# DRY AND WET TORREFACTION OF MICROALGAL BIOMASS FOR BIOCHAR PRODUCTION AS BIOENERGY SOURCES

GAN YONG YANG

FACULTY OF ENGINEERING
UNIVERSITY OF MALAYA
KUALA LUMPUR

2020

# DRY AND WET TORREFACTION OF MICROALGAL BIOMASS FOR BIOCHAR PRODUCTION AS BIOENERGY SOURCES

## GAN YONG YANG

## THESIS SUBMITTED IN FULFILMENT OF THE REQUIREMENTS FOR THE DEGREE OF ENGINEERING

## FACULTY OF ENGINEERING
## UNIVERSITY OF MALAYA
## KUALA LUMPUR

## 2020

# UNIVERSITY OF MALAYA
## ORIGINAL LITERARY WORK DECLARATION

Name of Candidate: Gan Yong Yang

Matric No: KVA 170027, 17006573/2

Name of Degree: PhD

Title of Project Paper/Research Report/Dissertation/Thesis ("this Work"): Dry and wet

torrefaction of microalgal biomass for biochar production as bioenergy sources

Field of Study: Energy

I do solemnly and sincerely declare that:

(1) I am the sole author/writer of this Work;
(2) This Work is original;
(3) Any use of any work in which copyright exists was done by way of fair dealing and for permitted purposes and any excerpt or extract from, or reference to or reproduction of any copyright work has been disclosed expressly and sufficiently and the title of the Work and its authorship have been acknowledged in this Work;
(4) I do not have any actual knowledge nor do I ought reasonably to know that the making of this work constitutes an infringement of any copyright work;
(5) I hereby assign all and every rights in the copyright to this Work to the University of Malaya ("UM"), who henceforth shall be owner of the copyright in this Work and that any reproduction or use in any form or by any means whatsoever is prohibited without the written consent of UM having been first had and obtained;
(6) I am fully aware that if in the course of making this Work I have infringed any copyright whether intentionally or otherwise, I may be subject to legal action or any other action as may be determined by UM.

     Candidate's Signature                 Date:

Subscribed and solemnly declared before,

     Witness's Signature                   Date:

Name:

Designation:

**ABSTRACT**

Increasing population in global and living standards have risen the consumption of global energy. Thermochemical conversion approaches hold great potential for the biomass conversion into energy applications. Among these approaches, torrefaction is a promising technique to enhance the biomass properties, making it more practical and suitable in biofuel applications. In this study, two different species of microalgae (third-generation biofuel feedstock) including *Chlorella vulgaris* ESP-31 and FSP-E were used as feedstocks for dry and wet torrefaction. Dry torrefaction of microalgae was performed at temperatures of 200, 250 and 300 ℃, and holding times of 15, 30, 45 and 60 min, respectively. Next, wet torrefaction of microalgae were conducted in water and dilute acidic solutions with the aid of microwaves irradiation at 160 ℃ and 10 min. The effects of sulfuric, phosphorus, and succinic acids on the microalgae with different percentages of chemical composition were investigated. The biochar produced from dry and wet torrefaction was performed fuel properties analysis and characterisation. In addition, TG-FTIR and double-shot Py-GC/MS approaches were executed to investigate the effects of torrefaction pre-treatment on microalgae pyrolysis. Furthermore, the kinetic modelling of microalgal biochar pyrolysis was carried out by using an independent parallel reaction model. As a result, dry torrefaction enhanced the HHV of microalga ESP-31 biochar (high-carbohydrate) by 45% with energy yield of 80% at 300 ℃ and 60 min. Torrefaction performance was highly affected by torrefaction temperature compared with holding time for microalgae and *Jatropha* biomass, but the solid yield of microalga ESP-31 significantly decreased with holding time at mild torrefaction (250 ℃) due to the high reactivity of the microalgae components (carbohydrates) at that temperature. For the wet torrefaction, the disruption of the microalga FSP-E (high-protein) was not notable in the acidic solutions. The HHV of microalga ESP-31 biochar produced by succinic acid wet torrefaction pre-treatment was enhanced by 40% with at least 45% of energy yield.

Thermogravimetric analysis revealed that the carbohydrate content of microalga ESP-31 has the highest degradation in sulfuric acid solution. For the evolved gas analysis, the microalgae pre-treated with sulfuric acid solution generated highest C–H absorption band in the pyrolysis gas. In the combustion TG-FTIR analysis, the intensity of O−H absorption band was removed in the first stage, indicating deoxygenation and dehydration process occurred in the wet torrefaction. In addition, the Py-GC/MS analysis revealed that only carbohydrate-derived products were decreased in the pyrolytic bio-oil of the microalgae pre-treated by the acidic solutions wet torrefaction. In contrast, carbohydrate- and lipid-derived products were decreased in the pyrolytic bio-oil of the microalgae pre-treated by the dry torrefaction. Lastly, the independent parallel reaction with four pseudo-components model successfully predicted the kinetic behaviours of carbohydrates, proteins, lipids and other components in microalgae. The results revealed the thermal degradation curve with a fit quality of at least 98% were predicted for microalgae pyrolysis kinetics. In short, wet torrefaction successfully enhanced the fuel properties of the microalgal biochar for biofuel applications.

Keywords: microalgae *Chlorella vulgaris*; biomass thermochemical conversion; dry and wet torrefaction; TG-FTIR and Py-GC/MS; kinetic modelling

# ABSTRAK

Peningkatan populasi dalam global dan taraf hidup meningkatkan penggunaan tenaga global. Penukaran termokimia mendekati potensi yang besar untuk menukar biomas menjadi aplikasi tenaga. Antara pendekatan ini, torrefaction merupakan teknik yang menjanjikan untuk meningkatkan sifat biomas, menjadikannya lebih praktikal dan sesuai dalam aplikasi biofuel. Dalam kajian ini, dua spesies mikroalgae yang berlainan (bahan bakar biofuel generasi ketiga) termasuk *Chlorella vulgaris* ESP-31 dan FSP-E telah digunakan sebagai bahan bakar untuk torrefaction kering dan basah. Torrefaction kering mikroalgae dilakukan pada suhu 200, 250 dan 300 ℃, dan memegang masa 15, 30, 45 dan 60 min. Seterusnya, torrefaction basah mikroalgae dilakukan di dalam air atau larutan asid cair dengan bantuan penyinaran gelombang mikro pada 160 ℃ dan 10 minit. Kesan daripada asid sulfur, fosforus, dan succinic kepada mikroalgae yang mempunyai peratusan komposisi kimia yang berbeza telah disiasatkan. TG-FTIR dan double-shot Py-GC/MS telah dilaksanakan untuk menyiasatkan kesan pra-rawatan torrefaction kepada mikroalga pyrolysis. Tambahan pula, pemodelan kinetik pyrolysis mikroalgae dilakukan dengan menggunakan model reaksi selari bebas. Akibatnya, torrefaction kering meningkatkan HHV microalga ESP-31 (karbohidrat yang tinggi) sebanyak 45% dengan hasil tenaga 80% pada 300 ℃ dan 60 min. Prestasi torrefaction sangat terjejas oleh suhu torrefaction berbanding dengan memegang masa bagi mikroalgae dan kernel binih *Jatropha*, tetapi hasil pepejal mikroalga ESP-31 berkurangan dengan memegang masa pada torrefaction ringan (250 ℃) disebatkan oleh kereaktifan komponen-komponen mikroalgae (karbohidrat) yang tinggi pada suhu tersebut. Bagi torrefaction basah, gangguan mikroalga FSP-E (protein yang tinggi) tidak ketara dalam larutan berasid. HHV bagi biochar mikroalga ESP-31 yang merawat dengan torrefaction basah dalam asid succinic meningkat sebanyak 40% dengan sekurang-kurangnya 45% hasil tenaga. Analisis termogravimetrik mendedahkan bahawa kandungan karbohidrat mikroalga ESP-

31 mempunyai degradasi tertinggi dalam larutan asid sulfurik. Bagi analisis gas yang berkembang, mikroalga yang dirawat dengan asid sulfuric menghasilkan gas dengan generasi penyerapan C−H tertinggi semasa pyrolysis. Dalam analisis TG-FTIR pembakaran, keamatan band penyerapan O−H telah dihapuskan di peringkat pertama, menunjukkan bahawa proses deoxygenation dan dehidrasi berlaku dalam torrefaction basah. Di samping itu, analisis Py-GC/MS menunjukkan bahawa hanya produk yang dihasilkan daripada karbohidrat telah berkurang dalam bio-minyak pyrolysis mikroalga yang dirawat sebelumnya oleh larutan berasid torrefaction basah. Sebaliknya, produk yang dihasilkan daripada karbohidrat dan lipid telah berkurang dalam bio-minyak pyrolysis mikroalga yang dirawat sebelumnya oleh torrefaction kering. Akhir sekali, tindak balas selari bebas dengan model yang mempunyai empat komponen pseudo berjaya meramalkan kelakuan kinetik karbohidrat, protein, lipid dan komponen lain dalam mikroalgae. Hasilnya telah berjaya menunjukkan lengkung degradasi haba dengan kualiti yang susuai sekurang-kurangnya 98% telah diramalkan untuk kinetik mikroalgae pyrolysis. Singkatnya, torrefaction basah berjaya meningkatkan sifat-sifat bahan api biochar mikroalgae untuk aplikasi biofuel.

Kata kunci: mikroalgae *Chlorella vulgaris*; penukaran termokimia biomas; torrefaction kering dan basah; TG-FTIR dan Py-GC/MS; pemodelan kinetik

# ACKNOWLEDGEMENTS

I hereby express my wholehearted appreciation to Dr. Ong Hwai Chyuan and Prof. Dr. Ling Tau Chuan, my research supervisors, for their enthusiastic encouragement, patient guidance and useful advice in this project. It would have been tougher journey to endure without his encouragement and assistance. My sincere thanks to my external supervisor, Prof. Dr. Chen Wei-Hsin form Department of Aeronautics and Astronautics, National Cheng Kung University, for his guidance and support throughout my research attachment in Taiwan.

My sincere thanks also go to Dr. Sheen Herng-Kuang from Taiwan Tai Sugar Research Cooperation and related member for their kind assistance and support in the lab facilities. Also, I would like to express my special thanks of gratitude to Prof. Jo-Shu Chang form Department of Chemical Engineering, National Cheng Kung University and related lab member for their support in the lab facilities and microalgae during my research in Taiwan.

I would also like to thank my fellow friends in the Faculty of Engineering, University of Malaya and Department of Aeronautics and Astronautics, National Cheng Kung University. All their willingness to help and sharing of knowledge in the related field help to keep my research work on schedule. Thank you to the laboratory technicians and staff for their help in offering me the resources and assistance.

Finally, I wish to thank my parents, family and friends for their support and encouragement throughout my studies.

# TABLE OF CONTENTS

# LIST OF FIGURES

# LIST OF TABLES

## LIST OF SYMBOLS AND ABBREVIATIONS

| | | |
|---|---|---|
| AAEMs | : | Alkali and alkaline earth metals |
| ACS | : | American Chemical Society |
| AOAC | : | Association of Official Agricultural Chemists |
| ASTM | : | American Society for Testing and Materials |
| atm | : | Atmospheric pressure |
| ATR | : | Attenuated total reflectance |
| C | : | Carbon |
| Ca | : | Calcium |
| $CH_4$ | : | Methane |
| Cl | : | Chlorine |
| CO | : | Carbon monoxide |
| $CO_2$ | : | Carbon dioxide |
| DAEM | : | Distributed Activation Energy Model |
| DSC | : | Differential scanning calorimetry |
| DTA | : | Differential thermal analysis |
| DTG | : | Differential thermogravimetric |
| FAME | : | Fatty acid methyl esters |
| FID | : | Flame ionization detector |
| Fe | : | Iron |
| FTIR | : | Fourier transform infrared |
| FWO | : | Flynn-Wall-Ozawa |
| GC | : | Gas chromatography |
| GC/MS | : | Gas chromatography coupled with mass spectrometer |
| H | : | Hydrogen |

| | | |
|---|---|---|
| $H_2$ | : | Hydrogen gas |
| $H_2SO_4$ | : | Sulfuric acid |
| $H_3PO_4$ | : | Phosphoric acid |
| HCl | : | Hydrochloric acid |
| HHV | : | Higher heating value |
| HMF | : | Hydroxymethylfurfural |
| HPLC | : | High-performance liquid chromatography |
| IPR | : | Independent parallel reaction |
| K | : | Potassium |
| KAS | : | Kissinger-Akahira-Sunose |
| kg | : | Kilogram |
| KOH | : | Potassium hydroxide |
| M | : | Mole |
| mg | : | milligram |
| min | : | minute |
| MJ | : | Megajoule |
| Mn | : | Manganese |
| MS | : | Mass spectrometer |
| ms | : | millisecond |
| N | : | Nitrogen |
| $N_2$ | : | Nitrogen gas |
| Na | : | Sodium |
| $NH_3$ | : | Ammonia |
| NO | : | Nitric oxide |
| O | : | Oxygen |
| PID | : | Proportional-integral-derivative |

| | | |
|---|---|---|
| PSO | : | Particle swarm optimisation |
| Py | : | Fast pyrolysis |
| RI | : | Refractive index |
| SEM | : | Scanning electron microscope |
| $SO_2$ | : | Sulphur dioxide |
| TG | : | Thermogravimetric analyser |
| TGA | : | Thermogravimetric analysis |
| TG-FTIR | : | Thermogravimetric analyser coupled with Fourier transform infrared spectrometer |
| TSI | : | Torrefaction severity index |
| $T_1$ | : | Temperature at which the conversion reaches 1% |
| $T_{99}$ | : | Temperature at which the conversion reaches 99% |
| $T_{max}$ | : | Temperature at which the maximum conversion rate occurs |
| XRD | : | X-ray diffraction |
| UV | : | Ultraviolet |
| vvm | : | Volume gas per volume of the medium per min |
| W | : | Watt |
| wt% | : | Weight percentage |
| ZSM-5 | : | Zeolite Socony Mobil-5 |
| % | : | Percentage |
| °C | : | Degree Celsius |
| $A$ | : | Pre-exponential factor ($s^{-1}$) |
| $c_i$ | : | Mass fraction of each component |
| $\left(\frac{d\alpha_i}{dT}\right)_{exp}$ | : | Conversion rates for experimental |
| $\left(\frac{d\alpha_i}{dT}\right)_{cal}$ | : | Conversion rates for calculated |

| | | |
|---|---|---|
| $Ea$ | : | Activation energy (kJ mol$^{-1}$) |
| $f(\alpha)$ | : | Reaction model |
| $Fit$ | : | Fit quality |
| $gbest$ | : | Global best position |
| $i$ | : | $i^{th}$ pseudo-component |
| $k$ | : | Number of iterations |
| $k(T)$ | : | Reaction rate constant (s$^{-1}$) |
| $m_f$ | : | Mass of the sample at final (800 °C) |
| $m_i$ | : | Mass of the sample at initial (105 °C) |
| $m_T$ | : | Mass of the sample at instantaneous |
| $N$ | : | Number of experimental points |
| $N_{particle}$ | : | Number of agents or particles sent to find the optimal solution |
| $OF$ | : | Objective function |
| $pbest_i$ | : | Best position experienced of the $i$-th particle |
| $R$ | : | Universal gas constant (9.314 J K$^{-1}$ mol$^{-1}$) |
| $rand()$ | : | Random number in the range [0,1] |
| $t$ | : | Conversion time (s) |
| $T$ | : | Absolute temperature (K) |
| $v_i$ | : | Position of the $i$-th particle |
| $x_i$ | : | Velocity of the $i$-th particle |
| $\alpha$ | : | Conversion degree |
| $\alpha_c$ | : | Momentum constant for adjusting the rate of change of the position |
| $\beta$ | : | Constant heating rate (°C s$^{-1}$) |
| $\beta_c$ | : | Momentum constant (0.5) |
| $\varphi_1$ | : | Cognitive learning rates |

$\varphi_2$   :   Social learning rates

# LIST OF APPENDICES

# INTRODUCTION

## 1.1 Research background

In the era of globalization, the demand of energy is increasing but fossil fuels are becoming limited. Thus, shortage supply of fossil fuel is the critical issue in this coming year due to the global increase in population. Combustion of fossil fuels produced carbon dioxide, that expected to change the climate (Li et al., 2013). The climate change will make the weather hotter and colder, as the consumption of electricity and energy increased. Among the fossil fuel, combustion of coal releases the highest carbon emission (Matter & Supply, 2012). The demand of energy supply can be overcome by using biomass renewable energy. In Malaysia, the biomass is not fully utilised for the energy production, while approximately 168 million tons of biomass produced every year. The biomass estimated produces more than 2400 MW of power, but only 773 MW is harvested (Ozturk et al., 2017).

Microalgal biomass is known as the third-generation biofuel feedstock and a potential resource for bioenergy industry due to fast growing organism (Ullah et al., 2015). Microalgal biomass is rich in nutritional contents such as carbohydrates, proteins, and lipids, which are suitable for biofuel production (Shuba & Kifle, 2018), foods (Smetana et al., 2017), soil additives (Fenton & Ó hUallacháin, 2012), livestock feeds (Madeira et al., 2017), pigments (Hu et al., 2017), nutraceuticals (Barba et al., 2015), and cosmetics (Wang et al., 2015a). After extraction of useful components, microalgal biomass has low heating value, high moisture and ash content, as well as hygroscopic nature. Direct combustion of microalgal biomass will contribute to greenhouse gases that will pollute the environment. These problems can be solved by converting the biomass into biochar through thermochemical conversion (Chang et al., 2015).

Biochar is a carbon-rich material from a biomass which is produced by thermochemical conversion process under limited of oxygen supply (Chang et al., 2015). In the past, biomass thermochemical conversion technologies have been neglected for energy generation due to low cost of fossil fuels. However, the increase in energy demands and environmental concerns related to fossil fuel energy generation caused these technologies revisit again. Hence, the use of renewable energy is increasing to replace the high pollutant non-renewable fossil fuel (Bujang et al., 2016).

The fundamental thermochemical conversion technologies involve torrefaction, pyrolysis, hydrothermal carbonization. Torrefaction is a thermal treatment process for improving the energy quality of solid biomass or pre-treatment of biomass for combustion, pyrolysis, gasification, and liquefaction. The temperature and holding time for torrefaction are normally in the ranges of 200−300 °C and 15−60 min (da Silva et al., 2017a). Pyrolysis of biomass is normally operated at temperature range of 300−700 °C, and the products are divided into 3 main categories: biochar, bio-oil, and bio-syngas (Kan et al., 2016). Hydrothermal carbonization is the heating of biomass in water at subcritical with temperatures of 180−250 °C and self-produced pressure up to 2 MPa to produce hydrochar as main output. Water acts as catalyst, medium and reactant during the carbonization process. Pyrolysis requires drying; however, hydrothermal carbonization can skip the drying process (Biller P, 2012).

Nevertheless, the researches on biochar production from the torrefaction are gaining attentions due to the high quality of solid biofuel obtained compared to pyrolysis (Sukiran et al., 2017). Torrefied biomass gives higher calorific value and carbon content, better grindability and hydrophobic, as well as low atomic ratio, ash and moisture contents compared to raw biomass (Wilk et al., 2015). Torrefaction changes biomass properties and increases energy quality of biomass, making it more practical and suitable to apply

in biofuel applications. The milder treatment condition of torrefaction gives higher solid mass yield and productivity compared to conventional pyrolysis with higher temperature (van der Stelt et al., 2011). Other than that, wet torrefaction or hydrothermal pre-treatment has gained attention as an efficient way to convert biomass of high moisture (Bach et al., 2017b; Shakya et al., 2017), which takes place in hot compressed water, where the pressure will be slightly higher than saturated vapor pressure of the torrefaction temperature (Bach & Skreiberg, 2016). Besides, wet torrefaction is a favourable pre-treatment method of pyrolysis for high quality of bio-oil (Triyono et al., 2019), while improving the combustion behaviour of biomass (Bach et al., 2017d).

Currently, several researches are focused in finding the effective technique to convert the high moisture microalgae into the biofuels and explore more new variations of microalgae species that can be employed as feedstock for bioenergy conversion process. The current research has showed that the technologies to produce energy from microalgae are still expensive and can cost more than the fossil fuel. Wet torrefaction was found to be an effective method to convert the high moisture biomass into biofuel by skipping the drying process. To date, the study on wet torrefaction technique using microalgae is still limited. Therefore, the sustainability of this research seems necessary to overcome these problems and improve the microalgal biochar quality that is expected to compete with fossil-based fuel.

## 1.2 Problem statement

Energy crisis is a growing problem in the country due to the volatile fuel prices and the limited amount of fossil fuel. Generally, Malaysia is still lack of literature study on torrefaction technique for solid biofuel production. Microalgae is recognized as favourable substitute for bioenergy production due to rapid growth, high biomass

3

production and carbon fixing efficiency compared to lignocellulosic biomass. Microalgae composition highly affected by the cultivation conditions and species, which will directly influence on the microalgae torrefaction performance. For this reason, the study of microalgae with different species and composition is important for torrefaction industry.

The third-generation biofuel feedstock, microalgal biomass on the torrefaction is still limited in the literature due to the high moisture content. The high moisture content of microalgae requires the large amount of energy to convert microalgae into biofuel. Wet torrefaction has been proven to convert the high-moisture biomass into the biofuel by skipping the drying step with a lower temperature. To date, the literature studies of microwave-assisted wet torrefaction of microalgae is still limited, whereas wet torrefaction in the various acidic solutions have not been reported. The current stage of converting microalgae into biochar is facing several challenges. Hence, wet torrefaction is potential to upgrade the microalgae into high quality renewable energy using lower temperature input.

Pyrolysis is a promising technique to convert microalgae into bio-oil at high temperatures (400–650 °C) and an inert condition. A variety of chemicals contained in the pyrolytic products including alkanes, hydrocarbons, aromatics, phenol derivatives, ketones, ethers, esters, sugars, water, and other substances. However, bio-oil produced from biomass pyrolysis exhibits disadvantages including low chemical and thermal stability, high oxygen and water content, and strong acidity which limit the use in energy applications and development. It is important to understand the biomass pyrolysis mechanism, as it can provide the fundamental knowledges on the selective pyrolysis process for obtaining a high-quality bio-oil. Thus, a new pre-treatment approach is necessary to overcome the microalgae bio-oil disadvantages.

In addition, it is important to study the microalgae pyrolysis characteristics and kinetics as its related to the products, reactions, and modelling processes at an industrial scale. Microalgae pyrolysis involves complex reactions and mechanism, which requires appropriate kinetic studies to understand the biomass reaction for reactor design. Although many studies concerning the microalgae pyrolysis kinetics have been carried out, the literature studies on the microalgae pyrolysis kinetic study of every single component are still limited. Moreover, the study on the wet torrefaction followed by microalgae pyrolysis kinetics is still absent. For this reason, the study wet torrefaction followed by pyrolysis behaviour and kinetic modelling of microalgae could be useful insights into the wet torrefaction pre-treatment on microalgae pyrolysis applications, as well as the reactor design for the biomass-to-energy process using Aspen Plus.

## 1.3    Research objectives

This research aims to investigate the biochar production from microalgae using advanced torrefaction techniques. Besides, this research attempts to obtain scientific overview of the microalgae biochar produced from both dry and wet torrefaction. The four main objectives of this research are as follows:

1.  To investigate the dry torrefaction performance and torrefaction severity of microalgae.

2.  To investigate the effect of advanced wet torrefaction technique on microalgal biomass in acidic solutions for co-production of biochar and sugar.

3.  To evaluate the effect of torrefaction for biofuel production using advanced TG-FTIR and Py-GC/MS approaches.

4.  To evaluate the effect of wet torrefaction on kinetic modelling of microalgae using independent parallel reaction.

## 1.4 Research hypothesis

Microalgae contributed by carbohydrates, proteins, lipids and other minor components. Different in the chemical composition in microalgae highly affected on the torrefaction performance. The high content of carbohydrates in microalgae will result in high enhancement of higher heating value (HHV) using low temperature torrefaction technique. Furthermore, the carbohydrates and proteins in the microalgae could be easily hydrolysed by acidic solutions. The high-pressure wet torrefaction technique will effectively hydrolyse carbohydrates and proteins in the microalgae and produced high HHV biochar. In addition, the complex structure of microalgae produced variety of chemicals contained in the bio-oil during pyrolysis. Dry and wet torrefaction can effectively remove the unwanted components to produce high quality bio-oil. Lastly, pyrolysis of microalgae involves complex reaction mechanism. Kinetic study using independent parallel reaction will provide useful insight to the pre-treatment operation and reactor design for biomass-to-energy industry.

## 1.5 Scope of the research

The research scope for this thesis is to investigate the biochar production from third-generation biofuel feedstock, microalgae as bioenergy using advanced torrefaction technique. The overall scope was divided in four main section based on the given objectives, which included experimental study of dry torrefaction, advanced wet torrefaction conversion technique, analysis of the effect of dry and wet torrefied biochar using TG-FTIR and Py-GC/MS approaches, and lastly the kinetics modelling of microalgae pyrolysis before and after wet torrefaction.

The research started with the conversion of microalgae to biochar using the dry torrefaction process. Two different microalga species, Chlorella *vulgaris* ESP-31 (high-

6

carbohydrate) and *Chlorella vulgaris* FSP-E (high-protein) were used as feedstocks for both dry and wet torrefaction. These microalgae were cultivated and collected from an open pond in southern of Taiwan. For the dry torrefaction, three different torrefaction temperatures of 200, 250 and 300 ℃ were applied, which is defined as light (200 ℃), mild (250 ℃) and severe (300 ℃) torrefaction, respectively (Zhang et al., 2018a). Four different holding time, namely, 15, 30, 45 and 60 min, were conducted for each dry torrefaction temperature. Next, the torrefaction performance using torrefaction severity index was implemented. Second-generation biofuel feedstock, *Jatropha* biomass was employed as comparison with the third-generation biofuel feedstock. Subsequently, wet torrefaction of the microalgae was carried out in a modified household microwave oven with maximum power of 800 W (Tatung TMO-231) with a hole on the roof of the oven to insert the reactor. In this study, four different solutions, namely, water, $H_2SO_4$, $H_3PO_4$ and succinic acid with concentration of 0.05 and 0.1 M were applied as wet torrefaction working fluids. Meanwhile, the basic characterisation on biochar fuel properties were carried out to analyse the torrefaction performance.

In order to further analyse the torrefied microalgae, thermogravimetric analysis (TGA) was performed by using a thermogravimetric analyser (Diamond TG/DTA, Perkin Elmer) coupled with Fourier transform infrared (FTIR) spectrometer (Perkin Elmer Spectrum 100) to evaluate the thermal behaviour and evolved gases analysis during the pyrolysis and combustion. A group of microalgae with the best torrefaction performance was selected for further analysis. The Py-GC/MS was implemented by using a pyrolyser (EGA/EY3030D) coupled with a gas chromatography-mass spectrometer (GC/MS, Agilent Technologies 7890A/5975C) to separate and identify the volatiles released during the pyrolysis. A two-stage thermal degradation (dry torrefaction as the first stage) of microalgae was applied by using a double-shot pyrolyser. Lastly, the obtained TGA and its derivative results were employed to conduct the kinetic modelling using an

independent parallel reaction (IPR) model. In addition, activation energy and pre-exponential factors of every single microalgae component were determined from the kinetic modelling data, together with the fit quality. The obtained results could be useful insights into the effect of wet torrefaction on microalgae pyrolysis applications, as well as the reactor design for the biomass-to-energy process.

## 1.6     Thesis outline

The format of this thesis follows the conventional format as mentioned in the University of Malaya guidelines. The overall outlines, as well as the organizational pattern of every chapter in this thesis are discussed in this section. The thesis comprises five chapters and each chapter is introduced as follows:

**Chapter 1**: This chapter defines the general background regarding biomass thermochemical conversion technique for biochar production, problem statement, research objectives, scope of the research and thesis outline.

**Chapter 2**: In this chapter, a literature review regarding the introduction on conversion process for biochar production, thermochemical conversion process of biomass especially on the torrefaction, and the quality of microalgal biochar produced under various torrefaction are presented, as well as the thermal analysis of the biochar using TG-FTIR and Py-GC/MS are summarised. Additionally, the kinetic modelling study of the microalgae pyrolysis using various techniques are discussed as well.

**Chapter 3**: The methodology of the research is presented in this chapter, which starts from the selection of the biomass, followed by the detailed explanation on the torrefaction process used in this study. Furthermore, the description on the characterisation and

analysis of the biochar produced from torrefaction are discussed, as well as the calculation of kinetic modelling.

**Chapter 4**: The results obtained from the research are presented in this chapter, together with the discussion and comparison with the results from the literature. First, the basic properties of biomass used in this study are discussed, following by the results and discussion on the dry and wet torrefaction process. Next, the in-depth analysis of the produced biochar using TG-FTIR and Py-GC/MS are included and explained, as well as the results of the kinetic modelling in the last section.

**Chapter 5**: This chapter contains a summary of the results and main conclusions associated with the research objectives. In addition, several future recommendations are provided in this chapter.

## LITERATURE REVIEW

### 2.1 Introduction

Energy crisis is a growing problem in the country due to the volatile fuel prices and the limited fossil deposited. The usage of fossil fuel or non-renewable energy emits vast volume of pollution gas and carbon dioxide during combustion, which is expected causes climate change. Besides, the continuous usage of fossil fuels for industry and transportation in the world have created the air pollutants. These phenomena increase weather hotness or coldness, thereby leading to increase consumption of energy and electricity. Hence, the development of renewable energy has rapidly increased due to these problems. The demand of energy supply can be overcome by using biomass renewable energy. Biomass energy is renewable in nature, which can replace the use of fossil fuels and reduce the environmental pollution.

Microalgae are an outstanding source of renewable energy due to its fast growth rate, short breeding cycle, and do not compete with second generation biofuel source for land (Goh et al., 2019). It is known as the third-generation biofuel source and a potential resource for bioenergy industry due to fast growing organism (Ullah et al., 2015). Generally, carbohydrates, proteins, and lipids are the main components in microalgae. The mass contents of these components are depending on the microalgae species, which will be directly affected on the biofuel characteristics. However, microalgae are not suitable to use as energy sources due to the high moisture content and low energy density. A proper treatment including thermochemical or biochemical conversion is required for converting the biomass into biofuel (Goyal et al., 2008; Pang, 2019).

Thermochemical conversion including torrefaction, pyrolysis, liquefaction and gasification have been successfully converted the microalgae into many energy applications (Chen et al., 2015f). Among these techniques, biomass pyrolysis is one of

the promising techniques for biofuel production in the form of char, oil and gas. High surface area of microalgal biochar produced by pyrolysis is suitable to use as bio-adsorbent for removing the contaminant in aqueous solution. Pyrolysis can produce biochar as solid biofuel, but the increased in calorific value of biochar is lower than torrefaction process. High quality of solid biofuel can be obtained from torrefaction of biomass as compared to pyrolysis (Sukiran et al., 2017). Torrefaction is a thermochemical conversion technique for production of coal fuel from biomass (da Silva et al., 2017b). The research of torrefaction of biomass has increased drastically to upgrade biomass as solid biofuel that can partly replace fossil fuel in industry (Chen et al., 2012b; Sukiran et al., 2017). Torrefied biomass gives high calorific value and carbon content, better grindability and hydrophobic, as well as low atomic ratio, ash and moisture content compared to raw biomass (Wilk et al., 2015). Torrefaction changes biomass properties and increases energy quality of biomass, making it more practical and suitable to be use as solid biofuel. The milder treatment condition of torrefaction gives higher solid mass yield and productivity compared to conventional pyrolysis with higher temperature (van der Stelt et al., 2011).

Recently, wet or hydrothermal torrefaction has gained attention as an efficient way to convert high moisture biomass (Bach et al., 2017b; Shakya et al., 2017). Wet torrefaction takes place in hot compressed water where the pressure will be slightly higher than saturated vapor pressure of the torrefaction temperature (Bach & Skreiberg, 2016). In addition, the latent heat of energy loss due to water vaporization can be avoided when the water remains in liquid phase. It is a promising technique for converting biomass into biochar with higher calorific values, energy yields and better hydrophobicity (Bach et al., 2013). Furthermore, wet torrefaction can work well with wet or even extremely wet biomass and enhance the removal of ash from biomass. Biochar is the main product after the wet torrefaction process while other side products such as sugar and sugar-based

derivatives will be produced as well (Yan et al., 2010). Besides, wet torrefaction is a favourable pre-treatment method of pyrolysis for high quality of bio-oil (Triyono et al., 2019), while improving the combustion behaviour of biomass (Bach et al., 2017d).

Thermal decomposition of microalgae components in the pyrolysis process can be divided into the degradation of carbohydrates, proteins, and lipids. The pyrolysis characteristic of every single component in the microalgae has been investigated through the TGA (Chen et al., 2018c). During the microalgae pyrolysis, pyrolysis gas is originated due to the degradation of microalgae components. The utilisation of TGA individually can only indicate the mass loss of biomass, and no evidence on the pyrolysis gas is revealed. The composition of pyrolysis gas in each weight loss step can be analysed by coupling the thermogravimetric analyser with Fourier-transform infrared spectroscopy (TG-FTIR) (Chen et al., 2019a; Lin et al., 2019). The information of the pyrolysis gas composition such as $CO_2$, CO, $H_2$, and $CH_4$ can be identified by FTIR. TG-FTIR has been applied to analyse the thermal behaviour and evolved gas on the torrefaction process and torrefied biomass (Chen et al., 2014b). The highest release of volatiles during torrefaction can be observed using DTG curves, and the functional groups of volatiles can be simultaneously determined using FTIR (Pahla et al., 2017). Meanwhile, the analytical pyrolyser coupling with gas chromatography and mass spectrometer (Py-GC/MS) has been successfully applied to evaluate the bio-oil composition of biomass fast pyrolysis. Py-GC/MS is an important analyser for biomass characterisation, it can effectively detect the pyrolytic products by comparing the total chromatographic peak areas obtained during the pyrolysis process at different conditions (Chen et al., 2018e; Chen et al., 2019c; Gao et al., 2013).

The study of the microalgae pyrolysis characteristics and kinetics is important as it is related to the products, reactions, and modelling processes at industrial scale (López-

González et al., 2014). Kinetics analysis is also known as an essential point in the thermal analysis to identify the mechanisms of biomass pyrolysis. Thermogravimetric analysis (TGA) has been widely applied to analyse the pyrolysis characteristics and kinetics of microalgae by identifying the weight loss of samples with the change of temperature precisely (Bach & Chen, 2017b). The data obtained from the TGA can be applied to determine the derivative thermogravimetric (DTG) analysis, which can evaluate the thermal behaviour of biomass. In general, the pyrolysis kinetics of biomass is expressed by the Arrhenius equation, which can determine the two important parameters including activation energy and pre-exponential factor to build the pyrolysis model. Pyrolysis kinetics of microalgae with different species have been studied in two different kinetic models including kinetic free and kinetic fitting (Gai et al., 2013), as well as catalytic pyrolysis kinetics (Xu et al., 2020). Kinetic fitting model is divided into single and multiple reaction models (Bach & Chen, 2017b). The single reaction model is very simple where microalgae are directly transformed into char and volatiles, providing a low fit quality to describe the microalgae pyrolysis. A modification of the multiple parallel reaction models based on the three main components of microalgae has been successfully used to describe the microalgae pyrolysis (Bach & Chen, 2017a).

To date, torrefaction process has received a lot of attention to convert the lignocellulosic biomass into biochar because of the significant increase in calorific value of biomass. However, the study on torrefaction technique using microalgae is still limited, especially on wet torrefaction. In this study, production process of microalgal biochar such as pyrolysis, hydrothermal carbonization and torrefaction are reviewed. This literature study aims to summarise and discuss the torrefaction process of microalgae biomass such as dry torrefaction and wet torrefaction. The fuel characteristics of torrefied microalgal biochar from previous studies are compiled. Lastly, the literatures related to

13

the in-depth biomass analysis using TG-FTIR and Py-GC/MS analytical techniques are reviewed, as well as the kinetic modelling study.

## 2.2    Thermochemical conversion

Biomass required some pre-treatment for better char yield and quality. Biochar is generally produced through thermochemical conversions including pyrolysis, torrefaction, and hydrothermal carbonization as shown in **Figure 2.1**. Pyrolysis mainly refers to slow pyrolysis, is a conventional way to produce biochar with high yield. As indicated in **Figure 2.1**, pyrolysis can be divided in slow and fast pyrolysis based on the different in heating rate and holding time. There are other recent development of biochar production including microwave-assisted pyrolysis, hydrothermal carbonization or torrefaction. Hydrothermal carbonization also produced a final carbonaceous material as the main product. Torrefaction is a method to upgrade the biomass with low energy content, whereas a high-quality solid biofuel is produced.
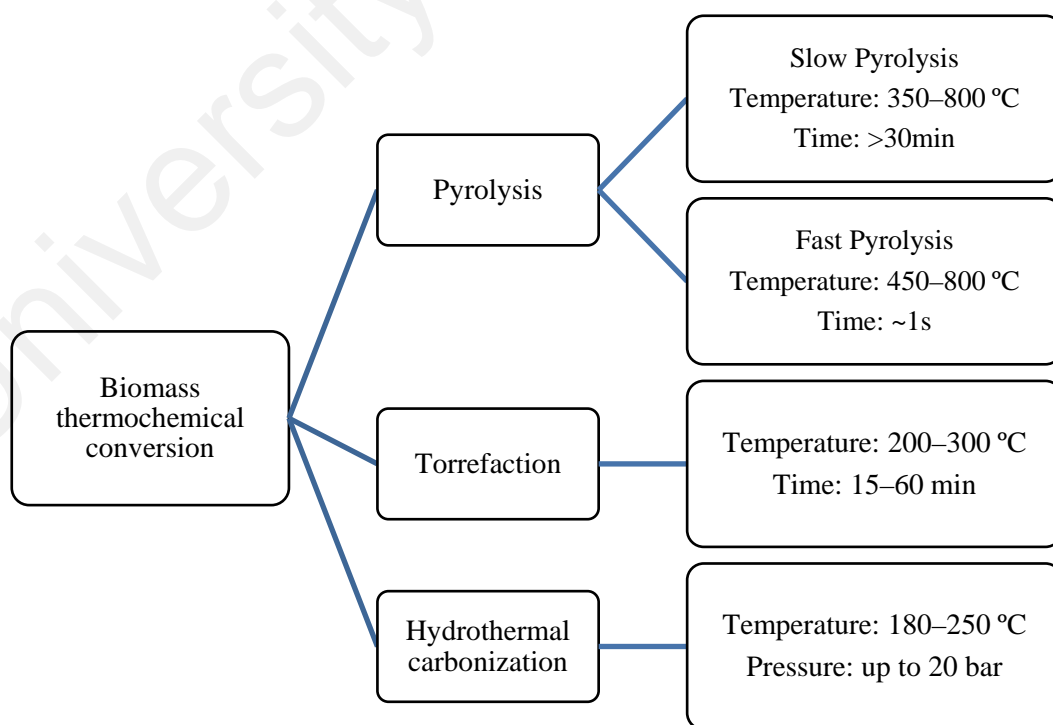


**Figure 2.1**: Biomass thermochemical conversion process

Second- and third-generation biofuels produced through the thermochemical conversion of biomass are important renewable sources for replacing fossil fuel (Chen et al., 2015f; Nicodème et al., 2018). Second-generation biofuel is produced using by-products of agricultural industries, but several disadvantages hinder the commercial application of this biomass (Yang et al., 2019b). Biofuel produced from algal biomass is categorised as third-generation biofuel, which can grow rapidly to produce high capacity of lipids for fuel synthesis (Adeniyi et al., 2018). Algae can be grown in nonarable lands and wastewater and do not compete for food production. In the upcoming years, algae are believed to be a future energy resource and be utilized in many industrial sectors (Mathimani et al., 2019).

### 2.2.1 Pyrolysis

Pyrolysis is an important thermochemical conversion process in which biomass is thermally degraded in the absence of oxygen, normally operated at atmospheric pressure (Bach & Chen, 2017b; Chen & Lin, 2016). After undergoing thermal decomposition, the products of pyrolysis include biochar, bio-oil, and non-condensable gases such as hydrogen, methane, syngas (a mixture of CO and $H_2$), carbon dioxide and other hydrocarbon gas. The yield of products mainly depends on the pyrolysis conditions. For example, biochar is the main product when the reaction temperature is under 450 °C, whereas bio-oil is the prime product in the range of 450−800 °C. High temperature beyond 800 °C lead to the formation of gases (Jahirul et al., 2012). Based on the experimental conditions (temperature, residence time, heating rate, and particle size), the pyrolysis processes have been divided into three types, including slow, fast and flash pyrolysis (Chen et al., 2015f).

The three major components in the lignocellulosic biomass are unevenly distributed in the cell wall. The hemicelluloses, cellulose, and lignin contents of the different types of lignocellulosic biomass can reach 15–30%, 40–60%, and 10–25%, respectively (Wang et al., 2017a). The interaction among the major components in biomass makes the biomass pyrolysis characterisation prediction simple based on the thermal behaviour of the individual components (Kan et al., 2016). However, hemicellulose is an amorphous structure with a low degree of polymerization. Hemicellulose degrades in two stages, which are the cracking of side unit within 100 °C and the centre wall decomposition at temperatures of 240–290 °C (Werner et al., 2014). Large-chain molecular-weight polymers that exist in crystalline cellulose require a higher decomposition temperature (320–360 °C) than hemicelluloses (Giudicianni et al., 2014). Lignin is a complex aromatic polymer structure that requires more than 500 °C to produce abundant oxygenated compounds (Zabeti et al., 2016). Meanwhile, microalgal biomass pyrolysis is also divided into three different reaction stages. The first stage occurs at temperatures below 200 °C, which separates water from microalgae. The second stage (200–600 °C) is the most reactive stage of the microalgal pyrolysis. Most of the microalgal components (carbohydrates, proteins, and lipids) are degraded completely to form chars and volatiles. The last stage of the microalgal pyrolysis starts from 600 °C, mainly due to the degradation of carbonaceous matters in the remaining solid residues (Bach & Chen, 2017b).

A complex biomass structure with different pyrolysis reaction conditions produces hundred types of oxygenated compounds with various properties. Bio-oil produced from biomass pyrolysis has high oxygen, water, and acid contents, which is unsuitable in petroleum infrastructure. Several studies have been conducted on the catalytic effects of thermochemical conversion processes, and positive effects have been reported. Catalytic pyrolysis is a process in which catalysts are utilized to enhance product yields based on

the need. Various catalysts, such as alkali and alkaline earth metals (AAEMs) (Trendewicz et al., 2015), zeolites (Williams & Nugranad, 2000), quartz sand (Aho et al., 2008), and iron (Fe) and Fe-based zeolites (Aho et al., 2010) have been employed to perform catalytic pyrolysis. Alkali and alkaline earth metals (AAEMs) in the pyrolysis of biomass generally generate encouraging results, which is effective catalysts in enhancing the biochar yield (Pütün, 2010; Wang et al., 2010), whereas zeolites in pyrolysis have been proven to enhance bio-oil yield and quality (Sebestyén et al., 2017).

Additionally, microwave-assisted pyrolysis has becoming a promising technique to produce high quality biochar, bio-oil and syngas. The use of microwave-assisted biomass conversion has successfully upgraded the agricultural biomass (Bundhoo, 2018; Lei et al., 2011). The advantages of microwave pyrolysis included high product yields, reduction of harmful chemical in bio-oil, energy and cost-saving. An electromagnetic wave is used in microwave technology to cause the oscillation between material molecules in order to generate heat. The technical advantages of microwave-assisted pyrolysis over conventional pyrolysis are as (1) a uniform microwave heating can be applied on larger biomass particles, (2) production of syngas with higher HHV, as it can be used for in-situ electricity for microwave generation, (3) cleaner products due to no agitation and fluidization in the process, and lastly, (4) mature technology with scale-up feasibility (Du et al., 2011). In addition, the biochar undergoes further chemical or thermal processing can be transformed into activated carbon (Spokas et al., 2011). During the pyrolysis, the release of volatiles in the biomass decreased the functional groups in biochar, making it a challenge as an effective adsorbent (Wang et al., 2015b). Nevertheless, the aid of microwave for pyrolysis can also be up-scaling in the future to convert agricultural biomass into biochar for applications such as soil fertilizer based on its economic production process.

Chemical treatment is one of the common reported methods to modify and improve the functionality, pore structure and surface area of biochar. The treatment involves one-step and two-step treatment procedures. Treatment of biochar after pyrolysis is proven to improve the performance of biochar as adsorbent (Wahi et al., 2017). Acid and alkaline treatment is suitable method to improve surface of biochar (Ahmed et al., 2016). Acid treatment is conducted to enhance the hydrophilicity of the materials, remove the mineral elements and also increase the acidic properties of the biochar (Ahmed et al., 2016). Phosphoric acid, nitric acid, hydrochloric acid and sulphuric acid are the common reagents used to modify the biochar surface properties (Nair & Vinu, 2016). In contrast, base treatment is applied to enhance the positively charges surface which may help in the adsorption of negatively charged pollutant (Ahmed et al., 2016). The common chemicals used for base treatment are potassium hydroxide and sodium hydroxide which able to increase the oxygen content and surface basicity of biochar (Wahi et al., 2017). Heavy metals can be absorbed by the organs in human and animal body, causing potentially damaging effects. Thus discharge of heavy metals into water supplies threatens ecosystem and human health (Bogusz et al., 2015). Recently, researchers found that modified biochar has improved the removal of contaminant and heavy metal from waste water (Ahmed et al., 2016).

### 2.2.2 Torrefaction

Torrefaction is divided into dry and wet torrefaction. Dry torrefaction converts raw biomass into biochar by heating at temperatures between 200 to 300 ºC, under atmospheric pressure with the absent of oxygen. Hydroxyl groups of the biomass are removed during torrefaction and producing hydrophobic groups. The major benefits of torrefied biomass are increased in HHV, energy density and carbon content while

18

decreased in atomic ratio and moisture content compared to raw biomass (Wilk et al., 2015). The biochar is the main product during the torrefaction, while bio-oil and biogas produced as by-products (Li et al., 2017b). Meanwhile, wet torrefaction used lower temperature and holding time to produce high energy dense biochar compared to dry torrefaction. Sub-critical water is used as reaction medium for wet torrefaction. The disadvantages of using wet torrefaction is high cost for setup and maintenance due to high pressure torrefaction process (Acharya et al., 2015).

During the torrefaction, the main constituents (hemicelluloses, cellulose and lignin) contained in lignocellulosic biomass will be thermally decomposed, especially the hemicellulose content (Chen & Kuo, 2011a). Chew and Doshi (2011) stated that the HHV of the woody and nonwoody biomass are increased up to 26 and 25 MJ/kg at torrefaction temperature of 300 °C, whereas the mass yield decreased to 24% for empty fruit bunches of palm oil. The increase in torrefaction temperature decreased the solid yield due to the chemical reactions, wherein the carbon retained in the biochar increased the HHV (Li et al., 2012). HHV enhancement cannot prevent the biomass weight loss. To clearly understand the weight loss and energy analysis of torrefaction, Chen et al. (2015d) and Zhang et al. (2018a) introduced the torrefaction severity index (TSI) to analyse the impact of torrefaction severity on the biomass torrefaction performance.

The knowledge of catalytic effect on biomass torrefaction is still limited recently. In recent studies, effect of catalysts has shown a positive effect on dry torrefaction (He et al., 2018). Na, K, Ca, and Mn metals bounded organically in biomass enhanced the biomass reactivity during torrefaction. Nonetheless, the effect of catalyst on the solid yield has been successful studied using TGA. The pine and spruce biomass with K and Na bounded organically resulted in more mass loss at temperatures of 240−280 °C when compared with their raw counterparts. It was shown that biomass organically bounded K

could provide shorter retention time (Shoulaifar et al., 2016). Saddawi et al. (2012) established that the mass loss decreases after removal of catalytic minerals (AAEMs) from biomass. The catalytic mineral contents (K, Na, Mg, and Ca) were removed by washing using water, hydrochloric acid and ammonium acetate. After pre-treatment and removal of AAEMs, biomass became less reactive to thermal degradation where increase in mass and energy yield were observed. Chen et al. (2016) studied the transformation and release features of Cl and K during biomass torrefaction at different particle sizes, temperatures, and holding times, and found that the high release of Cl and K increased the weight loss of the biomass. The release ratio of Cl was significantly affected by the particle size at 350 ℃.

### 2.2.3 Hydrothermal carbonization

Hydrothermal carbonization is the heating of biomass in water at subcritical with temperature (180−250 ℃) and self-produced pressure up to 20 bar to produce hydrochar as main output. Water acts as catalyst, medium and reactant during the carbonization process. Biomass with high moisture content is suitable to use hydrothermal carbonization compare to conventional pyrolysis (Álvarez-Murillo et al., 2016). Its dehydrated water content of biomass using pressure by saving time and energy to dry the biomass. Fuel properties of the biomass can be improved through this process and the hydrochar produced can be used as fertilizer to improve the soil properties (Kim et al., 2017). Hydrothermal carbonization has been widely used to improve the physical and chemical properties of wet biomass for the agriculture applications (Dai et al., 2017; Fakkaew et al., 2017).

In this process, biomass can be converted into high quality biofuel products, by controlling the process variables such as reaction temperature, holding time, pressure,

biomass feedstocks and the aid of catalysts (Tekin et al., 2014). In term of these process variables, temperature plays the most important factor in the hydrothermal carbonization process followed by holding time and biomass feedstocks (Nizamuddin et al., 2017). A high yield of solid product can be obtained by using lower reaction temperature, but the physical and chemical characteristics differ with the change in temperature. For a high reaction temperature carbonization, a biochar with high carbon content and low hydrogen and oxygen content is produced, as well as high HHV. Moreover, biochar produced from this process has a unique composition which is comparable with bituminous coal quality (Heilmann et al., 2010). The biochar produced has the properties of uniform spherical particles, controlled porosity, functional surfaces ($-$OH, C$=$O, $-$COOH), easily controlled surface chemistry and electronic properties, and can bind $CO_2$ from the plant precursor if the carbon is negative (Titirici et al., 2012).

## 2.3    Torrefaction of microalgae

### 2.3.1    Dry torrefaction

Dry torrefaction, or in another word mild pyrolysis or low temperature pyrolysis. Torrefaction is a process to improve the characteristic of biochar close to coal fuel. The process destroys the structure of biomass but upgraded the biomass calorific value and energy density (Sukiran et al., 2017). The general process of microalgae dry torrefaction is shown in **Figure 2.2** (Chen et al., 2015e) and the literature survey of torrefaction of microalgae and others biomass is presented in **Table 2.1**. Torrefaction of biomass is classified into light, mild and severe torrefaction with temperatures of 200$-$235, 235$-$275 and 275$-$300 °C, respectively. This significantly affects the carbon, oxygen and hydrogen contents, ash content, calorific values, hydrophobicity, moisture, and biochar yield (Wu et al., 2012). Today, dry torrefaction is facing economic challenges to produce high

quality microalgal biochar. The high moisture content of microalgae is required to pre-drying before the torrefaction. The moisture content of biomass should be less than 10 wt% to achieve high performance torrefaction (Bach & Skreiberg, 2016). For biomass with moisture content of 50−60 wt%, 3−5 MJ of energy is required to reduce the moisture content to 10−15 wt%. Thus, the overall performance of dry torrefaction is low due to high operating cost in thermal drying (Fagernäs et al., 2010).
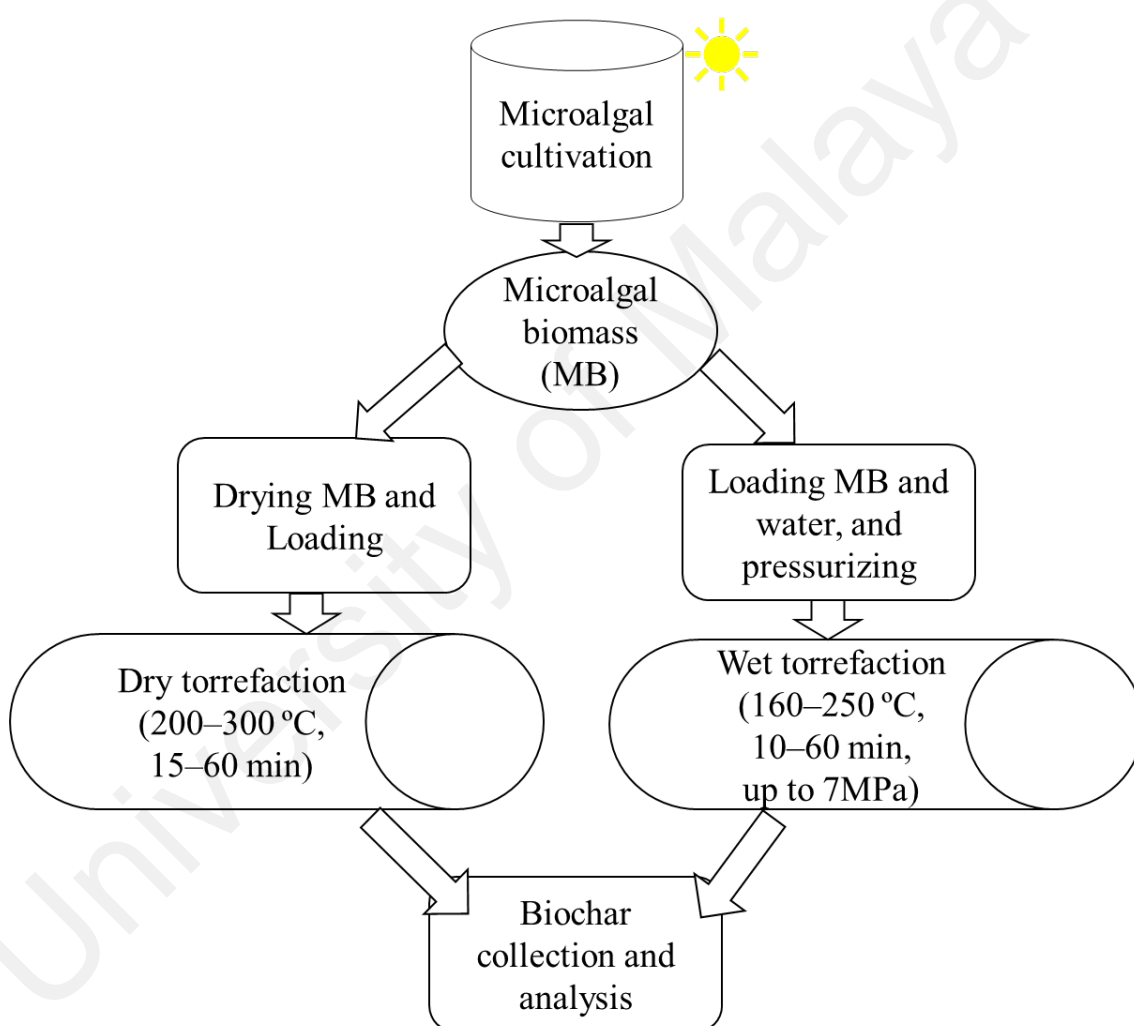


**Figure 2.2: General process of dry and wet torrefaction of microalgae**

**Table 2.1: Dry torrefaction of microalgal biomass and others biomass under different conditions**

| Biomass feedstock | Media | Temperature (°C) | Holding Time (min) | Solid yield (%) | References |
|---|---|---|---|---|---|
| **Microalgae** | | | | | |
| *Chlamydomonas* sp. JSC4 | Nitrogen | 200 | 30 | 93.9 | (Chen et al., 2016) |
| | | 250 | 15 | 92.7 | |
| | | 250 | 30 | 82.3 | |
| | | 250 | 60 | 64.2 | |
| | | 300 | 30 | 51.3 | |
| *Scenedesmus obliquus* CNW-N | Nitrogen | 200 | 60 | 86.37 | (Chen et al., 2014g) |
| | | 225 | | 82.74 | |
| | | 250 | | 76.45 | |
| | | 275 | | 67.19 | |
| | | 300 | | 63.23 | |
| *Chlamydomonas* sp. JSC4 | Nitrogen | 200 | 60 | 86.87 | (Chen et al., 2014e) |
| | | 225 | | 77.31 | |
| | | 250 | | 59.57 | |
| | | 275 | | 47.07 | |
| | | 300 | | 40.57 | |
| *Chlorella sorokiniana* CY1 | Nitrogen | 200 | 60 | 85.76 | |
| | | 225 | | 77.22 | |
| | | 250 | | 55.67 | |
| | | 275 | | 45.65 | |
| | | 300 | | 38.33 | |
| *Chlamydomonas* sp. JSC4 | Nitrogen | 200−300 | 15−60 | 50.8−95.7 | (Chen et al., 2015e) |
| *Chlorella vulgaris* ESP-31 | Nitrogen | 200−300 | 15−60 | 53.0−96.8 | (Chen et al., 2015d) |
| *Chlorella vulgaris* ESP-31 | $CO_2$ | 200−300 | 15−60 | − | (Chen et al., 2015d) |

**Table 2.1, continued**

| Biomass feedstock | Media | Temperature (°C) | Holding Time (min) | Solid yield (%) | References |
|---|---|---|---|---|---|
| **Others Biomass** | | | | | |
| Energy Sorghum | Nitrogen | 250−300 | 30 | 43−65 | (Yue et al., 2017) |
| Sweet Sorghum | | | | 51−70 | |
| Sugarcane bagasses | Nitrogen | 230 | 180 | 75 | (Granados et al., |
| | | 250 | | 66 | 2017) |
| | | 270 | | 53 | |
| | | 290 | | 47 | |
| Jatropha-seed residue | Nitrogen | 260−300 | 10−60 | − | (Hsu et al., 2017) |
| Empty Fruit Bunch | Nitrogen | 200 | 30 | 72.0 | (Uemura et al., 2017) |
| | Combustion gas | 200 | 30 | 67.0 | |
| Corncob | Nitrogen | 220−300 | 30 | 69.38−95.03 | (Li et al., 2017b) |
| | | | | 67.20−94.99 | |
| | $CO_2$ | 220−300 | 30 | | |
| Leucaena with microwave | Nitrogen | 100−250 W | 15−30 | 17.25−72.30 | (Huang et al., 2017a) |
| Cymbopogon citrates residue with microwave | Nitrogen | 200 | 30−40 | 81.50 | (Tan et al., 2017) |
| | | 250 | | 74.30 | |
| | | 300 | | 61.20 | |
| Sewage sludge with microwave | Nitrogen | 100W | 30 | ~72 | (Huang et al., 2017b) |
| | | 150−200W | | ~40 | |
| | | 400W | | ~9 | |

The torrefaction characteristic of microalgae has been studied by several researchers under torrefaction temperatures of 200−300 °C and holding times of 15−60 min (Chen et al., 2015e; Chen et al., 2016; Wu et al., 2012). Nitrogen gas is one of the commonly used torrefaction gas to prevent oxidation of the biochar. Chen et al. (2014e) investigated the thermal degradation of raw microalgal biomass, which includes the dehydration (25−200 °C), decomposition of carbohydrates and proteins (200−350 °C), lipid decomposition (350−550 °C), and other microalgae components (550−800 °C). Thus, torrefaction must be carried out at above 200 °C to upgrade the biomass. Carbohydrates, proteins and lipids are retained in the microalgae for torrefaction at 200 to 250 °C because a higher temperature is required to initiate the thermal degradation of carbohydrates (Chen et al., 2016). Increasing torrefaction temperature significantly affects the decomposition of microalgal biomass. Hence, torrefaction has an obvious impact on decomposition of carbohydrates, proteins and lipids at severe temperature (300 °C) (Chen et al., 2016)

Recently, torrefaction using non-inert gas is being implemented to save inert nitrogen gas and energy (Uemura et al., 2017). Oxidative reactions will occur for non-inert gas (combustion gas or $CO_2$) due to the oxygen content, hence upgrades the biomass in oxidative torrefaction (Rousset et al., 2012). The end products of torrefaction using combustion gas are $CO_2$ and CO in gas phase, whereas water, pheno and acetic acid in liquid phase. This process can be further improved with the assistance of microwave due to higher heating efficiency and power density, better heat transfer and process control, faster internal heating, and more uniform heat distribution (Huang et al., 2016; Huang et al., 2017b; Ren et al., 2014). Researchers have depicted interest in microwave torrefaction compared with conventional torrefaction. The feedstock properties of torrefied municipal solid waste biomass such as grindability, energy density, lessened moisture adsorption and energy yield are improved with the aid of microwave torrefaction at microwave power 250 to 750W, with lesser holding time. Microwave torrefaction of biomass

produces biochar which is similar to coal and carbon-neutral fuel (Iroba et al., 2017). The properties such as calorific value and fuel ratio of Leucaena biochar derived from microwave torrefaction are increased with raising microwave power and processing time, however, the mass and energy yield of the biochar declined (Huang et al., 2017a).

### 2.3.2    Wet torrefaction

Wet torrefaction or hydrothermal torrefaction is another type of thermochemical conversion of biomass. The process takes place in an inert condition with temperatures of 160−250 °C, which is relatively low compared to dry torrefaction (Bach & Skreiberg, 2016). Water is the most important solvent with plenty of attractive properties as a reaction medium and solvent for extraction, where the properties of water can be changed by varying the temperature and pressure. Water in subcritical condition acts as a reaction medium in wet torrefaction. In comparison with ambient water, subcritical water possesses attractive physical and chemical properties. The low dielectric constant of subcritical water enhanced the ionic reaction (Yu et al., 2008). Subcritical water effectively solubilises most of the biomass elements and suitable for biomass degradation reaction. The subcritical water is kept in liquid phase during wet torrefaction process to avoid loss of energy in the form of latent vaporization heat. Temperature of subcritical water is below critical temperature of water (374 °C) and higher than saturated vapor pressure of water at wet torrefaction temperature (Bach & Skreiberg, 2016). Overly elevated pressure did not further promote the reaction rate but risen the cost immensely. The pressure of the wet torrefaction is raised by water vapor, which highly depends on volume of reactor and water (Inagaki et al., 2010). Wet torrefaction is an attractive method to produce high quality biochar using low temperature and holding time. The ash components can be removed during wet torrefaction for a better quality biochar (Bach et

al., 2013). In accordance to review, the concept of wet torrefaction is identical to hydrothermal carbonization, still, there exists a major difference between them. The wet torrefaction aims to produce higher quality biochar for energy while hydrothermal carbonization aims to produce charcoal with high carbon content to use as fuel, soil fertilizer and adsorbent (Bach et al., 2014).

Recently, wet torrefaction is a promising method for biochar production due to its ability to convert wet biomass into biochar without drying process (Bach et al., 2016). Wet biomass sample with water is placed in pressurise reactor chamber to upgrade biomass and remove the moisture content of biomass. The main reaction of dry torrefaction will only occur when the moisture content in the biomass is lessen. The advantage of wet torrefaction is to reduce the cost of drying wet biomass. This is because high pressure dewatering is more efficient than thermal drying in dry torrefaction (Laurila et al., 2014). Besides, energy consumption is a highlighted issue for wet torrefaction to produce biochar. Large amount of energy is consumed to heat the voluminous water in the process of wet torrefaction. Low solid loaded to reactor offers fast conversion, but high energy consumed. It can be achieve economically by loading 15−20 wt% of biomass in water (Peterson et al., 2008). Generally, it needs 7−20% of the biochar energy to produce this biochar (Bach & Skreiberg, 2016). Thus, strategic control to recover the heat and mass during wet torrefaction process can effectively reduce the cost compared to dry torrefaction.

The mechanism of wet torrefaction differs from thermal treatment mechanism of dry torrefaction which involves decarboxylation, dehydration, decarbonylation, demethoxylation, condensation, and aromatization chemical reactions (Acharya et al., 2015). Hydrolysis is the first process in wet torrefaction due to the reaction of biomass with subcritical water. The hydrogen bonds in subcritical water split-up the ether and ester

bonds between monomeric sugars and cause biomass polymer's activation energy to decrease (Libra et al., 2011). Thus, degradation of hemicelluloses is higher in wet torrefaction compared to dry torrefaction. For lignocellulosic biomass, hemicellulose is depolymerized to oligomers and monomers through hydrolysis while the cellulose and lignin are partly depolymerized depend on the experimental condition of wet torrefaction (He et al., 2018). **Table 2.2** shows the biomass undergoing wet torrefaction. After the wet torrefaction of biomass, biochar can be obtained by separating the water with a filter. In addition, the biochar produced can be used directly as solid biofuel.

**Table 2.2: Wet torrefaction of microalgal biomass and others biomass under different conditions**

| Biomass feedstock | Media | Temperature (℃)/ Pressure | Holding Time (min) | Solid yield (%) | Reference(s) |
|---|---|---|---|---|---|
| *Microalgae* | | | | | |
| *Chorella vulgaris* ESP-31 with microwave | Nitrogen | 160−180 ℃ 2-3 bar | 5−30 | 51.84−62.92 | (Bach et al., 2017b) |
| *Others biomass* | | | | | |
| Sugarcane bagasses with microwave | Nitrogen | 180 ℃ | 5 15 30 | 70.4 66.1 60.8 | (Chen et al., 2012d) |
| Norwegian forest residue | Nitrogen CO₂ | 175−225 ℃, 70 bar | 30 | − | (Bach et al., 2015a) |
| Corncobs | Nitrogen | 175 ℃ 185 ℃ 195 ℃ | 5 | 77.68−53.03 | (Zheng et al., 2015) |
| Norway spruce and birch wood | Nitrogen | 175−225 ℃ 70 bar | 10−60 | 58.02−88.27 | (Bach et al., 2015b) |
| Rice husk | Nitrogen | 150−240 ℃ | 60 | 47.9−86.7 | (Zhang et al., 2017a) |
| Humulus lupulus, Plumeria alba and Calophyllum inophyllum | − | 260 ℃ | 10 | 26.5−50.9 | (Yang et al., 2015b) |
| Filtered multiple solid waste | − | 120−190 ℃ 2−12 bar | 30,60 | − | (Mu'min et al., 2017) |
| Duckweed | Nitrogen | 130−250 ℃ | 60 | 30.4−64.8 | (Zhang et al., 2016a) |

### 2.3.3 Factor affecting biochar quality and yield

The solid yield of the biochar is mainly affected by torrefaction temperature and holding time (Chen et al., 2014e; Yang et al., 2015b). The increase in torrefaction temperature and holding time produce low solid yield of microalgal biochar during dry torrefaction. This is due to high degradation of carbohydrates and proteins at high temperature and holding time (Chen et al., 2014e). The solid yield of microalgal biochar decreases to around 50% corresponding to high torrefaction severity at temperatures of 275−300 °C for dry torrefaction (Chen et al., 2016). The solid yield of biomass for wet torrefaction gives the same respond as dry torrefaction that also decrease dramatically at severe temperature and high holding time (Zhang et al., 2017a; Zheng et al., 2015). For non-isothermal dry torrefaction, different heat rates were used for same mean temperature (250 °C), solid yield decreases with increasing heat rate (Chen et al., 2014g). The weight loss of microalgae at high heating rate is low at initial torrefaction period but the weight loss increases substantially at the final torrefaction period due to high temperature (Chen et al., 2014g). Thus, this shows that thermal degradation of non-isothermal torrefaction microalgae is faster than isothermal torrefaction.

As discussed before by Bach and Skreiberg (2016), wet torrefaction requires relatively low temperature and holding time to produce the same solid yield compared to dry torrefaction. Reaction medium used by wet torrefaction (hydrothermal treatment) is more reactive than inert media in dry torrefaction. Chen et al. (2015d) and Bach et al. (2017b), who work on dry torrefaction and wet torrefaction of *Chlorella vulgaris* ESP-31, proved that solid yield of microalgae can be achieved approximately 52% via dry torrefaction at 300 °C for 60 min or via wet torrefaction at 180 °C for 10 min or 170 °C for 30 min. Yan et al. (2009) investigated that solid yields of Loblolly pine via wet torrefaction at 260 °C for 5 min were approximately same as solid yields via dry torrefaction at 300 °C for 80

min. The results indicated that wet torrefaction produces the same amount of solid yield at low torrefaction temperature and holding time compared to dry torrefaction.

Furthermore, torrefaction using non-inert gas results in different solid yield compared to inert gas (Chen et al., 2015d; Eseltine et al., 2013). Dry torrefaction of microalgal biomass by using non-inert gas, $CO_2$ atmospheres independently as torrefaction gas shows that the solid yield is lesser than using inert nitrogen gas (Chen et al., 2015d). This may results from $CO_2$ reaction with the carbon in the biochar known as Boudouard reaction (Eseltine et al., 2013), therefore producing low yield in solid. The results are corresponding to the torrefaction of other biomass using non-inert gas that produces low solid yield in comparison to inert nitrogen gas (Chen et al., 2014f; Uemura et al., 2015; Uemura et al., 2017). The results are similar to wet torrefaction of forest residues that produce lesser solid yield using $CO_2$ torrefaction gas (Bach et al., 2015a). Up to now, the study of wet torrefaction of microalgal biomass using non-inert gas is still absent. The effects of $CO_2$ for wet torrefaction of Norwegian forest residues show up faster than $N_2$ gas. It produces less solid product with low HHV while improving the volume to remove the ash elements in the biochar (Bach et al., 2015a). The $CO_2$ also gives better grindability and hydrophobicity compared to $N_2$. Meanwhile, the ash content of forest can remove up to 60−69% using $CO_2$ compared to $N_2$ wet torrefaction which is a mere 14−26% (Bach et al., 2015a).

Microalgal biomass is rich in carbohydrates, proteins, and lipids, which differs from lignocellulosic biomass that mainly consists of cellulose, hemicelluloses and lignin (Ho et al., 2010). FTIR spectroscopy and TG are used to clearly reveal the chemical structures and composition of torrefied microalgal biochar (Chen et al., 2014g; Chen et al., 2016). In dry torrefaction of microalgae, the carbohydrates are destroyed first followed by protein disruption and partial lipids consumed with increasing of torrefaction temperature

and holding time (Chen et al., 2016). The mild torrefaction with temperature around 250 °C shows higher protein content with more degradation of carbohydrates in the sample (Chen et al., 2016). For wet torrefaction, the degradation behaviours of carbohydrates and proteins are similar to dry torrefaction (Bach et al., 2017b).

For lignocellulose biomass at light torrefaction, hemicelluloses in biomass is the most active and will be demoted to some level, whereas the cellulose and lignin are not affected notably. Hence, the weight loss of biomass slightly decreases, while calorific value only increases in a small degree (Chen et al., 2015g). During mild torrefaction of biomass, hemicellulose decomposition is strengthened and is generally used up. This causes the cellulose starting to drain to certain level. Hemicellulose is completely used up during severe torrefaction and cellulose is destroyed to a certain degree. The weight of the biomass decreases when fuel energy density increases. A biomass with higher lignin content produces higher solid yield and thermal stability during wet torrefaction. This is due to the higher decomposition temperature of lignin compared to cellulose and hemicelluloses since the contribution of lignin to the char is very compelling. Reduction of solid yield is not largely due to decomposition of hemicelluloses but both the cellulose and hemicelluloses (Yang et al., 2015b).

### 2.3.4 Properties of biochar as solid biofuel

There are three main indicators to analyse the fuel properties of biochar which comprises of HHV, energy yield, and H/C and O/C atomic ratio (Chen et al., 2015g). The HHV is the amount of heat released when the biomass is burned. The HHV is commonly measured by using a bomb calorimeter in the laboratory. The energy yield is the energy ratio between the torrefied biomass and raw biomass. It is calculated by multiplication of solid yield and HHV enhancement factor (Chen et al., 2015d). There is a strong

correlation between solid yield and energy yield, as the energy yield is directly proportional to solid yield.

When biomass undergoes torrefaction, the carrier gas such as $N_2$ transfers heat to the biomass to upgrade the biochar fuel properties. It is done by reducing the moisture, hygroscopic range and increasing grindability (Chen et al., 2015e; Kambo & Dutta, 2015). Water and low HHV volatile organic compounds are released from biomass to increase the HHV and storage life without fuel degradation of the biochar (Martín-Lara et al., 2017). The increase in HHV of biochar may also due to the decrease of C−O bonds in woody biomass and also C−C energy bond is higher than C−O bond (Chen & Kuo, 2011b). The biomass with high torrefaction temperature provides the highest enhancement of HHV. However, the biochar is not the best sample due to low solid yield. Certain quantity of mass is volatilizing during torrefaction. Low solid yield in high torrefaction temperature can greatly affect the energy yield obtained of the biochar (Iáñez-Rodríguez et al., 2017).

Atomic H/C and O/C ratio are plotted on Van Krevelen diagram to analyse the fuel properties of biochar (Van Krevelen, 1950). The H/C and O/C ratio of microalgal biochar is decreasing with increasing of torrefaction temperature and holding time while the properties of biochar are approaching towards solid biofuel (Wu et al., 2012). The reason of H/C ratio decreases during increasing of torrefaction temperature and holding time is because of the increase in carbon elements. This happens since the formation of hydrocarbon gases that contain hydrogen are generated after 350 ℃. The O/C ratio decreased during torrefaction is due to generation of volatiles rich in oxygen such as CO, $CO_2$ and $H_2O$ (Martín-Lara et al., 2017).

### 2.3.4.1 Higher Heating Value (HHV) and energy yield

Biomass with high HHV is important for industry's applications, which can be improved by torrefaction process. A list of ultimate analysis and HHV of the raw microalgal biomass is summarised in **Table 2.3**. The carbon content and HHV of raw microalgal biomass is different for every biomass, which is ranged between 37−53% and 16−23 MJ/kg. *Chlorella vulgaris* ESP-31 and *Chlamydomonas* sp. JSC4 microalgae after the oil extraction have low HHV compared to raw microalgae. This is due to low lipids in the microalgal residue that has higher HHV compared with carbohydrates and proteins (Chen et al., 2015e).

**Table 2.3: Ultimate analysis and higher heating value of raw microalgae**

| Sample | Ultimate analysis (wt%) | | | | HHV (MJ/kg) | References |
|---|---|---|---|---|---|---|
| | C | H | N | O | | |
| *Chlorella vulgaris* ESP-31 | 53.01 | 8.67 | 3.26 | 35.05 | 22.02 | (Bach et al., 2017b) |
| *Chlorella vulgaris* ESP-31 residues | 47.78 | 7.85 | 4.14 | 40.23 | 17.90 | (Chen et al., 2015d) |
| *Sprirulina platensis* (SP) | 45.70 | 7.71 | 25.69 | 11.26 | 20.46 | (Wu et al., 2012) |
| SP residue | 50.53 | 7.40 | 24.29 | 11.69 | 22.84 | |
| *Chlamydomonas* sp. JSC4 (C. sp. JSC4) | 50.59 | 8.12 | 2.60 | 38.69 | 19.27 | (Chen et al., 2015e) |
| C. sp. JSC4 residues | 48.06 | 7.62 | 3.81 | 40.51 | 16.91 | |
| C. sp. JSC4 residues | 41.49 | 6.83 | 3.34 | 48.34 | 16.27 | (Chen et al., 2016) |
| *Scenedesmus obliquus* CNW-N | 37.37 | 5.80 | 6.82 | 50.02 | 16.10 | (Chen et al., 2014g) |
| C. sp. JSC4 residues | 40.32 | 7.38 | 2.61 | 44.50 | 17.41 | (Chen et al., 2014e) |
| *Chlorella sorokiniana* CY1 residues | 45.07 | 7.64 | 3.88 | 35.52 | 20.40 | |
| *Chlorella vulgaris* | 42.51 | 6.77 | 6.64 | 27.95 | 16.80 | (Wang et al., 2013) |
| *Chlorella vulgaris* remnants | 45.04 | 6.88 | 9.79 | 29.42 | 19.44 | |

**Table 2.4** demonstrates the improvement of HHV of torrefied microalgae and others biomass in dry and wet torrefaction. The HHV of microalgae is improved by increasing the torrefaction temperature and time, which is similar to another biomass (Bach et al., 2017b). The torrefied microalgae can reach the range of coal that cycles around 25−35 MJ/kg at high torrefaction temperature (Chen et al., 2015g). In wet torrefaction, oxygen and negative contribution to the HHV are removed from wet torrefied biomass to increase the HHV. Oxygen reacts with hydrogen to form $H_2O$ and reacts with volatile carbon to form $CO_2$ (Bach & Skreiberg, 2016). The HHV of the torrefied microalgae and others biomass increased with either increasing wet torrefaction temperature or holding time. In wet torrefaction, the effect of temperature is more apparent than holding time (Bach & Skreiberg, 2016).

In high torrefaction temperature, the HHV enhancement factor is increased with decreasing energy yield (Chen et al., 2015e). The HHV value of a torrefied biomass increased almost linearly with mass loss, producing lower energy yield as a result from low solid yield. Torrefied microalgae with low energy yield and solid yield will produce a solid biofuel with higher HHV and smaller mass that is convenient for storage and transportation in the fuel industry. Nevertheless, the energy yield of microalgal biochar greater than 95%, the enhancement of the HHV is less than 10%, indicating that the energy densification is insufficient (Chen et al., 2015d). Chen et al. (2015d) points out that a high energy yield and high enhancement of HHV of torrefied microalgae can be obtained by using low temperature torrefaction and longer holding time.

**Table 2.4: Ultimate analysis and fuel properties of torrefied microalgal biochar and others biochar**

| Sample | Temperature and duration | Ultimate analysis (wt %), dry-ash-free | | | | HHV (MJ/kg) | H/C ratio | O/C ratio | Energy yield (%) | Reference(s) |
|---|---|---|---|---|---|---|---|---|---|---|
| | | C | H | N | O | | | | | |
| *Microalgae* | | | | | | | | | | |
| *Chlorella vulgaris* ESP.31 | 200−300 °C 15−60 min | 49.12−65.30 | 7.93−5.10 | 5.00−6.72 | 37.96−22.87 | 17.9−25.2 | 1.94−0.94 | 0.58−0.26 | − | (Chen et al., 2015d) |
| *Chalamydomonas* sp. JSC4 residue | 200−300 °C 15−60 min | 51.58−72.60 | 7.22−4.42 | 4.00−6.49 | 37.20−16.50 | 17.65−24.77 | 1.90−0.73 | 0.73−0.17 | 99.8−74.3 | (Chen et al., 2015e) |
| *S.obliquus* CNW-N | 200−300 °C 60 min | 36.93−39.26 | 5.47−3.63 | 6.53−7.38 | 28.21−23.19 | − | 1.67−1.18 | 0.57−0.44 | − | (Chen et al., 2014g) |
| *Chlorella vulgaris* ESP.31 by wet torrefaction | 170 °C 30 min | 59.03 | 7.82 | 8.62 | 24.53 | 26.02 | 1.59 | 0.31 | 62.95 | (Bach et al., 2017b) |
| *Chlamydomonas* sp. JSC4 | 300 °C 30 min | 63.64 | 5.01 | 5.99 | 25.36 | − | 0.94 | 0.30 | − | (Chen et al., 2016) |
| *Others biomass* | | | | | | | | | | |
| Humulud lupulud, Plumeria alba, Calophyllum inophyllum | 260 °C 10 min | 60.5 60.7 59.1 | 6.0 6.8 4.9 | 2.7 0.6 0.3 | 30.8 31.9 35.7 | 25.3 25.7 23.6 | − | − | 38.5 45.7 65.2 | (Yang et al., 2015b) |

**Table 2.4, continued**

| Sample | Temperature and duration | Ultimate analysis (wt %), dry-ash-free | | | | HHV (MJ/kg) | H/C ratio | O/C ratio | Energy yield (%) | Reference(s) |
|---|---|---|---|---|---|---|---|---|---|---|
| | | C | H | N | O | | | | | |
| *Jatropha*-seed residue | 300 °C 30 min | 61.1 | 5.2 | 4.2 | 20.7 | 27.01 | 1.01 | 0.25 | − | (Hsu et al., 2017) |
| Waste bamboo chopsticks | 290 °C 40 min | 55.48 | 5.41 | 0.214 | 38.32 | 23.04 | 1.17 | 0.52 | − | (Chen et al., 2017b) |
| Landfill food waste | 275 °C 40 min | 61.22 | 5.77 | 3.37 | 29.65 | 26.15 | 0.48 | 0.09 | 77.2 | (Pahla et al., 2017) |
| Energy sorghum Sweet sorghum bagasse | 275 °C, 300 °C, 30 min | 55.25 59.30 | 4.90 4.56 | 1.73 0.92 | 38.13 35.23 | 23.80 26.88 | − | − | 73 70 | (Yue et al., 2017) |
| Sunflower seed shell | 300 °C 60 min | 69.5 | 5.30 | 0.50 | 24.6 | 27.6 | 0.92 | 0.27 | − | (Bilgic et al., 2016) |

### 2.3.4.2 Hydrophobicity and moisture content

Microalgal biomass and residues contain high moisture content compared to torrefied microalgae (Chen et al., 2015e; Wu et al., 2012). Moisture content is non-combustible and reduces combustor temperature of solid biofuel (Wu et al., 2012). The moisture content of microalgal biochar can reduce by torrefaction at high temperature and holding time (Chen et al., 2016). Moisture content of torrefied microalgae reduced below 1% at 300 ºC torrefaction temperature. The functional group of O−H bond of microalgal microalgae can be analysed using Fourier transform infrared (FTIR) analysis. The wave number of water molecules or O−H bond range between $3029-3639$ $cm^{-1}$ (Duygu et al., 2012). Hydroxyl group (O−H bond) of the microalgal biomass is destroyed during torrefaction, prevent formation of hydrogen bonds with water (Wu et al., 2012). Thus, the microalgal biomass is converted from hygroscopic biomass into hydrophobic (Chen et al., 2016), same results are done by using others biomass (Chen et al., 2015g). Conversion of hydrophobic structure can also be clearly observed through moisture content of torrefied microalgae (Chen et al., 2016). Wet torrefaction microalgae also destroyed the O−H bond, show that less water absorbs by torrefied microalgae during storage (Bach et al., 2017b). The hydrophobicity of microalgae is improved by wet torrefaction. In short, wet torrefaction provides better hydrophobic product at high temperature and holding time (Bach et al., 2017b).

### 2.3.4.3  Atomic H/C and O/C ratio

H/C and O/C atomic ratios of torrefied biomass in Van Krevelen diagram are important component to solid biofuel (Lu & Chen, 2013). The atomic ratio can be determined by weight percentage of C, H, N and O. The weight percentages of C, H, N and O of raw and torrefied microalgal biomass are presented in **Table 2.4**. The torrefaction process of microalgal biomass involves dehydration and devolatilization reaction that is closely related to composition of carbon, hydrogen and oxygen (Wu et al., 2012). These elements of the raw microalgae are altered after the torrefaction. The carbon content of the torrefied microalgae tends to increase with increasing of torrefaction temperature and holding time. On the other hand, the hydrogen and oxygen contents decreased with torrefaction severity (Chen et al., 2016; Wu et al., 2012). The loss of hydrogen and oxygen has the largest influence on torrefaction process due to the devolatilization and dehydration of the biomass (Wu et al., 2012). Thus, the H/C and O/C of torrefied microalgae can be decreased with increasing torrefaction temperature and holding time but the decrease of H/C ratio is larger than O/C atomic ratio (Chen et al., 2015e).

By comparing with to solid fuels, the atomic H/C and O/C value are 0.78−1.26 and 0.22−0.38 for lignite, 0.34−0.98 and 0.01−0.25 for coal, and 0.02−0.37 and 0−0.03 for anthracite, respectively (Prins, 2005). Chen et al. (2016) and Chen et al. (2015e) reported that the H/C and O/C atomic ratio microalgal biomass are increased after the torrefaction. The H/C and O/C ratios of *Chlamydomonas sp.* JSC4 torrefied microalgae was reduced from 1.90 to 0.73 and 0.68 to 0.17 at 300 ℃ for 60 min, which is within the range of coal. The low H/C and O/C of torrefied microalgae can reduce thermodynamic loss of smoke and vapor from excessive oxidation (Bergman et al., 2005). The effects of temperature and holding time on atomic H/C and O/C value for wet and dry torrefaction of microalgae are the same, as reported by Bach et al. (2017a).

### 2.3.4.4  Ignition and burnout temperature

The assurance in term of storage and delivery of fuel used in industry is vital. It is analysed based on the ignition and burnout temperature of biomass or biochar (Du et al., 2010). Ignition temperature is the minimum temperature when fuel ignites spontaneously without external sources. Burnout temperature is used to determine the temperature when the fuel is depleting. Ignition and burnout temperature of biomass is important to evaluate fuel properties and combustor design (Du et al., 2007). For dry torrefaction, the ignition and burnout temperature of raw and torrefied microalgae is slightly affected by torrefaction temperature (<250 °C) and holding time (<30 min). The ignition and burnout temperature rises when torrefaction is at 300 °C and 30 min due to the damage of proteins and carbohydrates of microalgae (Chen et al., 2016). Same trend is observed for torrefaction of others biomass (Pala et al., 2014; Zhang et al., 2016c), ignition and burnout temperature risen as torrefaction severity increases. Thus, fuel properties of microalgal biochar has improved in terms of storage and delivery by using dry torrefaction at high torrefaction temperature and holding time.

Wet torrefaction of microalgae and other biomass observed a different trend for increasing torrefaction temperature and holding time (Bach et al., 2017a; Zhang et al., 2016a). Wet torrefied microalgae have lower ignition temperature compared to raw microalgae. The microalgae has lower ignition temperature when there is increasing in torrefaction temperature and holding time (Bach et al., 2017a). In comparison to wet torrefaction of duckweed samples, ignition temperature increased (255.5−286.9 °C) along with torrefaction temperature from 130 to 250 °C (Zhang et al., 2016a). This is affected by first stage leftward shifting of devolatilization peaks in torrefied microalgae (Bach et al., 2017a). Burnout temperature observes no trend for changing wet torrefaction condition for microalgae, but the burnout temperature of torrefied microalgae is higher than raw microalgae (Bach et al., 2017a). Besides, the burnout temperature perceives an

inverse trend for wet torrefaction temperature for duckweed sample while raw biomass has higher burnout temperature compared to torrefied biomass (Zhang et al., 2016a). The burnout temperature decreases with increasing torrefaction temperature. Thus, the char produced by microalgal biomass is more thermally stable compared to raw microalgae due to higher burnout temperature after wet torrefaction (Bach et al., 2017a).

## 2.4 Analytical techniques for thermochemical conversion behaviour

Lignocellulosic biomass is mainly composed of cellulose, hemicelluloses, and lignin, while non-lignocellulosic or algal biomass is mainly made up of protein, carbohydrate, and lipid (Zhang et al., 2018a). The difference between the chemical compositions directly affects chemical reactivity. Wet chemistry analysis is required to analyse the biomass properties due to the biomass samples are insoluble in conventional solvents (Krasznai et al., 2018). Analytical thermal degradation techniques have been implemented for the characterisation of the composition and structure of biomass samples (Carrier et al., 2011). A comprehensive study of the latest techniques could facilitate the development of pyrolysis industries (Oyedun et al., 2014). There are three stages in thermal decomposition of biomass during pyrolysis: (1) the first stage occurs below 200 °C, including moisture removal and the devolatilization of light volatiles; (2) the second stage occurs within the temperature range of 200−675 °C in which thermal decomposition starts with the decomposition of hemicelluloses and cellulose; and (3) the third stage occurs above 675 °C in which the decomposition reaction is slowed down. The decomposition of lignin is possible when the temperature reaches up to 1170 °C, starting from 455 °C (Hassan et al., 2016).

TGA is the most common thermal analysis technique to analyse the composition of the biomass by measuring the change in weight with temperature and time (Bach & Chen,

2017b). The differential thermogravimetric (DTG) curve is obtained by differentiating the TGA curve to determine the physical and chemical properties of biomass (Yahiaoui et al., 2015). The applied atmosphere can be inert or oxidative; even vacuum can be applied for TGA. Besides TGA, thermal decomposition using an analytical pyrolyser has also been used, where the samples are heated to a given temperature in an inert atmosphere with a heating rate of 0.1−20 °C/ms (Xu et al., 2018a). FTIR is one of the most important analytical techniques to analyse the chemical composition of biomass (Fan et al., 2012). Lignocellulosic fibres appear differently in structure and arrangement from different types of biomass, but all the biomass consists the similar chemical compositions such as hemicelluloses, cellulose, and lignin with different percentages in the composition  (Fan et al., 2012). The greatest invention of FTIR is that the analysis of samples can be done in different states such as solid (powder), liquid, and gas phases.

### 2.4.1    Thermogravimetric analyser

Thermogravimetric analyser (TG) is an important thermal analysis for gas-solid reactions. TG has been used frequently in the laboratory biomass analysis and coal conversion by varying the process parameters such as temperature, time and heating rate (Carrier et al., 2011). Time-dependent weight change curve of biomass in isothermal or non-isothermal heating is the basis for characterizing the devolatilization processes, quantification of release rates and the kinetic reaction (Bach & Chen, 2017b). TG is made up of a balance coupled to a calorimeter, a controller, and a computer. The particles are heated through radiation in the thermo-analyser. The balance directly measures the weight loss of the tested sample as a function of time. The calorimeter gives the time dependence of both the heat flow and the temperature of the sample. Thermo-analytical techniques are divided into TGA, differential scanning calorimetry (DSC) and differential thermal

analysis (DTA). These thermo-analytical techniques are used to examine the thermal behaviour of biomass and to identify the kinetic parameters of the thermal reaction (Skreiberg et al., 2011). **Figure 2.3** presents the general setup system of a TG.
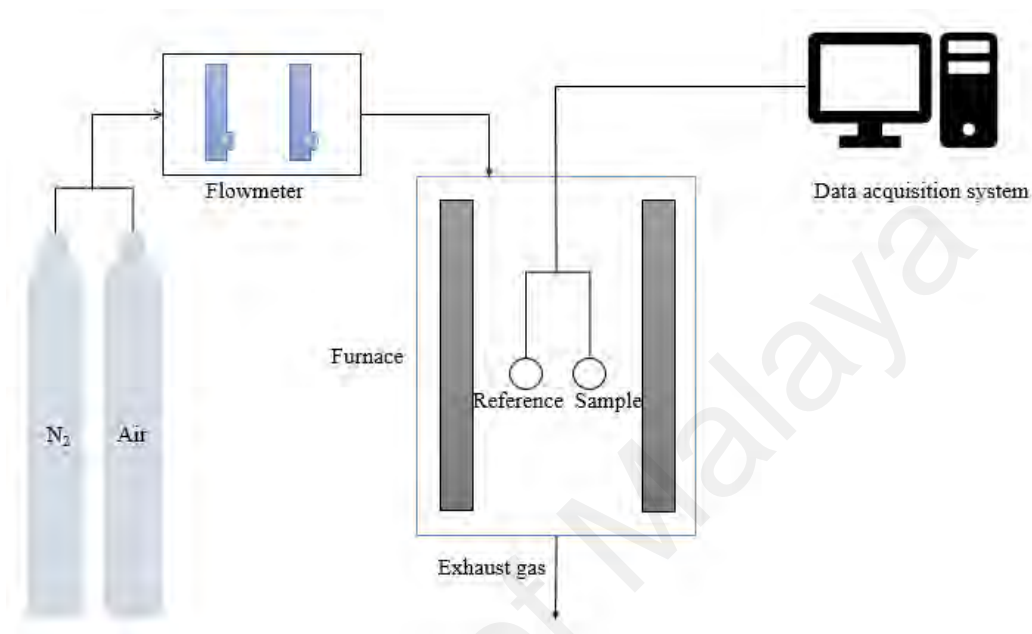


**Figure 2.3: Schematic of thermogravimetric analyser setup**

Thermal decomposition of biomass constituents like hemicelluloses, cellulose, and lignin is based on their chemical compositions and structures (Chen et al., 2015g). Hemicellulose consists of an amorphous structure with a lower degree of polymerization and belong to a group of heterogeneous polysaccharides obtained through various biosynthetic routes. Decomposition of hemicelluloses consist of two stages, including the cracking of side unit within 100 °C in the first stage and the second stage with the decomposition of the centre wall within a temperature range of 240−290 °C (Werner et al., 2014). Cellulose is a crystalline material consisting of large chain molecular-weight-polymer. More time is required to decompose cellulose in contrast to hemicelluloses, because of its better thermal stability. Cellulose takes around 320 to 360 °C temperatures for the thermal breakdown, yielding anhydrous cellulose and levoglucosan as primary products (Giudicianni et al., 2014). Lignin comprises of a complex aromatic polymer

structure, which includes sinapyl alcohol, coniferyl alcohol, and p-coumaryl alcohol linked by double bonds or carbon-carbon linkages (Mamaeva et al., 2016b). The temperature more than 500 °C results in its conversion, producing abundant oxygenated compounds such as phenols.

### 2.4.1.1 Torrefaction characteristics and performance

Torrefaction characteristics of biomass using a TG has been investigated by a number of researchers, as shown in **Table 2.5**. The study of biomass torrefaction using a TG can be separated into two sections such as the analysis of the torrefaction process and torrefaction performance of biomass. The first work using a TG to analyse biomass torrefaction characteristics can refer to the study of Chen and Kuo (2010), in which four different biomass materials were torrefied at two different temperatures of 240 (light) and 275 °C (severe). It was found that biomass thermal degradation at 240 °C was due to the decomposition of hemicelluloses, and cellulose was further decomposed at 275 °C. **Figure 2.4** shows the TGA and DTG torrefaction of four different biomass at severe torrefaction. The weight loss of the biomass during the torrefaction also depends on the reactivity of biomass. In the process of torrefaction, willow and bamboo can be categorized into relatively active species arising from a more apparent weight loss. Alternatively, wood and coconut shells can be classified as relatively inactive products due to less weight loss during torrefaction. In addition, the results also highlighted that biomass torrefaction with 1 h duration was an appropriate operation for producing biochar with higher energy density. Chen and Kuo (2011a) evaluated the effect of isothermal torrefaction of all single components of lignocellulosic biomass (hemicelluloses, cellulose, lignin and xylan) using TGA. For hemicelluloses, the torrefaction temperatures of 200 and 225 °C have no significant effect on thermal degradation, whereas a weight

loss of 19.5 and 52.6 wt% was observed for 250 and 275 °C. The weight loss of hemicelluloses was only 16.8 wt% for torrefaction temperature of 300 °C due to the large degradation of hemicelluloses before 300 °C. Besides, the thermal degradation of cellulose only significant at the torrefaction temperature of 275 °C. The decrease in the weight is linearly proportional to the torrefaction duration, implying that the torrefaction duration plays an important role in the thermal degradation of cellulose at 275 °C. For lignin, thermal degradation at torrefaction temperature of 300 °C was not notable, with only 7.4 wt% of lignin degraded. Torrefaction at 250 °C has the maximum impact of thermal degradation of xylan compared to 275 and 300 °C. The torrefaction duration is sensitive to the 200, 225, and 250 °C, whereas the effect of duration on weight loss was not notified at 275 and 300 °C. Eseltine et al. (2013) used a TG to study the thermal degradation of the biomass during the torrefaction process. An increase in the torrefaction temperature resulted in an intensified weight loss during the torrefaction process. The non-inert gas $CO_2$ showed a higher decrease in mass loss compared to inert gas with increasing the torrefaction temperature. The degradation of hemicelluloses was evidently observed with the torrefaction temperature of 200 °C, while the degradation of cellulose only occurred when the temperature was higher than 240 °C.
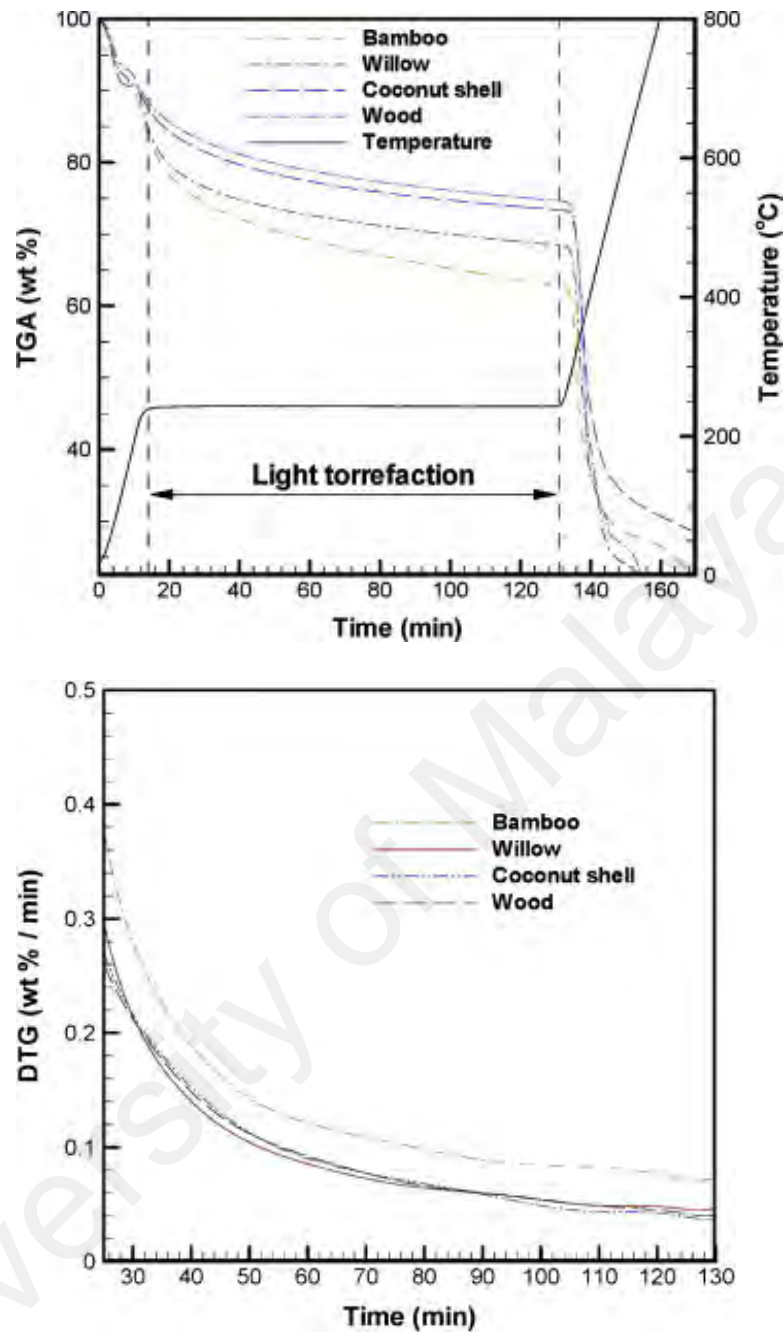
**Figure 2.4: TGA and DTG torrefaction of four different biomass at severe**

**torrefaction**

**(Reprinted from Chen and Kuo (2010), with permission from Elsevier)**

**Table 2.5: Summary of torrefaction process and torrefied biomass characterisation using TG**

| Biomass | Torrefaction temperature (°C) | Holding time | Main finding | References |
|---|---|---|---|---|
| *Torrefaction process* | | | | |
| Sugarcane bagasse | 230, 290 | 3 hours | • Maximum mass loss was 2.6 times faster with a temperature of 290 °C (0.005 to 0.013 $s^{-1}$). | (Granados et al., 2017) |
| Woody biomass | 200–300 | 60 min | • Weight loss increased with increasing temperature.<br>• $CO_2$ gas increased in weight loss. | (Eseltine et al., 2013) |
| Rubber wood with $K_2CO_3$ impregnated | 150, 200, 250, 300 | 120 min | • No thermal decomposition occurred at 150 °C.<br>- Solid yield decreased with increasing in $K^+$ concentration at 250 °C.<br>- Increase with increasing in $K^+$ concentration to 0.012M and 0.022M at 300 °C.<br>• 28% of torrefaction time could be reduced with potassium impregnated. | (Safar et al., 2019) |
| Woody biomass in Costa Rica | 225, 250, 275, 300 | 20, 30, 40 min | • Maximum devolatilization rate was 4.16, 1.80 and 0.70%/min for light, middle, and severe torrefaction.<br>• Weight loss during torrefaction Light: 3−6%; middle: 9−14%; severe: 11−16%. | (Moya et al., 2018) |
| Douglas fir sawdust | 250, 275, 300 | 1 hour | • The decomposition of biomass is doubled at 300 °C compared to 275 °C.<br>• Large decomposition on hemicelluloses and cellulose. | (Ren et al., 2013) |
| Food waste | 225, 275 | 40 min | • Less weight loss up to 40 min at 225 °C.<br>• More volatile release and low mass yield at 300 °C. | (Pahla et al., 2017) |

**Table 2.5, continued**

| Biomass | Torrefaction temperature (°C) | Holding time | Main finding | References |
|---------|-------------------------------|--------------|--------------|------------|
| *Chlamydomonas sp.* JSC4 *Chlorella sorokiniana* CY1 | 200, 225, 250, 275, 300 | 60 min | • High weight loss in the initial torrefaction stage.<br>• Amplitude of DTG curves rose with increasing torrefaction temperature.<br>• Torrefaction duration was important for mild torrefaction (250 °C). | (Chen et al., 2014e) |
| *Scenedesmus obliquus* CNW-N | 200-300 | 60 min | • High torrefaction temperature led to higher weight loss.<br>• Non-isothermal torrefaction has higher thermal degradation than isothermal torrefaction. | (Chen et al., 2014g) |
| ***Pyrolysis of Torrefied biomass*** | | | | |
| Bamboo Banyan Willow | 230, 260, 290 | 1 hour | • Bamboo was more sensitive to torrefaction.<br>• Lignin was pointed out in 290 °C. | (Chen et al., 2011b) |
| Rice straw Pine straw | 250 | 15 min | • Gas-pressurized torrefaction promoted decomposition of cellulose.<br>• Higher char yield obtained by gas-pressurized torrefaction compared to atmospheric pressure. | (Tong et al., 2018) |
| Rice husk | 210, 240, 270 | 1 hour | • Decrease in the value of mass loss.<br>• Decrease in $DTG_{mas}$ value.<br>• Leaching and torrefaction influence on $T_{max}$ and $T_i$. | (Zhang et al., 2018c) |

**Table 2.5, continued**

| Biomass | Torrefaction temperature (°C) | Holding time | Main finding | References |
|---|---|---|---|---|
| Poplar Fir | 200–230 | 1000 min | • Hemicellulose degraded. <br> • Amorphous cellulose decomposed. <br> • Increase in crystallinity of cellulose. <br> • Degree of polymerization in cellulose and lignin decreased. | (Chen et al., 2018d) |
| Washed rice husk | 250, 280 | 20 min | • Increase the initial decomposition temperature. <br> • High degradation on hemicellulose content. <br> • Lignin content increased. | (Zhang et al., 2016b) |
| *Camellia* shell | 260 | 30 min | • Structure changes and part of organic compound decompose at low temperature. <br> • In dry torrefaction, maximum weight loss peak shifted from 286 to 346 °C. <br> • Hemicelluloses were decomposed in wet torrefaction. | (Xu et al., 2018b) |
| Bamboo | 230, 250 | 60 min | • $O_2$ gas was more effective to remove hemicelluloses. <br> • Increase in initial decomposition temperature and maximum mass loss rate. <br> • Less $CO_2$ gas released at initial decomposition temperature. | (Su et al., 2018) |

Microalgae consist of different chemical components compared to lignocellulosic biomass. TG is evidently shown the changes in chemical composition of raw and torrefied microalgal biomass such as carbohydrates, proteins, and lipids. The carbohydrates are firstly destroyed in torrefaction of microalgae, followed by disruption of proteins and partially consumed the lipids with increasing of torrefaction severity (Chen et al., 2016). The combustion behaviour of wet torrefied microalgal biomass has been studied by Bach et al. (2017b) using a TG. During the wet torrefaction, the degradation of small organic molecules caused the torrefied microalgal biomass more reactive than raw microalgae at lower temperatures (<275 °C). For higher temperatures (>275 °C), the torrefied microalgae were thermally stable than raw microalgae due to the low thermally stable components eliminated during the wet torrefaction, while retaining the high thermal stable components.

TG has been used to analyse the thermal decomposition behaviour and torrefaction performance of torrefied biomass. Tong et al. (2018) proved gas pressurize torrefaction significantly decomposed the cellulose at 250 °C, while the cellulose remained when using carrier gas with atmospheric pressure torrefaction. The gas pressurized torrefaction converted the part of the volatile matter to fixed carbon by promoting the aromatization reactions. Chen et al. (2018d) found that the torrefaction treatment of woody biomass at temperatures of 200−240 °C significantly degraded hemicelluloses. The amorphous cellulose was decomposed which tended to increase the crystallinity of cellulose. Su et al. (2018) used a TG to evaluate the torrefied bamboo biomass pre-treated by different flue gases. The hemicelluloses of torrefied bamboo decomposed severely with the use of an oxygenated atmosphere.

Furthermore, the combustion behaviour of the torrefied biomass was studied by using the air atmosphere in TG. The DTG curve in the combustion was classified into four main stages including dehydration, volatile release, volatile combustion, and combustion of residue char (Xin et al., 2019a). Barzegar et al. (2019) evaluated the combustion behaviour of torrefied wood

biomass under different torrefaction conditions. The mass loss due to the dehydration was not detected in the TGA curve, indicating the hydrophobic nature of torrefied wood biomass. Furthermore, the TGA curve revealed that the ignition temperature of biomass delayed by about 5 $^{\circ}$C after the torrefaction at temperatures of 250 and 300 °C whereas the ignition temperature of the biomass was further delayed after the torrefaction at 350 $^{\circ}$C. This is because most of the hemicelluloses and cellulose were degraded during the torrefaction pre-treatment at a temperature of 350 °C, remaining the decomposition of lignin in the combustion. Tu et al. (2018) investigated the combustion properties of dry and wet torrefaction of the camellia shell. The dry torrefaction showed low activation energy (43.26 kJ/mol) and ignition temperature (290 °C) compared to wet torrefaction. Zhang et al. (2017a) evaluated the combustion behavior of wet torrefied duckweed biomass using a TG. The ignition temperature of the wet torrefied biomass increased with increasing torrefaction temperature from 130 to 250 °C, whereas the burnout temperature decreased. This implied that wet torrefaction significantly decreased the whole combustion process duration. The combustion behavior of wet torrefied microalgal biomass has been studied by Bach et al. (2017b). During the wet torrefaction, the degradation of small organic molecules caused the torrefied microalgal biomass more reactive than raw microalgae at lower temperatures (<275 °C). For higher temperatures (>275 °C), the torrefied microalgae were thermally stabled than raw microalgae due to the low thermally stable components eliminated during the wet torrefaction, while retaining the high thermal stable components.

### 2.4.1.2 Pyrolysis characteristics

TG was applied to understand the pyrolysis characteristics of single components in biomass such as degradation of hemicelluloses, cellulose, and lignin in lignocellulosic biomass (Burhenne et al., 2013), as well as carbohydrates, proteins, and lipids in non-lignocellulosic biomass (Chen et al., 2018c). The study on the pyrolysis characteristics of biomass components

is important in order to understand the thermal cracking mechanisms during the biomass decomposition (Zheng et al., 2019). Thermal decomposition of biomass constituents including hemicelluloses, cellulose, and lignin is based on their chemical compositions and structure (Chen et al., 2015g). Hemicelluloses consist of an amorphous structure with a lower degree of polymerization. Hemicelluloses belong to a group of heterogeneous polysaccharides obtained through various biosynthetic routes (Werner et al., 2014). Decomposition of hemicelluloses divided into two stages, including the cracking of side unit within 100 °C in the first stage and the decomposition of the center wall with a peak and a shoulder within a temperature range of 240−290 °C in the second stage. Cellulose is a crystalline material consisting of large chain molecular-weight-polymer. More time is required to decompose cellulose in contrast to hemicelluloses, because of its better thermal stability. Cellulose degrades around 320 to 360 °C temperatures for the maximum thermal breakdown, yielding anhydrous cellulose and levoglucosan as primary products (Giudicianni et al., 2014). Lignin comprises a complex aromatic polymer structure, which includes sinapyl alcohol, coniferyl alcohol, and p-coumaryl alcohol linked by double bonds or carbon-carbon linkages (Mamaeva et al., 2016a). A wide range of temperatures resulted in its conversion, producing abundant oxygenated compounds such as phenols. Lignin produces more solid residues (43%) in comparison to hemicelluloses (32%) and cellulose (5%) (Zabeti et al., 2016). The thermal degradation of microalgae was different from the lignocellulosic biomass and coal pyrolysis (Lu et al., 2013; Rizzo et al., 2013). The degradation of carbohydrates, proteins, and lipids are the main reaction during the pyrolysis of microalgae. Bach and Chen (2017b) reveal that the thermal decomposition of carbohydrates and proteins occur at a temperature range of 200–430 °C, these two components will merge to form a DTG peak. A higher temperature is needed for the degradation of lipid (430–530 °C). **Table 2.6** shows the list of the latest studies on the pyrolysis characteristic of biomass during the thermochemical conversion using a TG.

**Table 2.6: Summary of pyrolysis characteristic of biomass during thermochemical conversion using TG**

| Biomass | Final temperature (°C) | Heating rate (°C/min) | Main finding | References |
|---|---|---|---|---|
| *Jatropha* de-oiled cake | 700 | 5 | • Maximum weight loss at 250–500°C.<br>• Large particle size observed early weight reduction. | (Sharma & Sheth, 2018) |
| Rapeseed straw<br>Rapeseed meal<br>Camellia seed shell<br>Camellia seed meal | 800 | 10, 20, 30, 40 | • Increase in heating rate shifted the thermal evolution profiles to a higher temperature. | (Chen et al., 2015c) |
| Hazelnut husk | 1000 | 5, 10, 20 | • Increase in heating rate delayed the peaks in DTG and slightly affected the amount of volatile matter form. | (Ceylan & Topçu, 2014) |
| Rice straw<br>Poplar wood<br>Waste tire (co-pyrolysis) | 750 | 20 | • Thermal degradation of biomass started from 200 °C.<br>• Decomposition of waste tire occurred at 380 °C.<br>• High percentage of waste tire during co-pyrolysis resulted in a high yield of biochar. | (Wang et al., 2018b) |
| Sawdust<br>Rice husk<br>Bamboo dust<br>(co-pyrolysis) | 900 | 10, 15, 20, 30 | • Solid residue decreased during co-pyrolysis<br>• Blend of sawdust and bamboo dust have low thermal stability due to high cellulose content. | (Mallick et al., 2018) |
| Rubber wood (Potassium catalyst with 0.004, 0.008, 0.012 and 0.022M) | 800 | 20 | • Peak in DTG curves shifted towards lower temperature with the increase of potassium concentration.<br>• Solid yield increased from 13.4 to 38.1 wt% with the increase in potassium concentration. | (Safar et al., 2019) |

**Table 2.6, continued**

| Biomass | Final temperature (°C) | Heating rate (°C/min) | Main finding | References |
|---|---|---|---|---|
| Yunnan pine (ZSM-5 catalyst) | 600 | 5, 10, 20, 40, 60 | • Decrease the initial decomposition temperature.<br>• Decrease the thermal decomposition temperature and heating rate.<br>• Activate the polymer chain and reduced the activation energy. | (Zheng et al., 2019) |
| *Chlamydomonas reinhardtii* | 900 | 100 | • 5−7% of the total volatiles released at 170−250 °C.<br>• 78% of volatile released and decomposition of hydrocarbon chains of fatty acid components at 300 °C and 410 °C. | (Kebelmann et al., 2013) |
| *Nannochloropsis sp.* | 900 | 10 | • Main decomposition for microalgae and its main components at temperature zone of 200–450 °C. | (Wang et al., 2017b) |
| Microalgae biomass | 800 | 10 | • The main thermal degradation occurred from 150 to 500 °C. | (Chen et al., 2018c) |
| Indonesian oil sands | 650 | 10 | • 550 °C is the final pyrolysis temperature with 25% of weight loss. | (Zhang et al., 2018d) |

Pyrolysis characteristics of biomass with different pyrolysis conditions such as pyrolysis temperature, heating rate, particle size, co-pyrolysis effect, and the presence of catalysis have been analysed using a TG (Sharma & Sheth, 2018; Wang et al., 2018b). The decomposition pattern of the main components in biomass with different heating rates remained unchanged, but the thermal evolution profiles of TG and DTG curves shifted towards higher temperatures with the increase of the heating rate (Quan et al., 2016). The temperature shift was also observed during the pyrolysis of bamboo (Chen et al., 2014a), oil-plant wastes (Chen et al., 2015c), hazelnut husk (Ceylan & Topçu, 2014), and oil palm biomass (Idris et al., 2010). Safar et al. (2019) evaluated the catalytic effect of potassium on biomass pyrolysis. A shoulder and a peak due to the degradation of hemicelluloses and cellulose were observed at temperatures of 319 °C and 366 °C, respectively. The peak shifted toward the lower temperatures with the increase of the potassium concentration, whereas the shoulder tended to disappear with the impregnation of potassium with 0.022 M. The solid remained after the pyrolysis with the increase of impregnated potassium from 13.4 to 38.1 wt%. Furthermore, Chen et al. (2012a) evaluated the effect of co-pyrolysis of *Chlorella vulgaris* microalgae and coal. The main pyrolysis temperature range of microalgae and coal blend (172–600 °C) was closed to the microalgae individually (168–555 °C), where thermal degradation of coal was at a temperature range of 320–1000 °C. Zheng et al. (2018) analysed the co-pyrolysis of Yunnan pine biomass and low-density polyethylene with the addition of a catalyst. After the addition of low-density polyethylene and ZSM-5 catalyst to biomass, a decrease in thermal decomposition temperature was observed, whereas the solid residual after the pyrolysis clearly affected due to the synergistic effect. The addition of ZSM-5 catalyst enhanced the reaction activity of co-pyrolysis while reducing the activation energy with unchanged reaction mechanism.

### 2.4.2    Evolved gas analysis

During the thermochemical conversion of biomass, vapours are originated and contain some oxygenated compounds. An insight into the mechanisms of vapor formation and reactions involved provide information about the degradation of hemicelluloses, cellulose, and lignin for lignocellulosic biomass and the degradation of carbohydrate, protein, and lipid for non-lignocellulosic biomass (Gu et al., 2013; Peng et al., 2015). The composition of the evolved gas in each weight loss step cannot be observed only by TG analysis. The information of mixed gases and functional groups can be evaluated by FTIR (Christensen et al., 2017), and the mixture composition such as $CO_2$, CO, $H_2$ and $CH_4$ can be identified. Thus, the coupling of TG with FTIR becomes a functional tool in the dynamic analysis as it continuously monitors both the time-dependent evolution of gases and the weight of the non-volatile materials (residue) (Shen & Gu, 2009; Shen et al., 2010).

**Table 2.7** includes a summary of studies using infrared spectroscopy for organic matter, biomass, biofuel analysis, and monitoring. In TG-FTIR, the transfer line between the TG and FTIR is maintained above 200 ℃ to ensure all the decomposition remained in gaseous form. The schematic of the TG-FTIR system is presented in **Figure 2.5**. Information about the evolution characteristics with time or temperature can be obtained by TG-FTIR. This analytical technique can be applied to the monitoring of biomass devolatilization by identifying the mass loss process, major volatile species, and their corresponding release temperature range. TG-FTIR provides useful information on the understanding of trace element release, reaction mechanisms, and kinetics of biomass combustion and gasification (Huang et al., 2018). Hence, TG-FTIR for thermal behaviour and evolved gas phase analysis have been getting more research attention on the broad field of fuel conversion processes during the last decade (Robinson et al., 2016; Seo et al., 2010).

**Table 2.7: Summary of the key studies using TG-FTIR for organic matter, biomass, biofuel analysis, and monitoring**

| Material | Technology | Compounds predicted | References |
|---|---|---|---|
| Marine sediment | TG-FTIR | $H_2O$; $CO_2$ and hydrocarbons | (Oudghiri et al., 2016) |
| Low-rank coal | TG-FTIR | $CH_4$; CO production | (Liu et al., 2016) |
| Coal NM, NX, HLJ, SD | FTIR | $CO_2$; $CH_4$ emission | (Song et al., 2017) |
| Wheat straw pellets | TG-FTIR and TG-GC/MS | Alcohol and glycerol | (Striūgas et al., 2017) |
| Paper mill sludge and combustible solid waste | TG-FTIR and Py-GC/MS | O−H, C−H, C=O, C−O, $SO_2$, NO, HCl, CO, $CH_4$ and CO | (Fang et al., 2017) |
| Rice straw and high-density polyethylene | TG-FTIR-MS | $H_2$, $H_2O$, $CO_2$, CO, aldehydes ($C_2H_4O$), alcohols ($C_2H_5OH$), carboxyls ($CH_3COOH$) and hydrocarbons ($CH_4$, $C_2H_2$, $C_2H_4$, $C_2H_6$, $C_3H_6$, $C_3H_8$) | (Kai et al., 2017) |
| Oil shale, Coal (lignite and bitumite) | TG-FTIR | Increase in the ratio of aromatic C−H/aliphatic C−H | (Li et al., 2016) |
| Waste tea | TG-FTIR | $CO_2$, $H_2O$, $CH_3COOH$, $C_6H_5OH$, C=C | (Tian et al., 2016) |
| Sphagnum peat | TG-FTIR | Tar, char, $CO_2$, CO, $CH_4$, $C_2H_6$, HCOOH, $CH_3CH_2COOH$, $C_4H_8$ and $CH_2CHCHO$ and some aromatic hydrocarbons | (Yang et al., 2016) |
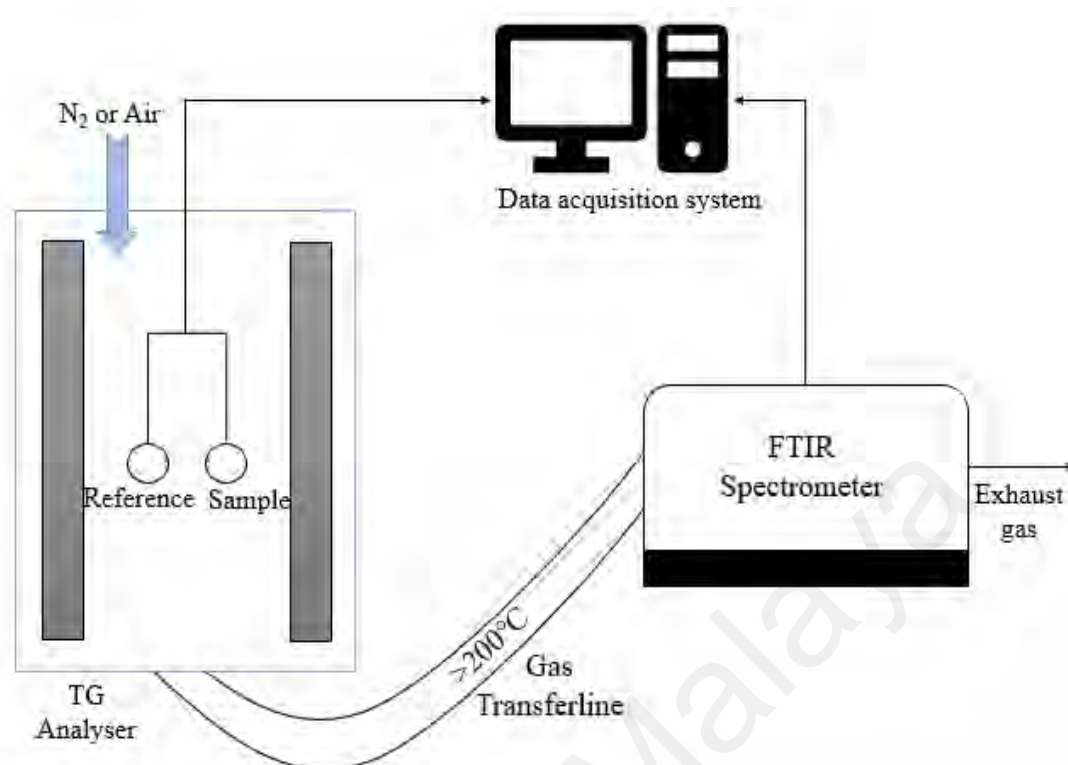
**Figure 2.5: A schematic of the TG-FTIR system**

The analysed results obtained by TG-FTIR provide knowledge about the classification of volatile compounds, including three stages. The first stage includes details about the gases evolved like CO and $CO_2$. Next, the second stage predicts the organic compounds responsible for thermal degradation like ketones and aldehydes. The third stage deals with the high temperature, where carbonization and char formation occur (Gu et al., 2013). The respective research attributes towards the development of industrial-scale production of biofuel. However, more knowledge is needed in understanding the nature of reaction mechanisms (Liu et al., 2011; Sadhukhan et al., 2008).

Torrefaction of biomass is an important pre-treatment technique to improve the physiochemical properties and the pyrolysis products of biomass (Chen et al., 2015b; Chen et al., 2011b). TG-FTIR has been applied to analyse the thermal behaviour and evolved gas on the torrefaction process and torrefied biomass (Chen et al., 2014b; Lv et al., 2015). The highest release of volatiles during torrefaction can be observed using DTG

curves, at the same time, the functional groups of the volatiles can be simultaneously determined using FTIR (Pahla et al., 2017). **Table 2.8** presents the literature using TG-FTIR for the evolved gas analysis on the torrefaction process and torrefied biomass. Lv et al. (2015) investigated the lignocellulosic components (cellulose, xylan, and lignin) torrefaction behaviour and evolved gas in isothermal conditions for 5 hours. Cellulose was thermally stable at short duration, but the degradation occurred dramatically afterward, especially at 280 ℃. The decomposition of xylan showed an increase in CO release with increasing temperature. For lignin, the decomposition reactions were more significant at low temperatures (220 and 250 ℃) with the emission of phenol.

**Table 2.8: A list of literature of TG-FTIR application on torrefaction performance and pyrolysis of torrefied biomass**

| Feedstock | Temperature (°C) | Time (min) | Outcome | References |
|---|---|---|---|---|
| *Torrefaction* | | | | |
| Rice husk | 200, 230, 260, 290 | 30 | • $CO_2$ and $H_2O$ showed high absorption peak.<br>• Organic carbohydrate (C=O) was detected.<br>• Volatile components (phenols, carbonyl compound, aromatic hydrocarbons, and low hydrocarbons) were enhanced by increasing the torrefaction temperature. | (Chen et al., 2014d) |
| Sewage sludge | 230−480 | 15 | • High torrefaction temperature produced higher gas yield. | (Hernández et al., 2017) |
| Sawdust | 230, 250, 270, 290 | 30 | • Only the characteristic of water appeared at the initial stage.<br>• Depolymerization occurred at 165 °C.<br>• Production of alkanes, aromatics, carbonyl and phenol from 248–290 °C.<br>• $CO_2$ was the main gaseous product at the end of torrefaction. | (Chen et al., 2011a) |
| Food waste | 225, 275, 300 | 40 | • The characteristic of water and $CO_2$ peak became more intense at high torrefaction temperatures.<br>• Release of carbonyl and aromatic compounds at 275 and 300 °C.<br>• Structural changes in biomass with the releases of phenol and aliphatic compounds. | (Pahla et al., 2017) |

**Table 2.8, continued**

| Feedstock | Temperature (°C) | Time (min) | Outcome | References |
|---|---|---|---|---|
| *Pyrolysis of Torrefied biomass* | | | | |
| Rice husk | 200, 230, 260, 290 | 30 | • $H_2O$, $CH_4$, CO, and $CO_2$ were detected first, then furans, ketones, phenols, and aldehydes evolved.<br>• Low spectral intensity and many absorption peaks disappeared at 290 °C. | (Chen et al., 2014b) |
| Herbaceous residues | 210, 240, 280 | 60 | • Formation of $CO_2$ shifted to a higher temperature.<br>• Absorbance of $CO_2$ peak decreased with increasing of torrefaction temperature.<br>• Formation of $CH_4$ through demethylation of hemicelluloses at low temperature.<br>• Amount of CO decreased with the increase of torrefaction temperature | (Xin et al., 2018) |
| Cotton stalks | 250 | 30 | • Shoulder peak disappeared in the torrefied biomass.<br>• Absorption intensity enhanced by water washing but decreases after torrefaction | (Cen et al., 2016) |
| Cotton stalks | 260 | 30 | • Strongest peaks were found at 35–38 min.<br>• Shoulder peak disappeared in the torrefied biomass. | (Chen et al., 2017a) |
| Mesquite Juniper wood | 240 | 60 | • High amounts of $CO_2$ and CO<br>• No significant changes of CO and $CH_4$ curve when using $N_2$ and $CO_2$ as torrefaction medium | (Eseltine et al., 2013) |

During the torrefaction process, depolymerization, devolatilization, and carbonization of the biomass chemical composition occur to produce a uniform black solid product, liquid (water, organics, and lipids), and non-condensable gas (CO, $CO_2$, and $CH_4$) (Shankar Tumuluru et al., 2011). The gaseous product during the torrefaction process can be observed by using TG-FTIR. Chen et al. (2014d) used TG-FTIR to evaluate the performance of torrefaction and evolved gas during the torrefaction of rice husk. The volatile release at the maximum mass loss with different torrefaction temperatures was observed using FTIR. The adsorption peaks of $CH_4$ and other gases such as phenols, a carbonyl compound, aromatic hydrocarbon, and low hydrocarbon were not detected during low torrefaction temperatures, whereas the adsorption peaks increased with the increase in torrefaction temperature. During the initial torrefaction stage or depolymerization stage, $CO_2$ peak was observed while the aromatic hydrocarbon and carbonyl compound characteristic peaks were restively weak, which indicated biomass under depolymerization and released limited amounts of CO, $CO_2$, and $H_2O$. The characteristic peaks for $CO_2$ and $H_2O$ were observed during the devolatilization stage. The absorption peaks indicated that phenol, carbonyl compounds, and aromatic hydrocarbons were relatively strong. Carbonization is the last stage of torrefaction, where the absorption peak was moderately decreased, revealing the end of the torrefaction process.

Torrefaction not only produces high-quality biochar but also is a promising biomass pre-treatment for pyrolysis (Chen et al., 2018e; Zhang et al., 2018c). TG-FTIR is widely applied on the pyrolysis, which can analyse the thermal degradation and real-time evolved gas functional group. This technique gives the advantages of less sample required and high accuracy to analyse on the torrefaction pre-treatment performance for pyrolysis (Chen et al., 2014b). Xin et al. (2018) revealed that torrefaction significantly affected the gaseous product released during the pyrolysis of herbaceous residues. A high decrease in

the $CO_2$ peak in pyrolysis was observed for torrefied biomass at 280 °C, stemming from the production of $CO_2$ mainly due to the decomposition of hemicelluloses and cellulose. High degradation of hemicelluloses and cellulose occurred at high torrefaction temperatures. In pyrolysis, the formation of $CH_4$ was mainly due to the demethylation of hemicelluloses at low temperatures (<400 °C). After the torrefaction at 280 °C, the maximum $CH_4$ release shifted to 430 °C, which was mainly ascribed by the decomposition of lignin. In addition, torrefaction decreased the oxygen content which would decrease the formation of CO during the pyrolysis.

In addition, TG-FTIR has been applied to analyse the torrefaction process and combustion behaviour of torrefied biomass using different torrefaction atmospheres ($N_2$ and $CO_2$) by Hernández et al. (2017). Combustion behaviour of torrefied biomass highly depended on the torrefaction temperature. The increase in torrefaction temperature increased the gas production. When $N_2$-torrefaction with a temperature higher than 330 °C was applied, the $SO_2$ produced during the combustion was reduced by more than 89%. By comparing the combustion produced gases ($CO_2$, $SO_2$, and $NH_3$) using different torrefaction atmospheres, more gas would be produced during the combustion for biomass torrefied by $CO_2$ compared to $N_2$ atmosphere. $CO_2$ atmosphere torrefaction could influence the torrefaction mechanisms and properties of the torrefied biomass at low temperatures.

## 2.5     Py-GC/MS analysis

More detailed information is needed in order to in-depth understanding of pyrolysis mechanism and process. The present of micro-pyrolyser coupling with gas chromatography and mass spectrometer (Py-GC/MS) has been successfully applied to evaluate the rapid pyrolysis products of biomass (Chen et al., 2019c). Py-GC/MS is an

important analyser for biomass characterisation, it can effectively detect the pyrolytic product distribution by comparing the total chromatographic peak areas obtained during the pyrolysis process at different conditions (Gao et al., 2013). The vapours generated during the pyrolysis without prior to condensation are transferred into the GC/MS analyser for detailed characterisation. The MS detector can qualitatively determine the vapours after the separation by GC. In Py-GC/MS, the residence time in the pyrolyser is very short (15−30 s), as compared with the residence time in convention pyrolysis reactors, which can prevent the secondary reactions in short residence time (Chen et al., 2019a; Liu et al., 2019a). The primary reactions of biomass pyrolysis can be effectively analysed by the Py-GC/MS. A list of summaries of the biomass pyrolysis characterisation using PyGC/MS is presented in **Table 2.9**.

**Table 2.9: Summaries of biomass pyrolysis using Py-GC/MS**

| Feedstock | Temperature (°C) | Time (s) | Main finding | References |
|---|---|---|---|---|
| **Microalgae** *Diplosphaera* sp. MM1 | 600 | 30 | • Microalgae cultivated in winery wastewater showed high C4−C10 and C11−C21 contents. | (Liu et al., 2019a) |
| *Chlorella vulgaris* | 400−800 | − | • HZSM-5 catalyst removed the heteronuclear atoms and converted into aromatic hydrocarbons.<br>• 53% of nitrogen released as ammonia at 800 ºC. | (Wang & Brown, 2013) |
| *Micractinium conductrix* | 550 | − | • Biomass harvested at late exponential phase (LEP) showed the highest aliphatic hydrocarbons content and lowest nitrogenous compounds. | (Wang et al., 2018c) |

| Feedstock | Temperature (℃) | Time (s) | Main finding | References |
|---|---|---|---|---|
| *Desmodesmus sp.* | 600 | 10 | • Py-GC/MS analysis of hydrothermal treatment microalgae oil mixed with zeolite H-ZMS-5.<br>• High yield of hydrocarbons.<br>• High nitrogen removal using zeolite catalyst. | (Torri et al., 2013) |
| *C.reinhardtii* (wild type and $CW15^+$) | 500 | − | • Identical protein and lipid derived from both types of microalgae | (Kebelmann et al., 2013) |
| *Chlorella vulgaris* | 700 | 20 | • Co-pyrolysis of microalgae and kitchen waste with additives.<br>• CaO reduced the acids by 85.9% for microalgae, 70.2% for kitchen waste and 81.7% for mixture of microalgae and kitchen waste. | (Chen et al., 2018a) |
| ***Others biomass*** | | | | |
| Pine wood | 360, 450, 500 and 550 | 6 | • Effect of biomass pre-treatment followed catalytic fast pyrolysis.<br>• The influences of temperature and catalyst loading were important than biomass pre-treatment. | (Xin et al., 2019b) |
| Brewer's spent grains | 300, 400, 500 and 600 | 15 | • Pyrolysis of biochar produced from hydrothermal carbonization.<br>• More furans and other cyclic oxygen compounds found in the biochar. | (Olszewski et al., 2019) |

| Feedstock | Temperature (°C) | Time (s) | Main finding | References |
|---|---|---|---|---|
| Bamboo waste | 600 | 15 | • Co-pyrolysis lignocellulosic biomass and amino acids.<br>• Increase phenols and O-species in bio-oil.<br>• Decrease cracking temperature and N-species. | (Chen et al., 2019a) |
| Pine wood | 350−600 | 20 | • Biomass pyrolysis with noble metal-like catalyst.<br>• $W_2C/AC$, $W_2N/AC$, $Mo_2C/AC$ and $Mo_2N/AC$.<br>• Lignin degradation was promoted to form stable monomeric phenolics. | (Lu et al., 2018) |
| Rice straw, cedar wood, dalbergia wood | First stage 270, 320, 360<br><br>Second stage 550 | 30 | • Two stage pyrolysis efficiently separate biomass pyrolysis products.<br>• Organic acids, alcohols, and aldehydes produced in first stage<br>• Phenolic substances in second stage | (Cai et al., 2019) |
| Rubber wood sawdust | First stage 200, 250, 300<br><br>Second stage 450, 500, 550 | − | • Torrefaction pre-treatment followed by pyrolysis.<br>• The content of oxygenated compounds in the bio-oil decreased with increasing of torrefaction temperature. | (Chen et al., 2018e) |

A complexity of the pyrolysis products is produced during the pyrolysis, which can be distributed into its three major components, namely, cellulose, hemicelluloses and lignin for lignocellulosic biomass (Yu et al., 2017). With the help of Py-GC/MS technology, the pyrolytic product distributions of three main components in the biomass during the primary pyrolysis were investigated systematically (Patwardhan et al., 2011a; Patwardhan et al., 2011b; Patwardhan et al., 2010). In contrast to lignocellulosic biomass,

three different major components including carbohydrates, proteins and lipids were analysed using the Py-GC/MS technology (Biller & Ross, 2014). Valdés et al. (2013) investigated the chemical composition of microalgae including carbohydrates, proteins and lipids under different culture conditions. A high correlation between the biochemical compositions between the conventional analytical methods and the novel Py-GC/MS was obtained.

Recently, Py-GC/MS also shows a positive result on the effect of pre-treatment on the biomass pyrolysis. Xin et al. (2019b) revealed the effect of pine wood biomass pre-treatment including torrefaction, acid-leaching, and acid-leaching followed by torrefaction on catalytic pyrolysis products by Py-GC/MS. The acid-leaching pre-treatment slightly lowered the aromatic compounds, whereas torrefaction pre-treatment showed the opposite site during the catalytic pyrolysis. Overall, the effect of temperature and catalyst loading were more significant on the pine wood pyrolysis. Olszewski et al. (2019) analysed the volatile matter released of the brewer's spent grains biochar from hydrothermal carbonization pre-treatment. The pyrolysis of biochar generated lesser N-compounds compared to raw biomass due to the Maillard reaction during the hydrothermal pre-treatment. Furthermore, Xing et al. (2016) studied the pyrolysis effect of copper and potassium impregnated wood dust biomass. The results revealed that the decomposition of hemicelluloses was enhanced with the increase of copper dosage, whereas a low level of cellulose and lignin degradation detected. In contrast, the potassium promoted the degradation of cellulose and lignin with minimum effect on hemicelluloses.

In addition, two stage thermal degradation of the biomass has been critically analysed by several researchers using Py-GC/MS. Zheng et al. (2015) evaluated the effect of dry and wet torrefaction of corncobs biomass on the fast pyrolysis using Py-GC/MS

technology. The analysis revealed that the wet torrefaction significantly enhanced the levoglucosan yield due to the decrease in the alkali metals. Zhang et al. (2018b) examined the two-stage thermal degradation of walnut shells using Py-GC/MS. Some value-added chemicals including furfural, levoglucosan, and 2-methoxy-4-methylphenol were enriched in the two-stage thermal degradation. Meanwhile, Zhang et al. (2019c) evaluated the effects of two-step pyrolysis of corncob coupled with water and acid pre-treatment using Py-GC/MS. The two-step pyrolysis enhanced the selectivity of ketones and phenols in first step and hydrocarbons in second step pyrolysis.

## 2.6    Kinetic modelling of microalgae

Kinetic modelling of biomass pyrolysis processes can be employed to define the main operating and design parameters for a reactor, which requires the information about pyrolysis kinetic parameters such as pre-exponential factor and activation energy. TGA is a common technology to obtain the experimental kinetic data, whereas the data is calculated through kinetic free and kinetic fitting model to obtain an effective activation energy for biomass pyrolysis (Bach & Chen, 2017b; Gai et al., 2013). In general, the pyrolysis kinetics of biomass is expressed by the Arrhenius's equation, which can determine the two important parameters including activation energy and pre-exponential factor to build the pyrolysis models.

Pyrolysis kinetic models have been successfully applied for microalgae. Similar chemical reactions occurred during the microalgae pyrolysis compared to others biomass, with number of substances and intermediates generated during the reactions. By using the simplest kinetics approach, the activation energy and pre-exponential factor can be estimated from the TGA. These methods known as kinetic-free model or isoconversional model due to the limited kinetic information. Kinetic-free model including Friedman,

Kissinger-Akahira-Sunose (KAS) and Flynn-Wall-Ozawa (FWO) methods using the differential and integral isoconversional methods to calculate the activation energy and pre-exponential factor of biomass pyrolysis from TGA data without the insight of reaction mechanisms (Das et al., 2017; Sharara et al., 2014). Other than that, the pyrolysis kinetics of microalgae also widely investigated using the simplified Distributed Activation Energy Model (DAEM) (Soria-Verdugo et al., 2018). These methods cannot regenerate the predicted TGA and DTG curves or the fit quality of experimental and modelling data. In contrast, kinetic fitting models are divided into single and multiple reaction models (Bach & Chen, 2017a). The single reaction model is very simple, as the microalgae are directly transformed into char and volatiles, providing a low fit quality to describe microalgae pyrolysis. A modification of the multiple parallel reaction models based on the three main components of microalgae have been successfully used to describe the microalgae pyrolysis (Bui et al., 2016).

Recently, the number of pyrolysis kinetics of microalgae is much lesser than that the bio-oil and biochar production studies from pyrolysis process in a lab-scale reactor. A list of TGA pyrolysis kinetics on various microalgae together with the activation energy are presented in **Table 2.10**. TGA pyrolysis normally conducted with a heating rate of 5−40 ºC/min and flow rates of 50−200 mL/min. In the literatures, kinetic free models are the most common methods to analysis the pyrolysis kinetics of microalgae. The activation energy of the microalgae are changes from species to species. The activation energy of microalgae can be ranged from 58−334 kJ/mol based on the **Table 2.10**. In addition, some research has conducted the multiple reaction model to study every single components of the microalgae in a kinetic fitting model. The activation energy of the carbohydrates, proteins and lipids of the microalgae are clearly calculated using this model.

**Table 2.10: Summaries of TGA pyrolysis kinetics on various microalgae**

| Microalgae | Heating rate (°C/min) | Kinetic model | Activation Energy (kJ/mol) | References |
|---|---|---|---|---|
| *Dunaliella tertiolecta* | 5−40 | KAS<br>FWO | 145.713<br>146.421 | (Shuping et al., 2010) |
| *Chlorella spp.*<br><br>*Nannochloropsis* | 15 | Freeman-Carroll | 71.3−72.9 | (Rizzo et al., 2013) |
| *Chlorella vulgaris* | 5−40 | FWO and KAS | First: 51<br>Second: 64 | (Agrawal & Chakraborty, 2013) |
| *Chlorella vulagris*<br><br>*Isochrysis galbana*<br><br>*Nannochloropsis gaditana* | 10−40 | Kissinger, Friedmen, FWO, KAS, DAEM | 135.6−337.1<br>148.4−309.4<br>137.4−373.0 | (Soria-Verdugo et al., 2018) |
| *Chlorella pyrenoidosa*<br><br>Bloom-forming cyanobacteria | 5−60 | Single-step global model | 143.71<br>173.46 | (Hu et al., 2015) |
| *Chlorella pyrenoidosa*<br><br>*Spirulina platensis* | 10−80 | Iso-conversional Vyazovkin approach | 58.85−114.5<br>74.35−140.1 | (Gai et al., 2013) |
| *Haematococcus pluvialis* | 20 | Friedman, FWO and Starink | 204.72 | (Gong et al., 2020) |
| *Nannochloropsis oculate*<br><br>*Tetraselmis sp.* | 5−20 | DAEM | 152.20<br>334 | (Ceylan & Kazan, 2015) |
| *Chlorella vulgaris* | 10−40 | DAEM | 150−250 | (Soria-Verdugo et al., 2017) |
| *Chlorella vulgaris* ESP-31<br><br>*Nannochloropsis oceanica* CY2<br><br>*Chlamydomonas sp.* JSC4 | 10 | Multiple reaction | Carbohydrate: 53.28−53.30<br>Protein: 142.61−188.35<br>Lipid: 40.21−59.23 | (Chen et al., 2018c) |

| Microalgae | Heating rate (ºC/min) | Kinetic model | Activation Energy (kJ/mol) | References |
|---|---|---|---|---|
| *Chlorella vulgaris* ESP-31 | 10 | Multiple reaction | Carbohydrate: 39.82 | (Bach & Chen, 2017a) |
| | | | Protein: 208.86 | |
| | | | Lipid: 48.61 | |
| | | | Others: 197.73 | |
| *Chlamydomonas* *Chlorella sorokiniana* | 20 | Multiple reaction | Hemicellulose: 113.12−117.12 | (Bui et al., 2016) |
| | | | Cellulose: 181.67−228.79 | |
| | | | Lignin: 61.74−66.39 | |
| | | | Lipid: 104.93−143.63 | |
| | | | Protein: 90.75−118.13 | |

KAS: Kissinger-Akahira-Sunose; FWO: Flynn-Wall-Ozawa; DAEM: Distributed Activation Energy Model

Up to date, microalgae pyrolysis has not been conducted at industrial scale yet. However, the data obtained from the pyrolysis kinetics are beneficial for the process design and up-scaling. A conceptual process modelling study and optimization is needed in the industrial deployment using a commercial simulator (Aspen Plus). The pyrolysis modelling can be analysed using kinetic reaction models based on the thermodynamic equilibrium calculations, which offers predictive simulations for large scale of biomass (Peters et al., 2017). In addition, a similar fundamental of Arrhenius's equation such as power law kinetic expressions was widely applied in theses kinetic schemes and pyrolysis kinetic studies. In short, an overview on the pyrolysis mechanism and process in the plant level, as well as the energy and environmental impact can be obtained from these models.

## 2.7    Research gap

To-date, much research on biomass torrefaction has been carried out to enhance the biomass fuel properties (Bach & Skreiberg, 2016; Chen et al., 2015g). Most of the existing study on the microalgae dry torrefaction mainly focuses on the temperature and holding time, but the comparison between the microalgae chemical composition including carbohydrates, proteins and lipids is not presented, as well as microalgae species. In the previous study of our group, dry torrefaction of microalgae was conducted using TG (Chen et al., 2014e), whereas only the weight loss of microalgae could be detected during torrefaction process. The detailed characterisation of microalgal biochar including HHV, FTIR, energy yield and thermal degradation analysis is still lacking. In the meantime, only one study was conducted by our research group on the microalgae wet torrefaction using water as reaction medium (Bach et al., 2017b). Wet torrefaction significantly reduces the temperature input to convert microalgae into biochar compared to dry torrefaction. To date, no literature on the microalgae wet torrefaction in acidic solutions have not been reported. Wet torrefaction in acidic solutions have shown positive results on the sugarcane bagasse (Chen et al., 2011c; Chen et al., 2012d), bamboo (Li et al., 2015)and macroalgae (Teh et al., 2017). The current stage of wet torrefaction of other biomass in acidic solution largely focuses on acid concentration, but the comparison between the acidic solution is not presented, especially on the organic and inorganic acid, neither has the differences in characteristics been clearly elucidated. In addition, the study on torrefaction pre-treatment and followed by the pyrolysis is gaining attention recently, namely two-stage thermal degradation. The literature studies on the two-stage thermal degradation mainly focused on the lignocellulosic biomass, which is studied on the products derived from hemicelluloses, cellulose, and lignin (Chen et al., 2019c; Sun et al., 2019; Zhu et al., 2019). However, a literature study on the two-stage thermal degradation of microalgae has not been reported, especially on the degradation of three

main microalgae components such as carbohydrates, proteins, and lipids. Although many studies concerning the microalgae pyrolysis kinetics have been carried out, the study on the wet torrefaction pre-treatment followed by microalgae pyrolysis kinetics is still absent, especially on the microalgae pyrolysis kinetic study of every single component. In addition, the comparison of the kinetic studies of microalgae *Chlorella vulgaris* with different chemical compositions is not presented.

For this reason, two different microalgae species including high-carbohydrate *Chlorella vulgaris* ESP-31 and high-protein Chlorella vulgaris FSP-E were employed as the feedstocks for dry and wet torrefaction. Dry torrefaction was conducted in a tube furnace to act as important literature for wet torrefaction process. The biochar produced from the dry torrefaction was characterised including solid yield, energy yield, HHV, FTIR, thermal degradation behaviour, and torrefaction severity index. A continuation study on the microalgae wet torrefaction was carried out based on the research of our team (Bach et al., 2017b). In this study, wet torrefaction of microalgae was further improved by using acidic solutions to increase the thermal degradation of low energy content components in microalgae at low temperature. Next, the effects of dry and wet torrefaction on microalgae pyrolysis were evaluated using TG-FTIR and double-shot Py-GC/MS approaches. The reaction mechanisms and product formations from the torrefaction followed by pyrolysis were addressed in detail. Lastly, the kinetic study of raw and pre-treated microalgae by wet torrefaction were investigated. The experimental results obtained from the microalgae pyrolysis kinetics can provide a useful insight to the pre-treatment operation and reactor design in biomass-to-energy industry.

# METHODOLOGY

## 3.1    Introduction

The chapter aims in providing the detail description of methods and procedures in this study. The overview of research activities is divided into four parts as shown in **Figure 3.1**, which is presented the four main objectives. In this study, third-generation biofuel feedstock was upgraded using advanced torrefaction process. Microalgae *Chlorella vulgaris* ESP-31 and FSP-E were used as feedstocks for dry and wet torrefaction. First, torrefaction severity index was applied to analyse the dry torrefaction performance of microalgae. Next, the advanced microwave-assisted wet torrefaction with the aid of acid catalyst was applied to upgrade the microalgae into biochar, as well as sugar and its derivative as by-products. The fuel properties, FTIR, XRD and SEM of the biochar produced from wet torrefaction was analysed critically. Furthermore, the microalgal biochar showed the better torrefaction performance were further investigated. The in-depth analysis of biochar produced from torrefaction was performed using TG-FTIR and Py-GC/MS analytical techniques. The thermal behaviour and evolved gas of biochar during the pyrolysis was investigated. Lastly, pyrolysis kinetics of torrefied microalgae were evaluated using the pyrolysis data obtained from TGA, with the aid of independent parallel reaction models to calculate the activation energy and pre-exponential factor of microalgae every single component.

| Experiment | Experiment in modified reactor | In-depth Analysis | Modeling |
|---|---|---|---|
| **Dry Torrefaction** | **Wet Torrefaction** | **TG-FTIR and Py-GC/MS** | **Kinetics study** |
| • Microalgae cultivation and pre-treatment | • Microwave reactor with hydrothermal condition | • Effect of dry and wet torrefaction | • Microalgae degradation |
| • *Chlorella vulgaris* ESP-31 (high-carbohydrate) and FSP-E (high- protein) | • Acid solution (organic and inorganic) | • Pyrolysis and combustion behaviour of torrefied microalgae | • Pyrolysis characterisation |
| • *Jatropha* biomass | • Wet torrefaction (160 $^{\circ}$C, 6 bar) | • Real-time evolved gas analysis using FTIR | • Pyrolysis kinetics of torrefied microalgae |
| • Torrefaction (200−300 °C, 15−60 min) | • Fuel properties analysis | • Single- and double-shot analysis | • Independent parallel reaction using four reaction model |
| • Fuel properties analysis | • Elemental and proximate analysis | • Production distribution of carbohydrates, proteins and lipids | • Conversion rate and degree of carbohydrates, proteins and lipids |
| • Characterisation | • Chemical and physical structure analysis | | • Activation energy and pre-exponential factor |
| • Torrefaction severity index | • Hydrolysates composition | | |

**Figure 3.1: Overview of research methodology**

## 3.2 Materials

Two different microalgae, *Chlorella vulgaris* ESP-31 (high-carbohydrate) and *Chlorella vulgaris* FSP-E (high-protein) were used as feedstocks for the dry and wet torrefaction. Sulphuric acid ($H_2SO_4$, 95−97%), succinic acid ($C_4H_6O_4$, 95%), phosphorus acid ($H_3PO_4$, 85%), n-Hexane ($C_6H_{14}$, 99%), phenol ($C_6H_6O$, 99%), ethanol ($C_2H_5OH$, 95%), potassium hydroxide (KOH, >85%, ACS reagent), 14% (v/v) boron trifluoride-

methanol (BF$_3$/CH$_3$OH, Sigma-Aldrich), D-(+)-glucose (C$_6$H$_{12}$O$_6$, 99.5%, ACS reagent), furfural (C$_5$H$_4$O$_2$, 99%, ACS reagent), and 5-(Hydroxymethyl)furfural (5-HMF, 99%, ACS reagent) were employed in this study. All the chemicals were used as received without any purification. Nitrogen, compressed air and purified helium were used for torrefaction process and detailed characterisation of biomass.

### 3.2.1    Biomass preparation

Microalgae were selected in this study because it is the third-generation promising feedstock for biofuel production and other valuable goods, which obtained from a research team by Prof Ju-Shu Chang, National Cheng Kung University, Taiwan. *Chlorella vulgaris* ESP-31 (high-carbohydrate) and *Chlorella vulgaris* FSP-E (high-protein) were cultivated and obtained from an open pond in southern of Taiwan (Wu et al., 2018). The microalga ESP-31 strain was precultured in a basal medium containing a KNO$_3$ concentration of 0.313 g L$^{-1}$, which is 25% of the original nitrogen source (KNO$_3$) (Tran et al., 2013). It was precultured at 25 °C for 4–5 days with CO$_2$ aeration (2% and 0.2 vvm) and illuminated at a light intensity of 60 μmol m$^{-2}$ s$^{-1}$. Next, the microalga was grown outdoors in a 450 L open pond (200 cm diameter × 15 cm depth) with CO$_2$ aeration at 2% and 0.05 vvm (volume gas per volume of the medium per min) for nearly 10 days to obtain the lipid content of 20–30% with a biomass concentration of 0.54 g L$^{-1}$. Microalga FSP-E was cultivated in a modified version of basal medium [19, 20], which consists of: KH$_2$PO$_4$, 1.25 g/L; MgSO$_4$·7H$_2$O , 1.0 g/L; CaCl$_2$·2H$_2$O, 0.1106 g/L; FeSO4·7H$_2$O, 0.0498 g/L; EDTA·2Na, 0.5 g/L; H$_3$BO$_3$, 0.1142 g/L; ZnSO$_4$·7H$_2$O, 0.0882 g/L; and Urea, 0.56 g/L (Chen et al., 2015a). It was precultured at room temperature, pH 6.8, and 300 rpm agitation with 2% CO$_2$ continuously aerated the culture medium at a rate of 0.2 vvm.

The microalgae were obtained by separating the liquid using large volume centrifuge (Himac CR21G, Hitachi). Next, the microalgae were then dehydrated in a drying oven at 85 °C for 48 h to provide a standard basis for the experiment. After that, the biomass was ground and passing through a 45-mesh sieve for torrefaction processes. The microalgal biomass were collected in sealed plastic bags and stored in a desiccator at room temperature until the experiments and analysis were carried out.

### 3.2.2    Chemical composition of microalgae

The chemical composition of microalgae including carbohydrates, proteins and lipids was determined on a dry basis according to the standard methods as reported in the literature. Phenol-sulfuric acid method was employed to determine the carbohydrate content of microalgae as described by Masuko et al. (2005). In general, 50 μL of microalgae was mixed with 150 μL of concentrated $H_2SO_4$ followed by 30 μL of phenol (5% w/v). The solution was heated in an incubator at 90 °C for 5 min and cooled to room temperature. After that, absorbance was measured at 490 nm by using a 96-well microplate, whereas the readings were then compared to a standard curve established using glucose standards. Meanwhile, the protein content was estimated according to the correlation reported in the literature (protein content = nitrogen content × 6.25) (Becker, 1994), whereas the elemental analyser (Elementar Vario EL III) was used to measure the total nitrogen content. The lipid content was analysed as fatty acid methyl esters (FAME) through the direct transesterification method (Yeh & Chang, 2011; Yeh & Chang, 2012). The microalgae were first washed with deionized water to remove the salt in the medium and dried by lyophilization. 8 mL of 0.5 N KOH in ethanol were mixed with a small number of lyophilized microalgal cells (0.04 g) and disrupted for 25 min using bed-beater (MM400, Retsch, Germany). Saponification was carried out by heating the mixture to

100 °C for 15 min and then cooled to room temperature. The esterification was carried out by adding 8 mL of 0.7 N HCl in methanol and 14% (v/v) $BF_3/CH_3OH$ into the mixture and heated to 100 °C for 15 min. Next, n-hexane was used as solvent to extract the FAME formed during the transesterification. After that, an external standard (methyl pentadecanoate (C15:0, Sigma) was added to the extracted FAME in order to determine the lipid content. Gas chromatography (GC-2014, Shimadzu, Japan) equipped with a flame ionization detector (FID) was used to analyse the composition of the FAME using a 100 m capillary column ($SP^{TM}$-2560, Supelco, Bellefonte, PA, USA) with an internal diameter of 0.25 mm. Ultra-pure helium with a constant flow rate of 1.0 mL/min was used as carrier gas. The temperature of injector and detector were both set at 260 °C, whereas oven temperature was initially set at 140 °C for 5 min and heated to 240 °C for 20 min with a heating rate of 4 °C/min.

## 3.3 Dry torrefaction process

Two different microalgae species were converted to solid biofuel using dry torrefaction. In addition, the effect of dry torrefaction on second-generation biofuel feedstock, de-oiled *Jatropha curcas* seed kernel biomass (*Jatropha* biomass) was investigated and compared with microalgal biomass. *Jatropha* seeds were obtained from a local company, Bionas. The seeds were cracked, and the shells were carefully removed. Meanwhile, the obtained kernels were used for oil extraction. The seed kernels were dried in an oven at 85 °C for 48 h to provide the standard basis of the experiment. The samples were ground and passing through an 18-mesh sieve for dry torrefaction process. This particle size was selected, because the small particle size of oil seed agglomerated the particles and decreased the oil yield (Zhong et al., 2018). Ultrasonic solvent extraction method was used to extract the seed kernel oil. The solvent used for extraction was n-

hexane. The extraction time via ultrasonic extraction in atmospheric pressure condition was dramatically low compared with Soxhlet extraction (Liu et al., 2014). Seed sample of 20 g was mixed with 120 mL of n-hexane for oil extraction. The extraction was carried out at 500 W and 20 Hz at an amplitude of 30% for 15 min. The oil content in the seed kernels were determined using Soxhlet extraction with n-hexane as solvent (Shah et al., 2005). The *Jatropha* biomass were dried and collected in sealed plastic bags and stored in a desiccator at room temperature until the experiments and analysis were carried out.

Dry torrefaction was conducted in Biofuel laboratory, Faculty of Engineering, University of Malaya. A schematic of the torrefaction setup is shown in **Figure 3.2**. A nitrogen gas tank was connected to the furnace to maintain the inert condition torrefaction. It was connected to a flow meter to control the gas flow rate. The furnace used for the experiment was a horizontal fixed-bed tube furnace with inner diameter of 5.5 cm, tube length of 80 cm and heated zone of 20 cm length.
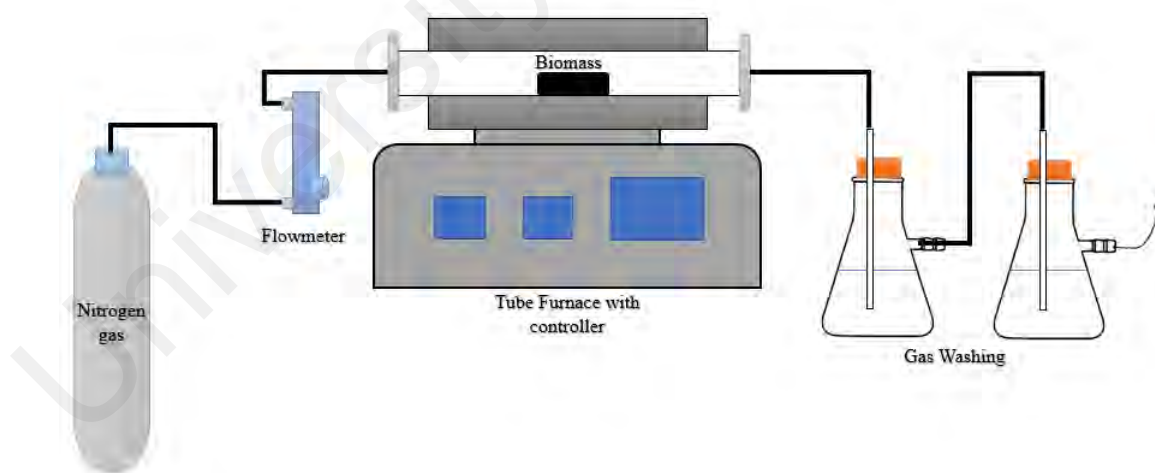


**Figure 3.2: Schematic of torrefaction setup**

In this study, three different torrefaction temperatures of 200, 250 and 300 °C were used as light (200 °C), mild (250 °C) and severe (300 °C) torrefaction, respectively (Zhang et al., 2018a). Four different holding time, namely, 15, 30, 45 and 60 min, were

conducted for each torrefaction temperature. For each run of the experiment, 5 g of biomass was measured and placed at the middle of the reactor tube using a combustion boat. Nitrogen gas with a flow rate of 200 mL/min was flowed into the furnace for 10 min before the torrefaction to provide an oxygen-free condition. Next, the biomass was then heated to the desired temperature at a rate heating rate of 10 °C/min, followed by holding for the required time. After the torrefaction, the reactor tube was cooled down to room temperature with the nitrogen flow. Finally, the torrefied samples were collected for further analysis.

The torrefaction severity index (TSI) was applied as an indicator to study the weight loss of biomass and a different combination of temperature and holding time that might be used to achieve the same degree of weight loss during torrefaction (Peng et al., 2013). The degree of biomass weight loss for different torrefaction conditions were analysed using TSI and defined as (Chen et al., 2015d; Zhang et al., 2018a):

$$TSI = \frac{WL_{T,t}}{WL_{300°C,60\,min}} = \frac{100 - SY_{T,t}}{100 - SY_{300°C,60min}} \tag{3.1}$$

where $WL_{T,t}$ represents the weight loss of the torrefied biomass at the specific temperature (T) and holding time (t), whereas SY represents the solid yield of the biomass. Within the ranges of torrefaction temperature and holding time, the torrefaction condition of 300 ºC and 60 min provides the highest degree of torrefaction, which is adopted as the reference operation.

## 3.4    Wet torrefaction process

Wet torrefaction of the microalgae was carried out in a modified household microwave oven with maximum power of 800 W (Tatung TMO-231) with a hole on the roof of the oven to insert the reactor. Wet torrefaction reactor was in a laboratory of Sugar Business

Division, Taiwan Sugar Corporation, Tainan. Microwave energy is capable of providing effective, selective, rapid, consistent, hot-spot based, energy efficient and homogenous heating in the thermochemical conversion process (Amin et al., 2019). In contrast, conventional heating through conduction, convection and radiation, which are generally slow, non-selective, less control and inefficient (Motasemi & Afzal, 2013; Zhang et al., 2017b). Water is a high microwave-absorbent material, the microwave absorbent absorbs microwave energy to create adequate thermal energy in order to achieve the temperatures required for extensive torrefaction to occur (Anuar Sharuddin et al., 2016). Through the rapid heating generated by microwave power, the microwave-assisted thermochemical conversion can achieve the temperature requirement in shorter amount of time which eventually leads to energy saving. **Figure 3.3** shows the experimental setup used for wet torrefaction. A Teflon cylindrical reactor (volume = 625 ml, length = 318 mm and inner diameter = 50 mm) was the main experimental reactor of the setup. The reactor was sealed tightly by a SUS316L stainless steel head which connected a pressure gauge, a back-pressure valve and a thermocouple. A proportional-integral-derivative (PID) temperature controller was connected to the thermocouple and microwave oven to monitor the temperature.
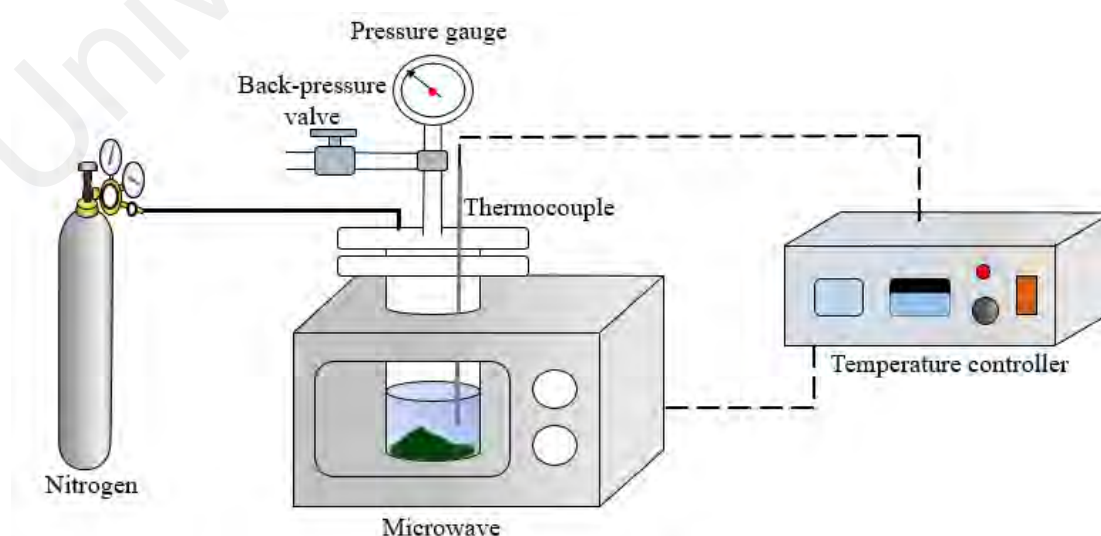


**Figure 3.3: Experimental setup of wet torrefaction process**

In this study, four different solutions, namely, water, $H_2SO_4$, $H_3PO_4$ and succinic acid with concentration of 0.05 M and 0.1 M were applied as wet torrefaction working fluids. The acidic solutions were applied in this study as it can accelerate the microalgae conversion and hydrolyse microalgae carbohydrate. For each run of the experiment, 20 g of dried microalgae and 100 mL of solution were mixed in the experimental reactor. Next, the reactor was tightly closed by stainless steel head and purged by nitrogen gas for 10 min to ensure an inert condition. Subsequently, the reactor was pressurized by compressed nitrogen gas to 3 bar. The reactor was heated to 160 ℃ and hold for 10 min when reactor reached the desired temperature. From the literature, these temperature and holding time were most suitable for co-production of biochar and sugar recovery (Teh et al., 2017). The reactor was heated by a microwave oven with 2.45 GHz frequency and operated with the current of 10 A. After the reaction completed, the reactor temperature was cooled by tuning off the power and released the gaseous. The aqueous mixture was separated by a centrifuge (Himac CF15RN, Hitachi) which operates at 8000 rpm for 10 min. The solid product was dried in the oven at 105 ℃ and 24 h after the separation. The dried solid product and hydrolysate were kept for further analysis. The experiment was conducted at least twice to ensure the repeatability.

The glucose and by-products were analysed by a high-performance liquid chromatography (HPLC) system equipped with a refractive index detector (RI 2000-F) and a UV detector (785A UV/VIS, Perkin Elmer), which conducted in a laboratory of Sugar Business Division, Taiwan Sugar Corporation, Tainan. A 300 mm × 8.8 mm ORH 801 column with a temperature of 80 ℃ was utilized. Ultrapure water with a flow rate of 0.3 mL/min was used as the mobile phase in the system. All the analysis was conducted more than twice to ensure the repeatability of the result, and the relative error was controlled below 5%.

### 3.5 Biomass and biochar characterisation

### 3.5.1 Torrefaction performance

The solid yield, HHV enhancement and energy yield are the important factors to evaluate the torrefaction performance and fuel properties of biochar (Sukiran et al., 2017).

#### 3.5.1.1 Solid yield

Solid yield is to determine the amount of biomass remained after the torrefaction process. The solid yield, which directly affected the energy yield, indicated the mass loss of the biomass during torrefaction (Zhang et al., 2018a). Initially, the weight of biomass before the torrefaction was measured using a weighing balance. After the torrefaction, the weight of the biochar was measured again to calculate the solid yield. The solid yield was calculated using equation (3.2) as follows:

$$Solid\ yield\ (\%) = \frac{weight\ of\ biochar\ (g)}{weight\ of\ biomass\ (g)}\ x\ 100 \tag{3.2}$$

#### 3.5.1.2 HHV enhancement factor

The HHV enhancement of biomass after the torrefaction was calculated based on the equation (3.3) as follows:

$$HHV\ Enhancement = \frac{HHV\ of\ torrefied\ biomass}{HHV\ of\ raw\ biomass} \tag{3.3}$$

First, the HHV of the raw biomass and torrefied biomass were analysed by a bomb calorimeter (IKA C5000) by referring to the ASTM D-5865 standard test method. Initially, ±0.5 g of sample was measured into the crucible and connected to an ignition thread, then placed in an oxygen bomb calorimeter. Oxygen gas with up to 40 atm was charged into the bomb and the secured oxygen bomb calorimeter was placed in the circulating water system. The measured mass of the sample was entered to the system for

the calculation of HHV. The operating time for each sample was ±6 min to completely burn and calculate the HHV, the heat quality produced by a complete combustion of sample mass is usually expressed in mega joules per kilogram. The calorimeter produces reliable results with good repeatability within 0.5% precision.

### 3.5.1.3 Energy yield

The biomass partly decomposes during the torrefaction process and producing various volatiles, which results in a mass loss and chemical energy to the gas phase. Energy yield was implemented to identify the energy remained in the biomass after the torrefaction, which can be calculated based on equation (3.4) as follows:

$$Energy\ yield\ (\%) = Solid\ yield\ \times\ HHV\ Enhancement \tag{3.4}$$

### 3.5.2 Elemental and proximate analyses

Element analysis of the microalgae were determined by an elemental analyser (2400 Series II CHNS/O, Perkin Elmer). It is based on the classic Pregl-Dumas method where samples are combusted in a pure oxygen environment, with the resultant combustion gases measured in an automated manner. It is ideal for quick determination of the content of carbon, hydrogen and nitrogen in organic and other material types. The furnace in the elemental analyser was heated from room temperature to 925 °C for combustion temperature and 640 °C for reduction before the analysis. Acetanilide was used as a sample to condition the column. During the analysis, each of the 4 samples in the path was placed with an acetanilide to act as the quality control sample for the elemental analysis.

In addition, the proximate analysis of microalgae were examined using a thermogravimetric analyser (Diamond TG/DTA, Perkin Elmer) based on ASTM D7582-15 method (Lee et al., 2017). First, ±10 mg of biomass was heated from room temperature to 110 ℃ with a heating rate of 5 ℃/min under the flow of $N_2$ gas and held for 10 min to determine the moisture content of biomass. Next, the biomass was heated to 800 ℃ with a similar heating rate and kept for 7 min to analyse the volatile matter. Thereafter, the gas was switched to oxygen in the TG chamber for the oxidation. The biomass was finally heated up to 900 ℃ and maintained for 30 min to determine the fixed carbon. The biomass weight was recorded until it reached a constant value. Finally, the ash content was measured by deducting the moisture, volatile matter and fixed carbon from 100%. The relative error of the results was controlled below 5%, and the average was obtained from the available data.

### 3.5.3 Chemical and physical structure characterisations

### 3.5.3.1 Solid Fourier transform infrared analysis

FTIR analysis was performed to analyse the change in functional groups on the raw, dry and wet torrefied microalgae using a Perkin Elmer Spectrum 100 equipped with an Attenuated Total Reflection (ATR) accessory. FTIR provides an infrared spectrum much more rapidly compared to the traditional spectrophotometer. The spectroscopy produces an infrared irradiation beam released from a glowing black-body source. Then, the beam passes through into interferometer where the spectral encoding takes place. The sample absorbs specific frequencies of energy when the beam enters the sample compartment, which is a unique characteristic of the sample from interferogram. Afterward, the special interferogram signals in energy versus time for all frequencies are measured by a detector. Meanwhile, a beam is superimposed to provide a reference (background) for the

instrument operation. Fourier transformation computer software is used to obtain the desired spectrum after the interferogram automatically subtracted the background spectrum of the sample spectrum. In each run, the background of FTIR were scanned for 16 times before analysis. The raw, dry and wet torrefied microalgae were prepared in powder form and the samples were placed on the spectra for the analysis. All the spectra were recorded within a range of $4000-650$ $cm^{-1}$ absorption band, and 16 scans were collected each run at room temperature with a spectral resolution of 4 $cm^{-1}$. The spectra were then ATR corrected and normalized in the Spectrum One Software. The pattern of absorption band will identify the changes in carbohydrates, proteins and lipids of the microalgae during the dry and wet torrefaction.

### 3.5.3.2 X-ray diffraction analysis

An X-ray diffractometer (D8 Advance ECO, Bruker) was used to carry out X-ray diffraction (XRD) analysis of the microalgae, which is providing full-sized goniometer class powder XRD under ambient and non-ambient conditions. XRD was carried out to investigate the effect of wet torrefaction on the crystalline cellulose and the mineral content of microalgae, as the related information on microalgae wet torrefaction in the past is still limited. First, the biomass powder was placed on an XRD plate and smoothen the surface of the biomass. Next, the plate was placed in the diffractometer and operated using a computer. In each analysis, the microalgae were analysed at the diffraction angle ($2\theta$) between 10 and $40^{o}$.

### 3.5.3.3  Surface morphology analysis

Scanning electron microscope (SEM) was applied to examine the effect of wet torrefaction on the physical changes and the surface morphology in microalgae. Field emission scanning electron microscope (Schottky, SU5000) was used in this study, which allows for a simple transition between high vacuum and variable pressure mode. The microalgae were placed above a coin using a copper tape. Next, the coin was coated with a layer of gold before place in the microscope. Thereafter, the sample was placed into the microscope for 30 min to ensure the vacuum condition. In this study, SEM images of microalgae with magnification factor of 500, 5000 and 15000 were taken for the analysis.

### 3.5.4  Thermal behaviour analysis

The thermal behaviour analysis of biomass and biochar were performed using a thermogravimetric analyser (TG, Diamond TG/DTA, Perkin Elmer). TG is an important thermal analysis for gas-solid reactions. TG has been used frequently in the laboratory biomass analysis and coal conversion by varying the process parameters such as temperature, time and heating rate (Carrier et al., 2011). The time-dependent weight change curve of biomass in isothermal or non-isothermal heating is the basis for characterizing the devolatilization processes, quantification of release rates and the kinetic reaction (Bach & Chen, 2017b). TG consists of a balance coupled with a calorimeter, a controller, and a computer. The particles are heated by radiation in the thermo-analyser. The balance directly measures the weight loss of the tested sample as a function of time. Two empty aluminium oxide crucibles were placed for the measurement. One of the crucibles was acted as reference while another for the measurement of sample weight. In each run, $\pm10$ mg of sample was heated from room temperature to 105 °C for 10 min to remove the moisture content and then heated to 800

°C. The heating rate of 20 °C/min and $N_2$ gas flow rate of 100 mL/min were used throughout the analysis.

## 3.6    Evolved gas analysis using TG-FTIR

### 3.6.1    Thermogravimetric analysis

TG coupled with a FTIR spectrometer (TG-FTIR) analysis was performed to evaluate the thermal behaviour and evolved gases from the microalgae pyrolysis and combustion, which was conducted in GenFUEL laboratory, Department of Aeronautics and Astronautics, National Cheng Kung University. Raw and wet torrefied microalgae ESP-31 (water, 0.1 M succinic acid, 0.1 M $H_3PO_4$ and 0.1 M $H_2SO_4$) were analysed by TG-FTIR technology. Microalga ESP-31 was selected for further analysis due to the high enhancement in HHV and outstanding performance in wet torrefaction. **Figure 3.4** presents the setup of TG-FTIR approach for evolved gas analysis of wet torrefied microalgae. TGA was carried out using a Perkin Elmer Diamond TG/DTA. In the pyrolysis of the microalgae, TGA was conducted using $N_2$ at a flow rate of 100 mL/min with a constant heating rate of 20 °C/min throughout the analysis. In each run, around 10 mg of microalga was heated from room temperature to 105 °C for 10 min to remove moisture and then heated to 800 °C. The weight loss and DTG throughout the analysis were monitored and recorded. Meanwhile, the experiment was repeated by changing the gas to air at a flow rate of 100 mL/min for the microalgae combustion. Similarly, the weight loss and DTG were monitored and recorded for combustion analysis. For the torrefaction of microalgae, around 10 mg of microalga was heated from room temperature to 105 °C for 10 min and then heated to the torrefaction temperature (200, 250 and 300 °C) for 20 min, followed by heating to 800 °C with a heating rate of 20 °C/min for pyrolysis.
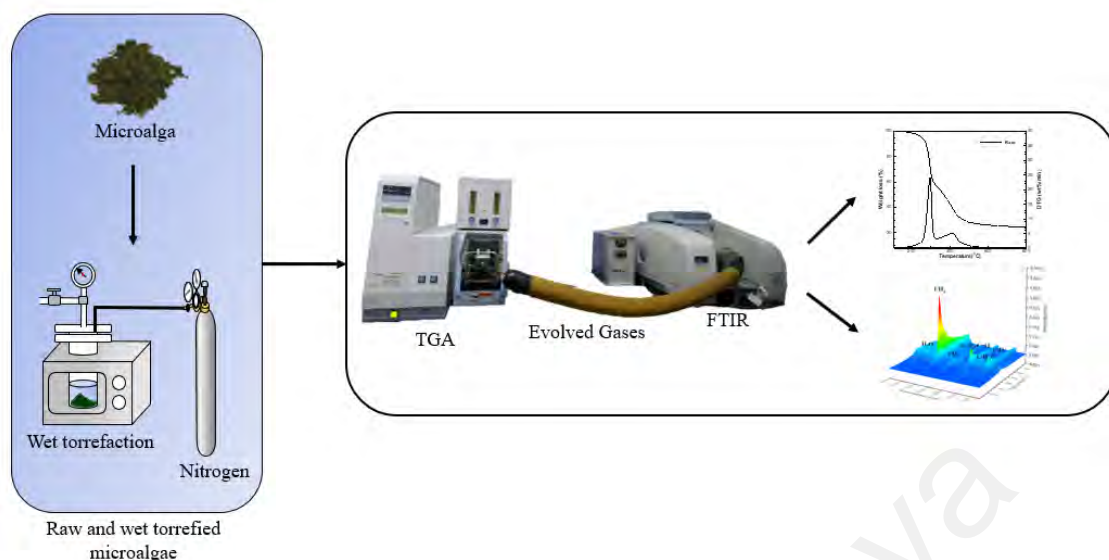
**Figure 3.4: The experiment procedures of TG-FTIR analysis on wet torrefied microalgae**

### 3.6.2 Gaseous Fourier transform infrared analysis

A FTIR spectrometer (Perkin Elmer Spectrum 100) was connected to a TG to evaluate the functional groups of evolved gases from the pyrolysis and combustion. A thermally insulated pipe with a temperature of 260 ℃ was connected between TG and FTIR to gather the signals of evolved gases. Before the experiment, the FTIR background was scanned with an average of 16 times to use as references. The FTIR absorbance was gathered every 5.25 s within the wavenumber range of 4000−650 cm$^{-1}$, while the absorbance data was collected simultaneously with TGA data. In addition, the evolved gas 3D FTIR absorbance for microalgae pyrolysis and combustion were investigated. Hence, a comprehensive insight into the formation of generated gases during the microalgae pyrolysis and combustion was obtained by combining the results of TGA and FTIR.

### 3.7 Py-GC/MS

The Py-GC/MS was implemented by using a pyrolyser (EGA/EY3030D) coupled with a gas chromatography-mass spectrometer (GC/MS, Agilent Technologies 7890A/5975C) to separate and identify the volatiles released during the fast pyrolysis of wet torrefied microalgae, which was conducted in Green Technology Research Institute, CPC Corporation, Kaohsiung, Taiwan. A two-stage thermal degradation (dry torrefaction pre-treatment as the first stage) of microalgae was practiced by using a double-shot pyrolyser. **Figure 3.5** presents the setup of the Py-GC/MS analysis of microalgae in single and double-shot pyrolysis. The column applied in the GC/MS system was an ultra-alloy capillary column (30 m–0.25 mm–0.25 μm). The oven temperature was initially set at 45 °C for 4 min and heated to 280 °C for 10 min with a heating rate of 6 °C/min. Ultra-pure helium with a constant flow rate of 1.0 mL/min was used as carrier gas throughout the experiment. The temperatures of GC/MS injector and interface were set at 275 and 300 °C to identify the pyrolysis volatiles. The mass spectra used for the mass selective detector were 40–550 $m/z$. The detected chromatographic peaks were determined according to the previous experimental mass spectrum data and the NIST library. The Py-GC/MS system was periodically calibrated to ensure measurement quality. The experiments were repeated at least twice to ensure the reproducibility and consistency of the data.
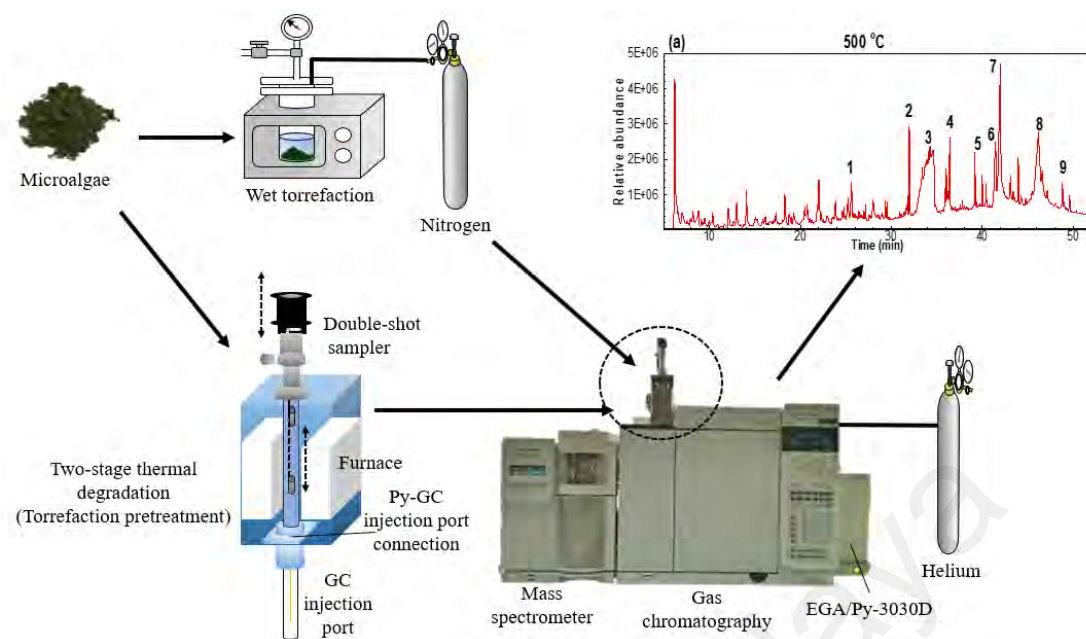
**Figure 3.5: The experiment procedures of Py-GC/MS analysis on wet torrefied microalgae and two-stage thermal degradation of microalgae**

### 3.7.1 Single-shot thermal degradation

The fast pyrolysis of raw and wet torrefied microalgae ESP-31 (water, 0.1 M succinic acid, 0.1 M $H_3PO_4$ and 0.1 M $H_2SO_4$) were carried out as single-shot on the Py-GC/MS at 500 °C for 30 s. Fast pyrolysis of 500 °C was applied because more than 95% of energy recovery can be achieved (Wang et al., 2013). For raw and wet torrefied microalgae, about 1.0 mg of microalga was loaded in the crucible and placed in the pyrolyser when the desired pyrolysis temperature was reached. Meanwhile, the produced volatiles were separated and identified by the GC/MS.

### 3.7.2 Double-shot thermal degradation

The double-shot was applied for dry torrefaction of microalga ESP-31 with three different temperature of 200, 250 and 300 ℃ (light, mild and severe torrefaction) for 20 min as the first shot, followed by 500 ℃ for 30 s as the second shot. The holding time was fixed at 20 min for torrefaction because most of the microalgae components have completely degraded (Chen et al., 2014e). For dry torrefaction, a hook was applied to fix the position of the crucible in the pyrolysis tube. The microalga loaded in the crucible was placed away from the furnace of the pyrolyser before reach the desired torrefaction temperature, as shown in **Figure 3.5**. Once the torrefaction temperature was achieved, the crucible was sent to the furnace of the pyrolyser for 20 min as the first stage torrefaction process. Then the volatiles were separated and sent to GC/MS to identify the components. Next, the crucible was sent back to the original place which beyond the furnace of the pyrolyser after the torrefaction process. Once the pyrolysis temperature was reached, the crucible was transferred back to pyrolyser for the second-stage pyrolysis. The produced volatiles were separated and identified again with the GC/MS, accomplishing the two-stage thermal degradation.

### 3.8    Kinetic modelling

### 3.8.1    Pyrolysis TGA

TGA of raw and wet torrefied microalgae ESP-31 (water and $H_2SO_4$) were carried out using a thermogravimetric analyser (Diamond TG/DTA, Perkin Elmer) to evaluate the pyrolysis kinetics. Currently, pyrolysis kinetics of various biomass has been successfully evaluated using TGA techniques. In each analysis, around 10 mg of microalga sample was weighed in an alumina crucible and placed into the analyser under a nitrogen flow rate of 100 mL/min. The sample was heated from room temperature to 105 ℃ at a heating

rate of 20 °C/min for 10 min to remove the moisture and heated to 800 °C for pyrolysis experiments. The TGA weight loss and the DTG was analysed and recorded for the kinetic study.

### 3.8.2    Independent parallel reaction (IPR)

The independent parallel reaction (IPR) model was used to simulate the pyrolysis kinetics of wet torrefied microalgae, as it is an effective kinetics modelling for every single components (Rueda-Ordóñez et al., 2015). Microalgae generally contributed by three main components including carbohydrates, proteins and lipids, as well as other minor components. For this reason, four parallel reaction models are required to describe the complexity of the microalgae pyrolysis, as this model presented a good model fitting and less calculating time reported in the literature (Bach & Chen, 2017a). These four components were separated and simulated independently. Hence, the decompositions of four independent parallel reactions for four pseudo-components are presented below:

$$\text{Microalgae} \begin{cases} Carbohdrate \xrightarrow{k_1} Char\,1 + Volatile\,1 \\ Protein \xrightarrow{k_2} Char\,2 + Volatile\,2 \\ Lipid \xrightarrow{k_3} Char\,3 + Volatile\,3 \\ Others \xrightarrow{k_4} Char\,4 + Volatile\,4 \end{cases} \tag{3.5}$$
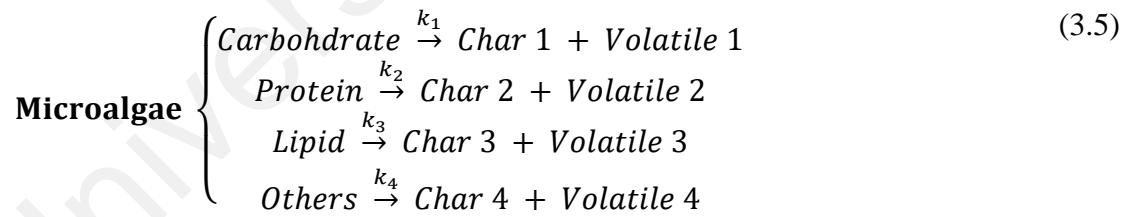
The typical non-isothermal kinetics for biomass pyrolysis is usually a function of temperature (T) multiply by a function of conversion degree (α), which is expressed as follows (Lu et al., 2013):

$$\frac{d\alpha}{dt} = k(T)f(\alpha) \tag{3.6}$$

In the above equation, $t, k(T)$, and $f(\alpha)$ are the conversion time (s), reaction rate constant (s$^{-1}$), and reaction model, respectively. Next, the microalgae conversion degree,

$\alpha$ is a normalized form of weight loss data during the microalgae decomposition, which is defined as:

$$\alpha = \frac{m_i - m_T}{m_i - m_f} \qquad (3.7)$$

where $m_i, m_T$ and $m_f$ represent the mass of the sample at initial (105 °C), instantaneous and final (800 °C) temperature, respectively. Based on the Arrhenius equation, the reaction rate constant of the pyrolysis is given as:

$$k(T) = A \exp\left(-\frac{Ea}{RT}\right) \qquad (3.8)$$

where $A, Ea, R$, and $T$ are the pre-exponential factor ($s^{-1}$), activation energy (kJ mol$^{-1}$), universal gas constant (9.314 J K$^{-1}$ mol$^{-1}$), and absolute temperature (K), respectively. The reaction function model used in this study is given as follows:

$$f(\alpha) = (1 - \alpha)^n \qquad (3.9)$$

where $n$ is the reaction order of the microalgae pyrolysis. In the non-isothermal pyrolysis, a constant heating rate, $\beta$ (°C s$^{-1}$) can be expressed as:

$$\beta = \frac{dT}{dt} \qquad (3.10)$$

Next, substituting equations (3.8), (3.9) and (3.10) into equation (3.6), the kinetic model in the explicit form is defined. For four reaction parallel models, the Arrhenius expression for the thermal degradation each microalgae components can be rewritten as follows (Chen et al., 2018c):

$$\frac{d\alpha_i}{dT} = \frac{A_i}{\beta} \exp\left(-\frac{Ea_i}{RT}\right) (1 - \alpha_i)^{n_i} \qquad (3.11)$$

where $i$ is the $i^{th}$ pseudo-component. The overall conversion rate as function of temperature (°C$^{-1}$) is the sum of the partial conversion rates of all the reactions as follows:

$$\frac{d\alpha}{dT} = \sum_i c_i \frac{d\alpha_i}{dT}, \qquad i = 1,2,3 \text{ and } 4 \tag{3.12}$$

$$\alpha_i = 1 - \exp\left(\frac{A_i}{\beta} \int_{T_o}^{T} e^{-\frac{Ea_i}{RT}} dT\right), \qquad for \ n_i = 1 \tag{3.13}$$

where $c_i$ is mass fraction of each component.

### 3.8.3 Fit quality

In order to evaluate the validity of the $A_i$, $Ea_i$, and $c_i$ calculated based on the predicted model, the curve fitting based on the non-linear least squares method was applied to compare the predicted and experimental curves, in which the objective function ($OF$) and fit quality ($Fit$) are defined as follows (Bach & Chen, 2017a):

$$OF = \sum_{i=1}^{N} \left[\left(\frac{d\alpha_i}{dT}\right)_{exp} - \left(\frac{d\alpha_i}{dT}\right)_{cal}\right]^2 \tag{3.14}$$

$$Fit\,(\%) = \left(1 - \frac{\sqrt{\frac{OF}{N}}}{\left[\left(\left(\frac{d\alpha_i}{dT}\right)_{exp}\right)\right]_{max}}\right) \times 100 \tag{3.15}$$

where $\left(\frac{d\alpha_i}{dT}\right)_{exp}$ and $\left(\frac{d\alpha_i}{dT}\right)_{cal}$ represent the conversion rates for experimental and calculated, respectively, while the $N$ is the number of experimental points. The algorithm of momentum-type particle swarm optimisation (PSO), based on the Chen et al. (2018c) was applied in this kinetic study to achieve the global optimization of the objective function. The equations of momentum-type PSO are defined as follows:

$$\vec{v}_i^{k+1} = \beta_c \times \Delta\vec{v}_i^k + \varphi_1 rand()(pbest_i - \vec{x}_i^k) + \varphi_2 rand()(gbest - \vec{x}_i^k) \qquad (3.16)$$

$$\vec{x}_i^{k+1} = \vec{x}_i^k + \alpha_c \times \vec{v}_i^{k+1}, i = 1,2,\ldots,N_{particle} \qquad (3.17)$$

where $v_i$ and $x_i$ are the position and velocity of the $i$-th particle as it scans in a $N_{var}$-dimension space, which is depending on the number of variables. $k$ represents the number of iterations and $\beta_c$ represents the momentum constant (0.5 in this study). $\varphi_1$ and $\varphi_2$ are the cognitive and social learning rates, respectively. Meanwhile, $rand()$, $pbest_i$, and $gbest$ are random number in the range [0,1], best position experienced of the $i$-th particle, and the global best position, respectively. $\alpha_c$ denotes as another momentum constant for adjusting the rate of change of the position. Lastly, $N_{particle}$ is the number of agents or particles sent to find the optimal solution.

In the initial step of PSO, the kinetic parameters are initialized with random values in the range of 0–100 for $E_a$ and $A$, and 0–0.5 for $c$, whereas the number of particles was set to 100. The kinetic parameters are optimized in this step. The obtained parameters are substituted into equations (3.12)−(3.14) in the second step to calculate the OF value. The comparison of OF value could obtain the best results (new $pbest_i$ and $gbest$ values) in the third step. The optimized criterion in this research would be examined when the $gbest$ value is smaller than $1 \times 10^{-5}$. The program would terminate and display the results when the optimized criterion is achieved or the iteration number reaches 2000. Moreover, these values should be in the normal range proposed in the literature. Then, the parameters will be reasonable to describe the pyrolysis kinetics of each case. Otherwise, the parameters would go back to the initial step to revise the value then return to the second step.

# RESULTS AND DISCUSSION

## 4.1 Introduction

The results obtained from the experimental were described, discussed and analysed in this chapter. First, the basic physiochemical properties of the microalgal biomass used in this study were presented and discussed, as well as the FTIR and TGA of the biomass are included. Next, the results and discussion on the dry torrefaction of two different species microalgae at three different torrefaction temperatures were carried out. The effect of dry torrefaction on biochar fuel properties such as solid yield, HHV enhancement and energy yield are examined. Meanwhile, discussion for the effect of torrefaction severity index on the HHV enhancement and energy yield were included as well. The next section discussed on the wet torrefaction performance of the microalgae in modified microwave reactor with the addition of acid catalysts. The analysis on the biochar fuel properties together with chemical, crystalline and physical structures of biochar were included, as well as the hydrolysates produced during the wet torrefaction. Furthermore, the microalgae with high torrefaction performance (microalga ESP-31, based on the previous results) was further investigated on the potential applications using advanced analytical techniques. The evolved gas of the pyrolysis and combustion of wet torrefied microalgae ESP-31 were analysed using FTIR in the next section. Meanwhile, Py-GC/MS was employed to analysis the bio-oil composition of microalgae after torrefaction. In addition, a double-shot thermal degradation was carried out to evaluate the effect of torrefaction on the microalgae pyrolysis. Lastly, the discussion on the pyrolysis kinetics and curve fitting of microalgae using independent parallel reaction were comprised in the last section. The effect of wet torrefaction on the conversion of carbohydrates, proteins, lipids and other components of microalgae were critically discussed.

## 4.2    Biomass basic properties

The composition, proximate, elemental and HHV analysis of two raw microalgae are presented in **Table 4.1**. The carbohydrate, protein and lipid content of the microalgae ESP-31 were 49.74, 14.94 and 23.39 wt%, respectively, while the microalgae FSP-E were 14.96, 64.78 and 14.70 wt%, respectively. The carbohydrate content of microalga ESP-31 was much higher than microalga FSP-E, while the protein content of microalga ESP-31 was noticeably lower than microalga FSP-E. The obtained weight percent of the volatile matter in the microalgae ESP-31 and FSP-E were 76.67 and 72.28 wt%, respectively. This implies that both microalgae possess high reactivity due to high percentage in volatile matter. The ash content of microalgae ESP-31 and FSP-E were 3.58 and 7.80 wt%, respectively. A high content of N element was observed on microalga FSP-E, mainly due to the high protein content in the microalga (Gai et al., 2015).

**Table 4.1: Characterisation of raw microalgae**

| Microalgae | ESP-31 | FSP-E |
|---|---|---|
| *Composition analysis (wt%, dry basis)* | | |
| Carbohydrate | 49.74 | 14.96 |
| Protein | 14.94 | 64.78 |
| Lipid | 23.39 | 14.70 |
| Others | 11.93 | 5.56 |
| | | |
| *Proximate analysis (wt%, dry basis)* | | |
| Volatile matter | 76.67 | 72.28 |
| Fixed carbon | 19.75 | 19.92 |
| Ash | 3.58 | 7.80 |
| | | |
| *Elemental analysis (wt%, dry-ash-free)* | | |
| C | 49.02 | 50.25 |
| H | 7.94 | 7.52 |
| N | 2.02 | 8.53 |
| O (by difference) | 41.02 | 33.70 |
| | | |
| H/C atomic ratio | 1.94 | 1.79 |
| O/C atomic ratio | 0.63 | 0.50 |
| HHV (MJ/kg) | 20.78 | 20.89 |

Furthermore, the chemical structures of raw microalgae were examined by FTIR spectra as presented in **Figure 4.1**. Numerous peaks were observed in the FTIR spectra indicated that the complexity of the microalgae structure. The peaks at around 900–1200 $cm^{-1}$, 1400–1600 $cm^{-1}$ and 2800–3000 $cm^{-1}$ represented the carbohydrate, protein and lipid composition of the microalgae (Bach et al., 2017b). For microalga ESP-31, a relatively high absorption on the C−O and O−H bond was detected due to the high carbohydrate content, as the O−H bond is the basic unit of polysaccharides (Wang et al., 2017b). In addition, the absorption of C−H for microalga ESP-31 was higher than microalga FSP-E

due to high lipid content for microalga ESP-31. Nonetheless, the N−H bond for microalga FSP-E was higher than microalga ESP-31 due to the high protein content. The FTIR result clearly presented that microalga ESP-31 is a microalga with high carbohydrate and lipid content, whereas microalga FSP-E is a high protein microalga.
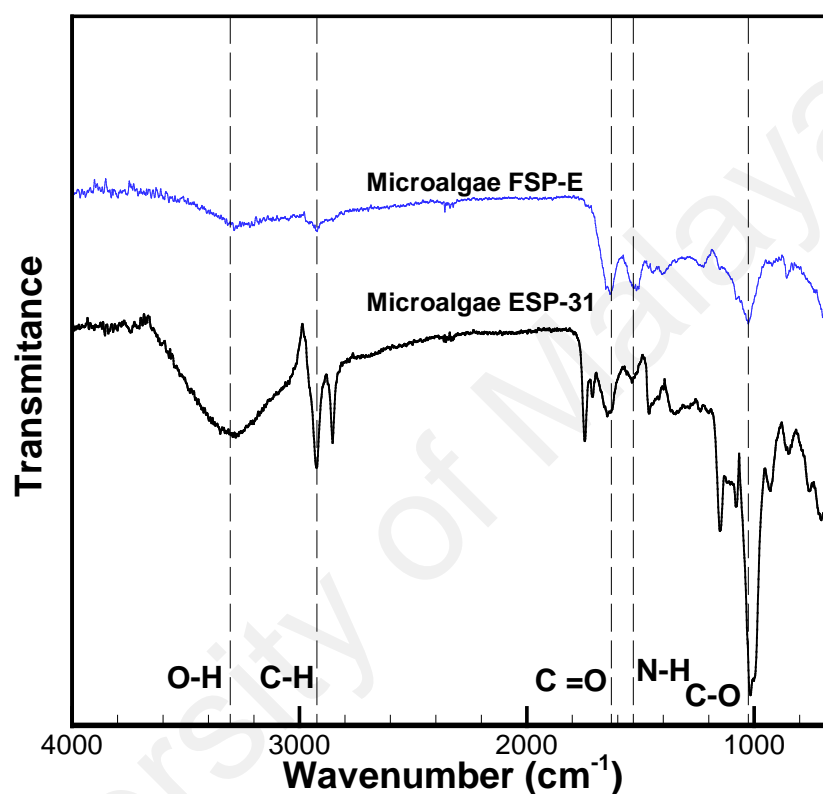


**Figure 4.1: FTIR analysis of raw microalgae**

The thermal decomposition behaviour of raw microalgae was studied by TGA and DTG as shown in **Figure 4.2**. From the literature, the weight loss for the first stage (200–350 °C) was mainly due to the decomposition of carbohydrates and proteins, whereas the second stage (350–550 °C) due to lipid decomposition (Chen et al., 2018b; Chen et al., 2014e). A relatively high first DTG peak was observed in the raw microalga ESP-31, indicating high decomposition of the carbohydrates as the microalga ESP-31 is rich in carbohydrate content. Moreover, a smaller second DTG peak was observed mainly due to the decomposition of the lipids. For microalga FSP-E, only one large peak with a

shoulder at low temperature were observed. Based on the composition analysis, the microalga FSP-E has relatively rich in protein content, which implies that the large peak was contributed by the large degradation of protein. Furthermore, the shoulder detected at low temperature might be due to the decomposition of carbohydrates and low volatile materials in the microalga.
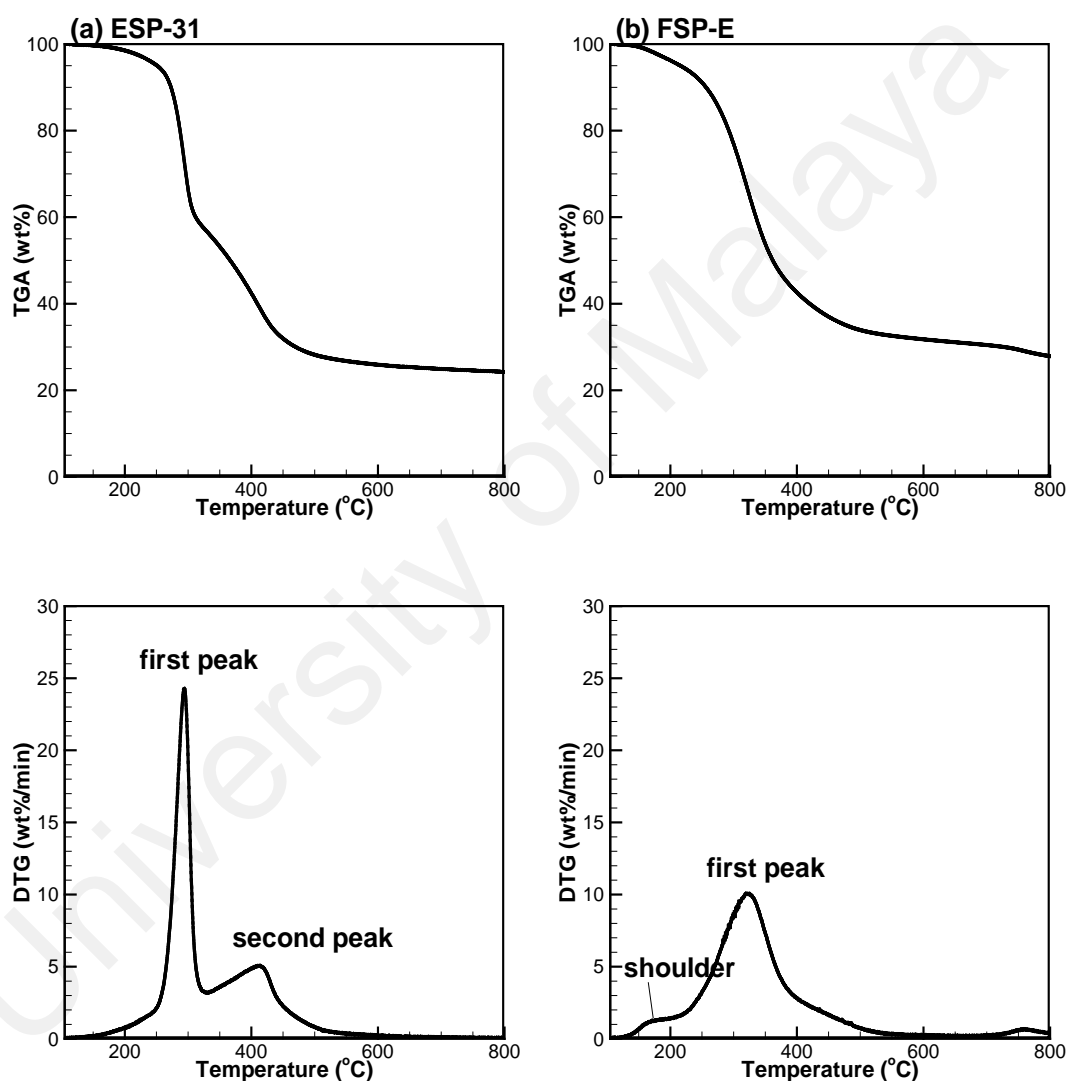


**Figure 4.2:** TGA and DTG curve of raw microalgae (a) ESP-31 and (b) FSP-E

## 4.3    Dry torrefaction

### 4.3.1    Biochar fuel analysis

The biochar fuel properties analysis and dry torrefaction performance of microalgae were analysed based on the solid yield, HHV enhancement and energy yield, as the key indicators (Bach et al., 2017b). The solid yield, HHV enhancement and energy yield of the biochar produced at different torrefaction temperatures (200–300 °C) and holding time (15–60 min) are presented in **Table 4.2**. The solid yield of torrefied microalga ESP-31, microalga FSP-E and *Jatropha* biomass ranged between 55.56–95.93%, 58.74–92.30%, and 63.46–94.47%, respectively. The solid yield decreased with the increase in temperature and holding time due to the large amount degradation of carbohydrates in severe torrefaction (Chen et al., 2014e), whereas degradation of hemicelluloses for *Jatropha* biomass (Li et al., 2012). At torrefaction temperature of 200 °C, high solid yield (>90 %) was obtained, and the decrease in the solid yield at that temperature was mainly caused by loss of water content (Xin et al., 2018), as well as the low degree of organic content.

**Table 4.2: Solid yield, HHV enhancement and energy yield of torrefied biomass**

| Biomass | Microalga ESP-31 | | | Microalga FSP-E | | | *Jatropha* biomass | | |
|---|---|---|---|---|---|---|---|---|---|
| Holding time (min) | Temperature (ºC) | | | | | | | | |
| | 200 | 250 | 300 | 200 | 250 | 300 | 200 | 250 | 300 |
| *Solid yield (%)* | | | | | | | | | |
| 15 | 95.93 | 86.76 | 59.55 | 92.30 | 84.79 | 66.17 | 94.47 | 84.00 | 68.90 |
| 30 | 95.15 | 72.54 | 57.15 | 91.73 | 80.90 | 61.05 | 92.54 | 82.51 | 66.25 |
| 45 | 93.85 | 70.12 | 56.18 | 90.98 | 78.52 | 59.69 | 92.29 | 82.08 | 65.46 |
| 60 | 93.59 | 67.37 | 55.56 | 90.60 | 77.52 | 58.74 | 91.88 | 80.56 | 63.46 |
| | | | | | | | | | |
| *HHV Enhancement* | | | | | | | | | |
| 15 | 1.02 | 1.09 | 1.39 | 1.02 | 1.04 | 1.14 | 1.06 | 1.13 | 1.21 |
| 30 | 1.02 | 1.22 | 1.42 | 1.03 | 1.06 | 1.16 | 1.08 | 1.15 | 1.23 |
| 45 | 1.03 | 1.24 | 1.44 | 1.04 | 1.08 | 1.17 | 1.08 | 1.19 | 1.23 |
| 60 | 1.03 | 1.31 | 1.45 | 1.04 | 1.11 | 1.18 | 1.08 | 1.19 | 1.24 |
| | | | | | | | | | |
| *Energy yield (%)* | | | | | | | | | |
| 15 | 97.57 | 94.55 | 83.06 | 94.53 | 88.51 | 75.46 | 99.79 | 94.85 | 83.62 |
| 30 | 96.98 | 88.70 | 81.36 | 94.39 | 85.93 | 70.88 | 99.78 | 95.24 | 80.73 |
| 45 | 96.90 | 87.27 | 81.15 | 94.58 | 84.66 | 69.77 | 99.70 | 97.79 | 80.61 |
| 60 | 96.55 | 88.00 | 80.59 | 93.77 | 86.16 | 69.08 | 99.58 | 96.08 | 78.90 |

The lowest solid yield of these biomass was observed at severe torrefaction condition (300 °C, 60 min). Notably, 40–44, 34–42, and 31–37 wt% of microalga ESP-31, microalga FSP-E and *Jatropha* biomass were thermally degraded at severe torrefaction. A similar phenomenon was observed for other species of microalgae (Chen et al., 2014g) and other biomass (da Silva et al., 2020), where the severe torrefaction showed the lowest solid yield. Microalga ESP-31 showed the highest weight loss among them, as this biomass is a carbohydrate-rich microalga, which is more sensitive at high temperature and easily degraded at severe torrefaction. *Jatropha* biomass showed the lowest weight loss, as this biomass comprised of hemicelluloses, cellulose and lignin, which is more thermal resistance to the torrefaction compared to the carbohydrates, proteins and lipids in the microalgae (Ubando et al., 2019). For the same torrefaction temperature, the holding time did not significantly change on solid yield for all the biomass. In contrast,

the solid yield of microalga ESP-31 significantly decreased with the holding time at mild torrefaction. The solid yield was decreased from 86.76 to 67.37 wt% for 15 to 60 min holding time. This scenario implied that torrefaction time played an important role for mild torrefaction due to high reactivity of the microalgae components (carbohydrates) at temperature of 250 ℃ (Chen et al., 2014e). The microalga FSP-E is a protein-rich microalga, where the protein is less reactive at mild torrefaction, which makes the holding time less significantly on this microalga. Similarly, cellulose in the *Jatropha* biomass is less reactive at mild torrefaction (Chen & Kuo, 2011a). It could be concluded that the increase in torrefaction temperature is more crucial to the thermal degradation of the biomass, while the holding time is only significant at mild torrefaction for microalga ESP-31.

The HHV enhancement of torrefied biomass increased with increasing of torrefaction temperature and holding time. From **Table 4.2**, the increase in HHV was highly affected by the torrefaction temperature compared with holding time. The increase in HHV was due to the increase in carbon content of torrefied product (Sabil et al., 2013). The mass loss had a strong correlation with the HHV for all the biomass (Peng et al., 2013). Evidently, the increase in HHV was most significant for microalga ESP-31 among them, as well as the highest mass loss. The enhancement of 45% was achieved at 300 ℃ and 60 min for microalga ESP-31, which is close to the results obtained from microalgae residues with different chemical composition (Chen et al., 2015d; Chen et al., 2016). Most of low volatiles and HHV components in the microalga ESP-31 were eliminated after the torrefaction process, remaining the high energy content components. Microalgae Chlamydomonas sp. JSC4 residues also presented high HHV enhancement after torrefaction at 300 ℃ due to the high carbohydrate content (Chen et al., 2015e). For microalga FSP-E, the lowest HHV enhancement among the biomass, this is because most of the low HHV protein remained in the biochar after the torrefaction, as the thermal

degradation of the microalgae protein was reported in a temperature ranges of 200−500 °C with the maximum degradation at 350−360 °C (Kebelmann et al., 2013). Torrefaction of microalga FSP-E only showed the enhancement of 18% at 300 °C and 60 min, which is relatively low compared to microalga ESP-31. Yu et al. (2018) showed that the HHV enhancement of high protein microalga FSP-E was less than 10%. The low HHV of the protein makes the microalga FSP-E not suitable to be used as solid biofuel.

The energy yield of the torrefied biomass clearly decreased with increasing torrefaction temperature compared with time. The energy yield changed from 69.08–99.79% for torrefaction temperatures (200–300 °C) and holding times (15–60 min). A relatively high energy yield was observed for all the biomass at light torrefaction, as only low volatile materials and moisture were removed in this stage. The microalga FSP-E showed the lowest energy yield due to the low HHV enhancement. At torrefaction temperature of 300 °C, the energy yield was less than 85% for all the biomass. This value was relatively low compared with other torrefaction temperatures (200 °C and 250 °C). The decrease in the energy yield was due to the decrease in mass yield caused by the biomass thermal degradation at high torrefaction temperature (Sabil et al., 2013).

### 4.3.2    Torrefaction severity index

In general, TSI is in the range of 0–1 based on previous definition (Zhang et al., 2018a). The values of TSI at the initial torrefaction and the torrefaction conditions of 300 °C and 60 min are zero and one, respectively. Meanwhile, the TSI of biomass at different operating conditions is presented in **Table 4.3**. Physically, the higher the value of TSI, the more sensitive the biomass weight loss to the torrefaction. It is a feasible parameter for indicating the level of biomass thermal degradation in the torrefaction. By plotting the profile distribution of HHV enhancement and energy yield versus TSI, the relationship

between the biomass degradation and the HHV enhancement could be significantly determined. Furthermore, the selection of biomass and torrefaction condition with the optimum torrefaction performance would be identified.

**Table 4.3: Torrefaction severity index of torrefied biomass at different operating conditions**

| Temperature (ºC) | Time (min) | Torrefaction severity index | | |
| --- | --- | --- | --- | --- |
| | | Microalga ESP-31 | Microalga FSP-E | *Jatropha* biomass |
| 200 | 15 | 0.09 | 0.19 | 0.15 |
| | 30 | 0.11 | 0.20 | 0.20 |
| | 45 | 0.14 | 0.22 | 0.21 |
| | 60 | 0.14 | 0.23 | 0.22 |
| 250 | 15 | 0.30 | 0.37 | 0.44 |
| | 30 | 0.62 | 0.46 | 0.48 |
| | 45 | 0.67 | 0.52 | 0.49 |
| | 60 | 0.73 | 0.54 | 0.53 |
| 300 | 15 | 0.91 | 0.82 | 0.85 |
| | 30 | 0.96 | 0.94 | 0.92 |
| | 45 | 0.99 | 0.98 | 0.95 |
| | 60 | 1.00 | 1.00 | 1.00 |

**Figure 4.3** and **Figure 4.4** represent the profile distribution of HHV enhancement and energy yield versus TSI for two different species of microalgae and *Jatropha* biomass. The slope of regression line stands for the sensitivity of the HHV enhancement and energy yield to TSI. In other words, the higher the gradient of the slope, the more sensitive the HHV enhancement and energy yield to TSI. Chen et al. (2015g) summarised the HHV enhancement profile of torrefied biomass versus the solid yield and showed that the data

did not display a strong linear distribution, whereas the profile of energy yield versus the solid yield exhibited a linear distribution with an $R^2$ value of 0.907. In this study, the HHV enhancement showed the linear distribution with the TSI, wherein the increase in weight loss will increase the HHV of the torrefied biomass, with a high $R^2$ value. The $R^2$ values of the microalga ESP-31, microalga FSP-E and *Jatropha* biomass were 0.99, 0.97 and 0.91, respectively. This result agreed with the results reported by Chen et al. (2011b) and Peng et al. (2013). The slope of the regression lines in **Figure 4.3** showed that the microalga ESP-31 had the greater influence on the HHV enhancement compared with microalga FSP-E and *Jatropha* biomass. The slope of the regression line of microalga ESP-31 was 0.48, whereas 0.18 and 0.20 were calculated for microalga FSP-E and *Jatropha* biomass, respectively. This finding indicated that the ratio of HHV enhancement and TSI of microalga ESP-31 was 4.8:10.

**(a) Microalga ESP-31**

y = 0.4779x + 0.9567
$R^2$ = 0.99

**(b) Microalga FSP-E**

y = 0.1826x + 0.9907
$R^2$ = 0.97

**(c) Jatropha biomass**

y = 0.2038x + 1.0466
$R^2$ = 0.91
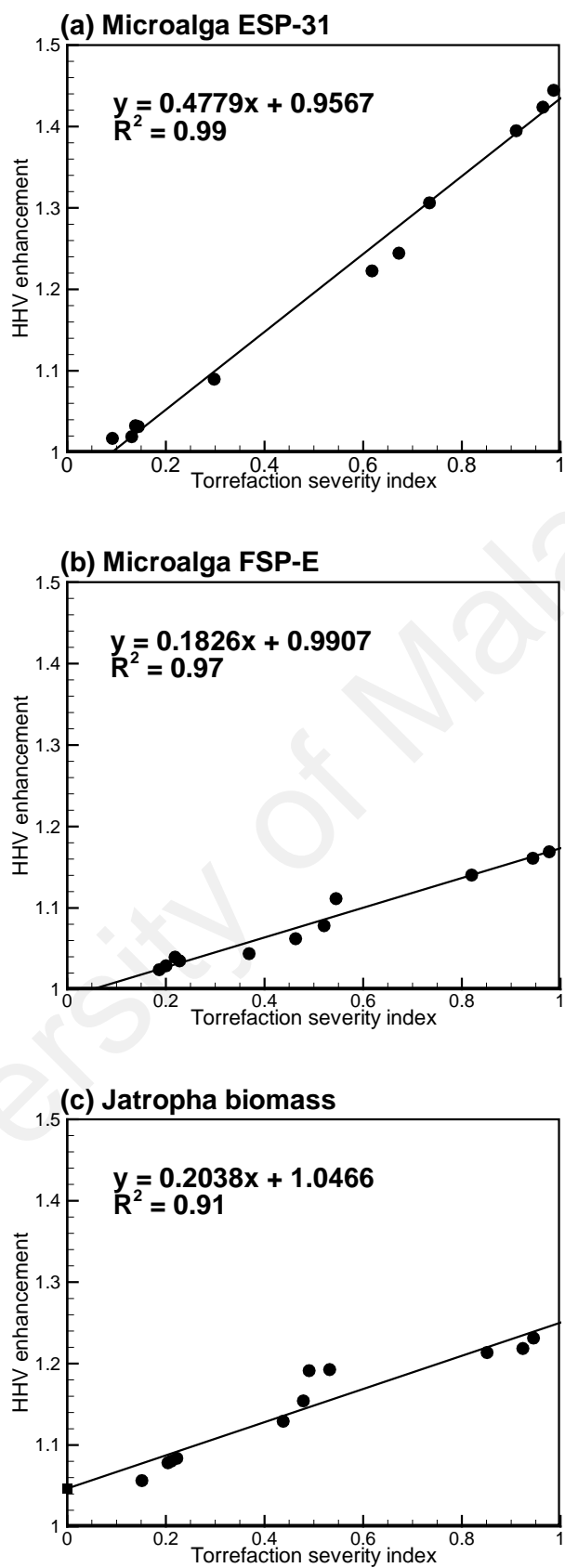
**Figure 4.3: HHV enhancement profiles of (a) microalga ESP-31, (b) microalga**

**FSP-E, and (c) *Jatropha* biomass**

**(a) Microalga ESP-31**

y = -17.988x + 99.333
$R^2$ = 0.99

**(b) Microalga FSP-E**

y = -31.577x + 101.01
$R^2$ = 0.99

**(c) Jatropha biomass**
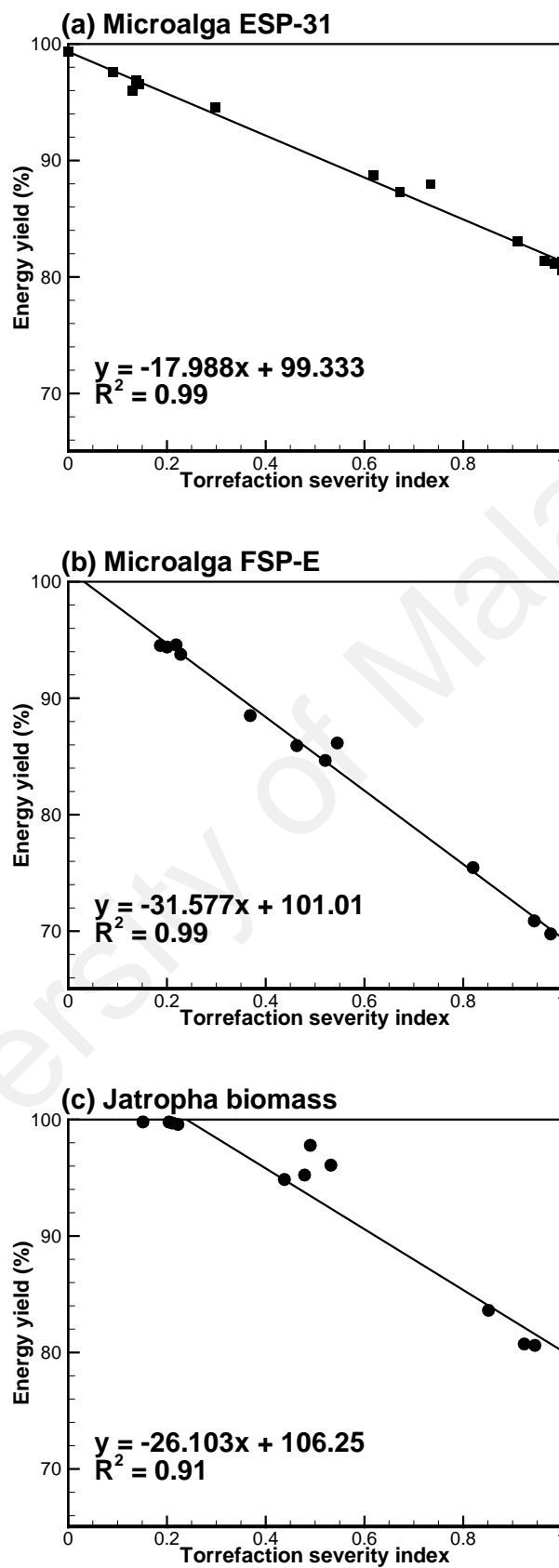
y = -26.103x + 106.25
$R^2$ = 0.91

**Figure 4.4: Energy yield profiles of (a) microalga ESP-31, (b) microalga FSP-E,**

**and (c) *Jatropha* biomass**

The total energy of the biomass tended to decrease with TSI increasing due to biomass weight loss. From **Figure 4.4**, negative slopes were observed for all the biomass, this is because the decreasing degree of solid yield is much higher than the increasing degree of HHV enhancement (Chen et al., 2011b). The slopes of regression lines of energy yield for microalga ESP-31, microalga FSP-E and *Jatropha* biomass were −17.99, −31.58 and −26.10, respectively. Similarly, a relatively high $R^2$ value was calculated for all the biomass with 0.99, 0.99 and 0.91 for microalga ESP-31, microalga FSP-E and *Jatropha,* respectively. Thus, the biomass torrefaction performance was successful predicted using TSI as a feasible indicator and microalga ESP-31 is more suitable to be converted into solid biofuel using torrefaction.

### 4.3.3    FTIR analysis

The chemical structures of raw and dry torrefied biomass examined by FTIR spectra are presented in **Figure 4.5**. The raw and torrefied biomass exhibited the same trend, but the spectra demonstrated that some peaks disappeared due to chemical bond breakage during the reaction. The stretching of the hydroxyl functional group (O–H bond) ranged between 3200 and 3570 cm$^{-1}$ (Coates, 2000). In the **Figure 4.5**, the band absorption at 3304 cm$^{-1}$ corresponds to the stretching of H-boned OH groups. The absorption clearly reduced after the torrefaction for all the biomass, especially in torrefaction at temperature of 300 ºC. Notably, the hygroscopic nature of biomass changed to hydrophobic after torrefaction to prevent the formation of hydrogen bond with O–H bond (Wu et al., 2012). Biomass with less moisture can store stably over a period, with a low risk of biological deterioration. Meanwhile, the transportation of hydrophobic biomass is cheaper, as lesser moisture in the biomass is delivered. Torrefied biomass became high-quality feedstock in gasification to produce good fuel properties of syngas (Chen et al., 2015g). The weight loss causes by dehydration reactions via bond scission with the removal of $H_2O$ between

250 and 300 °C. The elimination of CO and $CO_2$ via carbonyl and carboxyl group formation reactions, which limits devolatilization and carbonisation to produce final tars and chars during gasification. In addition, the peak between 2850 and 3000 $cm^{-1}$ indicated the presence of the aliphatic groups (stretching of C–H bond). Torrefaction did not change the C–H bond stretching vibrations assigned to the aliphatic group (Li et al., 2018).
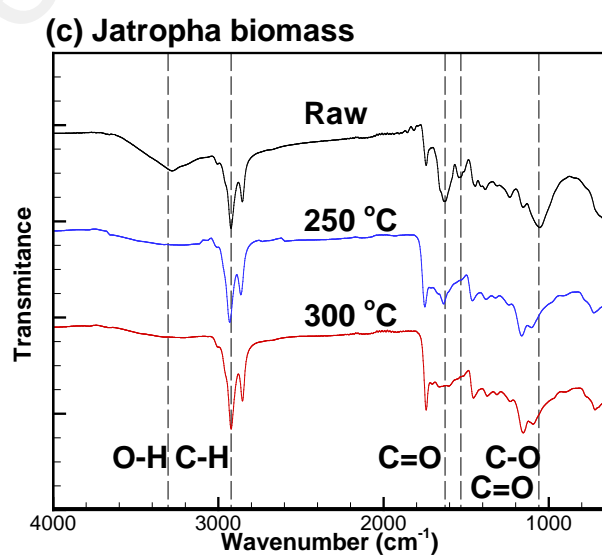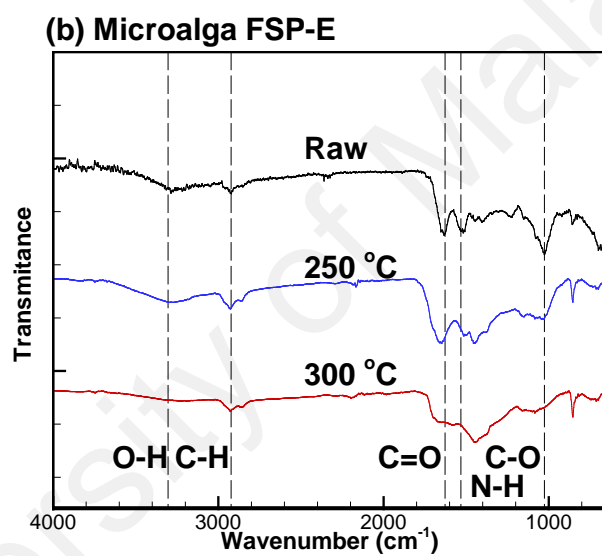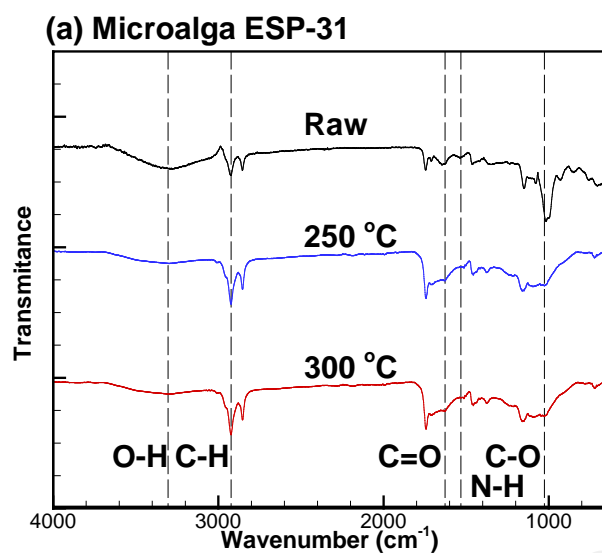
**Figure 4.5: FTIR analysis of raw and dry torrefied (a) microalga ESP-31, (b) microalga FSP-E, and (c) *Jatropha* biomass**

For microalgal biomass, the adsorption at 1532 and 1628 cm$^{-1}$ correspond to the C=O and N–H of amide associated with protein. It was observed that the adsorption peak was minimised after the torrefaction, indicating the degradation of proteins during the torrefaction, as the thermal degradation of the microalgae protein was reported in a temperature ranges of 200−500 °C (Kebelmann et al., 2013). In contract, these adsorptions for *Jatropha* biomass attributed to the aromatic skeletal in lignin and unconjugated C=O in hemicelluloses (Fan et al., 2020). The intensity for *Jatropha* biomass after torrefaction was evidently lower than the raw biomass, indicating the part of the lignin fraction underwent thermal degradation during torrefaction. In **Figure 4.5a** and **Figure 4.5b**, the peak at around 900−1200 cm$^{-1}$ represents C−O stretching bond, indicating the presence of carbohydrate composition in microalgae (Bach et al., 2017b). The peak can be clearly observed for raw microalgae, whereas this peak was eliminated after to torrefaction. From the literature, the decomposition carbohydrate of the microalgae occurred at temperature ranges of 200−350 °C (Chen et al., 2014e). For Jatropha biomass, the absorption at 1060 cm$^{-1}$ represents the C−O stretching bond of the hemicelluloses and cellulose (Park et al., 2013), which was decreased after the torrefaction. The decrease in C−O bond was mainly due to dehydration and decarboxylation of carbohydrates in the biomass (Li et al., 2018).

### 4.3.4    Thermal decomposition behaviour of torrefied biomass

The TGA and DTG curves of raw and torrefied biomass (250 °C and 300 °C; 60 min) were performed to determine the impact of the torrefaction on biomass as shown **Figure 4.6**. From the previous studies, the initial stage of weight loss (<200 °C) occurred due to the moisture loss (Sricharoenchaikul & Atong, 2009). The weight loss of the biomass at initial stage significantly minimised for the torrefied biomass, indicating dehydration occurred during the torrefaction. In the devolatilization stage, the weight loss of

112

microalgal biomass is different from the *Jatropha* biomass. For microalgal biomass, the weight loss at temperatures of 200–350 °C was mainly due to the decomposition of carbohydrates and proteins. Furthermore, lipid decomposition was occurred at the temperatures of 350–550 °C, while the degradation of carbonaceous matters in the biochar at a very slow rate occurred in the third stage (550−800 °C) (Chen et al., 2018b; Chen et al., 2014e). In contrast, for *Jatropha* biomass, the thermal decomposition of the hemicelluloses was observed at the first stage of degradation (200–350 °C), the second weight loss was due to cellulose degradation (275–350 °C), and lastly the lignin composition degraded at a wide range of temperatures (300–1000 °C). From the TGA curve, the increase in torrefaction temperature progressively decreased the thermal degradation of biomass, which was consistent with the results of Chen et al. (2011b). Besides, the initial decomposition temperature of the torrefied biomass increased with increasing torrefaction temperature. The weight loss of torrefied biomass at high torrefaction temperature (300 °C) was relatively low compared with low torrefaction temperature (250 °C), because the low volatile components was pyrolytically carbonised or polymerised (Hsu et al., 2017). A relatively more carbon in retained in the biomass after the torrefaction at 300 ºC, hence the TGA curve goes down slowly.

From **Figure 4.6a,** a large DTG peak of 27.27 wt%/min at 294 °C and the second DTG peak of 5.09 wt%/min at 413 °C were observed for microalgae ESP-31. There was no first DTG peak observed for the torrefied microalgae, implying most of the carbohydrates and part of the protein were eliminated during the torrefaction at temperatures of 250 and 300 ºC. Meanwhile, the peak observed from the torrefied microalgae was likely due to the thermal degradation of lipids, formed char, and other components in the microalgae (Chen et al., 2016), which cannot be decomposed during the torrefaction. From **Figure 4.6b**, a shoulder and a peak were identified for raw microalga FSP-E. The shoulder significantly removed for torrefied microalgae at temperatures of 250 and 300 ºC,

indicating the low volatile matters and carbohydrates were decomposed completely. The first peak was slightly reduced and shifted to a higher temperature for torrefaction at 250 ºC. This result revealed part of the proteins was decomposed, while the torrefaction has light impact on lipid composition. In addition, the DTG peak of the torrefied microalgae at temperature of 300 ºC was also due to the thermal degradation of lipids, formed char, and other components. From **Figure 4.6c**, a shoulder and two DTG peaks (322 and 385 °C) were observed for *Jatropha* biomass, which is differed from the microalgal biomass. the maximum weight loss of the *Jatropha* biomass occurred between 250 and 450 °C, as most of the hemicelluloses and cellulose remained in the biomass after the oil extraction (Chen & Kuo, 2011a). A shoulder and a first peak were mainly due to the decomposition of hemicelluloses and cellulose, whereas the second peak was likely due to decomposition of cellulose and lignin in the biomass (Xin et al., 2018). During torrefaction temperature of 250 °C, the first DTG peak moved to 338 °C, thereby signifying that a large amount of hemicellulose was degraded. One of the peaks at DTG disappeared for the torrefied *Jatropha* biomass at 300 °C, thereby demonstrating that several hemicelluloses and a part of cellulose were destroyed during torrefaction, whereas maintained a large amount of lignin in the biochar. Lignin is rich in carbon and high in calorific value, which is the main heating content in the biomass (White, 1987). In the torrefaction process, the degradation of the biomass components is dominated by dehydration and devolatilization of hemicelluloses component and part of the primary lignin sections (Chew & Doshi, 2011).
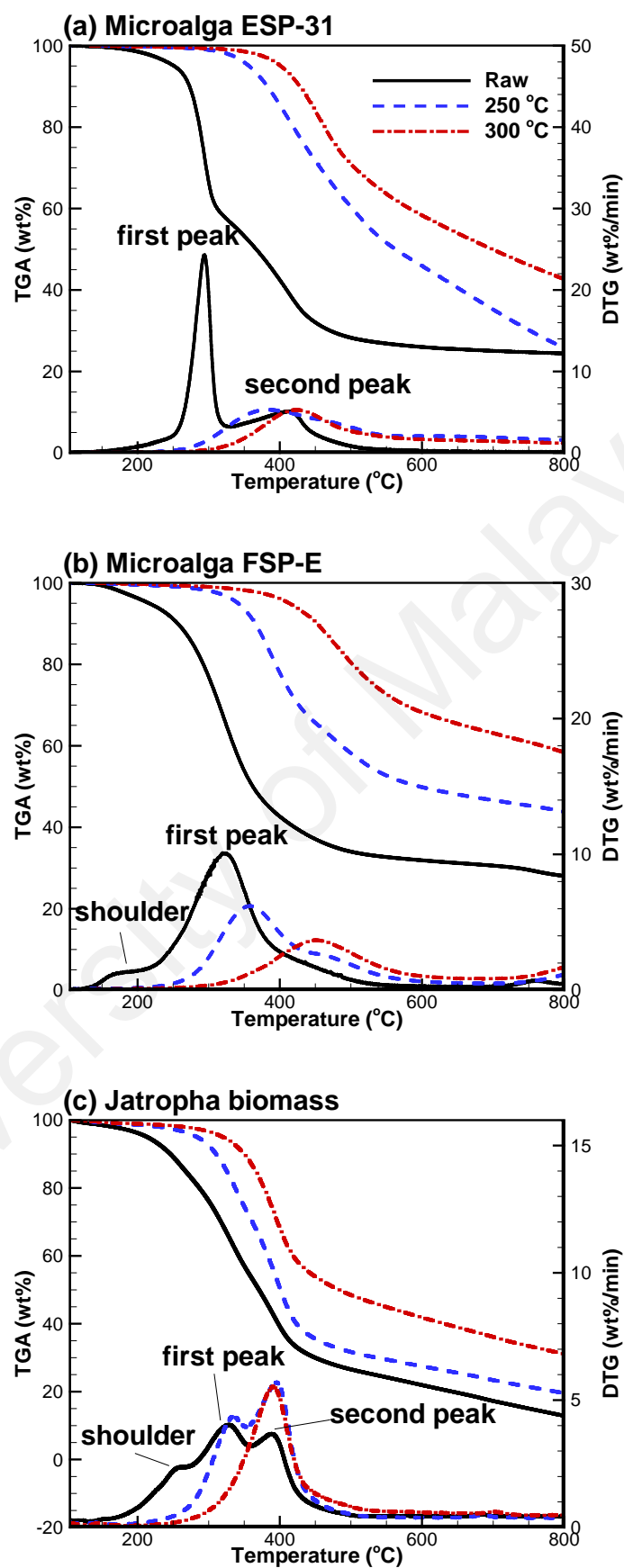
**Figure 4.6: TGA and DTG analysis of raw and dry torrefied (a) microalga ESP-31,**

**(b) microalga FSP-E, and (c) *Jatropha* biomass**

**4.4    Wet torrefaction**

**4.4.1    Biochar fuel analysis**

The solid yield, HHV enhancement and energy yield are the key indicators to investigate on the biochar fuel properties and wet torrefaction performance (Bach et al., 2017b). The solid yield represented the mass loss of the microalgae during wet torrefaction, which will directly influenced on the energy yield (Zhang et al., 2018a). The HHV enhancement reflects on both energy output and energy densification of the obtained biochar (Chen et al., 2012b). **Figure 4.7** shows the effects of the acidic solutions on the solid yield, HHV enhancement and energy yield of the torrefied microalgae (a) ESP-31 and (b) FSP-E.
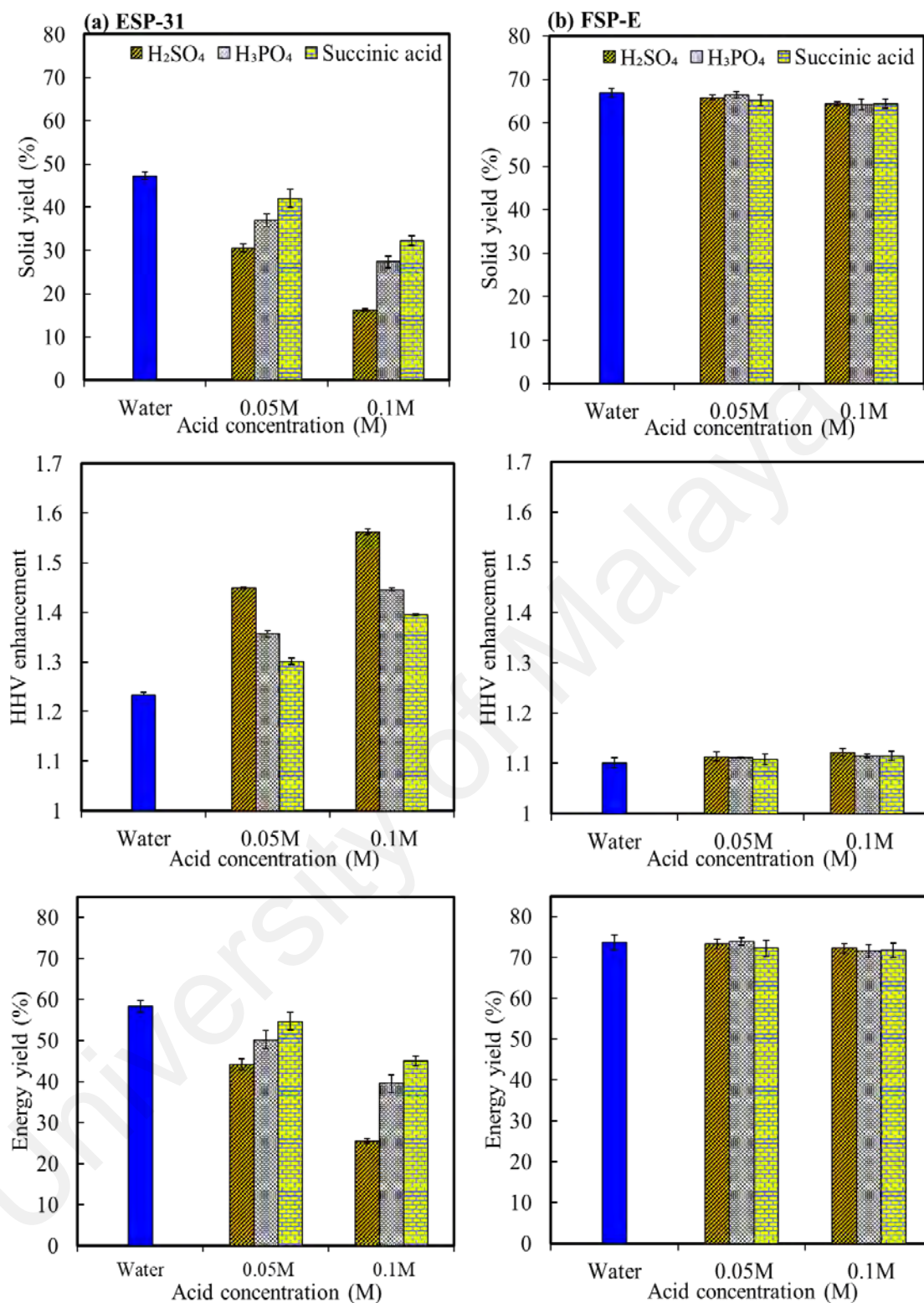
**Figure 4.7: Solid yield, HHV enhancement and energy yield of biochar (a) ESP-31, (b) FSP-E**

The solid yield of wet torrefied microalgae ESP-31 and FSP-E ranged between 16.30–47.25% and 64.20–66.90%, respectively. When microalgae were torrefied in acidic solutions, the solid yield was reduced due to the large amount of biomass degradation, similar to the trend as shown in wet torrefaction of sugarcane bagasse in acidic solution (Chen et al., 2012d). The solid yield decreased with the increase in acid concentration for microalga ESP-31, whereas no significant changes were found for microalga FSP-E. The use of 0.1 M $H_2SO_4$ showed the lowest solid yield among the acidic solutions due to the extra $H^+$ ion which created a high acidic medium (Teh et al., 2017). The main component for microalga ESP-31 is carbohydrates, which has poor hydrolysis resistance and is highly reactive during the wet torrefaction process (Wilson & Novak, 2009), enabling it prone to hydrolysis in acid solution into fermentable sugar (Chen et al., 2013). The high degradation rate of carbohydrates explains the low solid yield in microalga ESP-31. For microalga FSP-E, the mass loss was mainly due to the solubilization of oxygen-rich material, whereas most of the protein content remained in the solid phase. A higher hydrothermal media temperature (200 °C) was required to enhance the extraction rate of protein in acidic solution (Jazrawi et al., 2015).

The HHV enhancement of wet torrefied microalgae ESP-31 and FSP-E ranged between 1.23–1.56 and 1.10–1.12, respectively. A similar phenomenon of HHV enhancement was discovered, where only HHV enhancement for microalga ESP-31 was affected by the acidic solutions during wet torrefaction. It was observed that the HHV enhancement was directly proportional to the mass loss of the microalgae, similar to the study of biomass TSI by Chen et al. (2019b). The highest HHV enhancement was observed for microalga ESP-31 when using 0.1 M $H_2SO_4$, where the highest mass loss was induced. For the microalga pre-treated in 0.05 M $H_2SO_4$, the HHV enhancement of 1.44 was achieved, which is close to the result obtained from the dry torrefaction at 300

°C and 60 min. In the literature, Chen et al. (2015d) revealed that the torrefaction of microalgae with torrefaction temperature of 300 °C and heating time of 60 min produced biochar with HHV enhancement of 1.41. Notably, the HHV of microalga ESP-31 biochar was enhanced by 40% when the microalga was torrefied in 0.1 M succinic acid at 160 °C. The HHV of biochar produced from wet torrefaction in succinic acid required a relatively low temperature to obtain a similar HHV enhancement of biochar produced from dry torrefaction. For microalga FSP-E, the HHV enhancement (1.10–1.12) of biochar was identical to the wet torrefaction of rice husk at temperature of 240 °C (Zhang et al., 2017a). Microalgae could be torrefied at a lower temperature compared to lignocellulosic biomass, mainly due to differences in structure and composition (Bach et al., 2017b).

At the same wet torrefaction conditions, the energy yield of microalgae was higher than the solid yield, indicating the HHV of microalgae after the wet torrefaction is always higher than raw microalga. The energy yield of wet torrefied microalgae ESP-31 and FSP-E ranged between 25.47–58.24% and 71.59–73.67%, respectively. Although the enhanced HHV for microalga ESP-31 in 0.1 M $H_2SO_4$ was high, the energy retained in the microalgae after the wet torrefaction was relativity low. The HHV could be enhanced up to 40% and at least 45% of the energy yield after wet torrefaction in the succinic acid solution. Organic acid could be an effective alternative to replace dilute $H_2SO_4$ in pre-treatment (Kootstra et al., 2009a; Kootstra et al., 2009b). For microalga FSP-E, there was no significant change in the energy yield because only a small change in solid yield and HHV enhancement were observed in the acidic solutions. Meanwhile, it was revealed that the solid and energy yield of wet torrefied microalgae were much lower compared to biochar produced in dry torrefaction, which was due to the dissolution of biomass organic compound in subcritical water (Gao et al., 2016).

**Table 4.4** shows the proximate and elemental analysis of wet torrefied microalgae. The carbonization effect of microalgae in acidic wet torrefaction can be clearly evaluated from elemental analysis. The carbon content of raw microalgae ESP-31 and FSP-E were 49.02 and 50.25%, respectively. It could be observed that the increase in the mass loss of the microalgae enhanced the carbon and nitrogen contents in the solid products, similar to the study as reported by Bach et al. (2017b). A high N content (8.53 wt%) for microalga FSP-E contains 64.78 wt% of protein as compared to microalga ESP-31 which has N and protein content of 2.02 and 14.94 wt% respectively. For microalga FSP-E, the N content in the microalga increased after pre-treatment in the acidic solutions but without any significant change in the solid yield. This incident could be deduced that the protein content in microalga FSE-E was not hydrolysed in the acidic solution at 160 ℃.

The volatile matter of microalga ESP-31 was enhanced after the wet torrefaction. The high percentage of volatile matter can relate to a better biofuel conversion process (Chaiwong et al., 2013). The low fixed carbon was observed for wet torrefied microalgae with the aid of acid due to the high volatile matter (Teh et al., 2017). However, the ash content of microalga ESP-31 was decreased after the wet torrefaction. This could be attributed to the demineralization process that occurs during wet torrefaction that reduces the ash content at the temperature of 150 ℃ (Zhang et al., 2017a). Furthermore, the pre-treatment in acidic solution removed the inorganic element in the biomass that assists in reducing the ash content (Wigley et al., 2015; Zhang et al., 2018c). The ash content of microalgae which was torrefied in the $H_3PO_4$ solution was relatively higher compared to other acidic solutions. It is because phosphorus is one of the elements that will produce ash during the combustion (Boström et al., 2012; Tan & Lagerkvist, 2011). The reduction of ash from the process is a positive attribute that makes microalgae a suitable source for power generation application. Liu et al. (2019b) revealed that the deashed microalgae

possesses stable combustion properties at high temperature zones and could be mixed with coal in combustion application.

**Table 4.4: Elemental analysis of wet torrefied microalgae**

| Microalgae | Solution | Acid (M) | Proximate analysis (dry basis, wt%) | | | Elemental analysis (dry-ash-free, wt%) | | | | Atomic ratio | |
|---|---|---|---|---|---|---|---|---|---|---|---|
| | | | VM | FC | Ash | C | H | N | O* | H/C | O/C |
| ESP-31 | Raw | - | 76.67±0.59 | 19.75±0.35 | 3.58±0.24 | 49.02±0.20 | 7.94±0.04 | 2.02±0.02 | 41.02±0.26 | 1.94 | 0.63 |
| | Water | - | 81.66±0.12 | 16.90±0.20 | 1.44±0.08 | 56.10±0.33 | 8.77±0.11 | 3.31±0.05 | 31.82±0.49 | 1.88 | 0.43 |
| | $H_2SO_4$ | 0.05 | 87.61±0.64 | 10.98±0.60 | 1.41±0.04 | 65.31±0.18 | 10.15±0.09 | 3.80±0.07 | 20.74±0.34 | 1.87 | 0.24 |
| | | 0.10 | 88.88±0.82 | 9.92±0.79 | 1.20±0.03 | 65.25±0.19 | 10.06±0.04 | 3.76±0.04 | 20.93±0.27 | 1.85 | 0.24 |
| | $H_3PO_4$ | 0.05 | 85.54±0.55 | 12.88±0.50 | 1.58±0.05 | 61.07±0.01 | 9.48±0.03 | 3.78±0.01 | 25.67±0.04 | 1.86 | 0.32 |
| | | 0.10 | 88.13±0.43 | 10.26±0.58 | 1.61±0.05 | 62.79±0.67 | 9.85±0.09 | 3.46±0.01 | 23.90±0.77 | 1.88 | 0.29 |
| | Succinic acid | 0.05 | 84.55±0.29 | 14.03±0.25 | 1.42±0.04 | 57.17±0.28 | 9.04±0.01 | 3.44±0.02 | 30.35±0.31 | 1.90 | 0.40 |
| | | 0.10 | 86.32±0.89 | 12.60±0.79 | 1.08±0.10 | 59.75±0.67 | 9.41±0.13 | 3.69±0.08 | 27.15±0.88 | 1.89 | 0.34 |
| FSP-E | Raw | - | 72.28±0.64 | 19.92±0.72 | 7.80±0.08 | 50.25±0.59 | 7.52±0.24 | 8.53±0.08 | 33.70±0.1 | 1.79 | 0.50 |
| | Water | - | 72.53±0.47 | 19.08±0.33 | 8.39±0.14 | 51.12±0.94 | 7.74±0.24 | 8.75±0.23 | 32.39±1.41 | 1.82 | 0.48 |
| | $H_2SO_4$ | 0.05 | 72.52±0.59 | 19.01±0.37 | 8.47±0.22 | 54.92±0.98 | 8.43±0.18 | 9.29±0.12 | 27.36±1.28 | 1.84 | 0.37 |
| | | 0.10 | 73.88±0.91 | 17.44±0.72 | 8.68±0.19 | 56.31±1.07 | 8.06±0.02 | 9.44±0.31 | 26.19±1.40 | 1.72 | 0.35 |
| | $H_3PO_4$ | 0.05 | 71.83±1.01 | 17.90±0.90 | 10.20±0.11 | 52.81±0.06 | 8.22±0.05 | 9.38±0.04 | 29.59±0.15 | 1.87 | 0.42 |
| | | 0.10 | 70.58±0.52 | 17.82±0.62 | 11.60±0.10 | 57.37±0.14 | 8.67±0.02 | 9.59±0.04 | 24.37±0.20 | 1.81 | 0.32 |
| | Succinic acid | 0.05 | 73.96±0.83 | 19.28±0.68 | 6.76±0.15 | 51.36±0.34 | 7.82±0.06 | 8.71±0.04 | 32.11±0.44 | 1.83 | 0.47 |
| | | 0.10 | 75.02±0.74 | 19.54±0.82 | 5.44±0.08 | 52.12±1.08 | 7.96±0.18 | 8.65±0.22 | 31.27±1.48 | 1.83 | 0.45 |

VM=Volatile matter
FC=Fixed carbon
*by difference

### 4.4.2 Chemical and crystalline structure characterisations

#### 4.4.2.1 FTIR analysis

The chemical structures of raw and wet torrefied microalgae in different acidic conditions were examined by FTIR spectra as presented in **Figure 4.8**. The spectra illustrated that most of the peaks remained after wet torrefaction but with varied intensity. The peaks at around 900–1200 cm$^{-1}$, 1400–1600 cm$^{-1}$ and 2800–3000 cm$^{-1}$ represent the carbohydrate, protein and lipid composition of the microalgae, respectively (Bach et al., 2017b). Based on **Figure 4.8a**, the peaks at 1532, 1628 cm$^{-1}$ (C=O and N–H of amide associated with proteins) and 2923 cm$^{-1}$ (C–H of C=CH– chains of lipids) were enhanced in acidic solutions when compared to raw microalgae and torrefied microalgae in water solution. This shows that the protein and lipid contents of microalga ESP-31 were enhanced in acidic wet torrefaction. The band absorption at 3304 cm$^{-1}$ corresponds to the stretching of H-bonded OH groups. For microalgae ESP-31 and FSP-E, the absorption decreased with wet torrefaction in the water solution, which reflects the process of deoxygenation and dehydration during wet torrefaction (Chen et al., 2012d; Zhang et al., 2019b). In contrast, the intensity of the band increased after wet torrefaction in the acidic solutions, indicating the presence of acid in microalgae after the wet torrefaction (Sindhu et al., 2010; Sindhu et al., 2011).
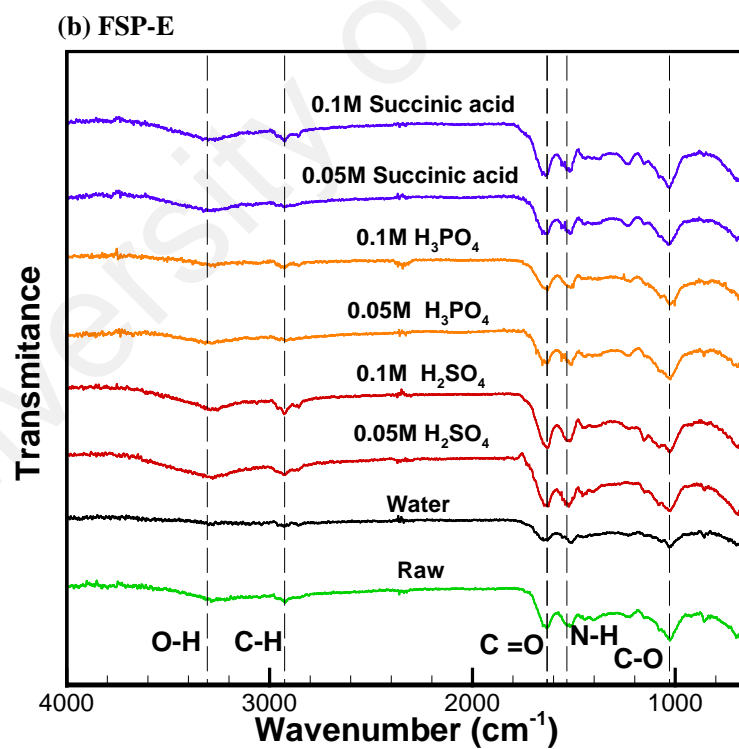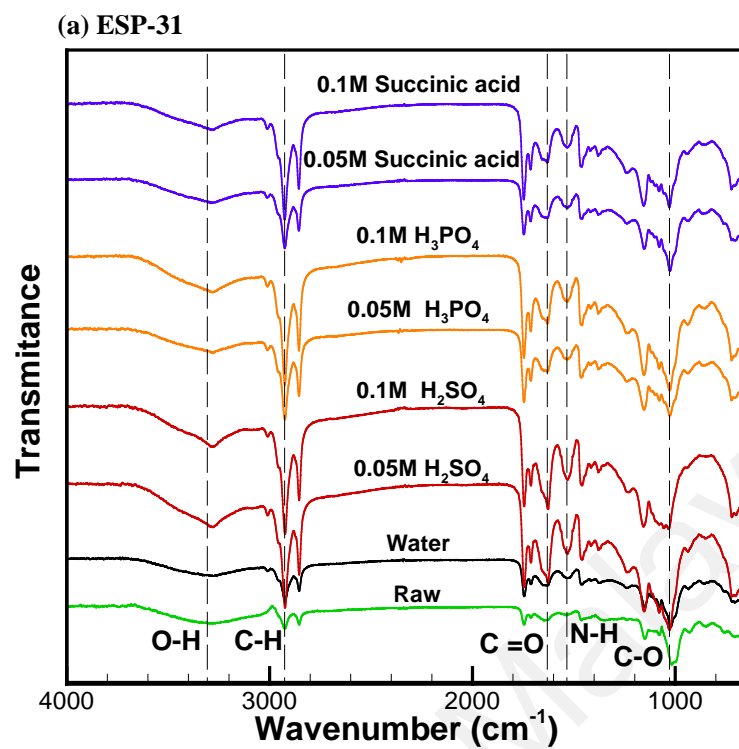
**Figure 4.8: FTIR analysis of wet torrefied microalgae (a) ESP-31 and (b) FSP-E**

### 4.4.2.2  XRD analysis

The XRD spectra of raw and torrefied microalgae are presented in **Figure 4.9** to analyse the crystalline cellulose structure. The carbohydrates of the microalgae mainly consist of starch and cellulose. The abundance of polysaccharide in microalgae *Chlorella vulgaris* is mainly contributed by starch, which is generally located in the chloroplast and composed of amylose and amylopectin (Safi et al., 2014). The cellulose in the microalgae is known as polysaccharide structure with large resistance, which is located on the microalgae cell wall as protective fibrous barrier. It was observed that a major diffraction peak of cellulose crystallographic plane occurred at 2θ with the range of 19–20º. The crystallographic plane of the microalgae usually ranges between 18–21º (Fabra et al., 2018; Huo et al., 2015), which is different from the lignocellulosic biomass that falls in the range of 22–23º (Chen et al., 2012c; Safar et al., 2019). **Figure 4.9a** shows the cellulose crystalline peaks increased after wet torrefaction, as the covered organic phase and starch could possibly dissolve into aqueous phase. However, cellulose crystalline peaks were further intensified when microalga ESP-31 was pre-treated in acidic solution. The cellulose crystalline structure was hardly destroyed by acidic solution pre-treatment with temperature as high as 180 °C (Chen et al., 2012c). The high concentration of crystalline cellulose remained after the wet torrefaction, which serves to enhance the formation of more cellulose-derived products during pyrolysis (Wang et al., 2018d). In contrast, the cellulose crystalline peaks in **Figure 4.9b** remained unchanged, indicating the cell structure of microalga FSP-E was not destroyed at low-temperature wet torrefaction. There were a number of semi-crystalline and poorly crystallized peaks detected at angles between 25 and 35º for raw microalga FSP-E, while no significant peak was observed for raw microalga ESP-31. Nanda et al. (2013) reported that part of the peaks in the XRD of biomass, biochar, and biomass ash were contributed by the minerals such as Na, Ca, Fe, Mg, Al, and Mn. After the wet torrefaction, the peak of microalga

FSP-E at around 26° was significantly decreased due to the demineralisation process (Zhang et al., 2017a). Based on the analyses of ash content and XRD, it could be concluded that the mineral content in the microalga FSP-E was higher than microalga ESP-31.

**(a) ESP-31**

0.1M Succinic acid

0.05M Succinic acid

0.1M H₃PO₄

0.05M H₃PO₄

0.1M H₂SO₄

0.05M H₂SO₄

Water

Raw

**(b) FSP-E**

0.1M Succinic acid

0.05M Succinic acid

0.1M H₃PO₄

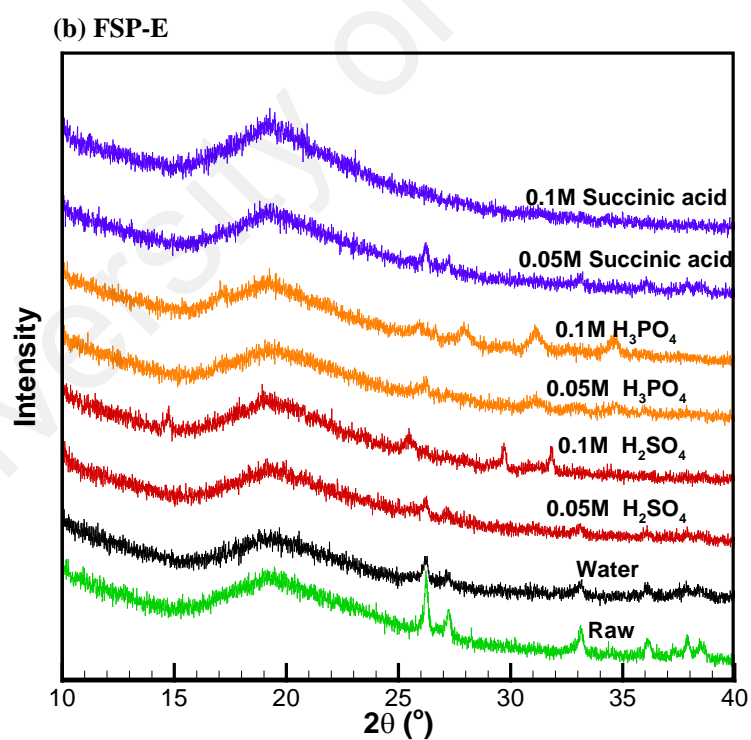0.05M H₃PO₄

0.1M H₂SO₄

0.05M H₂SO₄

Water

Raw
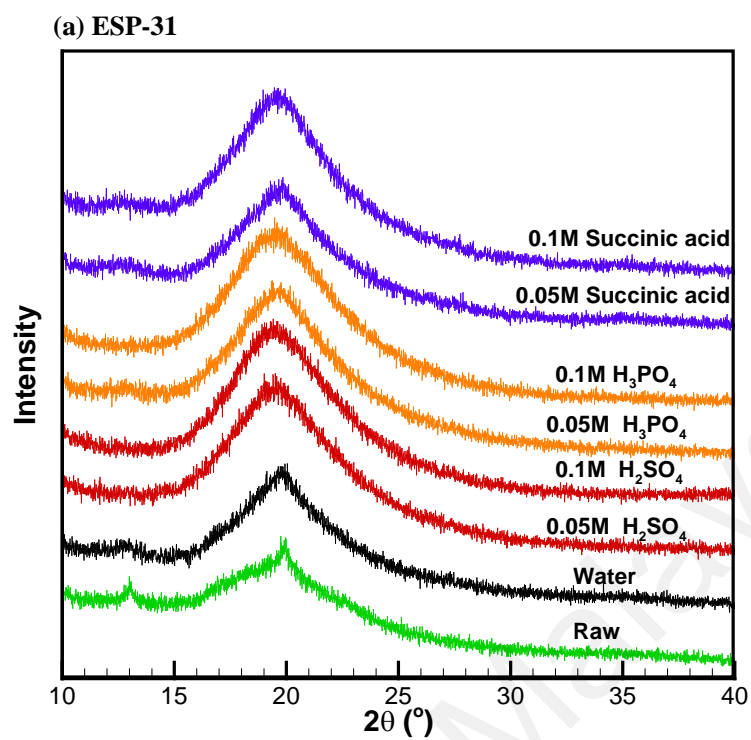
**Figure 4.9: XRD analysis of wet torrefied microalgae (a) ESP-31 and (b) FSP-E**

### 4.4.3 SEM surface analysis

The SEM images of raw and wet torrefied microalgae with different acidic solutions are demonstrated in **Figure 4.10** and **Figure 4.11**. The microalgae morphology with the magnification of 500, 5000 and 15000 were analysed. The surface morphology of microalga ESP-31 was influenced by the wet torrefaction as shown in **Figure 4.10**. By observing the raw microalga ESP-31 using SEM, some pores and cracks were observed on the surface and internal structure. When the microalgae were pre-treated in wet torrefaction, the disruption on the surface and porous structure was clearly observed. A larger pore structure in biochar is beneficial to improve the combustion properties of biochar (Zhang et al., 2019a). Pores in the biochar are responsible for the transport of oxygen gas into the deep inside of the biochar structure (Dudzińska, 2014). At the initial stage, self-heating of biochar is determined by amount of oxygen absorbed in porous structure of the biochar. In addition, a clear porous structure was observed on the surface of wet torrefied microalgae, which was contributed by the release of volatile and degradation of carbohydrates (Bach et al., 2017b; Zhang et al., 2019b). This phenomenon promoted the low solid and energy yield of the microalgae after torrefaction. For raw microalga FSP-E, no obvious cracks and pores were observed on the surface, as shown in **Figure 4.11**. After the wet torrefaction, the small porous holes observed on the surface of the microalgae with the magnification of 5000, which is similar to those reported by Liu et al. (2019b). The small porous holes could be due to the decomposition of the low volatile matters and carbohydrates of the microalgae during the wet torrefaction. Meanwhile, small porous holes were increased for the microalgae undergoes wet torrefaction in $H_2SO_4$ due to the extra $H^+$ ions.

| Biomass | ×500 | ×5000 | ×15000 |
|---------|------|-------|--------|
| Raw | | | |
| Water | | | |
| 0.05 M H₂SO₄ | | | |
| 0.1 M H₂SO₄ | | | |
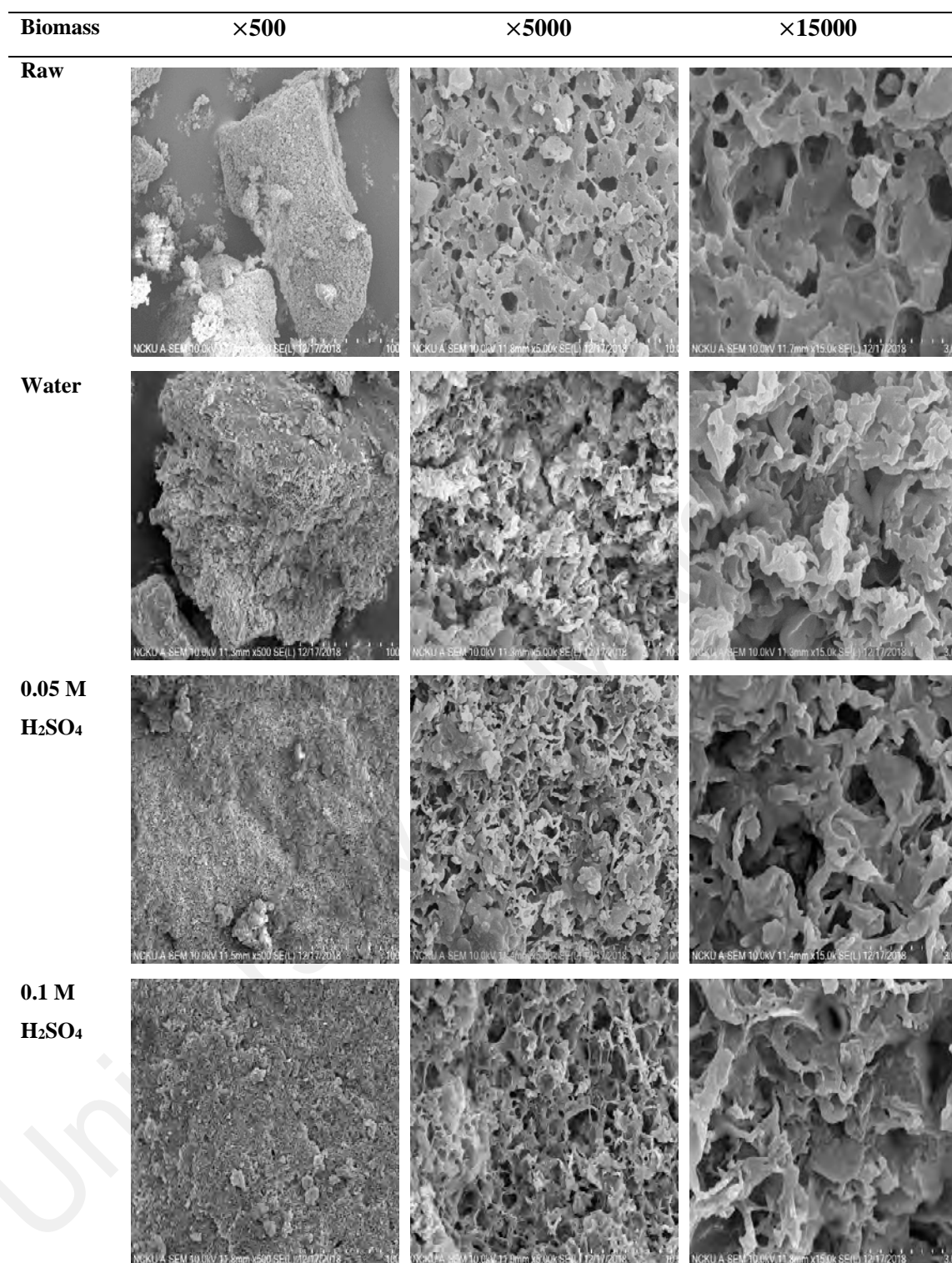


**Figure 4.10: SEM images of microalga *Chlorella vulgaris* ESP-31 with different**

**types of acid treatment**

| Biomass | ×500 | ×5000 | ×15000 |
|---------|------|-------|--------|
| 0.05 M H$_3$PO$_4$ | | | |
| 0.1 M H$_3$PO$_4$ | | | |
| 0.05 M Succinic acid | | | |
| 0.1 M Succinic acid | | | |

**Figure 4.10, continued**

130

| Biomass | ×500 | ×5000 | ×15000 |
|---------|------|-------|--------|
| Raw | | | |
| Water | | | |
| 0.05 M H₂SO₄ | | | |
| 0.1 M H₂SO₄ | | | |
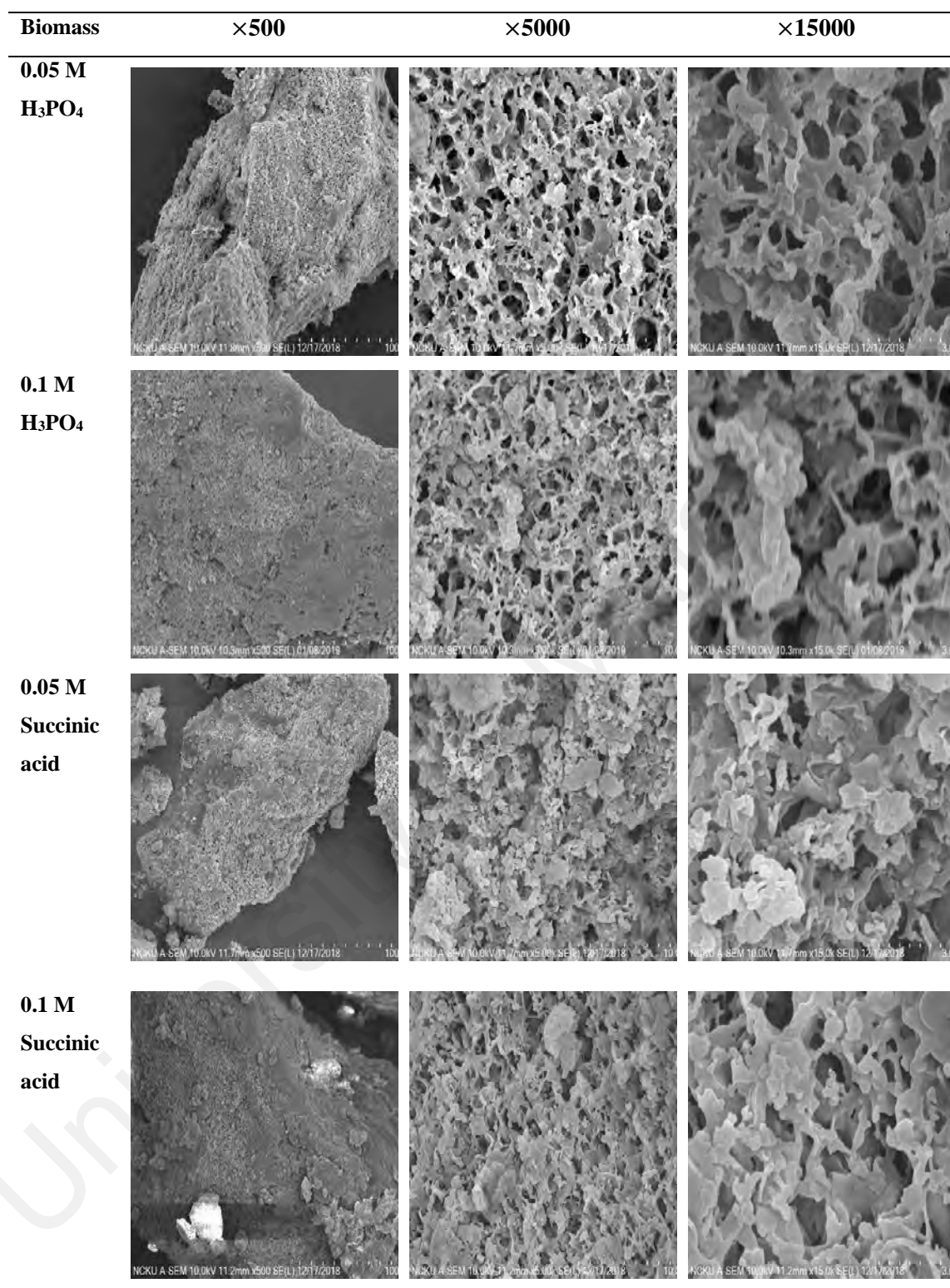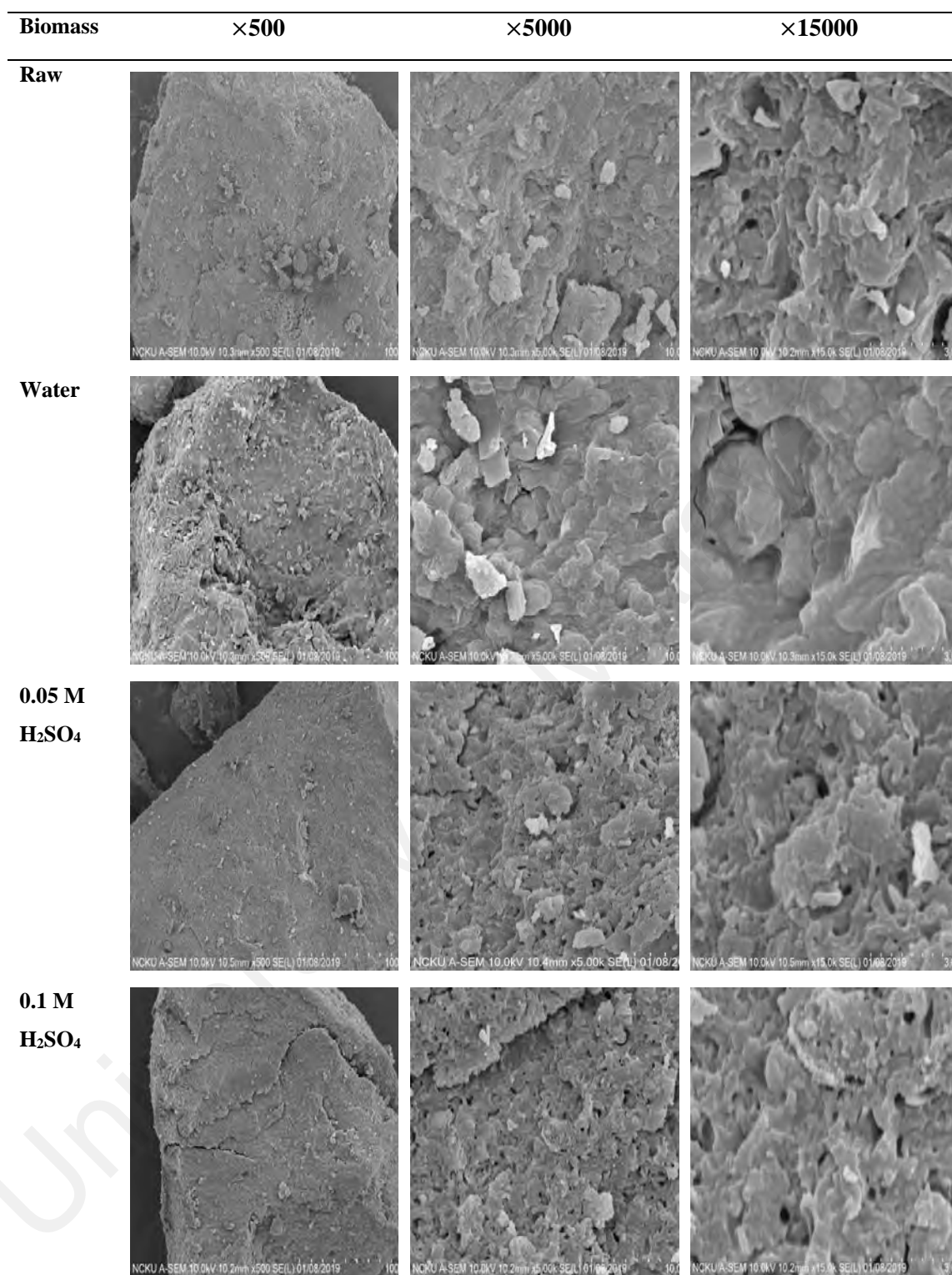


**Figure 4.11: SEM images of microalga Chlorella vulgaris FSP-E with different**

**types of acid treatment**

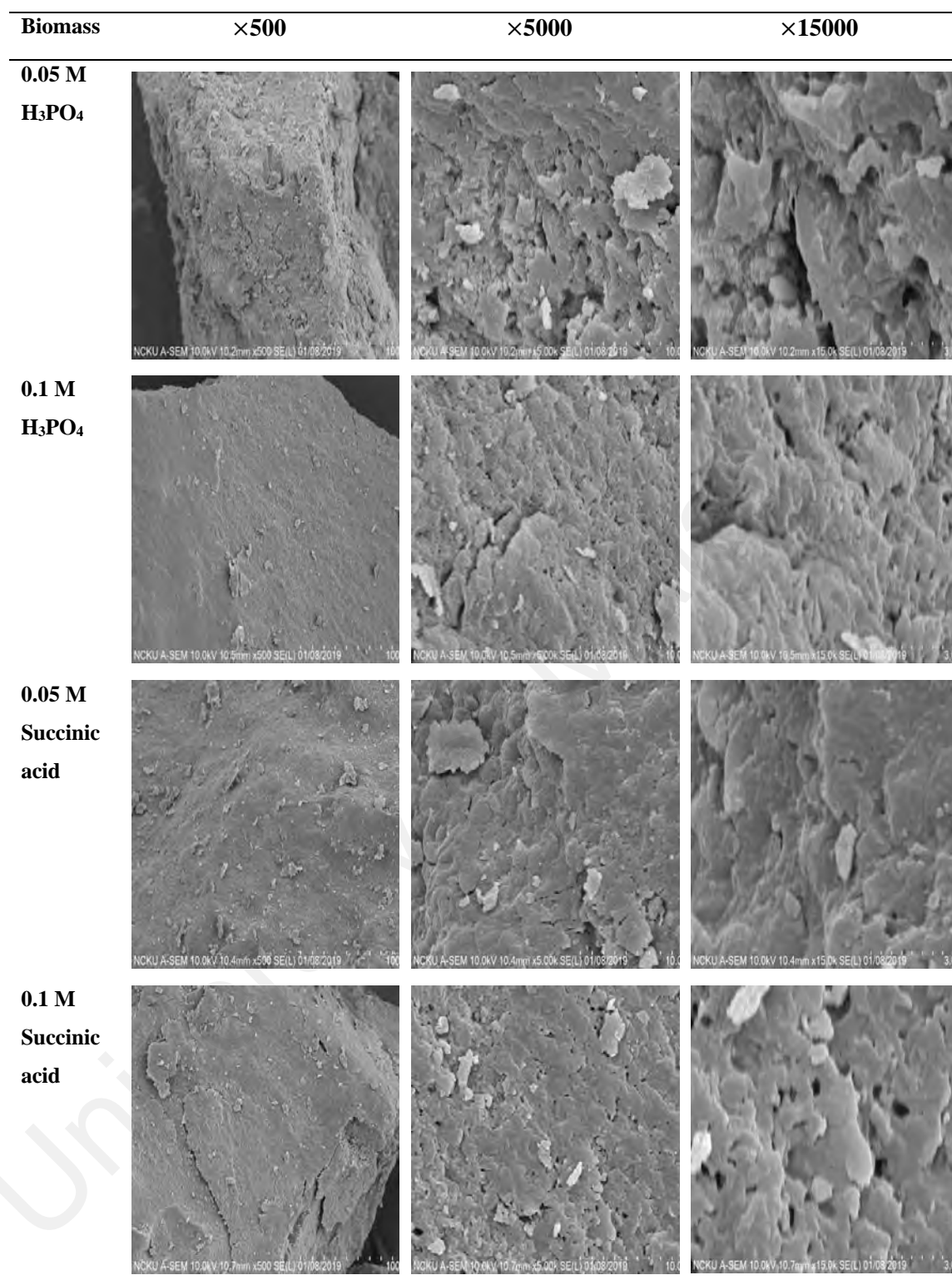| Biomass | ×500 | ×5000 | ×15000 |
|---|---|---|---|
| 0.05 M H₃PO₄ | | | |
| 0.1 M H₃PO₄ | | | |
| 0.05 M Succinic acid | | | |
| 0.1 M Succinic acid | | | |



**Figure 4.11, continued**

### 4.4.4 Thermal decomposition behaviour

In order to study the effectiveness of microalgae wet torrefaction in acidic solutions, the thermal decomposition behaviour of raw and wet torrefied microalgae was performed to analyse the changes of the chemical compositions in microalgae pre-treated by wet torrefaction. The TGA and DTG curves of raw and wet torrefied microalgae studied in an N$_2$ environment in a temperature range of 105−800 °C are presented in **Figure 4.12** and **Figure 4.13**. The weight loss for the first stage (200–350 °C) was mainly due to the decomposition of carbohydrates and proteins, whereas the second stage (350–550 °C) was due to lipid decomposition (Chen et al., 2018b; Chen et al., 2014e). Based on the DTG curve in **Figure 4.12a**, it was noticed that the first peak decreased after low-temperature wet torrefaction, whereas the second peak was intensified. The decrease in the first peak was mainly due to carbohydrate decomposition, as was reported previously that higher wet torrefaction temperature was required to degrade the proteins. The result was different from the dry torrefaction of microalgae. The torrefaction temperature of 200 °C and above were required to decrease and shift the first peak (Chen et al., 2016). The degradation of the first peak decreased with the use of acidic solutions. Then, the peak was further decreased with the increase in acid concentration, comparable to the trend exhibited by macroalgae (Teh et al., 2017), bamboo (Li et al., 2015) and sugarcane bagasse (Chen et al., 2012c) in other studies. In contrast, microalga FSP-E only produced one DTG peak due to the different in the chemical composition, as shown in **Figure 4.12b**. A shoulder in the raw microalga was removed after the wet torrefaction in water and acidic solutions, indicating the low volatile materials were completely decomposed. In addition, it was noticed that the first peak slightly increased after wet torrefaction, but the first peak was not shifted to higher or lower temperature. The change in the first peak after wet torrefaction was mainly due to carbohydrate decomposition and the increase in the protein

content. Furthermore, the first peak was slightly decreased with the increase in the acid concentration due to the increase in the carbohydrate decomposition.

From **Figure 4.13a**, it was observed that the order of the carbohydrate decomposition is in the sequence of $H_2SO_4$ > $H_3PO_4$ > succinic acid > water. Succinic acid is an organic acid, which is relatively weak and safe compared to the inorganic acids. The decrease in first peak was comparatively lower by using succinic acid compared to other acidic solutions. The use of $H_2SO_4$ in wet torrefaction of microalga ESP-31 showed the highest degradation in the carbohydrates compared to $H_3PO_4$, succinic acid and water for the acid concentration of 0.05 and 0.1 M. Teh et al. (2017) revealed that the use of 160 °C with 0.1 M $H_2SO_4$ was the optimum condition to hydrolyse carbohydrates in macroalgae. As shown in **Figure 4.13b**, no obvious modification to the DTG curve was shown when microalga FSP-E was torrefied in different acidic solutions. Microalga FSP-E contains relatively low carbohydrates and high proteins, hence resulting in fewer changes in the first peak as compared to microalga ESP-31. For microalga FSP-E, it was observed that no significant changes to solid yield and HHV enhancement in the different acidic solutions, as supported by the evidence of TGA and DTG curves as shown in **Figure 4.13b**.
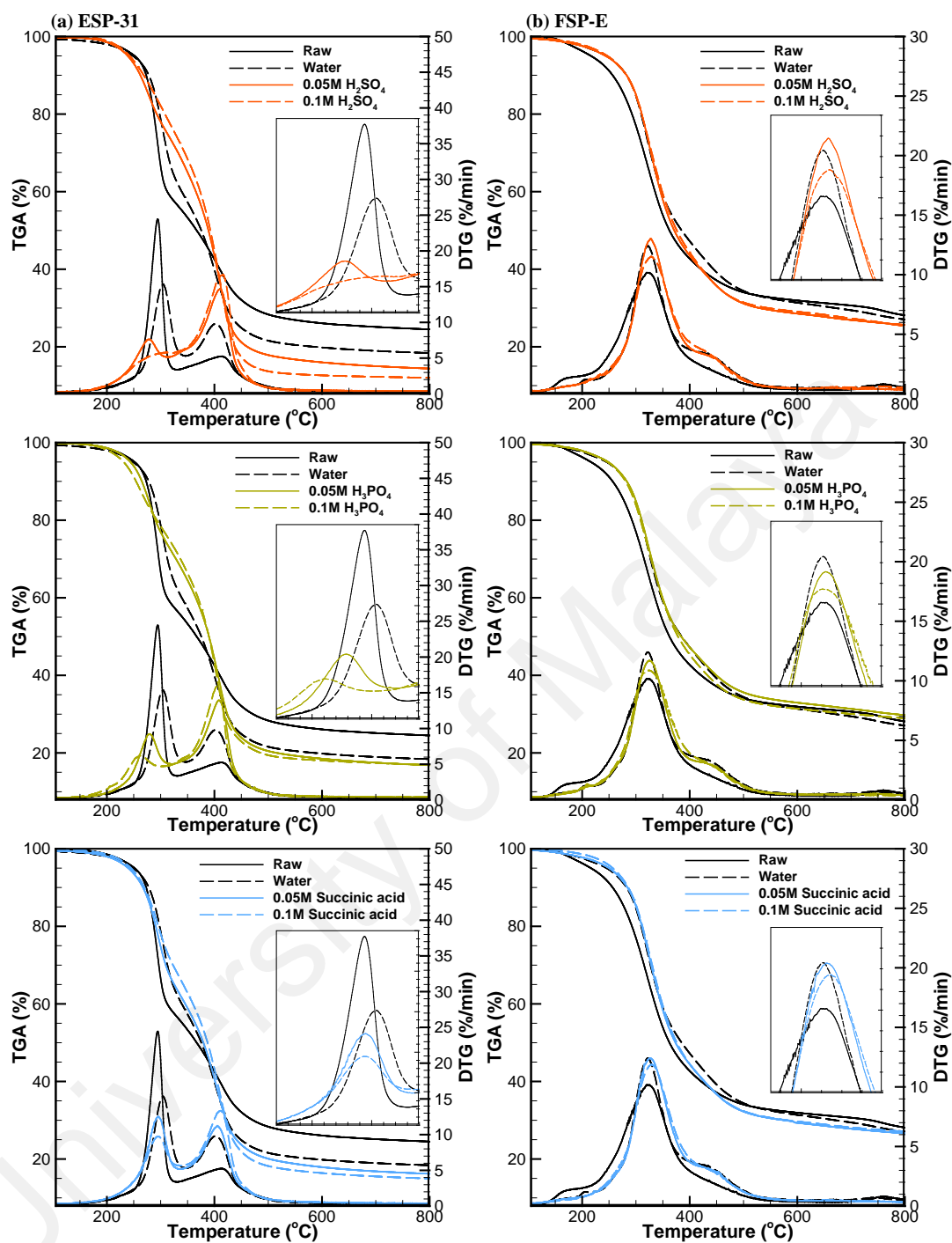
**Figure 4.12: Thermal decomposition behaviour of wet torrefied microalgae using different acid concentration (a) ESP-31 and (b) FSP-E**
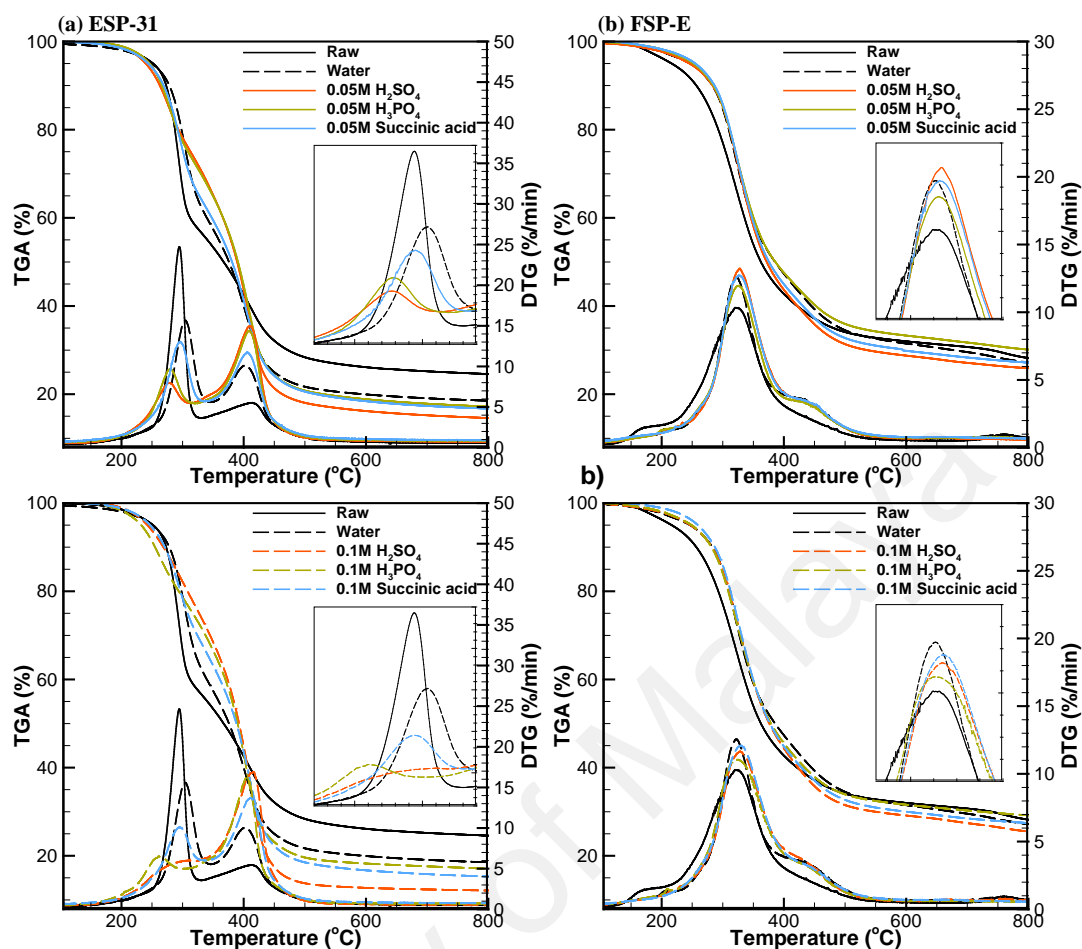
**Figure 4.13: Thermal decomposition behavior of wet torrefied microalgae with different type of acid (a) ESP-31 and (b) FSP-E**

### 4.4.5   Hydrolysates

The glucose and the by-products produced by 20 g of microalgae hydrolysis are presented in **Table 4.5**. Starch is the most abundant polysaccharide in microalgae *Chlorella vulgaris* (Safi et al., 2014). Starch is easier to be hydrolysed in hydrothermal water as compared to cellulose, where the by-products such as 5-hydroxymethylfurfural (5-HMF) and furfural can be produced easily (Nagamori & Funazukuri, 2004). The production of the by-products inhibits bioethanol production and requires costly downstream waste treatment (Chen et al., 2013). Hydrolysis was the first reaction step occurred during the wet torrefaction (Acharya et al., 2015). Carbohydrates in the

microalgae will be break down and hydrolysed into monomers such as fermentable sugars (Zabed et al., 2020). The glucose extracted from the microalgae is fermentable sugar, which can be metabolised by microorganisms to carry out bioconversion into bioethanol through fermentation process (Phwan et al., 2018). For wet torrefaction of microalga FSP-E, relatively low glucose was extracted due to the low carbohydrate content in the microalga. The amount of glucose extracted from the microalga ESP-31 was distinctively higher than microalga FSP-E. After wet torrefaction of microalga ESP-31 in water solution, 1.65 g/L of glucose with relatively low 5-HMF and furfural were formed. Most of the carbohydrate was not hydrolysed and remained in the microalga. The glucose content increased to 35.39 g/L when microalga was torrefied in 0.1 M $H_2SO_4$ solution, owing to the extra $H^+$ ions produced by sulfuric acid which created more acidic solution. A high extraction of glucose caused the low solid and energy yield as shown in **Figure 4.7**. Jeong et al. (2012) revealed that $H_2SO_4$ was the most favourable catalyst for glucose production among the four different types of acid catalysts (HCl, $H_2SO_4$, $HNO_3$, and $H_3PO_4$). Choi et al. (2015) proved that the cell structure of microalgae was hydrolysed in hydrothermal $H_2SO_4$ treatment via the production of high sugar content. In contrast to $H_2SO_4$, $H_3PO_4$ is a weak acid that produces less glucose content due to incomplete carbohydrate hydrolysis. At the same time, high 5-HMF content was produced, mainly ascribing to the nature of the inorganic acid which could influence the production of 5-HMF (Chheda et al., 2007). Since 5-HMF comprises of aldehydes and hydroxymethyl groups, it can be further converted into a sequence of high quality fuels such as 2,5-dimethylfuran and 5-ethoxymethyfurfural, as well as high-value chemicals including levulinic acid, 2,5-dimethyltetrahydrofuran and 2-hexanol (Wang et al., 2019). Among the three acids used, lowest glucose content was produced by using succinic acid due to the nature of weak organic acid as compared to the inorganic acid. Thus, higher wet

torrefaction temperature, heating time and acid concentration are required to hydrolyse the carbohydrates using organic acid.

Table 4.5: Concentration of glucose and by-products

| Microalgae | Solution | Acid concentration (M) | Glucose (g/L) | 5-HMF (g/L) | Furfural (g/L) |
|---|---|---|---|---|---|
| ESP-31 | Water | - | 1.65 | 0.07 | 0.02 |
| | $H_2SO_4$ | 0.05 | 6.45 | 0.27 | 0.07 |
| | | 0.1 | 35.39 | 1.69 | 0.25 |
| | $H_3PO_4$ | 0.05 | 4.88 | 0.31 | 0.08 |
| | | 0.1 | 9.66 | 1.33 | 0.32 |
| | Succinic | 0.05 | 1.95 | 0.35 | 0.08 |
| | acid | 0.1 | 3.49 | 0.49 | 0.10 |
| FSP-E | Water | - | 0.62 | - | - |
| | $H_2SO_4$ | 0.05 | 0.69 | - | - |
| | | 0.1 | 0.71 | - | - |
| | $H_3PO_4$ | 0.05 | 0.64 | - | - |
| | | 0.1 | 0.68 | - | - |
| | Succinic | 0.05 | 0.70 | - | - |
| | acid | 0.1 | 0.71 | - | - |

## 4.5 In-depth analysis of microalgae using TG-FTIR and Py-GC/MS approaches

### 4.5.1 Thermal behaviour analysis using TG

#### 4.5.1.1 Pyrolysis behaviour of wet torrefied microalgae

The pyrolysis TGA and DTG curves of raw and wet torrefied microalgae ESP-31 in water and three different acidic solutions are shown in **Figure 4.14**. The curves were employed to study the real-time evolved gas by coupling the TG with FTIR, which means the thermal degradation of the microalgae and the evolved gas during the pyrolysis from 105 to 800 ℃ could be examined simultaneously. At the early stage of the pyrolysis (<200 ℃), part of the weight loss was observed in the TGA curve due to the dehydration process of the microalgae (Bach & Chen, 2017b). The main thermal degradation of microalgae pyrolysis occurred at temperatures higher than 200 ℃, which can be divided into three main stages. The first stage (200−350 ℃) resulted in the thermal degradation of

carbohydrates and proteins, the second stage (350−550 °C) resulted in the thermal degradation of lipids, while the degradation of carbonaceous matters in the biochar occurred at a very slow rate in the third stage (550−800 °C) (Chen et al., 2014e). For the raw microalga, a large DTG peak of 27.27 wt%/min at 294 °C and the second DTG peak of 5.09 wt%/min at 413 °C were observed in the first and second stages. A large degradation of the raw microalga in the first stage was due to the high carbohydrate composition (49.7%). Based on the DTG curve in **Figure 4.14a**, the first peak (15.15 wt%/min) of the wet torrefied microalga in the water was decreased and slightly shifted to higher temperature, whereas the second peak (9.61 wt%/min) was slightly intensified. During the wet torrefaction, the destruction of the microalgae cell wall and structure could occur. Part of the carbohydrates was hydrolysed due to the poor hydrolysis resistance and high reactivity to the wet torrefaction process (Bach et al., 2017b), as the carbohydrates were more solubilized than the proteins at low temperature (Bougrier et al., 2008). After the torrefaction in the acidic solutions, the first DTG peak further decreased with the enhancement of the second DTG peak. The first DTG peaks of the wet torrefied microalgae in succinic acid, $H_3PO_4$ and $H_2SO_4$ were 9.46, 5.96 and 5.53 wt%/min, respectively, while the second DTG peaks were 13.06, 15.68 and 16.40 wt%/min, respectively. The $H_2SO_4$ showed the highest reduction in the first peak because of the high acidic medium which was created by the extra $H^+$ ion. In contrast to $H_2SO_4$, $H_3PO_4$ was less aggressive than $H_2SO_4$, providing less degradation of the carbohydrates compared to $H_2SO_4$. Succinic acid is an organic acid, which creates less acidic medium and less hazardous compared to the inorganic acid. The degradation of the carbohydrates was comparatively lower when using succinic acid compared to $H_3PO_4$ and $H_2SO_4$.
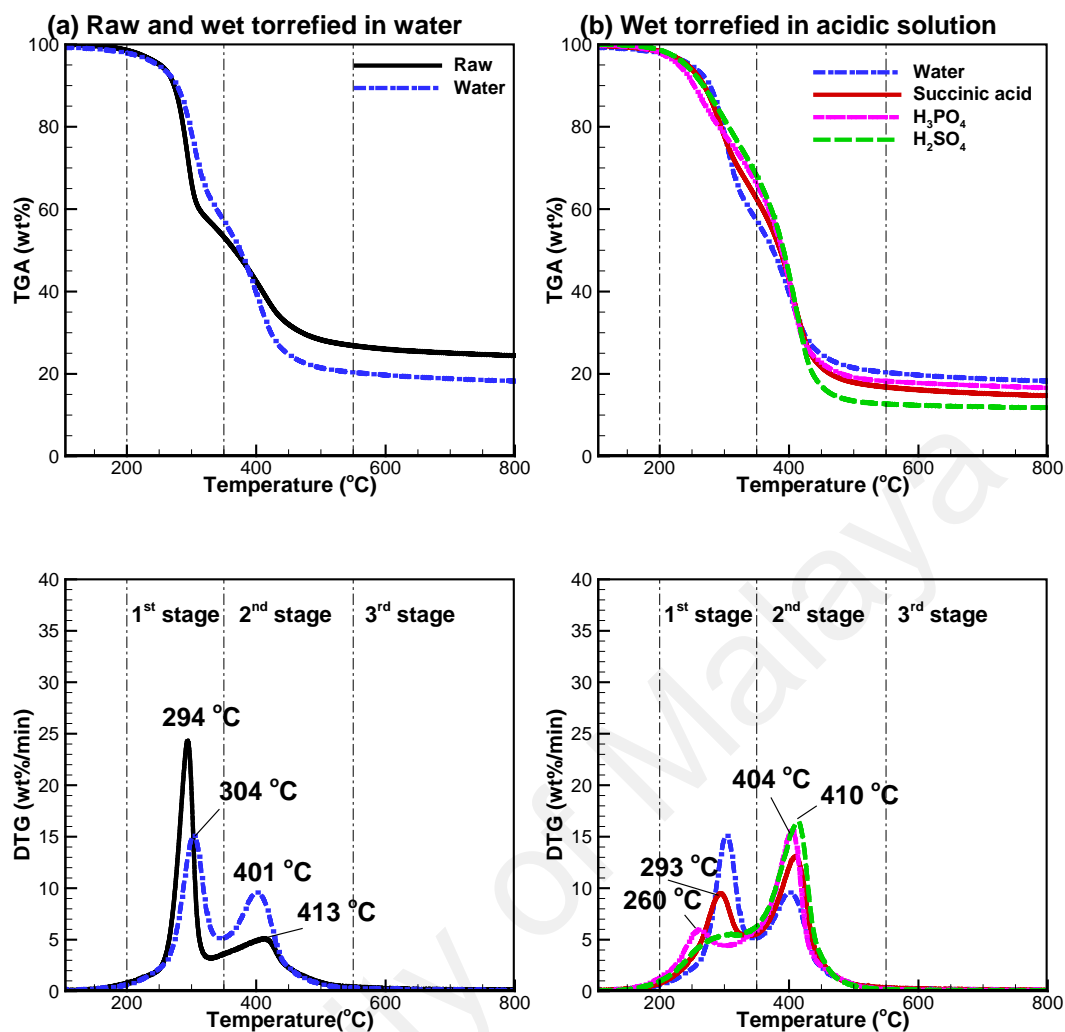
**Figure 4.14: Pyrolysis TGA and DTG curves of microalgae (20 °C/min, 100 mL/min of N₂): (a) raw and wet torrefied in water and (b) wet torrefied in acidic solutions**

### 4.5.1.2 Combustion behaviour of wet torrefied microalgae

The combustion TGA and DTG curves of raw and wet torrefied microalgae are shown in **Figure 4.15**. The weight loss in the TGA curve depicts the combustion process including dehydration, removal of volatile, volatile ignition, and char combustion (Magdziarz & Wilk, 2013). Based on the TGA and DTG curves, the wet torrefied microalgae in acidic solutions are more reactive than the raw and wet torrefied microalgae

in the water at temperatures lower than 275 °C, which may be attributed to the cell destruction during the acid hydrolysis (Harun & Danquah, 2011). The detailed combustion behaviour of microalgae was examined in the DTG curve. Similar to the pyrolysis, the dehydration of the microalgae occurred at an early stage, which was less than 200 °C (Lee et al., 2019). The first stage (200−350 °C) mainly showed the devolatilization and oxidative reactions of the low thermal combustion of carbohydrates and proteins (Chen et al., 2016). The second stage (350−500 °C) indicated the devolatilization and combustion of more thermal stable components such as lipids, while the third stage elucidated the combustion of the produced chars at high temperature (Liu et al., 2019b). The largest DTG peak (30.91 wt%/min) at 291 °C and the shoulder (5.00 wt%/min) at 337 °C of the raw microalga corresponded to the carbohydrate and protein combustion. The first DTG peak was decreased after the wet torrefaction in water and acidic solutions, contributing by the thermal degradation of carbohydrates during the wet torrefaction. The DTG peak (7.04 wt%/min) of the wet torrefied microalga in water developed at 361 °C, probably due to the combustion of char produced from the decomposition of carbohydrates and proteins during the pre-treatment (Chen et al., 2016). It was noticed that only one DTG peak was observed on the second stage for the wet torrefied microalgae. Repolymerization reactions of the microalgae to other components could take place during the hydrothermal pre-treatment (Lee et al., 2018). In addition, the char combustion DTG peaks of the wet torrefied microalgae were wider and allocated at higher temperatures compared to the raw microalga. This phenomenon indicated that the char produced from the wet torrefied microalgae were more stable and less reactive (Bach et al., 2017b).
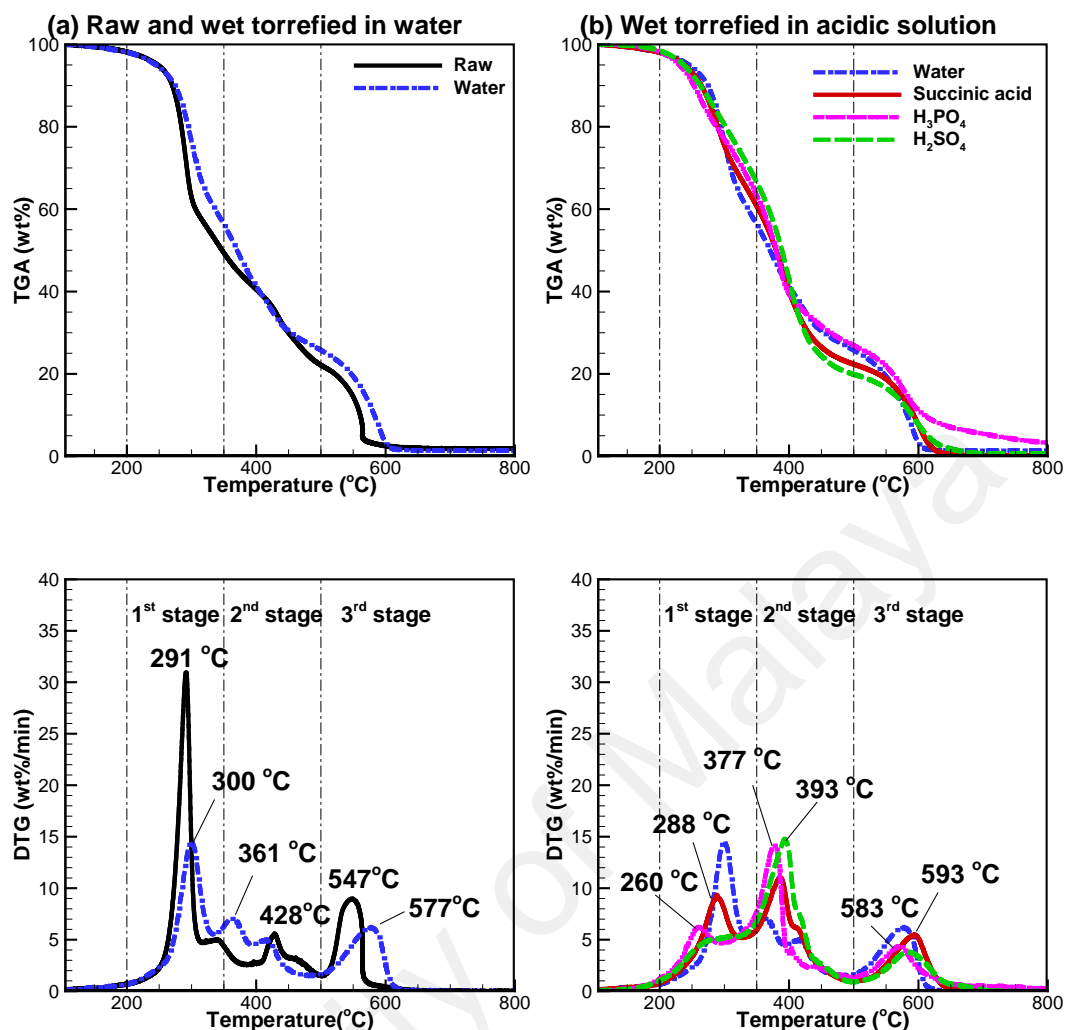
**Figure 4.15: Combustion TGA and DTG curves of microalgae (20 °C/min, 100 mL/min of air): (a) raw and wet torrefied in water and (b) wet torrefied in acidic solutions**

### 4.5.1.3 Torrefaction behaviour

The torrefaction TGA and DTG curves of the raw microalga torrefied at three different temperatures (200, 250 and 300 °C) for 20 min are presented in **Figure 4.16**. The first DTG peak represents the torrefaction of microalgae, while the second DTG peak stands for the pyrolysis of the torrefied microalgae. After the torrefaction, the solid yields of the microalgae at 200, 250, and 300 °C were 91.32, 66.42, and 50.50 wt%, respectively. The

TGA and DTG curves describe that the thermal degradation of microalgae was not significant in light torrefaction (200 °C). A small first DTG peak of 0.61 wt%/min was observed mainly due to the dehydration of the microalgae in light torrefaction. In contrast, a wider range of first DTG curve with a peak of 2.22 wt%/min was observed at mild torrefaction, which indicated the weight loss of the microalgae increased with the holding time. This scenario implied that torrefaction time played an important role for mild torrefaction due to the high reactivity of the microalgae components at a temperature of 250 °C (Chen et al., 2014e). During the severe torrefaction, an extreme weight loss was also noticed at the beginning of the torrefaction temperature. The maximum DTG peak of 21.96 wt%/min was determined due to the thermal degradation of the carbohydrates in the microalgae, corresponding to the devolatilization process (Chen et al., 2016). By comparing the DTG peaks during the torrefaction, a high torrefaction temperature provided a high DTG peak. It could be concluded that the increase in torrefaction temperature is more crucial to the thermal degradation of the microalgae, while the holding time is only significant at mild torrefaction.
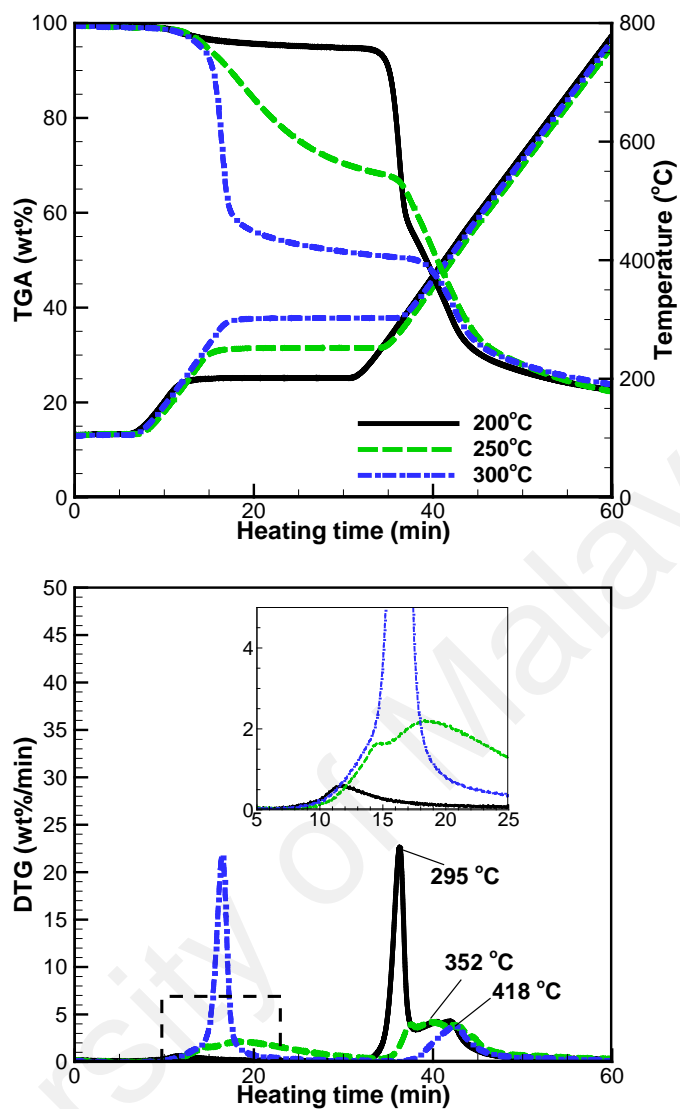
**Figure 4.16: Torrefaction TGA and DTG curve of microalgae**

### 4.5.2 Evolved gas analysis using TG-FTIR

### 4.5.2.1 Pyrolysis gas

The three-dimensional FTIR spectra of the pyrolysis gas analysis of raw and wet torrefied microalgae are displayed in **Figure 4.17**. **Table 4.6** shows the summary of FTIR functional groups and wavenumbers of gaseous products during the pyrolysis. $H_2O$, $C-H$, $CO_2$, $CO$, $C=C$, $C=O$, and $C-O$ were the gaseous products from the main reaction stage of the microalgae pyrolysis. The evolution of gaseous products corresponded to the weight loss of microalgae displayed in the TGA curve. A relatively flat profile at the early stage of the pyrolysis ($<200\ ℃$) indicated no gas release from the dehydration process of the microalgae. The pyrolysis gas was observed when the temperature was higher than $200\ ℃$, where the main thermal degradation of the microalgae components occurred, as shown in **Figure 4.14**. The emission of $CO_2$ significantly decreased after the wet torrefaction, especially in acidic solutions. The non-condensable gas including $CO_2$ and $CO$ were released during the torrefaction (Niu et al., 2019). The intensity of the $C-H$ absorption band was observed with the order of water, succinic acid, $H_3PO_4$ and $H_2SO_4$, which can be attributed to the high lipid decomposition. A similar trend was found in the pyrolysis DTG peak in the second stage. The $C-H$ absorption band could be determined after the microalgae pyrolysis process, which was caused by the secondary cracking and methanation of bio-oil (Widyawati et al., 2011).
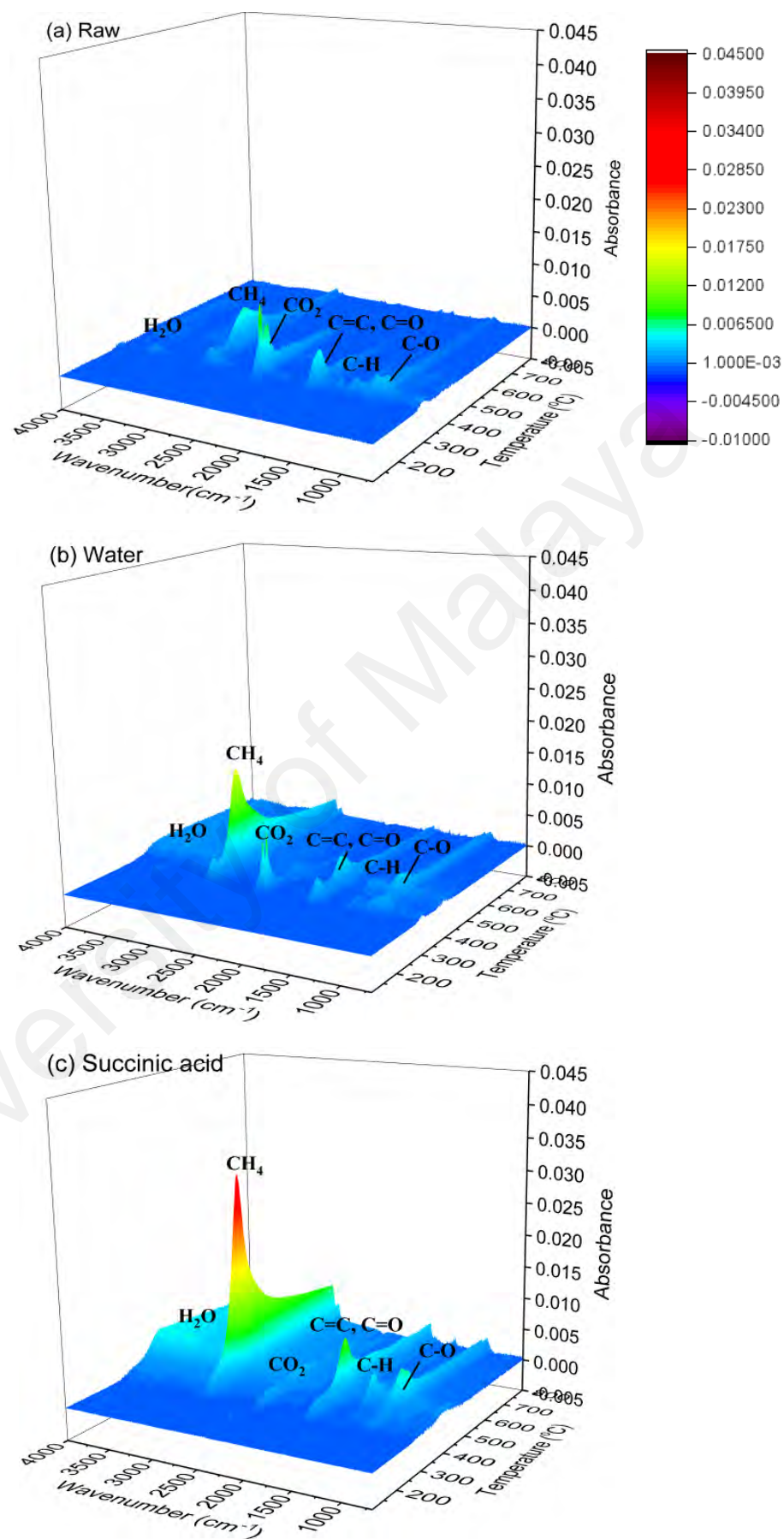
**Figure 4.17: 3D analysis of raw and wet torrefied microalgae pyrolysis gas**
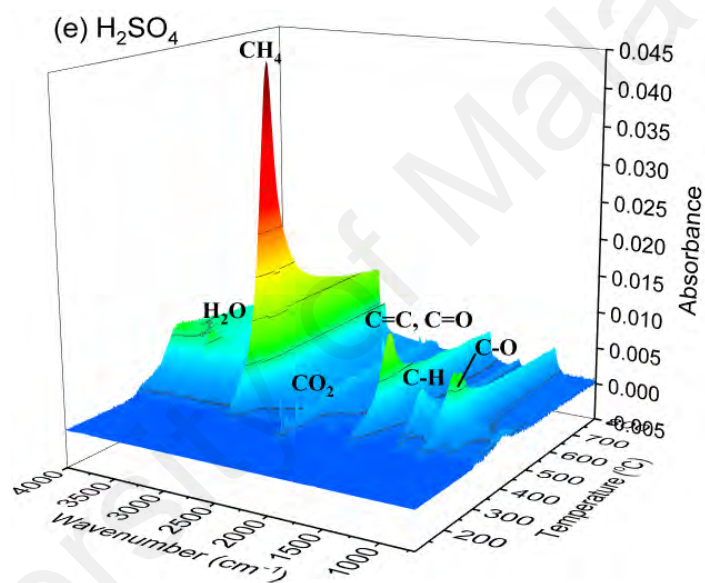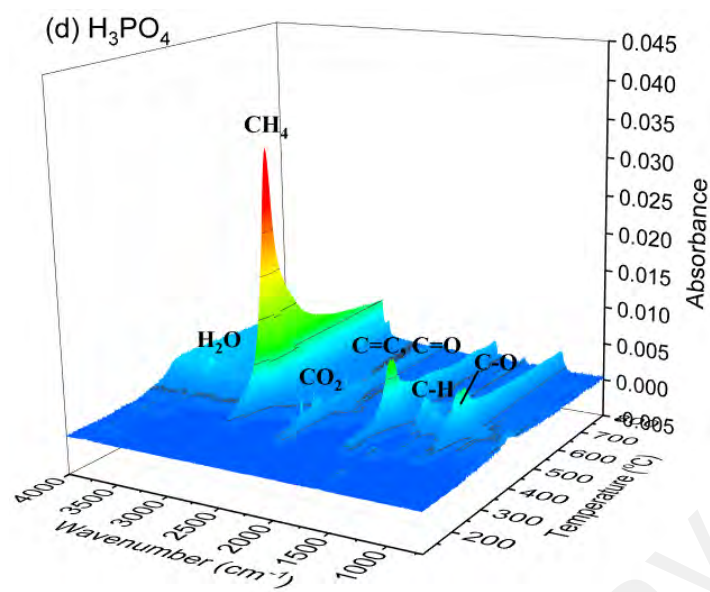
**Figure 4.17, continued**

**Table 4.6: Summary of functional groups and wavenumber of gaseous products during pyrolysis and combustion**

| Assignment | Wavenumber (cm$^{-1}$) | Possible compounds (Peng et al., 2015; Wang et al., 2018a) |
|---|---|---|
| O−H | 4000−3500 | Water, alcohols and carboxylic acids |
| C−H | 3000−2850 (2932) | Alkanes stretch, Hydrocarbons |
| O=C=O | 2400−2240, 780−560 | $CO_2$ |
| C−O | 2240−2060 | CO |
| C=O, C=C | 1850−1600 | Ketones, aldehydes, carboxylic acids, primary amides, esters |
| O−H | 1875−1275 | Water |
| C−O, O−H | 1300−950 | Ethers, alcohols, phenols |

In **Figure 4.17**, several peaks of gaseous products were detected at the temperatures of the first and second DTG peaks. In order to provide a deep analysis of the pyrolysis gas characteristic from the raw and wet torrefied microalgae, the FTIR spectra were selected based on the DTG peak temperature of each stage as shown in **Figure 4.18**. The first stage of the pyrolysis gas was mainly contributed by the thermal degradation of the microalgae carbohydrates, whereas the second stage was contributed by the thermal degradation of microalgae lipids. Marcilla et al. (2009) evaluated the pyrolysis gas of each microalgae single component by using glucose, glutamine and tripalmitine as carbohydrate, protein and lipid, respectively. The absorption band of the glucose presented a low intensity of C–H at 2850–2970 cm$^{-1}$, whereas the important absorption band corresponding to $CO_2$ emission appeared at 2250–2400 cm$^{-1}$. At the same time, the absorption bands of C=O and C–O could be identified in the FTIR spectra. The low intensity of C–H band could be related to the lipid components decomposition. The $CO_2$ absorption band was more important than other adsorption bands in the FTIR spectra for glutamine, whereas the C–H and C=O were the important adsorption band in tripalmitine.
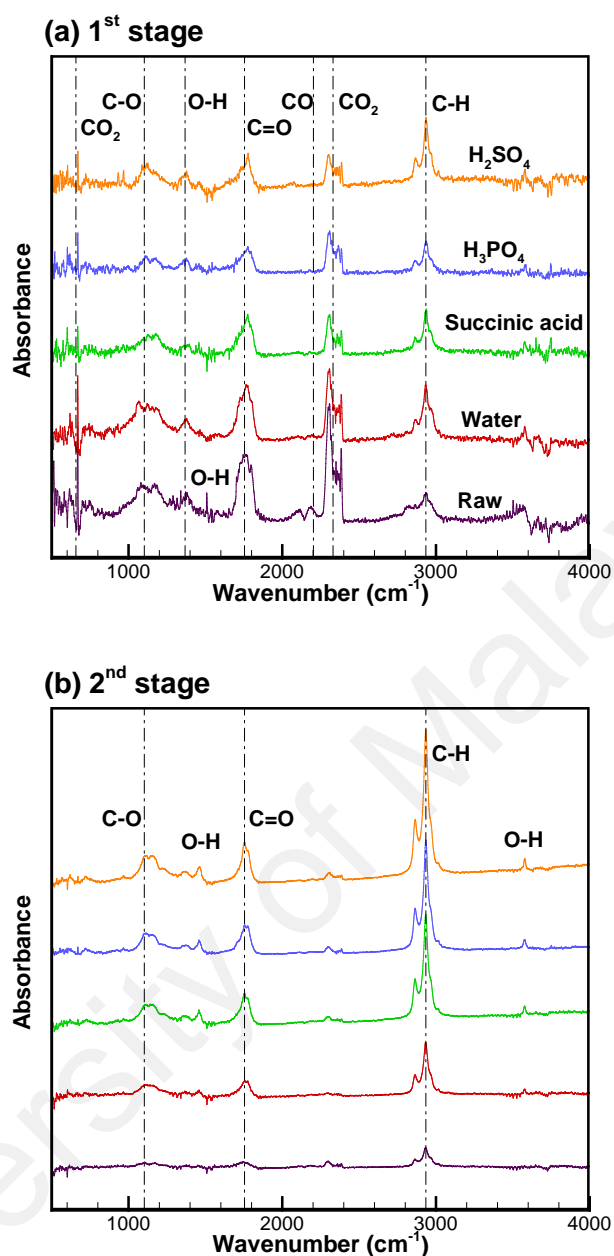
**Figure 4.18: FTIR spectra of gaseous released during the pyrolysis at first and second DTG peaks**

The absorption band on the water in the first stage was observed in the raw microalga with the vibrational modes contributed to the range of 1875–1275 cm$^{-1}$, indicating the release of water during the pyrolysis at the first stage. For raw microalga, $CO_2$, C=O, and C–O absorption bands were clearly determined in the first stage of FTIR spectra due to the degradation of carbohydrates (Peng et al., 2015). The C–H absorption band

corresponded to the small amount of lipid degradation as the degradation of lipid could occur in a temperature range of 170–580 °C (Chen et al., 2016). Furthermore, a small CO absorption band was detected in a range of $2240-2060$ cm$^{-1}$ in the raw microalga, whereas the CO absorption band was removed after the wet torrefaction, indicating no CO gas released during the pyrolysis of wet torrefied microalgae. Meanwhile, the $CO_2$ absorption band decreased dramatically in the wet torrefied microalgae, especially in acidic solutions. This is because the release of $CO_2$ during the pyrolysis was dominant by the degradation of carbohydrates and proteins (Marcilla et al., 2009), as most of the microalgae carbohydrates were hydrolysed in acidic solutions. Wang et al. (Wang et al., 2018a) proved that the acid pre-treatment could significantly reduce $CO_2$ emission during the microalgae pyrolysis due to the hydrolysis of carbohydrates.

In the second stage of the thermal degradation, C−O, C=O, and C−H absorption bands were not clearly detected for the raw microalga. This could be explained by the low lipid composition in the raw microalga and the limited thermal degradation of microalgae components in the second stage as shown in **Figure 4.14**. After the wet torrefaction in water and acidic solutions, it could be clearly observed that the absorption band of the C−H was enhanced, indicating the large lipid decomposition in the wet torrefied microalgae which created the aliphatic hydrocarbons including alkanes and alkenes. The lipids would crack into long-chain of fatty acids or alcohols during the pyrolysis (Li et al., 2017a), which increased the absorption band of C−O and C=O. The O−H absorption band which appeared in the ranges of $4000-3500$ cm$^{-1}$ and $1875-1275$ cm$^{-1}$ was still able to be detected in the wet torrefied microalgae in acidic solutions, although the previous studies have reported that deoxygenation and dehydration process occurred in the wet torrefaction (Chen et al., 2012d; Zhang et al., 2019b). The O−H absorption band appeared in the FTIR spectra after the wet torrefaction in the acidic solutions might be due to the presence of acid in the microalgae (Sindhu et al., 2011).

#### 4.5.2.2 Combustion gas

The raw and wet torrefied microalgae combustion gas analysis in three dimensional FTIR spectra is displayed in **Figure 4.19**. The gaseous products of the microalgae combustion were similar to those from microalgae pyrolysis, which was contributed by $H_2O$, C−H, $CO_2$, CO, C=C, C=O, and C−O from the main reaction stage of the combustion. A summary of FTIR functional groups and wavenumber of gaseous products during combustion is presented in **Table 4.6**. The absorption bands were clearly determined at the main combustion reaction (200−700 ℃), which could be divided into three main stages, including the combustion of carbohydrates and proteins, lipids, and char formation as presented in **Figure 4.15**. As the temperature increased from 200 ℃, the FTIR spectra revealed the release of $H_2O$, $CO_2$, and CO with some other organic volatile compounds with C=O and C−C absorption bands. The release of $CO_2$ at the first stage of combustion was due to the combustion of organic carbon, whereas CO formed was due to the incomplete combustion of carbon ($C + O_2 \rightarrow CO_2/CO$) (Oudghiri et al., 2016). For the raw microalga, the C−H absorption band was not detected due to the low lipid composition. As discussed in the pyrolysis of microalgae, the detection of C−H absorption band was mainly from the degradation of lipids. Hence, the C−H absorption band was discovered in the second stage of the combustion (350−500 ℃) on the wet torrefied microalgae. Most of the C−H absorption band was only detected in the second stage of the combustion. When the temperature of combustion was higher than 500 ℃, $CH_4$ would be oxidized into $CO_2$, as reported by Huang et al. (Huang et al., 2018).
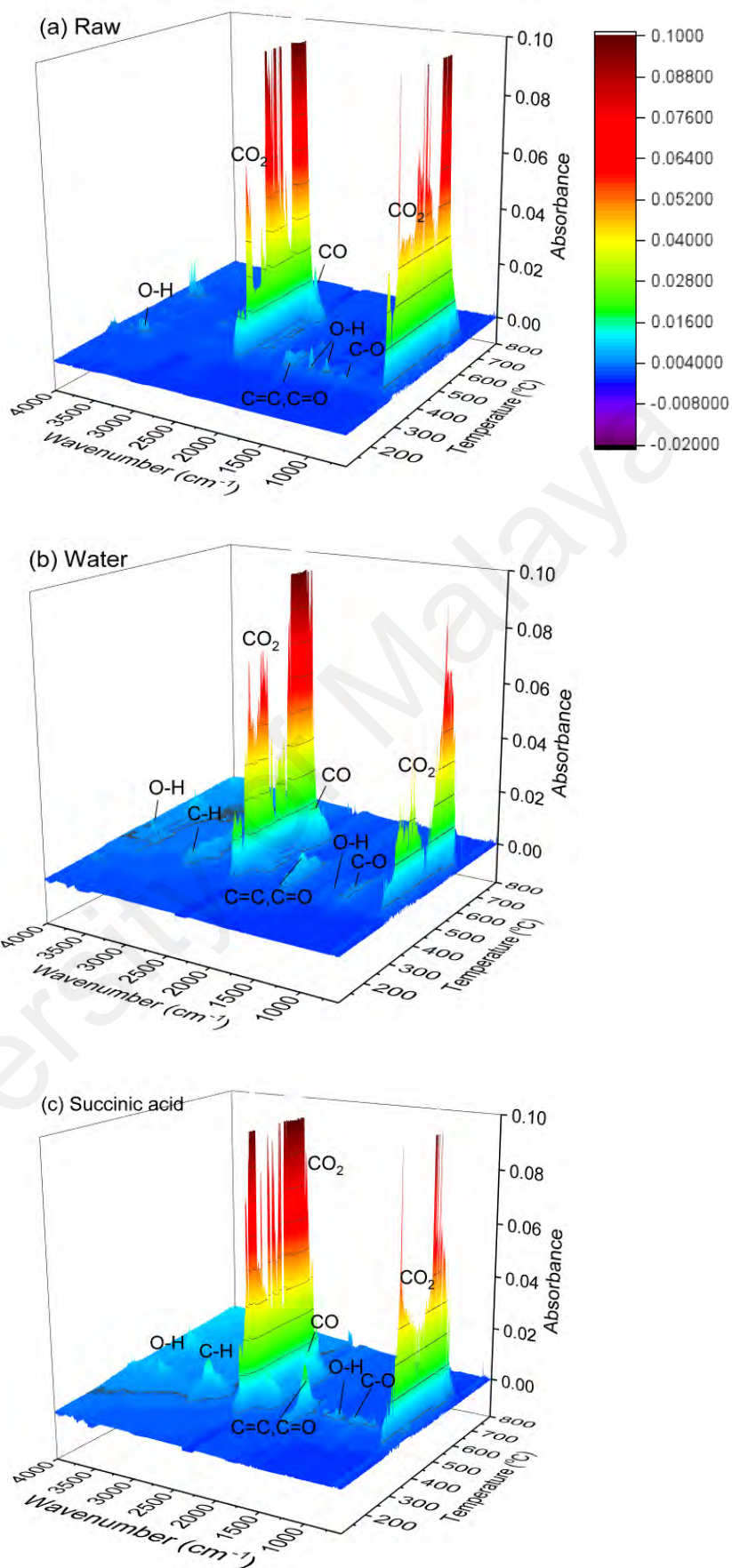
**Figure 4.19: 3D analysis of raw and wet torrefied microalgae combustion gas**
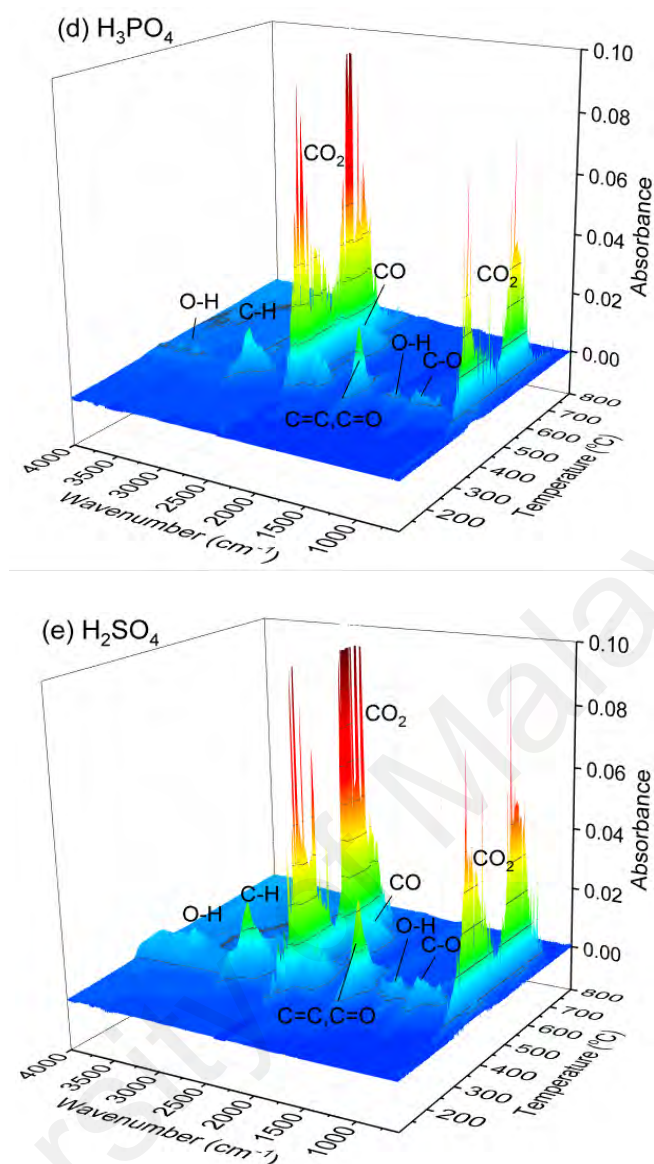
**Figure 4.19, continued**

Similarly, the large absorption peaks of the gaseous products were detected at the DTG peak temperature. The FTIR spectra of combustion were selected based on the DTG peak temperature of each stage, as presented in **Figure 4.20**. The first, second and third stages of combustion gas were mainly contributed by the thermal degradation of the microalgae carbohydrates, proteins, lipids and produced char. The absorption band of water in the first stage was observed in the raw microalga, indicating the water was not completely released during the dehydration stage. The intensity of O−H absorption band was removed in the first stage for wet torrefied microalgae, indicating deoxygenation and

dehydration processes occurred in wet torrefaction (Chen et al., 2012d; Zhang et al., 2019b). Besides, a similar trend on the CO and $CO_2$ absorption bands in the combustion of wet torrefied microalgae was observed, where the CO and $CO_2$ were removed and reduced in the wet torrefied microalgae due to the hydrolysis of carbohydrates in the wet torrefaction process. In the first stage of pyrolysis and combustion of microalgae components, similar gaseous products were released. During the combustion stage of microalgae lipids (the second stage), the emissions of $CO_2$ and CO were discovered, whereas no changes on the absorption band for the wet torrefied microalgae. Wet torrefaction in water and acidic solutions did not destroy the lipid structure in the microalgae. After the wet torrefaction, C=O and C−H absorption bands were intensified due to the enrichment of lipid composition in the microalgae. At the third stage of combustion, $CO_2$ and CO were the only gaseous products detected in the FTIR spectra. The C−H absorption band was not discovered because $CH_4$ and carbonyls were suppressed at high temperatures with the existence of $O_2$ (Yang et al., 2015a).
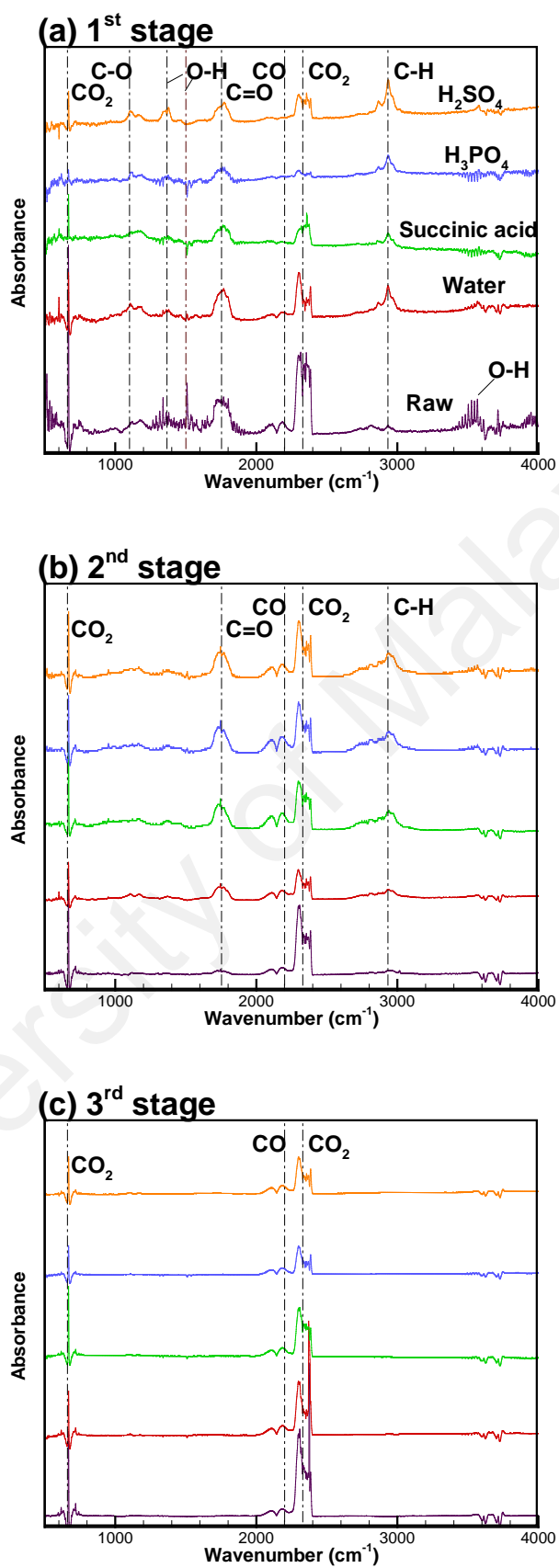
**Figure 4.20: FTIR spectra of gaseous released during the combustion at first,**

**second and third DTG peaks**

### 4.5.3 Py-GC/MS analysis

### 4.5.3.1 Single-shot thermal degradation

During the fast pyrolysis of microalgae, several reactions occur including dehydration, decarboxylation, fragmentation, polymerization, and rearrangement. The pyrolysis of microalgae can be divided into the pyrolysis of carbohydrates, proteins, and lipids (Chen et al., 2018c). The complexity of the microalgae components released numerous products during the pyrolysis including hydrocarbons, acids, alcohols, phenols, sugars, nitrogenous compounds, furans, aromatics, and others (Li et al., 2019). **Figure 4.21** shows the single-shot Py-GC/MS pyrograms of the raw and wet torrefied microalgae at 500 °C, whereas **Table 4.7** presents the main products contained in the pyrolysis volatiles. Several peaks in the Py-GC/MS pyrograms were diminished after the torrefaction pre-treatment, indicating the change in the microalgae bio-oil composition after pre-treatment. The absorption peak of furfural (1), 2-furancarboxaldehyde, 5-methyl (2), and 1,4:3,6-dianhydro-.alpha.-d-glucopyranose (3) were clearly reduced. These products mainly produced from the hydrolysis and cracking of microalgae carbohydrates (Hu et al., 2019), whereas the carbohydrate composition in the microalgae was significantly reduced after the wet torrefaction as reported previously. In addition, the peak of beta.-D-glucopyranose, 1,6-anhydro- (5), produced from the pyrolysis of carbohydrates was clearly eliminated in the pyrograms for the microalgae pre-treated with $H_3PO_4$ and $H_2SO_4$ solutions (Sotoudehniakarani et al., 2019). Most of the carbohydrates were hydrolysed into simple sugar when the microalgae were pre-treated in the $H_3PO_4$ and $H_2SO_4$ solutions.
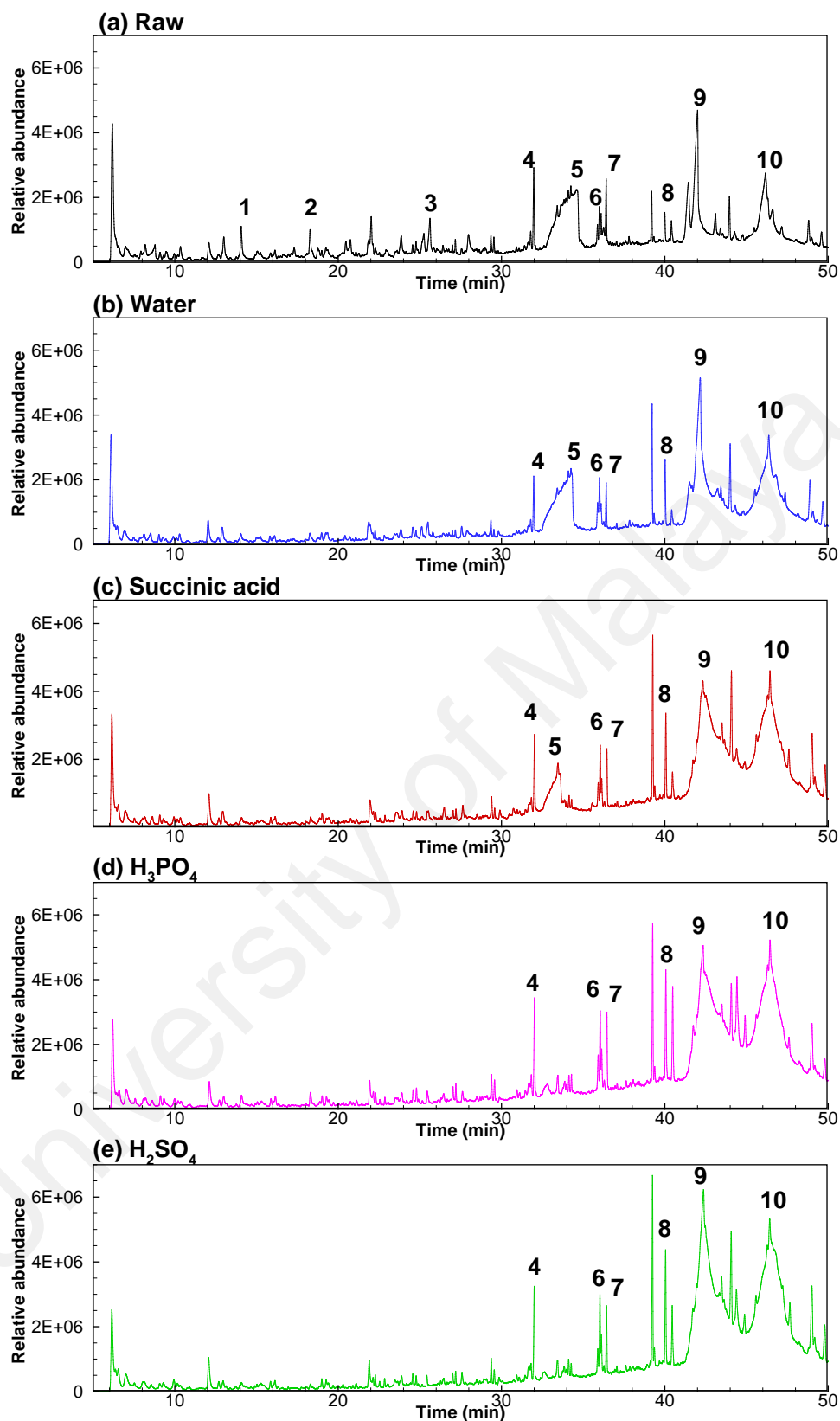
**Figure 4.21: Py-GC/MS pyrograms of microalgae pre-treatment using wet torrefaction in different acids**

**Table 4.7: Main components contained in pyrolysis volatiles in Py-GC/MS**

| No. | Name | Formula | Retention time | Relative content (%) | | | | | | | | | | |
| --- | --- | --- | --- | --- | --- | --- | --- | --- | --- | --- | --- | --- | --- | --- |
| | | | | Raw | Wet torrefaction pre-treatment (160 °C) | | | | Dry torrefaction pre-treatment | | | | | |
| | | | | | Water | Succinic acid | $H_3PO_4$ | $H_2SO_4$ | 200 °C | | 250 °C | | 300 °C | |
| | | | | | | | | | FS | SS | FS | SS | FS | SS |
| 1 | Furfural | $C_5H_4O_2$ | 14.01 | 0.99 | 0.37 | 0.24 | 0.27 | 0.21 | – | 0.77 | – | 0.41 | 1.29 | – |
| 2 | 2-Furancarboxaldehyde, 5-methyl | $C_6H_6O_2$ | 18.28 | 0.84 | 0.29 | 0.18 | 0.27 | 0.12 | – | – | 3.80 | 0.44 | 1.39 | – |
| 3 | 1,4:3,6-Dianhydro-.alpha.-d-glucopyranose | $C_6H_8O_4$ | 25.62 | 1.14 | 0.42 | 0.20 | – | – | – | 1.07 | – | 1.34 | 4.08 | 0.45 |
| 4 | Pentadecane | $C_{15}H_{32}$ | 31.98 | 1.40 | 1.00 | 0.88 | 1.05 | 0.98 | – | 1.51 | – | 1.00 | – | 2.94 |
| 5 | beta.-D-Glucopyranose, 1,6-anhydro- | $C_6H_{10}O_5$ | 34.24 | 17.44 | 13.8 | 5.15 | 0.81 | 0.39 | 18.28 | 20.31 | 24.65 | 18.10 | 29.18 | 0.26 |
| 6 | 8-Heptadecene | $C_{17}H_{34}$ | 36.00 | 1.28 | 1.57 | 1.30 | 1.29 | 1.36 | – | 2.20 | – | 1.52 | – | 2.87 |
| 7 | Heptadecane | $C_{17}H_{36}$ | 36.41 | 1.26 | 0.75 | 0.73 | 0.84 | 0.84 | – | 1.31 | – | 1.01 | – | 2.06 |
| 8 | Cyclopentadecanone, 2-hydroxy- | $C_{15}H_{18}O_2$ | 39.34 | 0.81 | 0.91 | 0.55 | 0.42 | 0.29 | – | 1.25 | 0.26 | 0.48 | 0.82 | – |
| 9 | n-Hexadecanoic acid | $C_{16}H_{32}O_2$ | 42.00 | 13.74 | 16.43 | 18.79 | 19.14 | 21.28 | – | 13.38 | – | 12.22 | 11.71 | 10.21 |
| 10 | Oleic acid | $C_{18}H_{34}O_2$ | 46.17 | 13.53 | 15.33 | 24.39 | 25.27 | 26.94 | 5.59 | 12.17 | 8.39 | 10.91 | 7.47 | 9.60 |

FS: First shot (dry torrefaction)

SS: Second shot (pyrolysis of torrefied microalgae)

**Figure 4.22** shows the distribution of main products produced during the pyrolysis of raw and wet torrefied microalgae. The fatty acids, N-containing compounds, and anhydrous sugars were derived from the lipids, proteins, and carbohydrates, respectively (Yang et al., 2019a). The main constituent of lipids existed in the form of triglycerides, which will crack into long-chain of fatty acids during the pyrolysis (Li et al., 2017a). N-hexadecanoic acid and octadecenoic acid were the main fatty acids derived from the microalgae in this study. Secondary cracking could occur to form short-chain hydrocarbon compounds at high pyrolysis temperature (>400 °C). It was observed that the fatty acids composition was increased after the wet torrefaction, especially in the acidic solutions. The enhancement of fatty acids composition is similar to the increase in the lipid content in the microalgae which is explained by the TGA curve in **Figure 4.14**, in a sequence of water, succinic acid, $H_3PO_4$, and $H_2SO_4$, respectively. The highest fatty acids composition (48.22%) was achieved for wet torrefied microalga in the $H_2SO_4$ solution, whereas only 29.24% detected in raw microalga. It is because most of the low volatile components and carbohydrates were hydrolysed in the acidic wet torrefaction. From the perspective of energy content, the abundance of fatty acids is beneficial to bio-oil quality and ease to upgrade into biofuel (Wang et al., 2013).
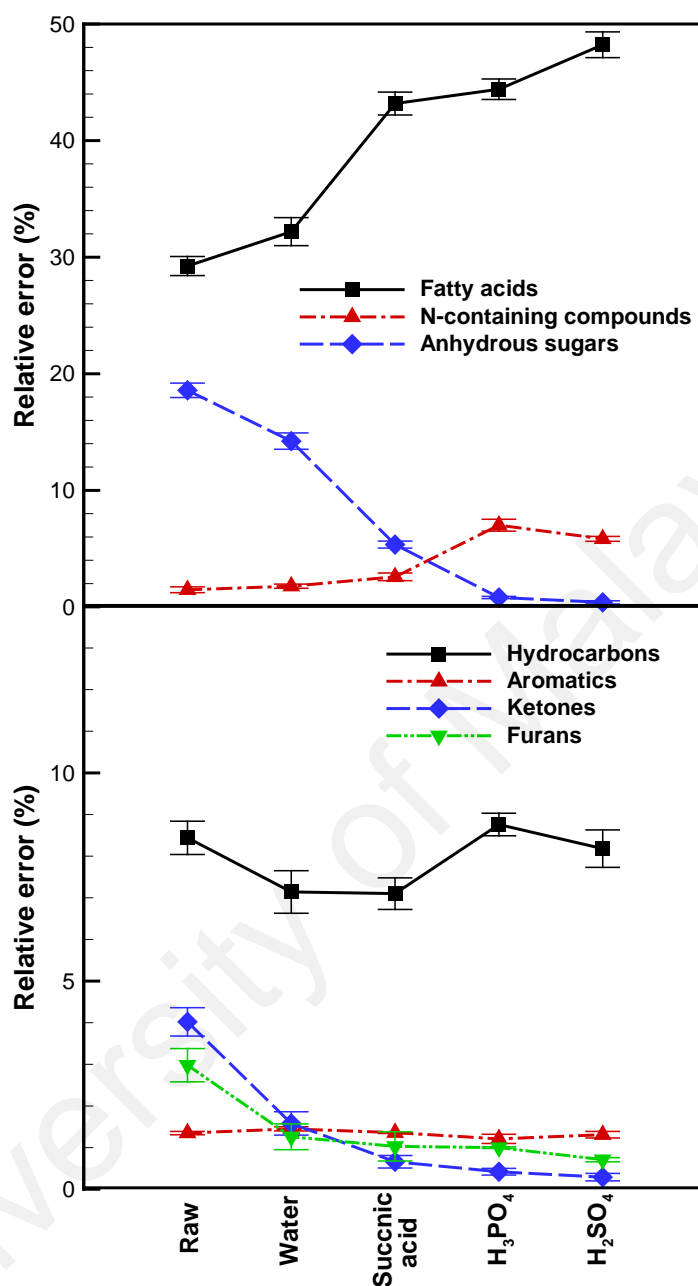
**Figure 4.22: Distributions of main products from pyrolysis of raw and wet torrefied microalgae**

During the pyrolysis of the proteins, the aromatic hydrocarbons (phenols, toluene, etc.) and N-containing compounds (indoles, pyridine, and nitriles) were found in the bio-oil composition, which were derived from the amino acids originated from proteins (Du et al., 2013). Furthermore, the aromatic hydrocarbons could also generate from the Diels-Alder cyclization of unsaturated lipids (Almeida et al., 2017), as the distribution of

aromatic compounds was not significantly changed after wet torrefaction, within the ranges of 1.21–1.45%. The N-containing compounds were slightly enhanced from 1.47 to 1.78% after the wet torrefaction in water, where the enhancement was further increased with the use of $H_3PO_4$ (7.01%) and $H_2SO_4$ (5.84%) in the wet torrefaction. It is because most of the protein remained in the microalgae after the wet torrefaction in acidic solutions, resulting an increase in the protein composition as the other components were degraded.

The carbohydrates of microalgae derived from the polysaccharides and oligosaccharides, The pyrolysis of carbohydrates would generate anhydrous sugars from hydrolysis reaction, and ketones and furans from cracking and decarboxylation reactions (Yang et al., 2019a). Relatively high contents of anhydrous sugars (18.58%), furans (2.98%) and ketones (4.02%) were noted in the pyrolysis of raw microalga. Meanwhile, the lowest anhydrous sugars (0.39%), furans (0.71%) and ketones (0.29%) were detected in the microalgae pre-treated by the $H_2SO_4$ in wet torrefaction. These products were reduced in a sequence of water, succinic acid, $H_3PO_4$, and $H_2SO_4$ due to the increase of hydrolysis reaction in wet torrefaction. In addition, the low carbohydrate composition in the microalgae yielded a low concentration of oxygenated compounds in bio-oil (Wang et al., 2013). The acids produced from the microalgae pyrolysis could be divided into linear acid (carbohydrates) and fatty acids (lipids) (Li et al., 2017a). Linear acids such as acetic acid are responsible for low pH and enhance the corrosive characteristics of bio-oil (Chen et al., 2014c). The production of acetic acid in the bio-oil was effectively avoided when the microalga was pre-treated with wet torrefaction using dilute $H_2SO_4$ solution, because of the low carbohydrate content.

### 4.5.3.2 Double-shot thermal degradation

The first stage of the double-shot thermal degradation was conducted by the torrefaction process at 200, 250 and 300 °C for 20 min. **Figure 4.23** demonstrates the Py-GC/MS pyrograms obtained from the microalgae torrefaction. The data illustrated that limited products were detected during the torrefaction at 200 and 250 °C, indicating the main microalgae components remaining after the torrefaction. This is because microalga was less reactive at the low-temperature torrefaction, whereby only a few organic compounds were converted into volatiles. Small peaks of anhydrous sugars and fatty acids were observed due to the degradation of carbohydrates and lipids. The degradation of lipids occurred in the temperature range of 170−580 °C with maximum degradation around 400 °C (Chen et al., 2016). Numerous products were detected during the torrefaction at 300 °C. The thermal degradation of microalga at the initial stage was more effective at severe torrefaction as shown in **Figure 4.16**. **Figure 4.24** shows the Py-GC/MS pyrograms obtained by the pyrolysis of torrefied microalgae. After the torrefaction at 200 °C, no significant change was detected in the bio-oil composition. Torrefaction at 200 °C only released low volatile compounds together with the dehydration process. The decrease in the furfural and 2-furancarboxaldehyde, 5-methyl peak were observed when the microalgae were pre-treated at 250 °C as first stage thermal degradation. As the temperature increased to 300 °C, the peak of beta.-D-glucopyranose, 1,6-anhydro- and n-hexadecanoic acid were diminished, indicating the carbohydrates and lipids of the microalgae were degraded during the torrefaction pre-treatment.
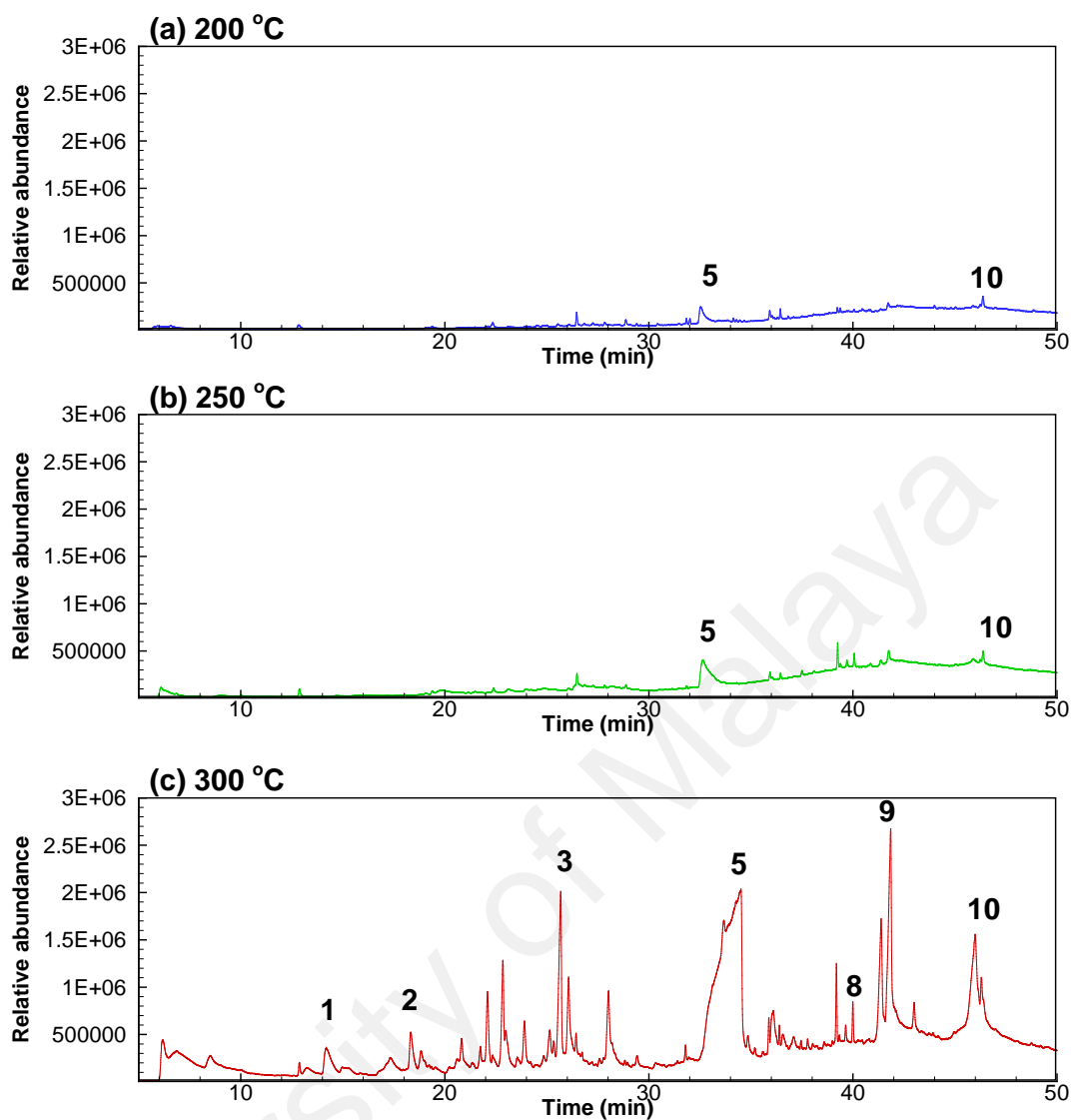
**Figure 4.23: Py-GC/MS of microalgae torrefaction at 200, 250 and 300 ºC**
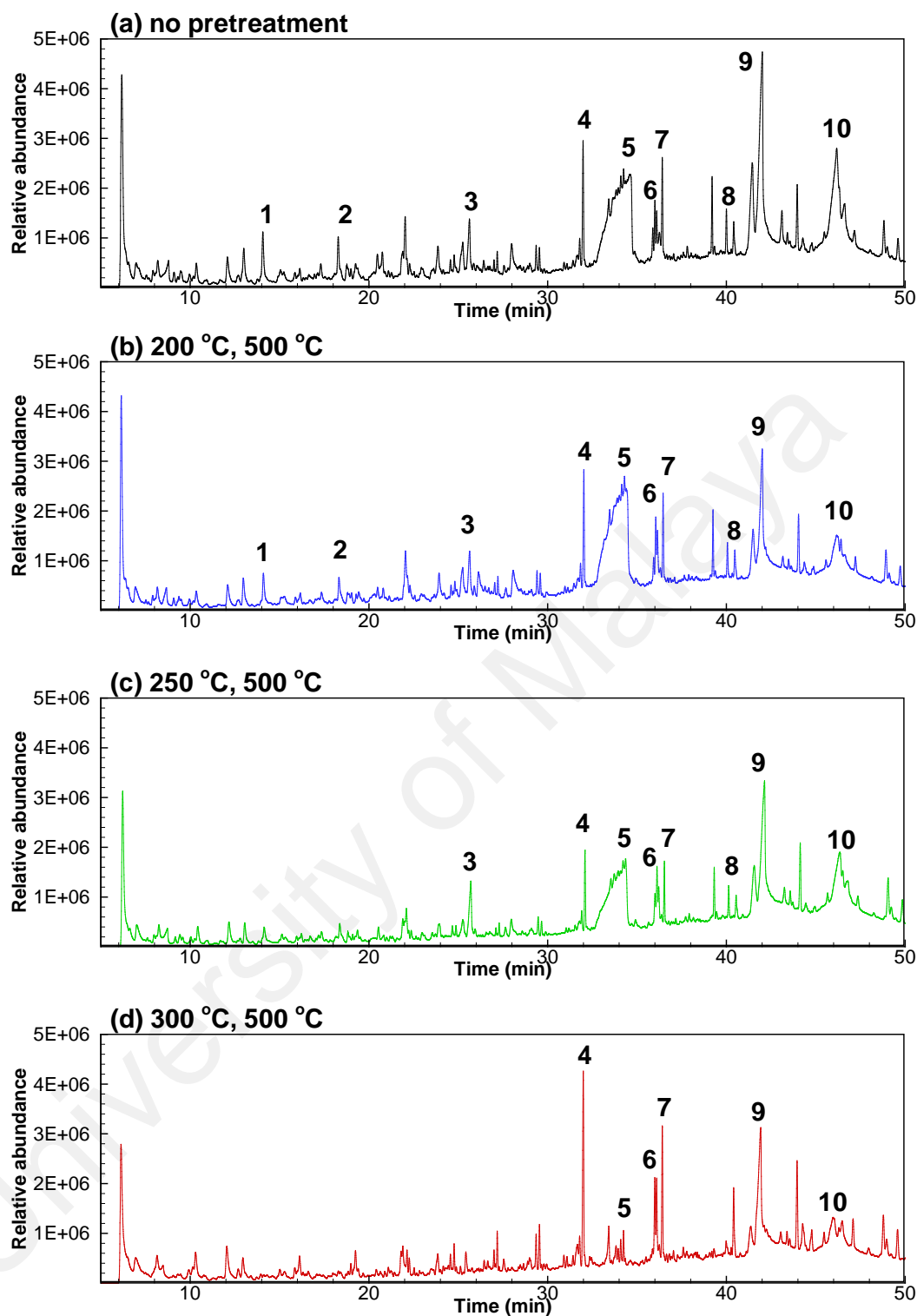
**Figure 4.24: Py-GC/MS of torrefied (200, 250 and 300 ºC) pre-treated microalgae**

**at 500 ºC, compared to non-torrefied microalgae**

Detailed distributions of the main products under the torrefaction and pyrolysis of torrefied microalgae are presented in **Figure 4.25**. From **Figure 4.25a**, it was found that the bio-oil composition from the torrefied microalgae was only contributed by the degradation of carbohydrates and lipids, whereas the products derived from the proteins including N-containing compounds and aromatics were not detected. The thermal degradation of the microalgae proteins was reported in a temperature range of $200-500$ °C with the maximum degradation at $350-360$ °C (Kebelmann et al., 2013). In this study, the protein content was relatively lower compared to those of carbohydrates and lipids, so the protein product could not be detected in the torrefaction process. With the increase of torrefaction temperature to 250 and 300 °C, the production of fatty acids, anhydrous sugars, ketones, furans, and hydrocarbons in the torrefaction bio-oil increased subsequently. The composition of fatty acids increased from 5.59 to 19.4%, whereas anhydrous sugars increased from 18.28% to 33.26%. This is because the thermal degradation of carbohydrates and lipids were more efficient in mild and severe torrefaction.
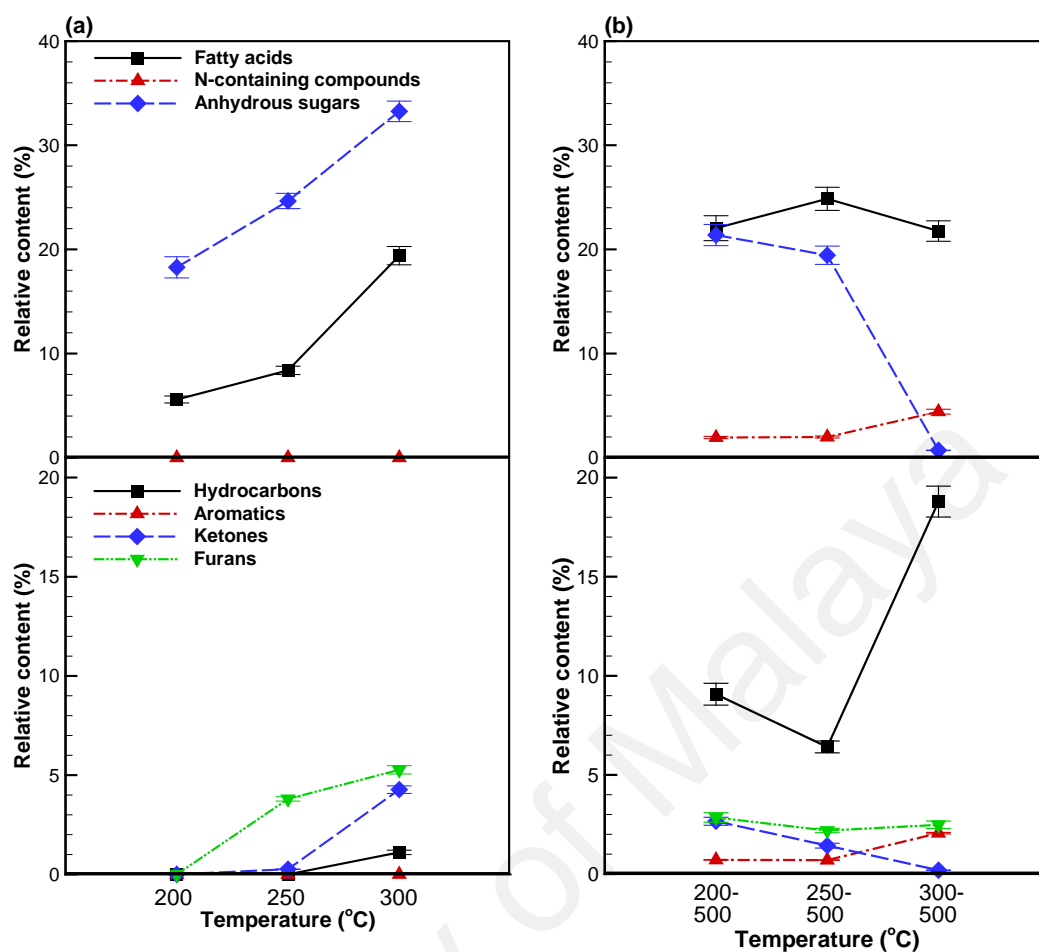
**Figure 4.25: Distributions of main products under (a) torrefaction and (b) pyrolysis of torrefied microalgae**

The pyrolytic products from the torrefied microalgae are presented in **Figure 4.25b**. It can be observed that the N-containing compounds (1.94 to 4.42%) were slightly enhanced with the torrefaction temperature. As the torrefaction temperature increased, the weight loss of microalgae increased, whereas the degradation of the proteins was relatively less than overall weight loss. In addition, a high yield of fatty acids was produced in the bio-oil when microalgae pre-treated at 250 °C was used. Carbohydrate degradation was more significant than lipid degradation during the torrefaction. The anhydrous sugars were close to zero (0.71%) after the 300 °C torrefaction, indicating most of the carbohydrates have been thermally degraded. Furthermore, severe torrefaction pre-treatment provided a high yield of the hydrocarbons (18.79%) in the pyrolytic bio-oil because the microalgae

lipid structure was destructed during the torrefaction. In the severe torrefaction, the structure of the biomass was altered, providing better pyrolysis behavior than the raw biomass (Dai et al., 2019).

### 4.5.3.3 Comparison of dry and wet torrefaction

In this study, the pyrolytic bio-oil produced from different pre-treatment techniques were analysed by identifying the major volatile components using single and double-shot Py-GC/MS. **Figure 4.26** presents the pyrolysis mechanism of torrefied microalgae based on the results obtained. The dry and wet torrefaction exhibited different mechanisms. In general, the mechanism occurring in dry torrefaction is the thermal treatment mechanism, which includes decarboxylation, decarbonylation, demethoxylation, derangement of intermolecular, condensation, and chemical reactions to aromatization (Funke & Ziegler, 2010). In this study, carbohydrates and lipids of microalgae were decomposed during the dry torrefaction. However, the presence of compressed water created the hydrolysis mechanism for the wet torrefaction process, whereas most of the carbohydrates would be hydrolysed due to poor hydrolysis resistance (Acharya et al., 2015).
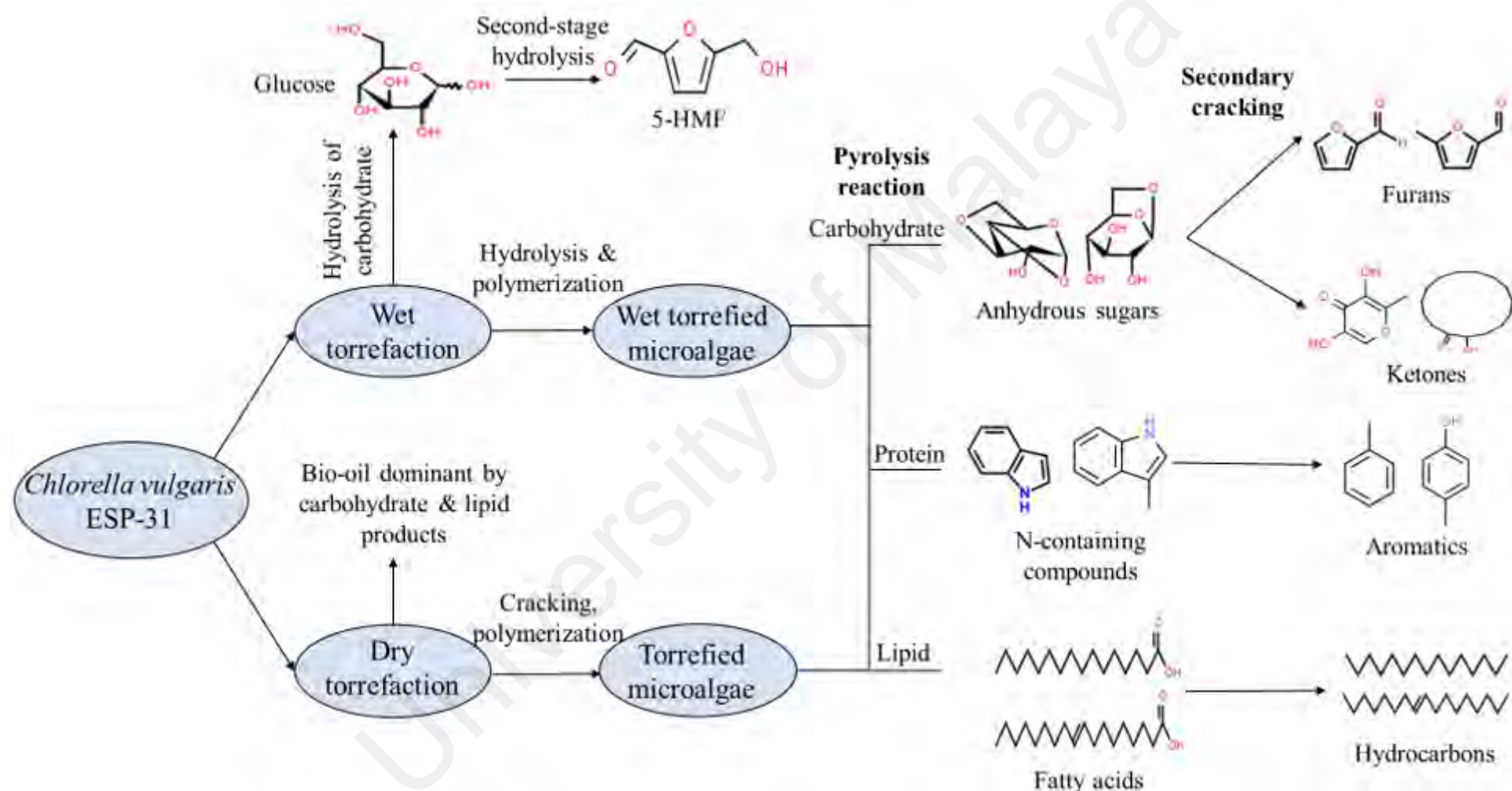
**Figure 4.26: Pyrolysis mechanism of torrefied microalgae**

As the discussion above, the product distribution of microalgae could be divided into pyrolysis of carbohydrates, proteins, and lipids to generate anhydrous sugars, N-containing compounds, and fatty acids, respectively. In the pyrolysis of wet torrefied microalgae, part of the carbohydrate derived products was decreased. The reduction of the carbohydrate products was decreased even more when microalgae were pre-treated in the acidic solutions. After the wet torrefaction in the dilute $H_2SO_4$ solution, most of the carbohydrate products in the bio-oil were removed. The removal of carbohydrates in the microalgae minimized the total water content in the bio-oil, as dehydration is the primary decomposition reaction in the pyrolysis of carbohydrates (Wang et al., 2017b). In addition, most of the carbohydrates in the microalgae was hydrolysed in the dilute $H_2SO_4$ solution, which is beneficial for the bioethanol production (Fasahati & Liu, 2015). In contrast, dry torrefaction not only limited the carbohydrate products in the pyrolytic bio-oil, whereas the lipid products were also changed during the pyrolysis. This process limited the usage of the bio-oil produced from dry torrefaction due to the complexity of the bio-oil. In the severe torrefaction, most of the carbohydrate products were released during the torrefaction, resulting in a limited amount of carbohydrate products in the pyrolytic bio-oil. Moreover, there was no significant change in the protein products after pre-treated in dry and wet torrefaction, indicating a higher temperature will be needed to remove the protein products.

In this study, wet torrefaction of microalgae was carried out in a modified microwave-assisted reactor in different types of acidic solutions. A relatively low wet torrefaction temperature (160 °C) with the aid of acid catalysts applied in this study has lower the energy input. Meanwhile, microwave irradiation uses lower energy input than thermal heating to heat the reaction medium to the desired temperature (Nizamuddin et al., 2018), which is more cost-effective. Dry torrefaction requires temperature of 300 °C to produce biochar with a similar HHV enhancement to wet torrefaction at 160 °C (30 MJ/kg), which

can be used in co-firing for steam generation or pyrolysis process. In term of energy required for biofuel production, dry torrefaction required large amount of energy to convert biomass into biochar as solid biofuel as higher temperature is needed, which is not suitable for large scale production. In the meantime, dry torrefaction destroys carbohydrates and lipids during composition. The bio-oil produced from dry torrefaction is not suitable to use as biofuel production due to its complexity. Wet torrefaction is a promising method for the large-scale production as it can fully utilise most of the components in the microalgae (liquid product as bioethanol production and solid product as solid biofuel), which also uses lower temperature compared to dry torrefaction. Although the mass production using dry torrefaction is applied in several industries, the energy required to convert the biomass into biofuel is relatively high. Wet torrefaction has shown the feasibility for the mass production of high-carbohydrate biomass. More study should be carried out on the reactor design for mass production purpose using wet torrefaction.

## 4.6 Kinetic modelling

### 4.6.1 Pyrolysis kinetics and curve fitting

Pyrolysis TGA of raw and wet torrefied microalgae ESP-31 in water and $H_2SO_4$ are presented in **Figure 4.27** to evaluate the thermal behaviour of microalgae. The weight loss at the temperatures below 200 ℃ was due to the release of moisture and low volatile materials. This was then followed by the main pyrolysis stage which is the decomposition of the microalgae main components including carbohydrates, proteins, lipids and other components occurred in a temperature range of 200−500 ℃. Several decomposition mechanisms involved in this stage including depolymerization, decarboxylation, and cracking (Peng et al., 2001). Based on the **Figure 4.27**, two derivative peaks were observed for raw microalga ESP-31. The first peak detected could be due to the thermal degradation of carbohydrates and proteins (Rizzo et al., 2013). Furthermore, the decomposition of lipids formed a second derivative peak for microalga ESP-31. The chemical composition analysis revealed that the raw microalga contained high carbohydrate content. For this reason, the first derivative peak of raw microalga mainly due to the carbohydrate decomposition. For the microalga pre-treated with wet torrefaction in water, the first peak clearly decreased, indicating the carbohydrate content was hydrolysed (Bach et al., 2017b). The peak was further decreased and formed a shoulder with the use of $H_2SO_4$ solution in wet torrefaction, in which the carbohydrate content was markedly reduced. As a result, the second peak was significantly enhanced.

**WT= wet torrefied microalgae**
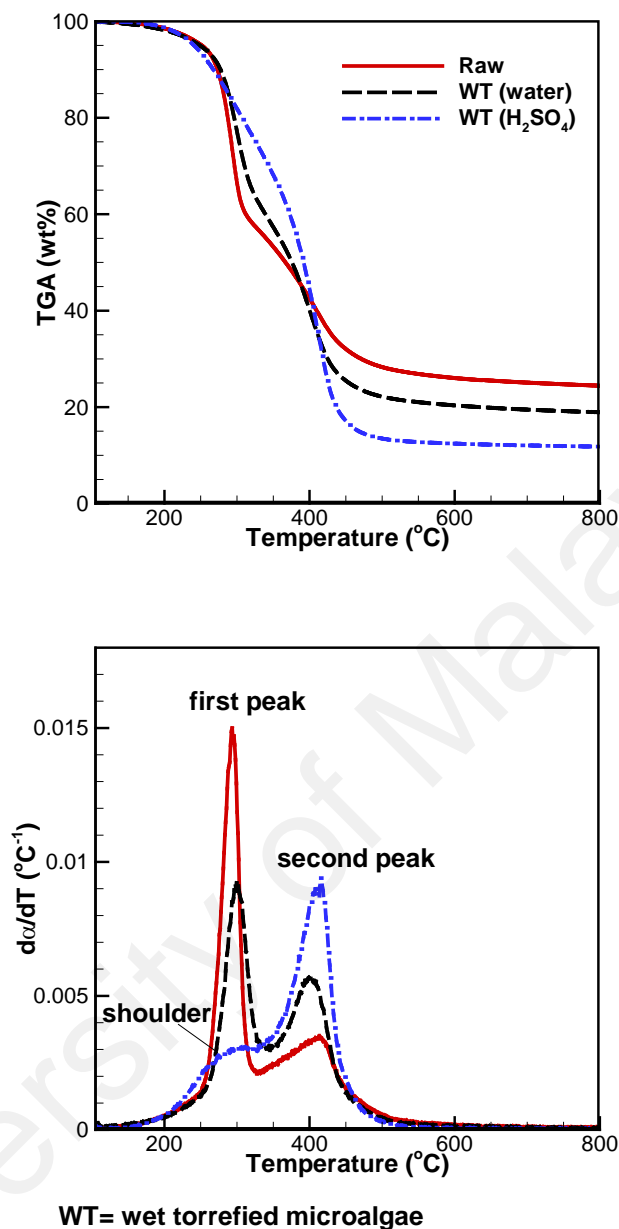
**Figure 4.27: Pyrolysis TGA of raw and wet torrefied microalgae ESP-31 in water and H₂SO₄**

The predicted curves of raw and pretreated microalgae ESP-31 were compared with the experimental curves, as presented in **Figure 4.28**. The result revealed that the predicted curves correspond well to the experimental curves using four reaction models. From the analysis of the kinetics illustrated below, the detailed mechanisms of microalgae components transformed during the wet torrefaction were identified.
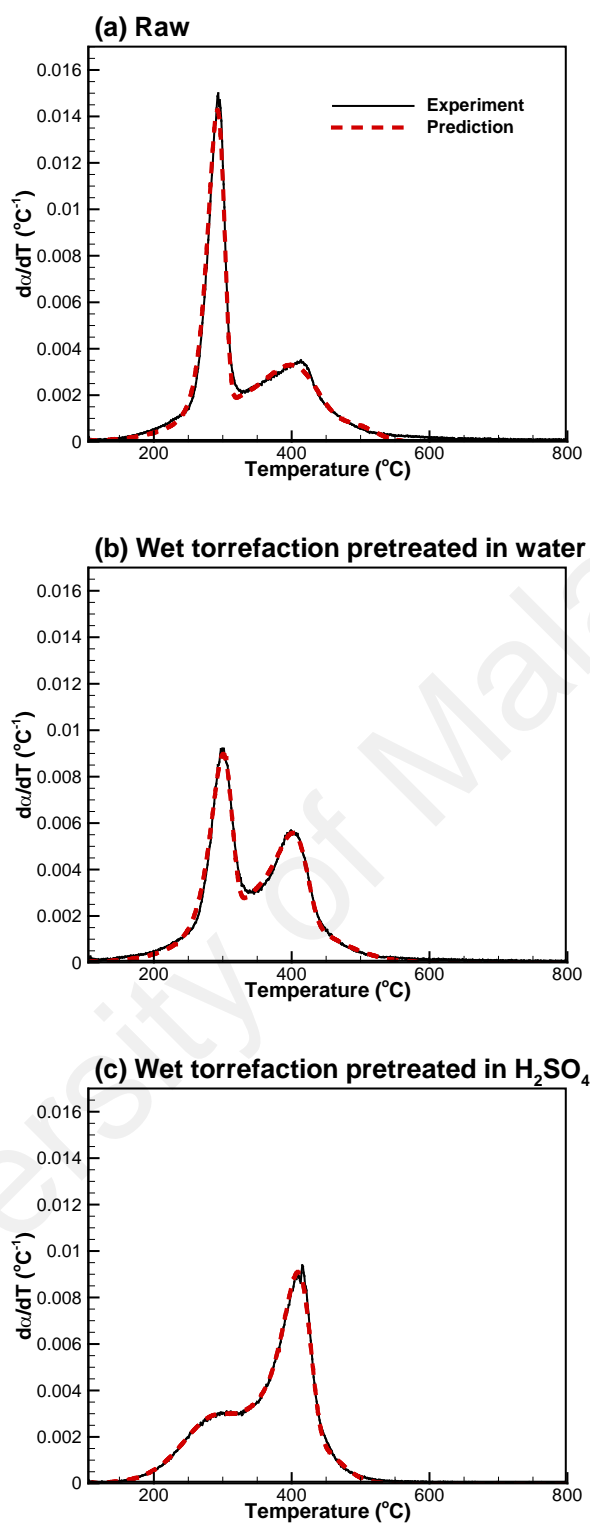
**Figure 4.28: Comparison of experimental and predicted curves of microalgae ESP-31 for (a) raw, (b) pre-treated in water, and (c) pre-treated in H₂SO₄**

### 4.6.1.1 Activation energy and pre-exponential factor

**Table 4.8** displays the detailed kinetic parameters of microalgae derived from the IPR kinetic modelling, as well as the fit quality of the predicted curve. The fit quality of raw and wet torrefied microalgae ESP-31 ranged between 98.27−99.05%. Overall, the fit quality of microalgae was achieved more than 98% using four reaction model, displaying good curves that match the experimental data. Meanwhile, the activation energies of carbohydrates, proteins, lipids, and others calculated from the predicted results are summarized in **Figure 4.29**. The activation energies of carbohydrates, proteins, lipids, and others ranged between 64.59−221.33, 43.78−61.38, 85.92−192.27, and 42.32−113.51 kJ mol$^{-1}$, respectively. For the raw microalga ESP-31, the activation energies for carbohydrates, proteins, and lipids were 221.33, 43.78, and 85.92 kJ mol$^{-1}$, respectively, which was close to the activation energies of microalgae *Chlamydomonas* JSC4 and *Chlorella sorokiniana* CY1 studied by Bui et al. (2016). This implies that the pyrolysis kinetics of microalga ESP-31 components could be predicted using the four parallel reaction model.

Moreover, the pre-exponential factor showed the similar trend with the activation energy for all the components. It was observed that the activation energy of carbohydrates decreased after the wet torrefaction in water, and further decreased in H$_2$SO$_4$ solution. A wide range of the carbohydrate activation energy was observed, as the carbohydrates have the larger impact among the other microalgae components in the wet torrefaction. Hence, the activation energy required for the thermal reaction of carbohydrates significantly decreased. In contrast to carbohydrates, the activation energy of lipids and proteins tend to increase after the wet torrefaction. However, there is no clear trend for the change of others in kinetic parameters.

**Table 4.8: Kinetic parameters of the main components of raw and wet torrefied**

**microalgae**

| Torrefaction condition | | $E_a$ (kJ mol$^{-1}$) | A (s$^{-1}$) | c (−) | Fit quality (%) |
|---|---|---|---|---|---|
| Raw | Carbohydrate | 221.33 | $7.17 \times 10^{18}$ | 0.40 | 98.84 |
| | Protein | 43.78 | $5.70 \times 10$ | 0.16 | |
| | Lipid | 85.92 | $3.56 \times 10^4$ | 0.32 | |
| | Others | 113.51 | $5.46 \times 10^5$ | 0.08 | |
| WT (Water) | Carbohydrate | 182.87 | $9.57 \times 10^{14}$ | 0.27 | 98.27 |
| | Protein | 46.96 | $4.92 \times 10$ | 0.23 | |
| | Lipid | 176.02 | $5.45 \times 10^{11}$ | 0.19 | |
| | Others | 42.32 | 7.43 | 0.27 | |
| WT ($H_2SO_4$) | Carbohydrate | 64.59 | $1.39 \times 10^4$ | 0.13 | 99.05 |
| | Protein | 61.38 | $1.32 \times 10^3$ | 0.25 | |
| | Lipid | 192.27 | $7.95 \times 10^{12}$ | 0.36 | |
| | Others | 73.31 | $2.16 \times 10^3$ | 0.24 | |

$E_a$ = activation energy
A = pre-exponential factor
c = contribution factor
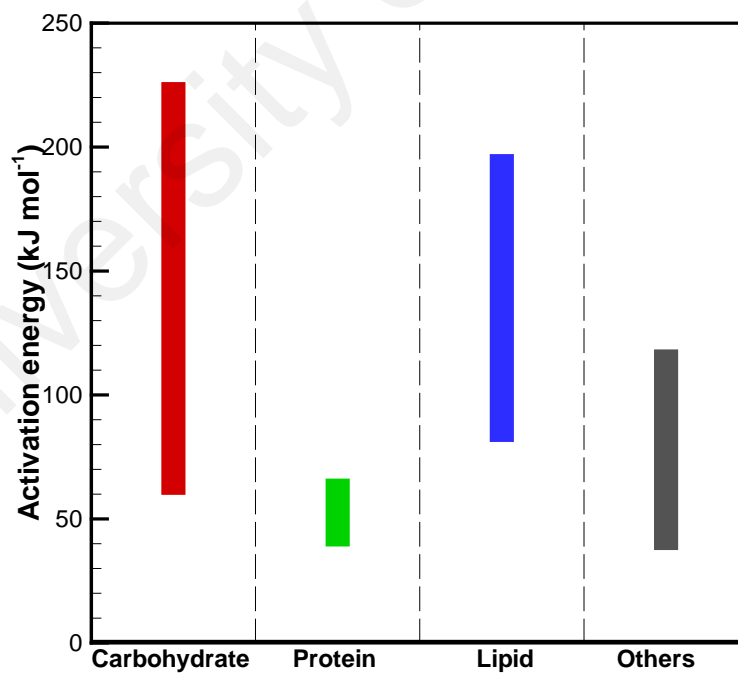


**Figure 4.29: The activation energy ranges of raw and wet torrefied microalgae**

**main components**

### 4.6.1.2 Contribution factor

Furthermore, the wet torrefaction significantly influenced on the kinetic parameters of the carbohydrates, lipids and others, but only slight effect on the protein based on the contribution factor (c) in **Table 4.8**. After the wet torrefaction, the c-value for the microalgae significantly changed due to the modification of the structures and properties of microalgae components. The c-value of the carbohydrates decreased from 0.40 to 0.27 after wet torrefaction in water and further reduced to 0.13 after wet torrefaction in acidic solution, which can be explained by the poor hydrolysis resistance of carbohydrates and ease to hydrolyse into fermentable sugar in $H_2SO_4$ solution (Chen et al., 2013; Wilson & Novak, 2009). This implies that the contribution of carbohydrates to the pyrolysis was decreased after the wet torrefaction. A similar c-value trend could be observed from the dry torrefaction and wet torrefaction of lignocellulosic biomass (Bach et al., 2015b; Broström et al., 2012). The c-value of hemicelluloses was decreased after the torrefaction due to the poor thermal resistance. Other than that, the c-value of proteins slightly increased after the wet torrefaction, most of the proteins retained in the microalgae, as higher temperature (>200 °C) is needed to extract the proteins in hydrothermal media (Jazrawi et al., 2015). The decrease in the c-value of lipids for the microalgae pre-treated in the water might due to the lipid destruction in the hydrothermal media and forming other components (Peterson et al., 2008). The slight increase in the proteins and lipids of microalgae pre-treated in $H_2SO_4$ solution could be due to the large decrease in carbohydrates. On top of that, the "others" in the wet torrefied microalgae stands for the torrefied part which was formed by destructing the main microalgae components (Bach et al., 2017c). Therefore, the c-value for others in the wet torrefied microalgae dramatically enhanced.

**4.6.2    Conversion rate and conversion degree of carbohydrates, proteins and lipids**

**4.6.2.1    Conversion rate as a function of temperature**

**Figure 4.30**, **Figure 4.31** and **Figure 4.32** present the conversion rate as a function of temperature and conversion degree for raw and wet torrefied microalgae. The changes of the conversion rate and conversion degree of carbohydrates, proteins, lipids and others of microalgae pre-treated with the wet torrefaction were investigated using four parallel reaction model. From the profile of raw microalga ESP-31 in **Figure 4.30a**, the first peak was mainly attributed to the degradation of carbohydrates and proteins, with small amount of lipid degradation. The second peak was mainly contributed by lipid degradation with small amount of proteins and others. Based on the results, it was observed that the maximum decomposition peak of carbohydrates was first began (292 ℃), followed by proteins (295 ℃) and lipids (399 ℃), which agreed with the literature done by Chen et al. (2016). Meanwhile, a delay in the second peak was identified at the temperature higher than 450 ℃, which was attributed by the other components with a maximum degradation temperature of 483 ℃. These components could be formed by the degradation of carbohydrates during the low temperature pyrolysis (Bach & Chen, 2017a). A similar phenomenon also found by Wang et al. (2017b), where the pyrolysis of carbohydrates isolated from the microalgae created a shoulder at temperatures higher than 400 ℃.
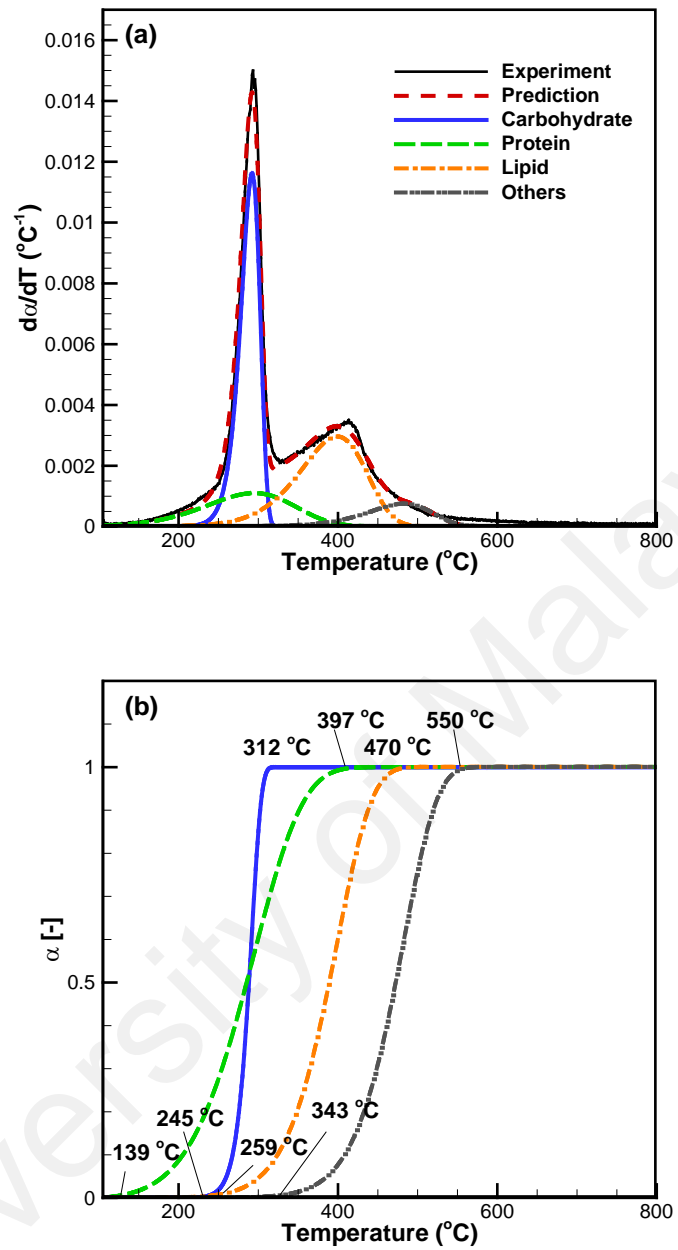
**Figure 4.30: Predicted pyrolysis kinetics of each component of raw microalgae**

**ESP-31 for (a) conversion rate and (b) conversion degree**
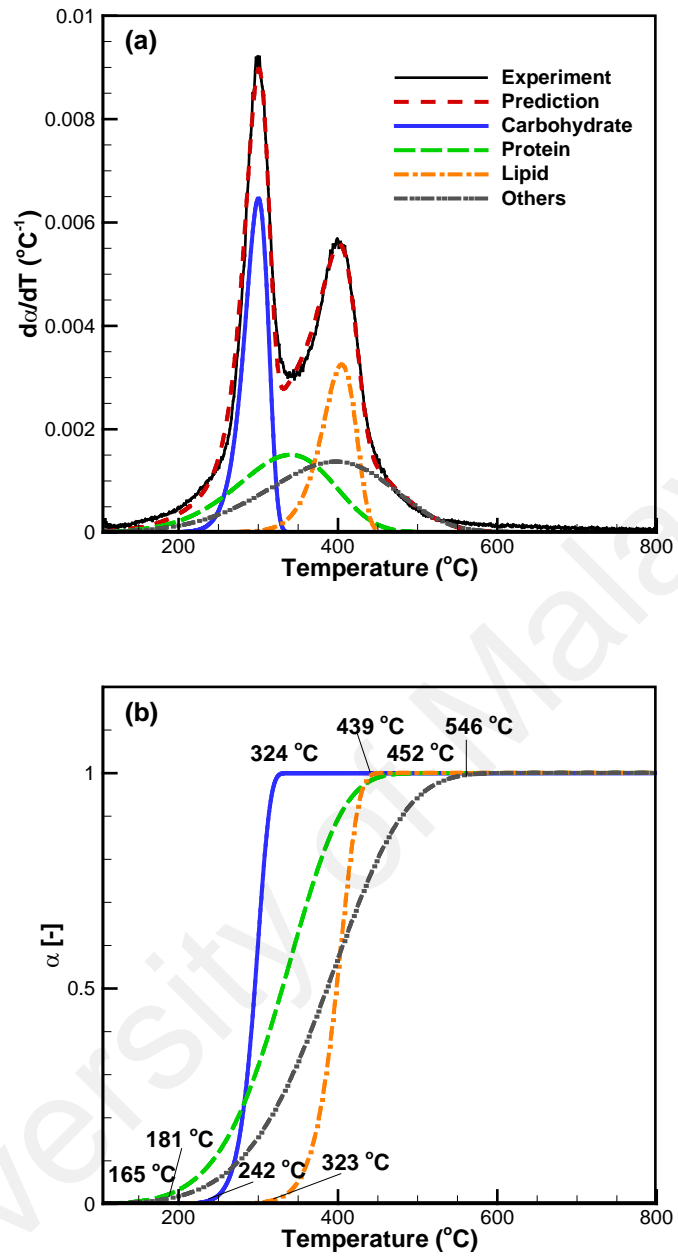
**Figure 4.31: Predicted pyrolysis kinetics of each component of wet torrefied microalgae ESP-31 in water for (a) conversion rate and (b) conversion degree**
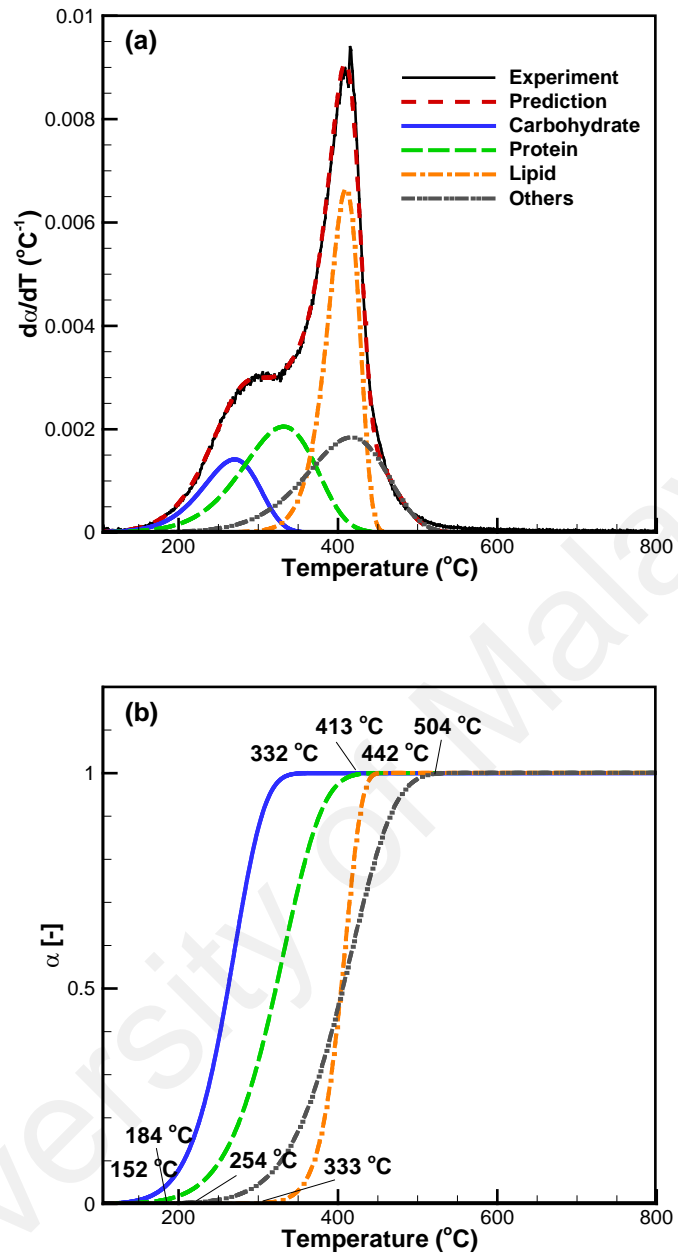
**Figure 4.32: Predicted pyrolysis kinetics of each component of wet torrefied microalgae ESP-31 in sulfuric acid for (a) conversion rate and (b) conversion degree**

In **Figure 4.31a**, the first peak of the wet torrefied microalgae in water was formed by the degradation of carbohydrates, proteins and part of the others, whereas the second peak was formed by degradation of lipids, others, and part of the proteins. It was observed that the others in the raw microalga only appeared at high temperature, but the others in wet torrefied microalgae appeared in a wide range of temperature. In general, thermal treatment mechanism of dry torrefaction includes dehydration, decarboxylation, decarbonylation, demethoxylation, derangement of intermolecular, condensation, as well as chemical reactions to aromatization (Funke & Ziegler, 2010). However, the wet torrefaction follows the mechanism of hydrolysis in the initial reaction due to the presence of compressed water, which helps to break the ester and ether bond of biomass complex polymeric chain (Acharya et al., 2015). During the hydrolysis, the microalgae components (carbohydrates, proteins, and lipids) are degraded into monomers and small chain polymers (Zabed et al., 2020). These intermediate products could be polymerized to form crossed linking carbon polymers (Sharma et al., 2020), known as torrefied products (others) in wet torrefaction (Bach et al., 2017c). Therefore, a larger degradation curve of others in wet torrefied microalgae was identified as compared to raw microalga. In **Figure 4.32a**, the first peak was disappeared and formed a shoulder in the conversion curve, but the shoulder was also attributed by the degradation of carbohydrates, proteins and part of the others, whereas the attribution of the second peak was similar to the wet torrefied microalgae in water.

The peak of carbohydrate curve was clearly minimized after wet torrefaction, while the wet torrefaction in $H_2SO_4$ shifted the carbohydrate curve to a lower temperature. This could be explained by the cracking and decomposition of the carbohydrates into small molecules during the wet torrefaction, whereas these small molecules have a lower degree of polymerization, as well as lower activation energies than carbohydrates. Thus, the activation energies of carbohydrate components decreased after the wet torrefaction, and

further decreased in the $H_2SO_4$ solution. When the microalgae pre-treated by the wet torrefaction in $H_2SO_4$ solution, the carbohydrates were further break down and remaining a very small amount of carbohydrate residue, as part of the carbohydrates were not hydrolysed into sugar (Ho et al., 2013). For the lignocellulosic biomass, the activation energy and the conversion curve of the hemicelluloses were decreased after the wet torrefaction due to the cracking and decomposition of hemicelluloses (Bach et al., 2015b). In contrast to carbohydrates, only small modification in the protein curve was detected for the wet torrefied microalgae. Proteins are made up by the peptide bonds which causes the proteins have much higher stability compared to the cellulosic materials during the hydrolysis (Rogalinski et al., 2008). Generally, a high hydrothermal temperature (230−250 °C) is required to hydrolyse the proteins into amino acids (Gu et al., 2020). In addition, lipids in the microalgae mainly in the form of saturated and non-saturated fatty acids as triacyl glycerides, which are easily to convert to free fatty acids in subcritical water due to the low dielectric constant at high temperature (>220 °C) (Guo et al., 2015). Hence, no majority change was detected in the lipid curve after the wet torrefaction due to the low temperature torrefaction (160 °C), as well as in $H_2SO_4$ solution.

### 4.6.2.2  Conversion degree

The conversion degree of microalgae every single component was further analysed to understand the thermal degradation process of each components. **Figure 4.30b**, **Figure 4.31b** and **Figure 4.32b** present the conversion degree (α) of four main components of microalgae with the temperatures $T_1$ and $T_{99}$ labelled on each curve to represent the temperature at which the conversion degree reaches 1 and 99%, respectively. From the curves, the pyrolysis sequence and reaction temperature of each component could be clearly analysed. Based on the **Figure 4.30b**, the proteins in the raw microalga was the

earliest component with the degradation process initiated at 139 °C, followed by carbohydrates at 245 °C and lipids at 259 °C, whereas the others began to decompose at the highest temperature (343 °C). Meanwhile, the carbohydrates were the first component reaches the conversion degree of 99% (312 °C), followed by proteins, lipids, and others at temperature of 397, 470, and 550 °C, respectively. The conversion degree of microalgae components pre-treated with wet torrefaction in water is presented in **Figure 4.31b**, indicates only small different in the outcomes compared to the carbohydrates, proteins and lipids of raw microalga, but there was a large change on others. The conversion degree of others began at temperature of 181 °C, which is much early than raw microalga due to the formation of torrefied products as explained previously. Meanwhile, the proteins were still the first component to decompose, but the initial conversion degree temperature shifted to higher temperature (165 °C), as most of the low thermal resistance proteins were removed during the wet torrefaction. In contrast, the temperature to achieve conversion degree of 99% (504 °C) significantly reduced after wet torrefaction in $H_2SO_4$ solution as shown in **Figure 4.32b**. This implies that $H_2SO_4$ significantly disrupted and hydrolysed the cell wall of the microalgae (Kim et al., 2016; Park et al., 2014). Similarly, the conversion degree of carbohydrates reaches 1% (152 °C) significantly reduced as most of the carbohydrate components were degraded to small molecules.

The detailed study of the thermal decomposition temperature ranges of each component, as well as the $T_1$, $T_{99}$, and $T_{max}$ are tabulated in **Table 4.9** and summarized in **Figure 4.33**. The carbohydrate decomposition temperature ranges of raw, wet torrefaction in water, and wet torrefaction in $H_2SO_4$ were 245−312, 242−324, and 153−332 °C, respectively. The thermal behaviours of carbohydrates react differently with respect to temperature gradient due to the change in chemical structures after the wet torrefaction. As investigated from the early studies (Fagerson, 1969; Pavlath & Gregorski,

1985), the initial decomposition temperature of carbohydrates could be occurred as low as 100 ℃ and last up to 450 ℃ or higher, whereas the thermal degradation of carbohydrates obtained in the present study was within this range. In addition, Vo et al. (2017) reported that the maximum decomposition of microalgae carbohydrates occurred at temperature of 290 ℃, which was close to the result obtained by the raw microalga (292 ℃). Meanwhile, the protein decomposition temperature ranges of raw, wet torrefaction in water, and wet torrefaction in $H_2SO_4$ were 139−397, 165−452, and 184−413 ℃, respectively, whereas those of lipid decomposition temperature ranges were 259−470, 323−439, and 333−442 ℃, respectively. Based on the study by Kebelmann et al. (2013), the decomposition temperature ranges of extracted proteins and lipids from microalgae were 200−500 and 170−600 ℃, respectively. The protein decomposition temperature ranges in this study are much lower compared to the literature, which might be due to the different in the microalgae structures. Furthermore, Wang et al. (2017b) revealed that the maximum degradation of proteins and lipids isolated from microalgae were 310 and 353 ℃, respectively, which was close to the results obtained in this study.

**Table 4.9: The initial and final temperatures for the conversion of the four main components**

| Torrefaction condition | Carbohydrate | | | Protein | | | Lipid | | | Others | | |
|---|---|---|---|---|---|---|---|---|---|---|---|---|
| | $T_1$ (°C) | $T_{99}$ (°C) | $T_{max}$ (°C) | $T_1$ (°C) | $T_{99}$ (°C) | $T_{max}$ (°C) | $T_1$ (°C) | $T_{99}$ (°C) | $T_{max}$ (°C) | $T_1$ (°C) | $T_{99}$ (°C) | $T_{max}$ (°C) |
| *Chlorella vulgaris* **ESP-31** | | | | | | | | | | | | |
| Raw | 244.56 | 311.65 | 292.29 | 139.21 | 396.85 | 295.70 | 259.15 | 469.93 | 398.94 | 342.82 | 549.83 | 483.38 |
| WT (Water) | 242.16 | 324.19 | 300.53 | 165.27 | 451.69 | 341.22 | 323.12 | 439.17 | 397.02 | 181.23 | 546.02 | 404.42 |
| WT ($H_2SO_4$) | 152.85 | 331.97 | 270.22 | 184.45 | 413.19 | 330.91 | 333.04 | 441.50 | 410.02 | 253.53 | 504.60 | 417.33 |

$T_1$=Temperature at which the conversion reaches 1%

$T_{99}$=Temperature at which the conversion reaches 99%

$T_{max}$= Temperature at which the maximum conversion rate occurs

**Figure 4.33: The decomposition temperature range of each microalgae component**

As observed in **Figure 4.33**, the carbohydrate decomposition temperature of microalgae wet torrefaction in $H_2SO_4$ covers a wide range. For the microalgae pre-treated in $H_2SO_4$, most of the carbohydrate structure was disrupted into small molecules, which could be degraded at lower temperature. For proteins, a wide range of decomposition temperature was observed with a minimum change after the wet torrefaction due to the strong peptide bonds as discussed previously. Meanwhile, a wide range of lipid degradation temperature of raw microalga were detected, similar to a study reported by Kebelmann et al. (2013). Generally, the lipid degradation in a wide temperature range of 170−580 °C (Chen et al., 2016). The narrow range of temperature degradation of microalgae after the wet torrefaction might be due to the degradation of low thermal resistant lipids during the wet torrefaction. However, the decomposition temperature of others was very different, which was due to the modification of the microalgae overall structures by the wet torrefaction pre-treatment.

# CONCLUSIONS AND RECOMMENDATIONS

## 5.1 Conclusions

Microalgal biomass are known as the third-generation biofuel feedstock for biorefinery which has successful converted to biochar by torrefaction. In this study, microalgal biomass were upgraded into biochar using dry and wet torrefaction techniques to improve the microalgal fuel properties and pyrolysis behaviour. For dry torrefaction, the fuel properties of the torrefied microalgae were improved via torrefaction at 300 °C at a holding time of 60 min. The HHV was enhanced by 45% with energy yield of 80% for microalga ESP-31 (high-carbohydrate). Dry torrefaction has less impact on the microalga FSP-E (high-protein) and Jatropha biomass (lignocelluloses) due to the different in chemical composition and structure. TSI indicated that increasing the weight loss also increased the HHV enhancement of the torrefied biomass. FTIR results revealed that the torrefaction diminished the O–H functioning group for all the biomass, especially in torrefaction at temperature of 300 °C, implying that the hygroscopic nature of biomass changed to hydrophobic after torrefaction to prevent the formation of hydrogen bond with O–H bond and improving the storage time of the biomass.

In addition, microwave-assisted wet torrefaction in acidic solution of microalgae have been performed in this study for co-production of solid biofuel and bioethanol. Generally, the fuel properties of the wet torrefied microalgae were enhanced with the increase of carbon content and HHV while decreasing ash content. For the wet torrefied microalgae in 0.05 M of $H_2SO_4$, the biochar HHV enhancement was similar to the dry torrefaction at 300 °C and 60 min. A lower temperature used in wet torrefaction can achieve similar HHV enhancement to the biochar produced from dry torrefaction, which eventually reduces the energy input for biofuel production. The highest HHV enhancement was achieved by using 0.1M $H_2SO_4$, but the least energy was retained in the microalgae. The ash content decreased when microalgae was performed with wet torrefaction in sulfuric

and succinic acid solutions, while using phosphorus acid showed an increase in ash content. TGA revealed that more carbohydrates were degraded in the acidic solutions, thus attaining high lipid content in the microalgae. The impact of acid solution to protein content of microalga FSP-E was negligible. The highest glucose was extracted in sulfuric acid solution due to the extra $H^+$ ion in the solution. Therefore, wet torrefaction in organic acid could be an alternative conversion process for solid biofuel production while sulfuric acid can be used for bioethanol production.

Furthermore, the effect of torrefaction pre-treatment on microalgae pyrolysis was studied using the TG-FTIR and double-shot Py-GC/MS. Wet torrefaction of microalga in $H_2SO_4$ showed the highest lipid composition leftover due to high degradation of carbohydrates caused by the extra $H^+$ ion acidic medium. The combustion char produced from the wet torrefied microalgae were more stable and less reactive compared to raw microalga. For the pyrolysis gas analysis, the intensity of C−H absorbance was increased in a sequence of water, succinic acid, $H_3PO_4$, and $H_2SO_4$. Most of the anhydrous sugars (carbohydrate products) in the pyrolysis bio-oil were reduced to 0.71 and 0.39% after pre-treated by dry torrefaction at 300 °C and wet torrefaction at 160 °C in $H_2SO_4$ solution, respectively. The fatty acids composition in the torrefaction bio-oil was increased from 5.59 to 19.4% when the dry torrefaction temperature increased from 200 to 300 °C, indicating the dry torrefaction not only removed the carbohydrate products in the bio-oil, whereas part of the lipid products was also eliminated. The pyrolytic bio-oil produced from the pre-treated microalgae by wet torrefaction in the $H_2SO_4$ solution was dominated by long-chain fatty acids, which is ready to convert into biofuel.

Lastly, pyrolysis kinetics was performed to analyse the kinetic parameters of every single component of raw and wet torrefaction microalga ESP-31, especially in water and $H_2SO_4$ due to the production of high-quality biochar based on the previous analysis. The

IPR model with four reaction model was successful predicted the pyrolysis kinetics of raw and wet torrefied microalgae. The results revealed that the thermal degradation curve with a fit quality of at least 98% were predicted for microalgae pyrolysis. This model predicted the thermal degradation temperature of carbohydrates, proteins, lipids, and others during the pyrolysis separately. For raw and wet torrefied microalgae, the activation energies for carbohydrates, proteins, lipids, and others ranged between 64.59−221.33, 43.78−61.38, 85.92−192.27, and 42.32−113.51 kJ mol$^{-1}$, respectively. Meanwhile, the activation energies and pre-exponential factor of carbohydrates decreased from 221.11 to 64.59 kJ mol$^{-1}$ and $7.17\times10^{18}$ to $1.39\times10^{4}$, respectively. Furthermore, wet torrefaction strongly affected the heights of derivative peak and decomposition temperature of each component significantly. The thermal degradation temperature of every single component after the wet torrefaction was clearly identify by using temperature indicators of $T_1$ (conversion degree reaches 1%) and $T_{99}$ (conversion degree reaches 99%). The pyrolysis kinetics of microalgae carbohydrates, proteins, lipids and others can be simulated readily to a certain fit quality using the IPR model.

Based on these conclusions, microalgae were successfully converted into biochar as bioenergy sources using dry and wet torrefaction. Dry torrefaction is a green alternative method for the biochar production. The fuel properties of biochar produced from microalga ESP-31 were close to the coal fuel, which could be used as co-firing in coal power plant. A low temperature wet torrefaction in acidic solutions can produce a similar HHV enhancement to the biochar produced from dry torrefaction. At the same time, wet torrefaction can fully utilise most of the components in the microalgae for biochar and sugar production. With the co-production of solid biochar as bioenergy sources and high glucose content in the liquid hydrolysate that can be utilized for bioethanol production, wet torrefaction in acidic solutions can be one of the conversion technologies towards application of renewable energy production. Furthermore, the methodology of this study

can be applied to high-carbohydrate biomass in future study for large scale production with minor modification of the current model. Next, TG-FTIR and Py-GC/MS were successfully investigated the microalgal biochar produced from dry and wet torrefaction. Dry torrefaction destroyed the carbohydrate and lipid components to produce torrefaction bio-oil rich in carbohydrate and lipid products. This process limited the usage of the torrefaction bio-oil due to the complexity of the bio-oil. Most of the carbohydrate products in the bio-oil were removed after pre-treated by wet torrefaction in sulfuric acid solution to improve the bio-oil quality by reducing acidity, water and oxygen contents. Microwave-assisted wet torrefaction at low temperature is a cost-effective pre-treatment technique to produce high-quality pyrolytic bio-oil, which can be scaled-up for the quantitative analysis in further research. Lastly, four reaction model was successfully predicted the pyrolysis kinetics of microalgae to understand the complex pyrolysis process of microalgae. Wet torrefaction strongly affected the kinetic parameters, conversion rate and conversion degree of each component for microalga ESP-31, which is the important parameters to be considered during the reactor design. The experimental results of microalgae pyrolysis kinetics are beneficial to pre-treatment operation and reactor design in the biomass-to-energy industry. In short, wet torrefaction conversion of microalgal biomass for bioenergy production was remarkably improved. The overall study offers a better understanding to the biochar production from microalgae biomass (third-generation biofuel feedstock).

**5.2     Recommendations for future work**

The recommendations are as follows:

1. The conventional torrefaction required higher energy input to convert the microalgae. Meanwhile, the microalgal species directly affected on the torrefaction performance due to the different in the chemical composition and structure. Hence, the selection on the microalgae used to upgrade as biofuel is very crucial. Furthermore, cultivation of the microalgae should be taken into consideration to produce the desired composition for biofuel production.

2. Wet torrefaction is found to be a promising method to produce high quality solid biofuel with high HHV and energy yields at low temperature and holding time. It is known as a new technique to conversion of microalgae to biochar by skipping drying process. Today, the cost of installing the setup of wet torrefaction is high in the current stage due to high pressure required. In-depth research should be conducted on energy and economic benefits of pilot scale wet torrefaction reactor. In addition, a detailed cost-effective analysis on the process of microalgae wet torrefaction needs to be conducted to serve as an important guideline for upscale and production of high energy content biochar in the future. Furthermore, the biochar produced from wet torrefaction shows an applicable approach as bio-adsorbent for water or soil. Application on water treatment using microalgal biochar may be applicable by applying further treatment into activated biochar.

3. The combination of TG and FTIR provides a very useful tool for determining the decomposition stage and evolved products during a biomass thermochemical conversion process. Homo-diatomic species such as $H_2$ is hardly detected using

TG-FTIR. The sample with similar functional groups such as different light hydrocarbons is difficult to distinguish by FTIR. A thermogravimetric analyser coupled with mass spectrometry (TG-MS) to measure the mass-to-charge ratio (*m/z*) of volatiles can be one of the solutions for the limitation. Meanwhile, TG-FTIR and Py-GC/MS are qualitative analysis, the bio-oil yield cannot be presented in current study, a scape up analysis can be conducted in further study for the quantitative analysis.

4. Pyrolysis kinetics using IPR models have successfully determined the kinetics of every single components. However, limited number of publications investigated the biomass pyrolysis kinetics using this method, it recommends that further kinetics studies of various biomass would use this model due to the advantages. Moreover, complex interactions between the chemistry and transport phenomena often arise at interparticle and intraparticle during the practical applications. The heat and mass transfer phenomena can be considered in the future work by using simulation. Thus, it suggests to further exploring on the detailed models coupling with heat, mass and momentum transports, to further understand the pyrolysis behaviour of microalgal particles during practical.

# REFERENCES

Acharya, B., Dutta, A., & Minaret, J. (2015). Review on comparative study of dry and wet torrefaction. *Sustainable Energy Technologies and Assessments, 12*, 26-37.

Adeniyi, O. M., Azimov, U., & Burluka, A. (2018). Algae biofuel: Current status and future applications. *Renewable and Sustainable Energy Reviews, 90*, 316-335.

Agrawal, A., & Chakraborty, S. (2013). A kinetic study of pyrolysis and combustion of microalgae Chlorella vulgaris using thermo-gravimetric analysis. *Bioresource Technology, 128*, 72-80.

Ahmed, M. B., Zhou, J. L., Ngo, H. H., Guo, W., & Chen, M. (2016). Progress in the preparation and application of modified biochar for improved contaminant removal from water and wastewater. *Bioresource Technology, 214*, 836-851.

Aho, A., Kumar, N., Eränen, K., Salmi, T., Hupa, M., & Murzin, D. Y. (2008). Catalytic pyrolysis of woody biomass in a fluidized bed reactor: Influence of the zeolite structure. *Fuel, 87*(12), 2493-2501.

Aho, A., Kumar, N., Lashkul, A. V., Eränen, K., Ziolek, M., Decyk, P., Salmi, T., Holmbom, B., Hupa, M., & Murzin, D. Y. (2010). Catalytic upgrading of woody biomass derived pyrolysis vapours over iron modified zeolites in a dual-fluidized bed reactor. *Fuel, 89*(8), 1992-2000.

Almeida, H. N., Calixto, G. Q., Chagas, B. M., Melo, D. M., Resende, F. M., Melo, M. A., & Braga, R. M. (2017). Characterization and pyrolysis of Chlorella vulgaris and Arthrospira platensis: potential of bio-oil and chemical production by Py-GC/MS analysis. *Environmental Science and Pollution Research, 24*(16), 14142-14150.

Álvarez-Murillo, A., Sabio, E., Ledesma, B., Román, S., & González-García, C. M. (2016). Generation of biofuel from hydrothermal carbonization of cellulose. Kinetics modelling. *Energy, 94*, 600-608.

Amin, M., Chetpattananondh, P., & Ratanawilai, S. (2019). Application of extracted marine Chlorella sp. residue for bio-oil production as the biomass feedstock and microwave absorber. *Energy Conversion and Management, 195*, 819-829.

Anuar Sharuddin, S. D., Abnisa, F., Wan Daud, W. M. A., & Aroua, M. K. (2016). A review on pyrolysis of plastic wastes. *Energy Conversion and Management, 115*, 308-326.

Bach, Q.-V., & Chen, W.-H. (2017a). A comprehensive study on pyrolysis kinetics of microalgal biomass. *Energy Conversion and Management, 131*, 109-116.

Bach, Q.-V., & Chen, W.-H. (2017b). Pyrolysis characteristics and kinetics of microalgae via thermogravimetric analysis (TGA): A state-of-the-art review. *Bioresource Technology, 246*, 88-100.

Bach, Q.-V., Chen, W.-H., Lin, S.-C., Sheen, H.-K., & Chang, J.-S. (2017a). Effect of Wet Torrefaction on Thermal Decomposition Behavior of Microalga Chlorella vulgaris ESP-31. *Energy Procedia, 105*, 206-211.

Bach, Q.-V., Chen, W.-H., Lin, S.-C., Sheen, H.-K., & Chang, J.-S. (2017b). Wet torrefaction of microalga Chlorella vulgaris ESP-31 with microwave-assisted heating. *Energy Conversion and Management, 141*, 163-170.

Bach, Q.-V., Chen, W.-H., Sheen, H.-K., & Chang, J.-S. (2017c). Gasification kinetics of raw and wet-torrefied microalgae Chlorella vulgaris ESP-31 in carbon dioxide. *Bioresource Technology, 244*, 1393-1399.

Bach, Q.-V., & Skreiberg, Ø. (2016). Upgrading biomass fuels via wet torrefaction: A review and comparison with dry torrefaction. *Renewable and Sustainable Energy Reviews, 54*, 665-677.

Bach, Q.-V., Tran, K.-Q., Khalil, R. A., Skreiberg, Ø., & Seisenbaeva, G. (2013). Comparative assessment of wet torrefaction. *Energy & Fuels, 27*(11), 6743-6753.

Bach, Q.-V., Tran, K.-Q., & Skreiberg, Ø. (2015a). Accelerating wet torrefaction rate and ash removal by carbon dioxide addition. *Fuel Processing Technology, 140*, 297-303.

Bach, Q.-V., Tran, K.-Q., & Skreiberg, Ø. (2016). Hydrothermal pretreatment of fresh forest residues: Effects of feedstock pre-drying. *Biomass and Bioenergy, 85*, 76-83.

Bach, Q.-V., Tran, K.-Q., & Skreiberg, Ø. (2017d). Combustion kinetics of wet-torrefied forest residues using the distributed activation energy model (DAEM). *Applied Energy, 185*, 1059-1066.

Bach, Q.-V., Tran, K.-Q., Skreiberg, Ø., Khalil, R. A., & Phan, A. N. (2014). Effects of wet torrefaction on reactivity and kinetics of wood under air combustion conditions. *Fuel, 137*, 375-383.

Bach, Q.-V., Tran, K.-Q., Skreiberg, Ø., & Trinh, T. T. (2015b). Effects of wet torrefaction on pyrolysis of woody biomass fuels. *Energy, 88*, 443-456.

Barba, F. J., Grimi, N., & Vorobiev, E. (2015). New approaches for the use of non-conventional cell disruption technologies to extract potential food additives and nutraceuticals from microalgae. *Food Engineering Reviews, 7*(1), 45-62.

Barzegar, R., Yozgatligil, A., Olgun, H., & Atimtay, A. T. (2019). TGA and kinetic study of different torrefaction conditions of wood biomass under air and oxy-fuel combustion atmospheres. *Journal of the Energy Institute*.

Becker, E. W. (1994). *Microalgae: biotechnology and microbiology* (Vol. 10): Cambridge University Press.

Bergman, P. C., Boersma, A., Zwart, R., & Kiel, J. (2005). Torrefaction for biomass co-firing in existing coal-fired power stations. *Energy Centre of Netherlands, Report No. ECN-C-05-013*.

Bilgic, E., Yaman, S., Haykiri-Acma, H., & Kucukbayrak, S. (2016). Limits of variations on the structure and the fuel characteristics of sunflower seed shell through torrefaction. *Fuel Processing Technology, 144*, 197-202.

Biller P, R. A., Skill SC, Lea-Langton A, Balasundaram B, Hall C, Riley R, Llewellyn CA. (2012). Nutrient recycling of aqueous phase for microalgae cultivation from the hydrothermal liquefaction process. *Algal Res, 1*, 70-76.

Biller, P., & Ross, A. B. (2014). Pyrolysis GC–MS as a novel analysis technique to determine the biochemical composition of microalgae. *Algal Research, 6*, 91-97.

Bogusz, A., Oleszczuk, P., & Dobrowolski, R. (2015). Application of laboratory prepared and commercially available biochars to adsorption of cadmium, copper and zinc ions from water. *Bioresource Technology, 196*, 540-549.

Boström, D., Skoglund, N., Grimm, A., Boman, C., Öhman, M., Broström, M., & Backman, R. (2012). Ash Transformation Chemistry during Combustion of Biomass. *Energy & Fuels, 26*(1), 85-93.

Bougrier, C., Delgenès, J. P., & Carrère, H. (2008). Effects of thermal treatments on five different waste activated sludge samples solubilisation, physical properties and anaerobic digestion. *Chemical Engineering Journal, 139*(2), 236-244.

Broström, M., Nordin, A., Pommer, L., Branca, C., & Di Blasi, C. (2012). Influence of torrefaction on the devolatilization and oxidation kinetics of wood. *Journal of Analytical and Applied Pyrolysis, 96*, 100-109.

Bui, H.-H., Tran, K.-Q., & Chen, W.-H. (2016). Pyrolysis of microalgae residues – A kinetic study. *Bioresource Technology, 199*, 362-366.

Bujang, A. S., Bern, C. J., & Brumm, T. J. (2016). Summary of energy demand and renewable energy policies in Malaysia. *Renewable and Sustainable Energy Reviews, 53*, 1459-1467.

Bundhoo, Z. M. A. (2018). Microwave-assisted conversion of biomass and waste materials to biofuels. *Renewable and Sustainable Energy Reviews, 82*(Part 1), 1149-1177.

Burhenne, L., Messmer, J., Aicher, T., & Laborie, M.-P. (2013). The effect of the biomass components lignin, cellulose and hemicellulose on TGA and fixed bed pyrolysis. *Journal of Analytical and Applied Pyrolysis, 101*, 177-184.

Cai, W., Liu, Q., Shen, D., & Wang, J. (2019). Py-GC/MS analysis on product distribution of two-staged biomass pyrolysis. *Journal of Analytical and Applied Pyrolysis, 138*, 62-69.

Carrier, M., Loppinet-Serani, A., Denux, D., Lasnier, J.-M., Ham-Pichavant, F., Cansell, F., & Aymonier, C. (2011). Thermogravimetric analysis as a new method to determine the lignocellulosic composition of biomass. *Biomass and Bioenergy, 35*(1), 298-307.

Cen, K., Chen, D., Wang, J., Cai, Y., & Wang, L. (2016). Effects of Water Washing and Torrefaction Pretreatments on Corn Stalk Pyrolysis: Combined Study Using TG-FTIR and a Fixed Bed Reactor. *Energy & Fuels, 30*(12), 10627-10634.

Ceylan, S., & Kazan, D. (2015). Pyrolysis kinetics and thermal characteristics of microalgae Nannochloropsis oculata and Tetraselmis sp. *Bioresource Technology, 187*, 1-5.

Ceylan, S., & Topçu, Y. (2014). Pyrolysis kinetics of hazelnut husk using thermogravimetric analysis. *Bioresource Technology, 156*, 182-188.

Chaiwong, K., Kiatsiriroat, T., Vorayos, N., & Thararax, C. (2013). Study of bio-oil and bio-char production from algae by slow pyrolysis. *Biomass and Bioenergy, 56*, 600-606.

Chang, Y.-M., Tsai, W.-T., & Li, M.-H. (2015). Chemical characterization of char derived from slow pyrolysis of microalgal residue. *Journal of Analytical and Applied Pyrolysis, 111*, 88-93.

Chen, C.-Y., Lee, P.-J., Tan, C. H., Lo, Y.-C., Huang, C.-C., Show, P. L., Lin, C.-H., & Chang, J.-S. (2015a). Improving protein production of indigenous microalga Chlorella vulgaris FSP-E by photobioreactor design and cultivation strategies. *Biotechnology Journal, 10*(6), 905-914.

Chen, C.-Y., Zhao, X.-Q., Yen, H.-W., Ho, S.-H., Cheng, C.-L., Lee, D.-J., Bai, F.-W., & Chang, J.-S. (2013). Microalgae-based carbohydrates for biofuel production. *Biochemical Engineering Journal, 78*, 1-10.

Chen, C., Ma, X., & He, Y. (2012a). Co-pyrolysis characteristics of microalgae Chlorella vulgaris and coal through TGA. *Bioresource Technology, 117*, 264-273.

Chen, D., Cen, K., Jing, X., Gao, J., Li, C., & Ma, Z. (2017a). An approach for upgrading biomass and pyrolysis product quality using a combination of aqueous phase bio-oil washing and torrefaction pretreatment. *Bioresource Technology, 233*, 150-158.

Chen, D., Zheng, Z., Fu, K., Zeng, Z., Wang, J., & Lu, M. (2015b). Torrefaction of biomass stalk and its effect on the yield and quality of pyrolysis products. *Fuel, 159*, 27-32.

Chen, D., Zhou, J., & Zhang, Q. (2014a). Effects of heating rate on slow pyrolysis behavior, kinetic parameters and products properties of moso bamboo. *Bioresource Technology, 169*, 313-319.

Chen, D., Zhou, J., & Zhang, Q. (2014b). Effects of Torrefaction on the Pyrolysis Behavior and Bio-Oil Properties of Rice Husk by Using TG-FTIR and Py-GC/MS. *Energy & Fuels, 28*(9), 5857-5863.

Chen, D., Zhou, J., Zhang, Q., & Zhu, X. (2014c). Evaluation methods and research progresses in bio-oil storage stability. *Renewable and Sustainable Energy Reviews, 40*, 69-79.

Chen, D., Zhou, J., Zhang, Q., Zhu, X., & Lu, Q. (2014d). Torrefaction of Rice Husk using TG-FTIR and its Effect on the Fuel Characteristics, Carbon, and Energy Yields. *BioResources, 9*(4).

Chen, H., Xie, Y., Chen, W., Xia, M., Li, K., Chen, Z., Chen, Y., & Yang, H. (2019a). Investigation on co-pyrolysis of lignocellulosic biomass and amino acids using TG-FTIR and Py-GC/MS. *Energy Conversion and Management, 196*, 320-329.

Chen, J., Fan, X., Jiang, B., Mu, L., Yao, P., Yin, H., & Song, X. (2015c). Pyrolysis of oil-plant wastes in a TGA and a fixed-bed reactor: Thermochemical behaviors, kinetics, and products characterization. *Bioresource Technology, 192*, 592-602.

Chen, L., Yu, Z., Liang, J., Liao, Y., & Ma, X. (2018a). Co-pyrolysis of chlorella vulgaris and kitchen waste with different additives using TG-FTIR and Py-GC/MS. *Energy Conversion and Management, 177*, 582-591.

Chen, Q., Zhou, J., Liu, B., Mei, Q., & Luo, Z. (2011a). Influence of torrefaction pretreatment on biomass gasification technology. *Chinese Science Bulletin, 56*(14), 1449-1456.

Chen, W.-H., Cheng, C.-L., Show, P.-L., & Ong, H. C. (2019b). Torrefaction performance prediction approached by torrefaction severity factor. *Fuel, 251*, 126-135.

Chen, W.-H., Cheng, W.-Y., Lu, K.-M., & Huang, Y.-P. (2011b). An evaluation on improvement of pulverized biomass property for solid fuel through torrefaction. *Applied Energy, 88*(11), 3636-3644.

Chen, W.-H., Chu, Y.-S., Liu, J.-L., & Chang, J.-S. (2018b). Thermal degradation of carbohydrates, proteins and lipids in microalgae analyzed by evolutionary computation. *Energy Conversion and Management, 160*, 209--219.

Chen, W.-H., Chu, Y.-S., Liu, J.-L., & Chang, J.-S. (2018c). Thermal degradation of carbohydrates, proteins and lipids in microalgae analyzed by evolutionary computation. *Energy Conversion and Management, 160*, 209-219.

Chen, W.-H., Huang, M.-Y., Chang, J.-S., & Chen, C.-Y. (2014e). Thermal decomposition dynamics and severity of microalgae residues in torrefaction. *Bioresource Technology, 169*, 258-264.

Chen, W.-H., Huang, M.-Y., Chang, J.-S., & Chen, C.-Y. (2015d). Torrefaction operation and optimization of microalga residue for energy densification and utilization. *Applied Energy, 154*, 622-630.

Chen, W.-H., Huang, M.-Y., Chang, J.-S., Chen, C.-Y., & Lee, W.-J. (2015e). An energy analysis of torrefaction for upgrading microalga residue as a solid fuel. *Bioresource Technology, 185*, 285-293.

Chen, W.-H., & Kuo, P.-C. (2010). A study on torrefaction of various biomass materials and its impact on lignocellulosic structure simulated by a thermogravimetry. *Energy, 35*(6), 2580-2586.

Chen, W.-H., & Kuo, P.-C. (2011a). Isothermal torrefaction kinetics of hemicellulose, cellulose, lignin and xylan using thermogravimetric analysis. *Energy, 36*(11), 6451-6460.

Chen, W.-H., & Kuo, P.-C. (2011b). Torrefaction and co-torrefaction characterization of hemicellulose, cellulose and lignin as well as torrefaction of some basic constituents in biomass. *Energy, 36*(2), 803-811.

Chen, W.-H., & Lin, B.-J. (2016). Characteristics of products from the pyrolysis of oil palm fiber and its pellets in nitrogen and carbon dioxide atmospheres. *Energy, 94*, 569-578.

Chen, W.-H., Lin, B.-J., Colin, B., Chang, J.-S., Pétrissans, A., Bi, X., & Pétrissans, M. (2018d). Hygroscopic transformation of woody biomass torrefaction for carbon storage. *Applied Energy, 231*, 768-776.

Chen, W.-H., Lin, B.-J., Huang, M.-Y., & Chang, J.-S. (2015f). Thermochemical conversion of microalgal biomass into biofuels: A review. *Bioresource Technology, 184*, 314-327.

Chen, W.-H., Lu, K.-M., Lee, W.-J., Liu, S.-H., & Lin, T.-C. (2014f). Non-oxidative and oxidative torrefaction characterization and SEM observations of fibrous and ligneous biomass. *Applied Energy, 114*, 104-113.

Chen, W.-H., Lu, K.-M., & Tsai, C.-M. (2012b). An experimental analysis on property and structure variations of agricultural wastes undergoing torrefaction. *Applied Energy, 100*, 318-325.

Chen, W.-H., Peng, J., & Bi, X. T. (2015g). A state-of-the-art review of biomass torrefaction, densification and applications. *Renewable and Sustainable Energy Reviews, 44*, 847-866.

Chen, W.-H., Tu, Y.-J., & Sheen, H.-K. (2011c). Disruption of sugarcane bagasse lignocellulosic structure by means of dilute sulfuric acid pretreatment with microwave-assisted heating. *Applied Energy, 88*(8), 2726-2734.

Chen, W.-H., Wang, C.-W., Kumar, G., Rousset, P., & Hsieh, T.-H. (2018e). Effect of torrefaction pretreatment on the pyrolysis of rubber wood sawdust analyzed by Py-GC/MS. *Bioresource Technology, 259*, 469-473.

Chen, W.-H., Wang, C.-W., Ong, H. C., Show, P. L., & Hsieh, T.-H. (2019c). Torrefaction, pyrolysis and two-stage thermodegradation of hemicellulose, cellulose and lignin. *Fuel, 258*, 116168.

Chen, W.-H., Wu, Z.-Y., & Chang, J.-S. (2014g). Isothermal and non-isothermal torrefaction characteristics and kinetics of microalga Scenedesmus obliquus CNW-N. *Bioresource Technology, 155*, 245-251.

Chen, W.-H., Ye, S.-C., & Sheen, H.-K. (2012c). Hydrolysis characteristics of sugarcane bagasse pretreated by dilute acid solution in a microwave irradiation environment. *Applied Energy, 93*, 237-244.

Chen, W.-H., Ye, S.-C., & Sheen, H.-K. (2012d). Hydrothermal carbonization of sugarcane bagasse via wet torrefaction in association with microwave heating. *Bioresource Technology, 118*, 195-203.

Chen, Y.-C., Chen, W.-H., Lin, B.-J., Chang, J.-S., & Ong, H. C. (2016). Impact of torrefaction on the composition, structure and reactivity of a microalga residue. *Applied Energy, 181*, 110-119.

Chen, Y.-H., Chang, C.-C., Chang, C.-Y., Yuan, M.-H., Ji, D.-R., Shie, J.-L., Lee, C.-H., Chen, Y.-H., Chang, W.-R., Yang, T.-Y., Hsu, T.-C., Huang, M., Wu, C.-H., Lin, F.-C., & Ko, C.-H. (2017b). Production of a solid bio-fuel from waste bamboo chopsticks by torrefaction for cofiring with coal. *Journal of Analytical and Applied Pyrolysis, 126*, 315-322.

Chew, J. J., & Doshi, V. (2011). Recent advances in biomass pretreatment – Torrefaction fundamentals and technology. *Renewable and Sustainable Energy Reviews, 15*(8), 4212-4222.

Chheda, J. N., Román-Leshkov, Y., & Dumesic, J. A. (2007). Production of 5-hydroxymethylfurfural and furfural by dehydration of biomass-derived mono- and poly-saccharides. *Green Chemistry, 9*(4), 342-350.

Choi, S.-A., Choi, W.-I., Lee, J.-S., Kim, S. W., Lee, G.-A., Yun, J., & Park, J.-Y. (2015). Hydrothermal acid treatment for sugar extraction from Golenkinia sp. *Bioresource Technology, 190*, 408-411.

Christensen, E., Evans, R. J., & Carpenter, D. (2017). High-resolution mass spectrometric analysis of biomass pyrolysis vapors. *Journal of Analytical and Applied Pyrolysis, 124*, 327-334.

Coates, J. (2000). Interpretation of infrared spectra, a practical approach. *Encyclopedia of analytical chemistry, 12*, 10815-10837.

da Silva, C. M. S., Carneiro, A. d. C. O., Vital, B. R., Figueiró, C. G., de Freitas Fialho, L., de Magalhães, M. A., Carvalho, A. G., & Cândido, W. L. (2017a). Biomass torrefaction for energy purposes–Definitions and an overview of challenges and opportunities in Brazil. *Renewable and Sustainable Energy Reviews*.

da Silva, C. M. S., Carneiro, A. d. C. O., Vital, B. R., Figueiró, C. G., Fialho, L. d. F., de Magalhães, M. A., Carvalho, A. G., & Cândido, W. L. (2017b). Biomass torrefaction for energy purposes – Definitions and an overview of challenges and opportunities in Brazil. *Renewable and Sustainable Energy Reviews*.

da Silva, J. C. G., Pereira, J. L. C., Andersen, S. L. F., Moreira, R. d. F. P. M., & José, H. J. (2020). Torrefaction of ponkan peel waste in tubular fixed-bed reactor: In-depth bioenergetic evaluation of torrefaction products. *Energy, 210*, 118569.

Dai, L., Wang, Y., Liu, Y., Ruan, R., He, C., Yu, Z., Jiang, L., Zeng, Z., & Tian, X. (2019). Integrated process of lignocellulosic biomass torrefaction and pyrolysis for upgrading bio-oil production: A state-of-the-art review. *Renewable and Sustainable Energy Reviews, 107*, 20-36.

Dai, L., Yang, B., Li, H., Tan, F., Zhu, N., Zhu, Q., He, M., Ran, Y., & Hu, G. (2017). A synergistic combination of nutrient reclamation from manure and resultant hydrochar upgradation by acid-supported hydrothermal carbonization. *Bioresource Technology, 243*, 860-866.

Das, P., Mondal, D., & Maiti, S. (2017). Thermochemical conversion pathways of Kappaphycus alvarezii granules through study of kinetic models. *Bioresource Technology, 234*, 233-242.

Du, S.-W., Chen, W.-H., & Lucas, J. (2007). Performances of pulverized coal injection in blowpipe and tuyere at various operational conditions. *Energy Conversion and Management, 48*(7), 2069-2076.

Du, S.-W., Chen, W.-H., & Lucas, J. A. (2010). Pulverized coal burnout in blast furnace simulated by a drop tube furnace. *Energy, 35*(2), 576-581.

Du, Z., Hu, B., Ma, X., Cheng, Y., Liu, Y., Lin, X., Wan, Y., Lei, H., Chen, P., & Ruan, R. (2013). Catalytic pyrolysis of microalgae and their three major components: Carbohydrates, proteins, and lipids. *Bioresource Technology, 130*, 777-782.

Du, Z., Li, Y., Wang, X., Wan, Y., Chen, Q., Wang, C., Lin, X., Liu, Y., Chen, P., & Ruan, R. (2011). Microwave-assisted pyrolysis of microalgae for biofuel production. *Bioresource Technology, 102*(7), 4890-4896.

Dudzińska, A. (2014). The Effect of Pore Volume of Hard Coals on Their Susceptibility to Spontaneous Combustion. *Journal of Chemistry, 2014*, 393819.

Duygu, D. Y., Udoh, A. U., Ozer, T. B., Akbulut, A., Erkaya, I. A., Yildiz, K., & Guler, D. (2012). Fourier transform infrared (FTIR) spectroscopy for identification of Chlorella vulgaris Beijerinck 1890 and Scenedesmus obliquus (Turpin) Kützing 1833. *African Journal of Biotechnology, 11*(16), 3817-3824.

Eseltine, D., Thanapal, S. S., Annamalai, K., & Ranjan, D. (2013). Torrefaction of woody biomass (Juniper and Mesquite) using inert and non-inert gases. *Fuel, 113*, 379-388.

Fabra, M. J., Martínez-Sanz, M., Gómez-Mascaraque, L. G., Gavara, R., & López-Rubio, A. (2018). Structural and physicochemical characterization of thermoplastic corn starch films containing microalgae. *Carbohydrate Polymers, 186*, 184-191.

Fagernäs, L., Brammer, J., Wilén, C., Lauer, M., & Verhoeff, F. (2010). Drying of biomass for second generation synfuel production. *Biomass and Bioenergy, 34*(9), 1267-1277.

Fagerson, I. S. (1969). Thermal degradation of carbohydrates; a review. *Journal of Agricultural and Food Chemistry, 17*(4), 747-750.

Fakkaew, K., Koottatep, T., & Polprasert, C. (2017). Faecal sludge treatment and utilization by hydrothermal carbonization. *Journal of Environmental Management*.

Fan, M., Dai, D., & Huang, B. (2012). Fourier transform infrared spectroscopy for natural fibres. In *Fourier transform-materials analysis*: InTech.

Fan, Y., Tippayawong, N., Wei, G., Huang, Z., Zhao, K., Jiang, L., Zheng, A., Zhao, Z., & Li, H. (2020). Minimizing tar formation whilst enhancing syngas production by integrating biomass torrefaction pretreatment with chemical looping gasification. *Applied Energy, 260*, 114315.

Fang, S., Yu, Z., Ma, X., Lin, Y., Lin, Y., Chen, L., Fan, Y., & Liao, Y. (2017). Co-pyrolysis characters between combustible solid waste and paper mill sludge by TG-FTIR and Py-GC/MS. *Energy Conversion and Management, 144*, 114-122.

Fasahati, P., & Liu, J. J. (2015). Economic, energy, and environmental impacts of alcohol dehydration technology on biofuel production from brown algae. *Energy, 93*, 2321-2336.

Fenton, O., & Ó hUallacháin, D. (2012). Agricultural nutrient surpluses as potential input sources to grow third generation biomass (microalgae): A review. *Algal Research, 1*(1), 49-56.

Funke, A., & Ziegler, F. (2010). Hydrothermal carbonization of biomass: A summary and discussion of chemical mechanisms for process engineering. *Biofuels, Bioproducts and Biorefining, 4*(2), 160-177.

Gai, C., Liu, Z., Han, G., Peng, N., & Fan, A. (2015). Combustion behavior and kinetics of low-lipid microalgae via thermogravimetric analysis. *Bioresource Technology, 181*, 148-154.

Gai, C., Zhang, Y., Chen, W.-T., Zhang, P., & Dong, Y. (2013). Thermogravimetric and kinetic analysis of thermal decomposition characteristics of low-lipid microalgae. *Bioresource Technology, 150*, 139-148.

Gao, N., Li, A., Quan, C., Du, L., & Duan, Y. (2013). TG–FTIR and Py–GC/MS analysis on pyrolysis and combustion of pine sawdust. *Journal of Analytical and Applied Pyrolysis, 100*, 26-32.

Gao, P., Zhou, Y., Meng, F., Zhang, Y., Liu, Z., Zhang, W., & Xue, G. (2016). Preparation and characterization of hydrochar from waste eucalyptus bark by hydrothermal carbonization. *Energy, 97*, 238-245.

Giudicianni, P., Cardone, G., Sorrentino, G., & Ragucci, R. (2014). Hemicellulose, cellulose and lignin interactions on Arundo donax steam assisted pyrolysis. *Journal of Analytical and Applied Pyrolysis, 110*, 138-146.

Goh, B. H. H., Ong, H. C., Cheah, M. Y., Chen, W.-H., Yu, K. L., & Mahlia, T. M. I. (2019). Sustainability of direct biodiesel synthesis from microalgae biomass: A critical review. *Renewable and Sustainable Energy Reviews, 107*, 59-74.

Gong, Z., Fang, P., Wang, Z., Li, X., Wang, Z., & Meng, F. (2020). Pyrolysis characteristics and products distribution of haematococcus pluvialis microalgae and its extraction residue. *Renewable Energy, 146*, 2134-2141.

Goyal, H. B., Seal, D., & Saxena, R. C. (2008). Bio-fuels from thermochemical conversion of renewable resources: A review. *Renewable and Sustainable Energy Reviews, 12*(2), 504-517.

Granados, D. A., Ruiz, R. A., Vega, L. Y., & Chejne, F. (2017). Study of reactivity reduction in sugarcane bagasse as consequence of a torrefaction process. *Energy, 139*, 818-827.

Gu, X., Ma, X., Li, L., Liu, C., Cheng, K., & Li, Z. (2013). Pyrolysis of poplar wood sawdust by TG-FTIR and Py–GC/MS. *Journal of Analytical and Applied Pyrolysis, 102*, 16-23.

Gu, X., Martinez-Fernandez, J. S., Pang, N., Fu, X., & Chen, S. (2020). Recent development of hydrothermal liquefaction for algal biorefinery. *Renewable and Sustainable Energy Reviews, 121*, 109707.

Guo, Y., Yeh, T., Song, W., Xu, D., & Wang, S. (2015). A review of bio-oil production from hydrothermal liquefaction of algae. *Renewable and Sustainable Energy Reviews, 48*, 776-790.

Handing Chen, X. C., Zhi Qiao, Haifeng Liu. (2016). Release and transformation characteristics of K and Cl during straw torrefaction and mild pyrolysis. *Fuel, 167*, 31-39.

Harun, R., & Danquah, M. K. (2011). Influence of acid pre-treatment on microalgal biomass for bioethanol production. *Process Biochemistry, 46*(1), 304-309.

Hassan, H., Lim, J. K., & Hameed, B. H. (2016). Recent progress on biomass co-pyrolysis conversion into high-quality bio-oil. *Bioresource Technology, 221*, 645-655.

He, C., Tang, C., Li, C., Yuan, J., Tran, K.-Q., Bach, Q.-V., Qiu, R., & Yang, Y. (2018). Wet torrefaction of biomass for high quality solid fuel production: A review. *Renewable and Sustainable Energy Reviews, 91*, 259-271.

Heilmann, S. M., Davis, H. T., Jader, L. R., Lefebvre, P. A., Sadowsky, M. J., Schendel, F. J., von Keitz, M. G., & Valentas, K. J. (2010). Hydrothermal carbonization of microalgae. *Biomass and Bioenergy, 34*(6), 875-882.

Hernández, A. B., Okonta, F., & Freeman, N. (2017). Sewage sludge charcoal production by N2- and CO2-torrefaction. *Journal of Environmental Chemical Engineering, 5*(5), 4406-4414.

Ho, S.-H., Chen, W.-M., & Chang, J.-S. (2010). Scenedesmus obliquus CNW-N as a potential candidate for CO2 mitigation and biodiesel production. *Bioresource Technology, 101*(22), 8725-8730.

Ho, S.-H., Huang, S.-W., Chen, C.-Y., Hasunuma, T., Kondo, A., & Chang, J.-S. (2013). Bioethanol production using carbohydrate-rich microalgae biomass as feedstock. *Bioresource Technology, 135*, 191-198.

Hsu, T.-C., Chang, C.-C., Yuan, M.-H., Chang, C.-Y., Chen, Y.-H., Lin, C.-F., Ji, D.-R., Shie, J.-L., Manh, D. V., Wu, C.-H., Chiang, S.-W., Lin, F.-C., Lee, D.-J., Huang,

M., & Chen, Y.-H. (2017). Upgrading of Jatropha-seed Residue after Mechanical Extraction of Oil via Torrefaction. *Energy*.

Hu, J., Nagarajan, D., Zhang, Q., Chang, J.-S., & Lee, D.-J. (2017). Heterotrophic cultivation of microalgae for pigment production: A review. *Biotechnology Advances*.

Hu, M., Chen, Z., Guo, D., Liu, C., Xiao, B., Hu, Z., & Liu, S. (2015). Thermogravimetric study on pyrolysis kinetics of Chlorella pyrenoidosa and bloom-forming cyanobacteria. *Bioresource Technology, 177*, 41-50.

Hu, Y., Gong, M., Feng, S., Xu, C., & Bassi, A. (2019). A review of recent developments of pre-treatment technologies and hydrothermal liquefaction of microalgae for bio-crude oil production. *Renewable and Sustainable Energy Reviews, 101*, 476-492.

Huang, J., Liu, J., Chen, J., Xie, W., Kuo, J., Lu, X., Chang, K., Wen, S., Sun, G., Cai, H., Buyukada, M., & Evrendilek, F. (2018). Combustion behaviors of spent mushroom substrate using TG-MS and TG-FTIR: Thermal conversion, kinetic, thermodynamic and emission analyses. *Bioresource Technology, 266*, 389-397.

Huang, Y.-F., Cheng, P.-H., Chiueh, P.-T., & Lo, S.-L. (2017a). Leucaena biochar produced by microwave torrefaction: Fuel properties and energy efficiency. *Applied Energy, 204*, 1018-1025.

Huang, Y.-F., Sung, H.-T., Chiueh, P.-T., & Lo, S.-L. (2016). Co-torrefaction of sewage sludge and leucaena by using microwave heating. *Energy, 116*(Part 1), 1-7.

Huang, Y.-F., Sung, H.-T., Chiueh, P.-T., & Lo, S.-L. (2017b). Microwave torrefaction of sewage sludge and leucaena. *Journal of the Taiwan Institute of Chemical Engineers, 70*, 236-243.

Huo, S., Wang, Z., Cui, F., Zou, B., Zhao, P., & Yuan, Z. (2015). Enzyme-Assisted Extraction of Oil from Wet Microalgae Scenedesmus sp. G4. *Energies, 8*(8).

Iáñez-Rodríguez, I., Martín-Lara, M. Á., Blázquez, G., Pérez, A., & Calero, M. (2017). Effect of torrefaction conditions on greenhouse crop residue: Optimization of conditions to upgrade solid characteristics. *Bioresource Technology, 244*(Part 1), 741-749.

Idris, S. S., Rahman, N. A., Ismail, K., Alias, A. B., Rashid, Z. A., & Aris, M. J. (2010). Investigation on thermochemical behaviour of low rank Malaysian coal, oil palm biomass and their blends during pyrolysis via thermogravimetric analysis (TGA). *Bioresource Technology, 101*(12), 4584-4592.

Inagaki, M., Park, K. C., & Endo, M. (2010). Carbonization under pressure. *New Carbon Materials, 25*(6), 409-420.

Iroba, K. L., Baik, O.-D., & Tabil, L. G. (2017). Torrefaction of biomass from municipal solid waste fractions II: Grindability characteristics, higher heating value, pelletability and moisture adsorption. *Biomass and Bioenergy, 106*, 8-20.

Jahirul, I. M., Rasul, G. M., Chowdhury, A. A., & Ashwath, N. (2012). Biofuels Production through Biomass Pyrolysis —A Technological Review. *Energies, 5*(12).

Jazrawi, C., Biller, P., He, Y., Montoya, A., Ross, A. B., Maschmeyer, T., & Haynes, B. S. (2015). Two-stage hydrothermal liquefaction of a high-protein microalga. *Algal Research, 8*, 15-22.

Jeong, T. S., Choi, C. H., Lee, J. Y., & Oh, K. K. (2012). Behaviors of glucose decomposition during acid-catalyzed hydrothermal hydrolysis of pretreated Gelidium amansii. *Bioresource Technology, 116*, 435-440.

Kai, X., Li, R., Yang, T., Shen, S., Ji, Q., & Zhang, T. (2017). Study on the co-pyrolysis of rice straw and high density polyethylene blends using TG-FTIR-MS. *Energy Conversion and Management, 146*, 20-33.

Kambo, H. S., & Dutta, A. (2015). Comparative evaluation of torrefaction and hydrothermal carbonization of lignocellulosic biomass for the production of solid biofuel. *Energy Conversion and Management, 105*, 746-755.

Kan, T., Strezov, V., & Evans, T. J. (2016). Lignocellulosic biomass pyrolysis: A review of product properties and effects of pyrolysis parameters. *Renewable and Sustainable Energy Reviews, 57*, 1126-1140.

Kebelmann, K., Hornung, A., Karsten, U., & Griffiths, G. (2013). Intermediate pyrolysis and product identification by TGA and Py-GC/MS of green microalgae and their extracted protein and lipid components. *Biomass and Bioenergy, 49*, 38-48.

Kim, D.-Y., Vijayan, D., Praveenkumar, R., Han, J.-I., Lee, K., Park, J.-Y., Chang, W.-S., Lee, J.-S., & Oh, Y.-K. (2016). Cell-wall disruption and lipid/astaxanthin extraction from microalgae: Chlorella and Haematococcus. *Bioresource Technology, 199*, 300-310.

Kim, D., Park, S., & Park, K. Y. (2017). Upgrading the fuel properties of sludge and low rank coal mixed fuel through hydrothermal carbonization. *Energy*.

Kootstra, A. M. J., Beeftink, H. H., Scott, E. L., & Sanders, J. P. M. (2009a). Comparison of dilute mineral and organic acid pretreatment for enzymatic hydrolysis of wheat straw. *Biochemical Engineering Journal, 46*(2), 126-131.

Kootstra, A. M. J., Beeftink, H. H., Scott, E. L., & Sanders, J. P. M. (2009b). Optimization of the dilute maleic acid pretreatment of wheat straw. *Biotechnology for Biofuels, 2*(1), 31.

Krasznai, D. J., Champagne Hartley, R., Roy, H. M., Champagne, P., & Cunningham, M. F. (2018). Compositional analysis of lignocellulosic biomass: conventional methodologies and future outlook. *Critical Reviews in Biotechnology, 38*(2), 199-217.

Laurila, J., Havimo, M., & Lauhanen, R. (2014). Compression drying of energy wood. *Fuel Processing Technology, 124*, 286-289.

Lee, J., Lee, K., Sohn, D., Kim, Y. M., & Park, K. Y. (2018). Hydrothermal carbonization of lipid extracted algae for hydrochar production and feasibility of using hydrochar as a solid fuel. *Energy, 153*, 913-920.

Lee, J., Sohn, D., Lee, K., & Park, K. Y. (2019). Solid fuel production through hydrothermal carbonization of sewage sludge and microalgae Chlorella sp. from wastewater treatment plant. *Chemosphere, 230*, 157-163.

Lee, X. J., Lee, L. Y., Gan, S., Thangalazhy-Gopakumar, S., & Ng, H. K. (2017). Biochar potential evaluation of palm oil wastes through slow pyrolysis: Thermochemical characterization and pyrolytic kinetic studies. *Bioresource Technology, 236*, 155-163.

Lei, H., Ren, S., Wang, L., Bu, Q., Julson, J., Holladay, J., & Ruan, R. (2011). Microwave pyrolysis of distillers dried grain with solubles (DDGS) for biofuel production. *Bioresource Technology, 102*(10), 6208-6213.

Li, B., Duan, Y., Luebke, D., & Morreale, B. (2013). Advances in CO2 capture technology: A patent review. *Applied Energy, 102*, 1439-1447.

Li, F., Srivatsa, S. C., & Bhattacharya, S. (2019). A review on catalytic pyrolysis of microalgae to high-quality bio-oil with low oxygeneous and nitrogenous compounds. *Renewable and Sustainable Energy Reviews, 108*, 481-497.

Li, H., Liu, X., Legros, R., Bi, X. T., Lim, C. J., & Sokhansanj, S. (2012). Torrefaction of sawdust in a fluidized bed reactor. *Bioresource Technology, 103*(1), 453-458.

Li, K., Zhang, L., Zhu, L., & Zhu, X. (2017a). Comparative study on pyrolysis of lignocellulosic and algal biomass using pyrolysis-gas chromatography/mass spectrometry. *Bioresource Technology, 234*, 48-52.

Li, M.-F., Shen, Y., Sun, J.-K., Bian, J., Chen, C.-Z., & Sun, R.-C. (2015). Wet Torrefaction of Bamboo in Hydrochloric Acid Solution by Microwave Heating. *ACS Sustainable Chemistry & Engineering, 3*(9), 2022-2029.

Li, S.-X., Chen, C.-Z., Li, M.-F., & Xiao, X. (2017b). Torrefaction of corncob to produce charcoal under nitrogen and carbon dioxide atmospheres. *Bioresource Technology*.

Li, S.-X., Chen, C.-Z., Li, M.-F., & Xiao, X. (2018). Torrefaction of corncob to produce charcoal under nitrogen and carbon dioxide atmospheres. *Bioresource Technology, 249*, 348-353.

Li, S., Ma, X., Liu, G., & Guo, M. (2016). A TG–FTIR investigation to the co-pyrolysis of oil shale with coal. *Journal of Analytical and Applied Pyrolysis, 120*, 540-548.

Libra, J. A., Ro, K. S., Kammann, C., Funke, A., Berge, N. D., Neubauer, Y., Titirici, M.-M., Fühner, C., Bens, O., Kern, J., & Emmerich, K.-H. (2011). Hydrothermal carbonization of biomass residuals: a comparative review of the chemistry, processes and applications of wet and dry pyrolysis. *Biofuels, 2*(1), 71-106.

Lin, B., Zhou, J., Qin, Q., Song, X., & Luo, Z. (2019). Thermal behavior and gas evolution characteristics during co-pyrolysis of lignocellulosic biomass and coal: A TG-FTIR investigation. *Journal of Analytical and Applied Pyrolysis, 144*, 104718.

Liu, C., Duan, X., Chen, Q., Chao, C., Lu, Z., Lai, Q., & Megharaj, M. (2019a). Investigations on pyrolysis of microalgae Diplosphaera sp. MM1 by TG-FTIR and Py-GC/MS: Products and kinetics. *Bioresource Technology, 294*, 122126.

Liu, H., Chen, Y., Yang, H., Gentili, F. G., Söderlind, U., Wang, X., Zhang, W., & Chen, H. (2019b). Hydrothermal carbonization of natural microalgae containing a high ash content. *Fuel, 249*, 441-448.

Liu, J., Chen, P., He, J., Deng, L., Wang, L., Lei, J., & Rong, L. (2014). Extraction of oil from Jatropha curcas seeds by subcritical fluid extraction. *Industrial Crops and Products, 62*, 235-241.

Liu, P., Wang, L., Zhou, Y., Pan, T., Lu, X., & Zhang, D. (2016). Effect of hydrothermal treatment on the structure and pyrolysis product distribution of Xiaolongtan lignite. *Fuel, 164*, 110-118.

Liu, Q., Zhong, Z., Wang, S., & Luo, Z. (2011). Interactions of biomass components during pyrolysis: A TG-FTIR study. *Journal of Analytical and Applied Pyrolysis, 90*(2), 213-218.

López-González, D., Fernandez-Lopez, M., Valverde, J. L., & Sanchez-Silva, L. (2014). Kinetic analysis and thermal characterization of the microalgae combustion process by thermal analysis coupled to mass spectrometry. *Applied Energy, 114*, 227-237.

Lu, J.-J., & Chen, W.-H. (2013). Product yields and characteristics of corncob waste under various torrefaction atmospheres. *Energies, 7*(1), 13-27.

Lu, K.-M., Lee, W.-J., Chen, W.-H., & Lin, T.-C. (2013). Thermogravimetric analysis and kinetics of co-pyrolysis of raw/torrefied wood and coal blends. *Applied Energy, 105*, 57-65.

Lu, Q., Zhou, M.-x., Li, W.-t., Wang, X., Cui, M.-s., & Yang, Y.-p. (2018). Catalytic fast pyrolysis of biomass with noble metal-like catalysts to produce high-grade bio-oil: Analytical Py-GC/MS study. *Catalysis Today, 302*, 169-179.

Lv, P., Almeida, G., & Perré, P. (2015). TGA-FTIR analysis of torrefaction of lignocellulosic components (cellulose, xylan, lignin) in isothermal conditions over a wide range of time durations. *BioResources, 10*(3), 4239-4251.

Madeira, M. S., Cardoso, C., Lopes, P. A., Coelho, D., Afonso, C., Bandarra, N. M., & Prates, J. A. M. (2017). Microalgae as feed ingredients for livestock production and meat quality: A review. *Livestock Science, 205*, 111-121.

Magdziarz, A., & Wilk, M. (2013). Thermogravimetric study of biomass, sewage sludge and coal combustion. *Energy Conversion and Management, 75*, 425-430.

Mallick, D., Poddar, M. K., Mahanta, P., & Moholkar, V. S. (2018). Discernment of synergism in pyrolysis of biomass blends using thermogravimetric analysis. *Bioresource Technology, 261*, 294-305.

Mamaeva, A., Tahmasebi, A., Tian, L., & Yu, J. (2016a). Microwave-assisted catalytic pyrolysis of lignocellulosic biomass for production of phenolic-rich bio-oil. *Bioresource Technology, 211*, 382-389.

Mamaeva, A., Tahmasebi, A., Tian, L., & Yu, J. (2016b). Microwave-assisted catalytic pyrolysis of lignocellulosic biomass for production of phenolic-rich bio-oil. *Bioresour Technol, 211*, 382-389.

Marcilla, A., Gómez-Siurana, A., Gomis, C., Chápuli, E., Catalá, M. C., & Valdés, F. J. (2009). Characterization of microalgal species through TGA/FTIR analysis: Application to nannochloropsis sp. *Thermochimica Acta, 484*(1), 41-47.

Martín-Lara, M. A., Ronda, A., Zamora, M. C., & Calero, M. (2017). Torrefaction of olive tree pruning: Effect of operating conditions on solid product properties. *Fuel, 202*, 109-117.

Masuko, T., Minami, A., Iwasaki, N., Majima, T., Nishimura, S.-I., & Lee, Y. C. (2005). Carbohydrate analysis by a phenol–sulfuric acid method in microplate format. *Analytical Biochemistry, 339*(1), 69-72.

Mathimani, T., Baldinelli, A., Rajendran, K., Prabakar, D., Matheswaran, M., Pieter van Leeuwen, R., & Pugazhendhi, A. (2019). Review on cultivation and thermochemical conversion of microalgae to fuels and chemicals: Process evaluation and knowledge gaps. *Journal of Cleaner Production, 208*, 1053-1064.

Matter, P., & Supply, U. W. (2012). ENVIRONMENTAL OUTLOOK TO 2050.

Motasemi, F., & Afzal, M. T. (2013). A review on the microwave-assisted pyrolysis technique. *Renewable and Sustainable Energy Reviews, 28*, 317-330.

Moya, R., Rodríguez-Zúñiga, A., Puente-Urbina, A., & Gaitán-Álvarez, J. (2018). Study of light, middle and severe torrefaction and effects of extractives and chemical compositions on torrefaction process by thermogravimetric analysis in five fast-growing plantations of Costa Rica. *Energy, 149*, 1-10.

Mu'min, G. F., Prawisudha, P., Zaini, I. N., Aziz, M., & Pasek, A. D. (2017). Municipal solid waste processing and separation employing wet torrefaction for alternative fuel production and aluminum reclamation. *Waste Management, 67*, 106-120.

Nagamori, M., & Funazukuri, T. (2004). Glucose production by hydrolysis of starch under hydrothermal conditions. *Journal of Chemical Technology & Biotechnology, 79*(3), 229-233.

Nair, V., & Vinu, R. (2016). Peroxide-assisted microwave activation of pyrolysis char for adsorption of dyes from wastewater. *Bioresource Technology, 216*, 511-519.

Nanda, S., Mohanty, P., Pant, K. K., Naik, S., Kozinski, J. A., & Dalai, A. K. (2013). Characterization of North American lignocellulosic biomass and biochars in terms

of their candidacy for alternate renewable fuels. *Bioenergy Research, 6*(2), 663-677.

Nicodème, T., Berchem, T., Jacquet, N., & Richel, A. (2018). Thermochemical conversion of sugar industry by-products to biofuels. *Renewable and Sustainable Energy Reviews, 88*, 151-159.

Niu, Y., Lv, Y., Lei, Y., Liu, S., Liang, Y., Wang, D., & Hui, S. e. (2019). Biomass torrefaction: properties, applications, challenges, and economy. *Renewable and Sustainable Energy Reviews, 115*, 109395.

Nizamuddin, S., Baloch, H. A., Griffin, G. J., Mubarak, N. M., Bhutto, A. W., Abro, R., Mazari, S. A., & Ali, B. S. (2017). An overview of effect of process parameters on hydrothermal carbonization of biomass. *Renewable and Sustainable Energy Reviews, 73*, 1289-1299.

Nizamuddin, S., Baloch, H. A., Siddiqui, M., Mubarak, N., Tunio, M., Bhutto, A., Jatoi, A. S., Griffin, G., & Srinivasan, M. (2018). An overview of microwave hydrothermal carbonization and microwave pyrolysis of biomass. *Reviews in Environmental Science and Bio/Technology, 17*(4), 813-837.

Olszewski, M. P., Arauzo, P. J., Wądrzyk, M., & Kruse, A. (2019). Py-GC-MS of hydrochars produced from brewer's spent grains. *Journal of Analytical and Applied Pyrolysis, 140*, 255-263.

Oudghiri, F., Allali, N., Quiroga, J. M., & Rodríguez-Barroso, M. R. (2016). TG–FTIR analysis on pyrolysis and combustion of marine sediment. *Infrared Physics & Technology, 78*, 268-274.

Oyedun, A. O., Tee, C. Z., Hanson, S., & Hui, C. W. (2014). Thermogravimetric analysis of the pyrolysis characteristics and kinetics of plastics and biomass blends. *Fuel Processing Technology, 128*, 471-481.

Ozturk, M., Saba, N., Altay, V., Iqbal, R., Hakeem, K. R., Jawaid, M., & Ibrahim, F. H. (2017). Biomass and bioenergy: An overview of the development potential in Turkey and Malaysia. *Renewable and Sustainable Energy Reviews, 79*, 1285-1302.

Pahla, G., Ntuli, F., & Muzenda, E. (2017). Torrefaction of landfill food waste for possible application in biomass co-firing. *Waste Management*.

Pala, M., Kantarli, I. C., Buyukisik, H. B., & Yanik, J. (2014). Hydrothermal carbonization and torrefaction of grape pomace: A comparative evaluation. *Bioresource Technology, 161*, 255-262.

Pang, S. (2019). Advances in thermochemical conversion of woody biomass to energy, fuels and chemicals. *Biotechnology Advances, 37*(4), 589-597.

Park, J.-Y., Oh, Y.-K., Lee, J.-S., Lee, K., Jeong, M.-J., & Choi, S.-A. (2014). Acid-catalyzed hot-water extraction of lipids from Chlorella vulgaris. *Bioresource Technology, 153*, 408-412.

Park, J., Meng, J., Lim, K. H., Rojas, O. J., & Park, S. (2013). Transformation of lignocellulosic biomass during torrefaction. *Journal of Analytical and Applied Pyrolysis, 100*, 199-206.

Patwardhan, P. R., Brown, R. C., & Shanks, B. H. (2011a). Product Distribution from the Fast Pyrolysis of Hemicellulose. *ChemSusChem, 4*(5), 636-643.

Patwardhan, P. R., Brown, R. C., & Shanks, B. H. (2011b). Understanding the Fast Pyrolysis of Lignin. *ChemSusChem, 4*(11), 1629-1636.

Patwardhan, P. R., Satrio, J. A., Brown, R. C., & Shanks, B. H. (2010). Influence of inorganic salts on the primary pyrolysis products of cellulose. *Bioresource Technology, 101*(12), 4646-4655.

Pavlath, A. E., & Gregorski, K. S. (1985). Atmospheric pyrolysis of carbohydrates with thermogravimetric and mass spectrometric analyses. *Journal of Analytical and Applied Pyrolysis, 8*, 41-48.

Peng, J. H., Bi, X. T., Sokhansanj, S., & Lim, C. J. (2013). Torrefaction and densification of different species of softwood residues. *Fuel, 111*, 411-421.

Peng, W., Wu, Q., Tu, P., & Zhao, N. (2001). Pyrolytic characteristics of microalgae as renewable energy source determined by thermogravimetric analysis. *Bioresource Technology, 80*(1), 1-7.

Peng, X., Ma, X., Lin, Y., Guo, Z., Hu, S., Ning, X., Cao, Y., & Zhang, Y. (2015). Co-pyrolysis between microalgae and textile dyeing sludge by TG–FTIR: Kinetics and products. *Energy Conversion and Management, 100*, 391-402.

Peters, J. F., Banks, S. W., Bridgwater, A. V., & Dufour, J. (2017). A kinetic reaction model for biomass pyrolysis processes in Aspen Plus. *Applied Energy, 188*, 595-603.

Peterson, A. A., Vogel, F., Lachance, R. P., Fröling, M., Antal Jr, M. J., & Tester, J. W. (2008). Thermochemical biofuel production in hydrothermal media: a review of sub-and supercritical water technologies. *Energy & Environmental Science, 1*(1), 32-65.

Phwan, C. K., Ong, H. C., Chen, W.-H., Ling, T. C., Ng, E. P., & Show, P. L. (2018). Overview: Comparison of pretreatment technologies and fermentation processes of bioethanol from microalgae. *Energy Conversion and Management, 173*, 81-94.

Prins, M. J. (2005). Thermodynamic analysis of biomass gasification and torrefaction.

Pütün, E. (2010). Catalytic pyrolysis of biomass: Effects of pyrolysis temperature, sweeping gas flow rate and MgO catalyst. *Energy, 35*, 2761-2766.

Quan, C., Gao, N., & Song, Q. (2016). Pyrolysis of biomass components in a TGA and a fixed-bed reactor: Thermochemical behaviors, kinetics, and product characterization. *Journal of Analytical and Applied Pyrolysis, 121*, 84-92.

Ren, S., Lei, H., Wang, L., Bu, Q., Chen, S., & Wu, J. (2013). Thermal behaviour and kinetic study for woody biomass torrefaction and torrefied biomass pyrolysis by TGA. *Biosystems Engineering, 116*(4), 420-426.

Ren, S., Lei, H., Wang, L., Yadavalli, G., Liu, Y., & Julson, J. (2014). The integrated process of microwave torrefaction and pyrolysis of corn stover for biofuel production. *Journal of Analytical and Applied Pyrolysis, 108*, 248-253.

Rizzo, A. M., Prussi, M., Bettucci, L., Libelli, I. M., & Chiaramonti, D. (2013). Characterization of microalga Chlorella as a fuel and its thermogravimetric behavior. *Applied Energy, 102*, 24-31.

Robinson, T., Bronson, B., Gogolek, P., & Mehrani, P. (2016). Sample preparation for thermo-gravimetric determination and thermo-gravimetric characterization of refuse derived fuel. *Waste Management, 48*, 265-274.

Rogalinski, T., Liu, K., Albrecht, T., & Brunner, G. (2008). Hydrolysis kinetics of biopolymers in subcritical water. *The Journal of Supercritical Fluids, 46*(3), 335-341.

Rousset, P., Macedo, L., Commandré, J. M., & Moreira, A. (2012). Biomass torrefaction under different oxygen concentrations and its effect on the composition of the solid by-product. *Journal of Analytical and Applied Pyrolysis, 96*, 86-91.

Rueda-Ordóñez, Y. J., Tannous, K., & Olivares-Gómez, E. (2015). An empirical model to obtain the kinetic parameters of lignocellulosic biomass pyrolysis in an independent parallel reactions scheme. *Fuel Processing Technology, 140*, 222-230.

Sabil, K. M., Aziz, M. A., Lal, B., & Uemura, Y. (2013). Synthetic indicator on the severity of torrefaction of oil palm biomass residues through mass loss measurement. *Applied Energy, 111*, 821-826.

Saddawi, A., Jones, J.M, Williams, A, Le Coeur. (2012). Commodity fuels from biomass through pretreatment and torrefaction: Effects of mineral content on torrefied fuel characteristics and quality *Energy and Fuels, 26*(11), 6466-6474.

Sadhukhan, A. K., Gupta, P., Goyal, T., & Saha, R. K. (2008). Modelling of pyrolysis of coal-biomass blends using thermogravimetric analysis. *Bioresource Technology, 99*(17), 8022-8026.

Safar, M., Lin, B.-J., Chen, W.-H., Langauer, D., Chang, J.-S., Raclavska, H., Pétrissans, A., Rousset, P., & Pétrissans, M. (2019). Catalytic effects of potassium on biomass pyrolysis, combustion and torrefaction. *Applied Energy, 235*, 346-355.

Safi, C., Zebib, B., Merah, O., Pontalier, P.-Y., & Vaca-Garcia, C. (2014). Morphology, composition, production, processing and applications of Chlorella vulgaris: A review. *Renewable and Sustainable Energy Reviews, 35*, 265-278.

Sebestyén, Z., Barta-Rajnai, E., Bozi, J., Blazsó, M., Jakab, E., Miskolczi, N., Sója, J., & Czégény, Z. (2017). Thermo-catalytic pyrolysis of biomass and plastic mixtures using HZSM-5. *Applied Energy, 207*, 114-122.

Seo, D. K., Park, S. S., Hwang, J., & Yu, T.-U. (2010). Study of the pyrolysis of biomass using thermo-gravimetric analysis (TGA) and concentration measurements of the evolved species. *Journal of Analytical and Applied Pyrolysis, 89*(1), 66-73.

Shah, S., Sharma, A., & Gupta, M. N. (2005). Extraction of oil from Jatropha curcas L. seed kernels by combination of ultrasonication and aqueous enzymatic oil extraction. *Bioresource Technology, 96*(1), 121-123.

Shakya, R., Adhikari, S., Mahadevan, R., Shanmugam, S. R., Nam, H., Hassan, E. B., & Dempster, T. A. (2017). Influence of biochemical composition during hydrothermal liquefaction of algae on product yields and fuel properties. *Bioresource Technology, 243*, 1112-1120.

Shankar Tumuluru, J., Sokhansanj, S., Hess, J. R., Wright, C. T., & Boardman, R. D. (2011). REVIEW: A review on biomass torrefaction process and product properties for energy applications. *Industrial Biotechnology, 7*(5), 384-401.

Sharara, M. A., Holeman, N., Sadaka, S. S., & Costello, T. A. (2014). Pyrolysis kinetics of algal consortia grown using swine manure wastewater. *Bioresource Technology, 169*, 658-666.

Sharma, H. B., Sarmah, A. K., & Dubey, B. (2020). Hydrothermal carbonization of renewable waste biomass for solid biofuel production: A discussion on process mechanism, the influence of process parameters, environmental performance and fuel properties of hydrochar. *Renewable and Sustainable Energy Reviews, 123*, 109761.

Sharma, R., & Sheth, P. N. (2018). Multi reaction apparent kinetic scheme for the pyrolysis of large size biomass particles using macro-TGA. *Energy, 151*, 1007-1017.

Shen, D. K., & Gu, S. (2009). The mechanism for thermal decomposition of cellulose and its main products. *Bioresour Technol, 100*(24), 6496-6504.

Shen, D. K., Gu, S., & Bridgwater, A. V. (2010). Study on the pyrolytic behaviour of xylan-based hemicellulose using TG–FTIR and Py–GC–FTIR. *Journal of Analytical and Applied Pyrolysis, 87*(2), 199-206.

Shoulaifar, T. K., DeMartini, N., Karlström, O., & Hupa, M. (2016). Impact of organically bonded potassium on torrefaction: Part 1. Experimental. *Fuel, 165*, 544-552.

Shuba, Eyasu S., & Kifle, D. (2018). Microalgae to biofuels: 'Promising' alternative and renewable energy, review. *Renewable and Sustainable Energy Reviews, 81*(Part 1), 743-755.

Shuping, Z., Yulong, W., Mingde, Y., Chun, L., & Junmao, T. (2010). Pyrolysis characteristics and kinetics of the marine microalgae Dunaliella tertiolecta using thermogravimetric analyzer. *Bioresource Technology, 101*(1), 359-365.

Sindhu, R., Binod, P., Satyanagalakshmi, K., Janu, K. U., Sajna, K. V., Kurien, N., Sukumaran, R. K., & Pandey, A. (2010). Formic Acid as a Potential Pretreatment

Agent for the Conversion of Sugarcane Bagasse to Bioethanol. *Applied Biochemistry and Biotechnology, 162*(8), 2313-2323.

Sindhu, R., Kuttiraja, M., Binod, P., Janu, K. U., Sukumaran, R. K., & Pandey, A. (2011). Dilute acid pretreatment and enzymatic saccharification of sugarcane tops for bioethanol production. *Bioresource Technology, 102*(23), 10915-10921.

Skreiberg, A., Skreiberg, Ø., Sandquist, J., & Sørum, L. (2011). TGA and macro-TGA characterisation of biomass fuels and fuel mixtures. *Fuel, 90*(6), 2182-2197.

Smetana, S., Sandmann, M., Rohn, S., Pleissner, D., & Heinz, V. (2017). Autotrophic and heterotrophic microalgae and cyanobacteria cultivation for food and feed: life cycle assessment. *Bioresource Technology, 245*(Part A), 162-170.

Song, H., Liu, G., Zhang, J., & Wu, J. (2017). Pyrolysis characteristics and kinetics of low rank coals by TG-FTIR method. *Fuel Processing Technology, 156*, 454-460.

Soria-Verdugo, A., Goos, E., García-Hernando, N., & Riedel, U. (2018). Analyzing the pyrolysis kinetics of several microalgae species by various differential and integral isoconversional kinetic methods and the Distributed Activation Energy Model. *Algal Research, 32*, 11-29.

Soria-Verdugo, A., Goos, E., Morato-Godino, A., García-Hernando, N., & Riedel, U. (2017). Pyrolysis of biofuels of the future: Sewage sludge and microalgae – Thermogravimetric analysis and modelling of the pyrolysis under different temperature conditions. *Energy Conversion and Management, 138*, 261-272.

Sotoudehniakarani, F., Alayat, A., & McDonald, A. G. (2019). Characterization and comparison of pyrolysis products from fast pyrolysis of commercial Chlorella vulgaris and cultivated microalgae. *Journal of Analytical and Applied Pyrolysis, 139*, 258-273.

Spokas, K. A., Novak, J. M., Stewart, C. E., Cantrell, K. B., Uchimiya, M., DuSaire, M. G., & Ro, K. S. (2011). Qualitative analysis of volatile organic compounds on biochar. *Chemosphere, 85*(5), 869-882.

Sricharoenchaikul, V., & Atong, D. (2009). Thermal decomposition study on Jatropha curcas L. waste using TGA and fixed bed reactor. *Journal of Analytical and Applied Pyrolysis, 85*(1), 155-162.

Striūgas, N., Skvorčinskienė, R., Paulauskas, R., Zakarauskas, K., & Vorotinskienė, L. (2017). Evaluation of straw with absorbed glycerol thermal degradation during pyrolysis and combustion by TG-FTIR and TG-GC/MS. *Fuel, 204*, 227-235.

Su, Y., Zhang, S., Liu, L., Xu, D., & Xiong, Y. (2018). Investigation of representative components of flue gas used as torrefaction pretreatment atmosphere and its effects on fast pyrolysis behaviors. *Bioresource Technology, 267*, 584-590.

Sukiran, M. A., Abnisa, F., Wan Daud, W. M. A., Abu Bakar, N., & Loh, S. K. (2017). A review of torrefaction of oil palm solid wastes for biofuel production. *Energy Conversion and Management, 149*, 101-120.

Sun, Y., He, Z., Tu, R., Wu, Y.-j., Jiang, E.-c., & Xu, X.-w. (2019). The mechanism of wet/dry torrefaction pretreatment on the pyrolysis performance of tobacco stalk. *Bioresource Technology, 286*, 121390.

Tan, I. A. W., Shafee, N. M., Abdullah, M. O., & Lim, L. L. P. (2017). Synthesis and characterization of biocoal from Cymbopogon citrates residue using microwave-induced torrefaction. *Environmental Technology & Innovation, 8*, 431-440.

Tan, Z., & Lagerkvist, A. (2011). Phosphorus recovery from the biomass ash: A review. *Renewable and Sustainable Energy Reviews, 15*(8), 3588-3602.

Teh, Y. Y., Lee, K. T., Chen, W.-H., Lin, S.-C., Sheen, H.-K., & Tan, I. S. (2017). Dilute sulfuric acid hydrolysis of red macroalgae Eucheuma denticulatum with microwave-assisted heating for biochar production and sugar recovery. *Bioresource Technology, 246*, 20-27.

Tekin, K., Karagöz, S., & Bektaş, S. (2014). A review of hydrothermal biomass processing. *Renewable and Sustainable Energy Reviews, 40*, 673-687.

Tian, L., Shen, B., Xu, H., Li, F., Wang, Y., & Singh, S. (2016). Thermal behavior of waste tea pyrolysis by TG-FTIR analysis. *Energy, 103*, 533-542.

Titirici, M.-M., White, R. J., Falco, C., & Sevilla, M. (2012). Black perspectives for a green future: hydrothermal carbons for environment protection and energy storage. *Energy & Environmental Science, 5*(5), 6796-6822.

Tong, S., Xiao, L., Li, X., Zhu, X., Liu, H., Luo, G., Worasuwannarak, N., Kerdsuwan, S., Fungtammasan, B., & Yao, H. (2018). A gas-pressurized torrefaction method for biomass wastes. *Energy Conversion and Management, 173*, 29-36.

Torri, C., Fabbri, D., Garcia-Alba, L., & Brilman, D. W. F. (2013). Upgrading of oils derived from hydrothermal treatment of microalgae by catalytic cracking over H-ZSM-5: A comparative Py–GC–MS study. *Journal of Analytical and Applied Pyrolysis, 101*, 28-34.

Tran, D.-T., Chen, C.-L., & Chang, J.-S. (2013). Effect of solvents and oil content on direct transesterification of wet oil-bearing microalgal biomass of Chlorella vulgaris ESP-31 for biodiesel synthesis using immobilized lipase as the biocatalyst. *Bioresource Technology, 135*, 213-221.

Trendewicz, A., Evans, R., Dutta, A., Sykes, R., Carpenter, D., & Braun, R. (2015). Evaluating the effect of potassium on cellulose pyrolysis reaction kinetics. *Biomass and Bioenergy, 74*, 15-25.

Triyono, B., Prawisudha, P., Aziz, M., Mardiyati, Pasek, A. D., & Yoshikawa, K. (2019). Utilization of mixed organic-plastic municipal solid waste as renewable solid fuel employing wet torrefaction. *Waste Management, 95*, 1-9.

Tu, R., Jiang, E., Yan, S., Xu, X., & Rao, S. (2018). The pelletization and combustion properties of torrefied Camellia shell via dry and hydrothermal torrefaction: A comparative evaluation. *Bioresource Technology, 264*, 78-89.

Ubando, A. T., Rivera, D. R. T., Chen, W.-H., & Culaba, A. B. (2019). A comprehensive review of life cycle assessment (LCA) of microalgal and lignocellulosic bioenergy products from thermochemical processes. *Bioresource Technology, 291*, 121837.

Uemura, Y., Saadon, S., Osman, N., Mansor, N., & Tanoue, K.-i. (2015). Torrefaction of oil palm kernel shell in the presence of oxygen and carbon dioxide. *Fuel, 144*, 171-179.

Uemura, Y., Sellappah, V., Trinh, T. H., Hassan, S., & Tanoue, K.-i. (2017). Torrefaction of empty fruit bunches under biomass combustion gas atmosphere. *Bioresource Technology, 243*, 107-117.

Ullah, K., Ahmad, M., Sofia, Sharma, V. K., Lu, P., Harvey, A., Zafar, M., & Sultana, S. (2015). Assessing the potential of algal biomass opportunities for bioenergy industry: A review. *Fuel, 143*, 414-423.

Valdés, F., Catalá, L., Hernández, M. R., García-Quesada, J. C., & Marcilla, A. (2013). Thermogravimetry and Py–GC/MS techniques as fast qualitative methods for comparing the biochemical composition of Nannochloropsis oculata samples obtained under different culture conditions. *Bioresource Technology, 131*, 86-93.

van der Stelt, M. J. C., Gerhauser, H., Kiel, J. H. A., & Ptasinski, K. J. (2011). Biomass upgrading by torrefaction for the production of biofuels: A review. *Biomass and Bioenergy, 35*(9), 3748-3762.

Van Krevelen, D. (1950). Graphical-statistical method for the study of structure and reaction processes of coal. *Fuel, 29*, 269-284.

Vo, T. K., Ly, H. V., Lee, O. K., Lee, E. Y., Kim, C. H., Seo, J.-W., Kim, J., & Kim, S.-S. (2017). Pyrolysis characteristics and kinetics of microalgal Aurantiochytrium sp. KRS101. *Energy, 118*, 369-376.

Wahi, R., Zuhaidi, N. F. Q. a., Yusof, Y., Jamel, J., Kanakaraju, D., & Ngaini, Z. (2017). Chemically treated microwave-derived biochar: An overview. *Biomass and Bioenergy, 107*, 411-421.

Wang, H.-M. D., Chen, C.-C., Huynh, P., & Chang, J.-S. (2015a). Exploring the potential of using algae in cosmetics. *Bioresource Technology, 184*, 355-362.

Wang, H., Gao, B., Wang, S., Fang, J., Xue, Y., & Yang, K. (2015b). Removal of Pb(II), Cu(II), and Cd(II) from aqueous solutions by biochar derived from KMnO4 treated hickory wood. *Bioresource Technology, 197*, 356-362.

Wang, H., Zhu, C., Li, D., Liu, Q., Tan, J., Wang, C., Cai, C., & Ma, L. (2019). Recent advances in catalytic conversion of biomass to 5-hydroxymethylfurfural and 2, 5-dimethylfuran. *Renewable and Sustainable Energy Reviews, 103*, 227-247.

Wang, J., Ma, X., Yu, Z., Peng, X., & Lin, Y. (2018a). Studies on thermal decomposition behaviors of demineralized low-lipid microalgae by TG-FTIR. *Thermochimica Acta, 660*, 101-109.

Wang, K., & Brown, R. C. (2013). Catalytic pyrolysis of microalgae for production of aromatics and ammonia. *Green Chemistry, 15*(3), 675-681.

Wang, K., Brown, R. C., Homsy, S., Martinez, L., & Sidhu, S. S. (2013). Fast pyrolysis of microalgae remnants in a fluidized bed reactor for bio-oil and biochar production. *Bioresource Technology, 127*, 494-499.

Wang, L., Chai, M., Liu, R., & Cai, J. (2018b). Synergetic effects during co-pyrolysis of biomass and waste tire: A study on product distribution and reaction kinetics. *Bioresource Technology, 268*, 363-370.

Wang, S., Dai, G., Yang, H., & Luo, Z. (2017a). Lignocellulosic biomass pyrolysis mechanism: A state-of-the-art review. *Progress in Energy and Combustion Science, 62*, 33-86.

Wang, S., Uzoejinwa, B. B., Abomohra, A. E.-F., Wang, Q., He, Z., Feng, Y., Zhang, B., & Hui, C.-W. (2018c). Characterization and pyrolysis behavior of the green microalga Micractinium conductrix grown in lab-scale tubular photobioreactor using Py-GC/MS and TGA/MS. *Journal of Analytical and Applied Pyrolysis, 135*, 340-349.

Wang, X., Sheng, L., & Yang, X. (2017b). Pyrolysis characteristics and pathways of protein, lipid and carbohydrate isolated from microalgae Nannochloropsis sp. *Bioresource Technology, 229*, 119-125.

Wang, X., Wu, J., Chen, Y., Pattiya, A., Yang, H., & Chen, H. (2018d). Comparative study of wet and dry torrefaction of corn stalk and the effect on biomass pyrolysis polygeneration. *Bioresource Technology, 258*, 88-97.

Wang, Z., Wang, F., Cao, J., & Wang, J. (2010). Pyrolysis of pine wood in a slowly heating fixed-bed reactor: Potassium carbonate versus calcium hydroxide as a catalyst. *Fuel Processing Technology, 91*(8), 942-950.

Werner, K., Pommer, L., & Broström, M. (2014). Thermal decomposition of hemicelluloses. *Journal of Analytical and Applied Pyrolysis, 110*, 130-137.

White, R. H. (1987). Effect of lignin content and extractives on the higher heating value of wood. *Wood Fiber Sci, 19*(4), 446-452.

Widyawati, M., Church, T. L., Florin, N. H., & Harris, A. T. (2011). Hydrogen synthesis from biomass pyrolysis with in situ carbon dioxide capture using calcium oxide. *International Journal of Hydrogen Energy, 36*(8), 4800-4813.

Wigley, T., Yip, A. C. K., & Pang, S. (2015). The use of demineralisation and torrefaction to improve the properties of biomass intended as a feedstock for fast pyrolysis. *Journal of Analytical and Applied Pyrolysis, 113*, 296-306.

Wilk, M., Magdziarz, A., & Kalemba, I. (2015). Characterisation of renewable fuels' torrefaction process with different instrumental techniques. *Energy, 87*, 259-269.

Williams, P. T., & Nugranad, N. (2000). Comparison of products from the pyrolysis and catalytic pyrolysis of rice husks. *Energy and Fuels, 25*(6), 493-513.

Wilson, C. A., & Novak, J. T. (2009). Hydrolysis of macromolecular components of primary and secondary wastewater sludge by thermal hydrolytic pretreatment. *Water Research, 43*(18), 4489-4498.

Wu, K.-T., Tsai, C.-J., Chen, C.-S., & Chen, H.-W. (2012). The characteristics of torrefied microalgae. *Applied Energy, 100*, 52-57.

Wu, W., Lin, K.-H., & Chang, J.-S. (2018). Economic and life-cycle greenhouse gas optimization of microalgae-to-biofuels chains. *Bioresource Technology, 267*, 550-559.

Xin, S., Huang, F., Liu, X., Mi, T., & Xu, Q. (2019a). Torrefaction of herbal medicine wastes: Characterization of the physicochemical properties and combustion behaviors. *Bioresource Technology, 287*, 121408.

Xin, S., Mi, T., Liu, X., & Huang, F. (2018). Effect of torrefaction on the pyrolysis characteristics of high moisture herbaceous residues. *Energy, 152*, 586-593.

Xin, X., Pang, S., de Miguel Mercader, F., & Torr, K. M. (2019b). The effect of biomass pretreatment on catalytic pyrolysis products of pine wood by Py-GC/MS and principal component analysis. *Journal of Analytical and Applied Pyrolysis, 138*, 145-153.

Xing, S., Yuan, H., Huhetaoli, Qi, Y., Lv, P., Yuan, Z., & Chen, Y. (2016). Characterization of the decomposition behaviors of catalytic pyrolysis of wood using copper and potassium over thermogravimetric and Py-GC/MS analysis. *Energy, 114*, 634-646.

Xu, F., Wang, B., Yang, D., Ming, X., Jiang, Y., Hao, J., Qiao, Y., & Tian, Y. (2018a). TG-FTIR and Py-GC/MS study on pyrolysis mechanism and products distribution of waste bicycle tire. *Energy Conversion and Management, 175*, 288-297.

Xu, X., Tu, R., Sun, Y., Li, Z., & Jiang, E. (2018b). Influence of biomass pretreatment on upgrading of bio-oil: Comparison of dry and hydrothermal torrefaction. *Bioresource Technology, 262*, 261-270.

Xu, Y., Hu, Y., Peng, Y., Yao, L., Dong, Y., Yang, B., & Song, R. (2020). Catalytic pyrolysis and liquefaction behavior of microalgae for bio-oil production. *Bioresource Technology, 300*, 122665.

Yahiaoui, M., Hadoun, H., Toumert, I., & Hassani, A. (2015). Determination of kinetic parameters of Phlomis bovei de Noé using thermogravimetric analysis. *Bioresource Technology, 196*, 441-447.

Yan, W., Acharjee, T. C., Coronella, C. J., & Vasquez, V. R. (2009). Thermal pretreatment of lignocellulosic biomass. *Environmental Progress & Sustainable Energy, 28*(3), 435-440.

Yan, W., Hastings, J. T., Acharjee, T. C., Coronella, C. J., & Vásquez, V. R. (2010). Mass and Energy Balances of Wet Torrefaction of Lignocellulosic Biomass. *Energy & Fuels, 24*(9), 4738-4742.

Yang, C., Li, R., Zhang, B., Qiu, Q., Wang, B., Yang, H., Ding, Y., & Wang, C. (2019a). Pyrolysis of microalgae: A critical review. *Fuel Processing Technology, 186*, 53-72.

Yang, J., Chen, H., Zhao, W., & Zhou, J. (2016). TG–FTIR-MS study of pyrolysis products evolving from peat. *Journal of Analytical and Applied Pyrolysis, 117*, 296-309.

Yang, S., Zhu, X., Wang, J., Jin, X., Liu, Y., Qian, F., Zhang, S., & Chen, J. (2015a). Combustion of hazardous biological waste derived from the fermentation of antibiotics using TG–FTIR and Py–GC/MS techniques. *Bioresource Technology, 193*, 156-163.

Yang, W., Shimanouchi, T., Iwamura, M., Takahashi, Y., Mano, R., Takashima, K., Tanifuji, T., & Kimura, Y. (2015b). Elevating the fuel properties of Humulus lupulus, Plumeria alba and Calophyllum inophyllum L. through wet torrefaction. *Fuel, 146*, 88-94.

Yang, Z., Wu, Y., Zhang, Z., Li, H., Li, X., Egorov, R. I., Strizhak, P. A., & Gao, X. (2019b). Recent advances in co-thermochemical conversions of biomass with fossil fuels focusing on the synergistic effects. *Renewable and Sustainable Energy Reviews, 103*, 384-398.

Yeh, K.-L., & Chang, J.-S. (2011). Nitrogen starvation strategies and photobioreactor design for enhancing lipid content and lipid production of a newly isolated microalga Chlorella vulgaris ESP-31: Implications for biofuels. *Biotechnology Journal, 6*(11), 1358-1366.

Yeh, K.-L., & Chang, J.-S. (2012). Effects of cultivation conditions and media composition on cell growth and lipid productivity of indigenous microalga Chlorella vulgaris ESP-31. *Bioresource Technology, 105*, 120-127.

Yu, J., Paterson, N., Blamey, J., & Millan, M. (2017). Cellulose, xylan and lignin interactions during pyrolysis of lignocellulosic biomass. *Fuel, 191*, 140-149.

Yu, K. L., Show, P. L., Ong, H. C., Ling, T. C., Chen, W.-H., & Salleh, M. A. M. (2018). Biochar production from microalgae cultivation through pyrolysis as a sustainable carbon sequestration and biorefinery approach. *Clean Technologies and Environmental Policy, 20*(9), 2047-2055.

Yu, Y., Lou, X., & Wu, H. (2008). Some Recent Advances in Hydrolysis of Biomass in Hot-Compressed Water and Its Comparisons with Other Hydrolysis Methods. *Energy & Fuels, 22*(1), 46-60.

Yue, Y., Singh, H., Singh, B., & Mani, S. (2017). Torrefaction of sorghum biomass to improve fuel properties. *Bioresource Technology, 232*, 372-379.

Zabed, H. M., Akter, S., Yun, J., Zhang, G., Zhang, Y., & Qi, X. (2020). Biogas from microalgae: Technologies, challenges and opportunities. *Renewable and Sustainable Energy Reviews, 117*, 109503.

Zabeti, M., Baltrusaitis, J., & Seshan, K. (2016). Chemical routes to hydrocarbons from pyrolysis of lignocellulose using Cs promoted amorphous silica alumina catalyst. *Catalysis Today, 269*, 156-165.

Zhang, C., Ho, S.-H., Chen, W.-H., Xie, Y., Liu, Z., & Chang, J.-S. (2018a). Torrefaction performance and energy usage of biomass wastes and their correlations with torrefaction severity index. *Applied Energy, 220*, 598-604.

Zhang, C., Wang, C., Cao, G., Chen, W.-H., & Ho, S.-H. (2019a). Comparison and characterization of property variation of microalgal biomass with non-oxidative and oxidative torrefaction. *Fuel, 246*, 375-385.

Zhang, D., Wang, F., Zhang, A., Yi, W., Li, Z., & Shen, X. (2019b). Effect of pretreatment on chemical characteristic and thermal degradation behavior of corn stalk digestate: Comparison of dry and wet torrefaction. *Bioresource Technology, 275*, 239-246.

Zhang, L., Huang, L., Li, S., & Zhu, X. (2018b). Study on two-step pyrolysis of walnut shell coupled with acid washing pretreatment. *Journal of Analytical and Applied Pyrolysis, 136*, 1-7.

Zhang, L., Li, S., Ding, H., & Zhu, X. (2019c). Two-step pyrolysis of corncob for value-added chemicals and high-quality bio-oil: Effects of alkali and alkaline earth metals. *Waste Management, 87*, 709-718.

Zhang, S., Chen, T., Li, W., Dong, Q., & Xiong, Y. (2016a). Physicochemical properties and combustion behavior of duckweed during wet torrefaction. *Bioresource Technology, 218*, 1157-1162.

Zhang, S., Chen, T., Xiong, Y., & Dong, Q. (2017a). Effects of wet torrefaction on the physicochemical properties and pyrolysis product properties of rice husk. *Energy Conversion and Management, 141*, 403-409.

Zhang, S., Dong, Q., Zhang, L., & Xiong, Y. (2016b). Effects of water washing and torrefaction on the pyrolysis behavior and kinetics of rice husk through TGA and Py-GC/MS. *Bioresource Technology, 199*, 352-361.

Zhang, S., Su, Y., Xu, D., Zhu, S., Zhang, H., & Liu, X. (2018c). Effects of torrefaction and organic-acid leaching pretreatment on the pyrolysis behavior of rice husk. *Energy, 149*, 804-813.

Zhang, Y., Chen, P., Liu, S., Peng, P., Min, M., Cheng, Y., Anderson, E., Zhou, N., Fan, L., Liu, C., Chen, G., Liu, Y., Lei, H., Li, B., & Ruan, R. (2017b). Effects of feedstock characteristics on microwave-assisted pyrolysis - A review. *Bioresour Technol, 230*, 143-151.

Zhang, Y., Yao, A., & Song, K. (2016c). Torrefaction of cultivation residue of Auricularia auricula-judae to obtain biochar with enhanced fuel properties. *Bioresource Technology, 206*, 211-216.

Zhang, Z., Ma, X., Li, H., Li, X., & Gao, X. (2018d). Understanding the pyrolysis progress physical characteristics of Indonesian oil sands by visual experimental investigation. *Fuel, 216*, 29-35.

Zheng, A., Zhao, Z., Chang, S., Huang, Z., Zhao, K., Wei, G., He, F., & Li, H. (2015). Comparison of the effect of wet and dry torrefaction on chemical structure and pyrolysis behavior of corncobs. *Bioresource Technology, 176*, 15-22.

Zheng, Y., Tao, L., Yang, X., Huang, Y., Liu, C., & Zheng, Z. (2018). Study of the thermal behavior, kinetics, and product characterization of biomass and low-density polyethylene co-pyrolysis by thermogravimetric analysis and pyrolysis-GC/MS. *Journal of Analytical and Applied Pyrolysis, 133*, 185-197.

Zheng, Y., Tao, L., Yang, X., Huang, Y., Liu, C., & Zheng, Z. (2019). Comparative study on pyrolysis and catalytic pyrolysis upgrading of biomass model compounds: Thermochemical behaviors, kinetics, and aromatic hydrocarbon formation. *Journal of the Energy Institute, 92*(5), 1348-1363.

Zhong, J., Wang, Y., Yang, R., Liu, X., Yang, Q., & Qin, X. (2018). The application of ultrasound and microwave to increase oil extraction from Moringa oleifera seeds. *Industrial Crops and Products, 120*, 1-10.

Zhu, X., Luo, Z., Diao, R., & Zhu, X. (2019). Combining torrefaction pretreatment and co-pyrolysis to upgrade biochar derived from bio-oil distillation residue and walnut shell. *Energy Conversion and Management, 199*, 111970.

# LIST OF PUBLICATIONS AND PAPERS PRESENTED

1. Gan, Y. Y., Ong, H. C., Show, P. L., Ling, T. C., Chen, W. H., Yu, K. L., & Abdullah, R. (2018). Torrefaction of microalgal biochar as potential coal fuel and application as bio-adsorbent. *Energy conversion and management*, *165*, 152-162.

2. Gan, Y. Y., Ong, H. C., Ling, T. C., Chen, W. H., & Chong, C. T. (2019). Torrefaction of de-oiled Jatropha seed kernel biomass for solid fuel production. *Energy*, *170*, 367-374.

3. Gan, Y. Y., Ong, H. C., Chen, W. H., Sheen, H. K., Chang, J. S., Chong, C. T., & Ling, T. C. (2020). Microwave-assisted wet torrefaction of microalgae under various acids for coproduction of biochar and sugar. *Journal of Cleaner Production*, 119944.

4. Gan, Y. Y., Chen, W. H., Ong, H. C., Sheen, H. K., Chang, J. S., Hsieh, T. H., & Ling, T. C. (2020). Effects of dry and wet torrefaction pretreatment on microalgae pyrolysis analyzed by TG-FTIR and double-shot Py-GC/MS. *Energy*, 210, 118579.

5. Gan, Y. Y., Chen, W. H., Ong, H. C., Lin, Y. Y., Sheen, H. K., Chang, J. S., & Ling, T. C. (2021). Effect of wet torrefaction on pyrolysis kinetics and conversion of microalgae carbohydrates, proteins, and lipids. *Energy Conversion and Management*, 227, 113609.